ENERGETIC STUDY OF A SOLAR ASSISTED GROUND SOURCE HEAT PUMP SYSTEM FOR DOMESTIC HEATING WITH PARAMETRIC ANALYSES VIA SIMULATION

Evangelos Sakellariou

JANUARY 2020

Thesis submitted in partial fulfilment of the requirements for the degree in Doctor of Philosophy

De Montfort University

Institute of Energy and Sustainable Development

Faculty of Computing, Engineering and Media

This research is sponsored by De Montfort University

Declaration

I herewith certify that all material in this dissertation which is not my own work has been duly acknowledged.

Evangelos Sakellariou

Acknowledgements

Although the PhD research is an individual effort, I am thankful to people and the De Montfort University which was the financial supporter of this work. First, I feel deeply grateful to De Montfort University which offered me this opportunity. It was an honor for me to be chosen by Professor Rick Greenough and Dr Andrew Wright to work on this project. Without the scholarship from the university, my plans for PhD degree would be unrealistic.

I was privileged to be supervised by a team which let me explore the wider field without imposing any restrictions and pressure on my work. My supervisory team consisted of Dr Andrew Wright and Dr Muyiwa Oyinlola. During the research, there were times which mountains had to be climbed in order to go further, in these instances their crucial advice made me to conserve time and energy. I would like to thank them for all they have offered to me. Along with the supervisory team, Professor Rick Greenough was a person acting as an advisor throughout all the research, the annual reviews and the small meetings were always a source for thoughts for me.

A vital person in the conducted research was Dr Petros Axaopoulos from University of West Attica. With Professor Axaopoulos, the additional experimentation and validation of the new photovoltaic thermal model was carried out. The professor's assistance regarding the simulation platform was important, since TRNSYS is a complicated software with minimum online assistance. Also, with Dr Petros Axaopoulos, I have discussed the developed metrics and their utility, without our collaboration my knowledge in the topic would be poorer. Therefore, I would like to thank him for all the time spent with me.

My research time was split between Leicester and Nafplio (Greece). Of course, when I was at the University, I had a place with a desk waiting for me to work. But, back in Greece, by having two children, one infant and one toddler, to work at home was an unachievable task. Therefore, the major working time was spent at the public library Palamedes and at Harvard's Hellenic studies center, both located in Nafplio. I feel grateful for the hospitality and place offered to me.

During my studies at De Montfort University, I met many colleagues doing their PhD in a variety of fields. Unfortunately, I did not spend enough time at the University in order to establish closer relations with all PhD students. But, when I was there, we always spent some time together. I would like to express my special appreciation to Carlos Naranjo Mendoza, who was the colleague working on a related with me the PhD topic. Also, I would like to thank Nittalin

Phunapai and Ozan Tasli, who are the persons along with Carlos whom I came closer and spent together most of the time being in Leicester.

Lastly, I would like to thank my wife Foteini for her patience and companionship, it was very hard to be away from time to time and let her alone with two baby daughters. Also, I would like to thank my mother in law Stella for her support during the studies, without her it would have been very hard to be away for studies. Stella was the person who kept the balance at home, by replacing me in many ways. Finally, I was very fortunate of meeting Christin Keen, she shared with me her house. Chris taught me how to grow potatoes and other vegetables on the allotment, also we did Sunday's bicycle rides with the cycling group "Spokes". Chris was the key person assisting me to maintain my motivation when I was in the UK, away from my family.

ABSTRACT

In this thesis, a solar assisted ground source heat pump system is energetically evaluated for the UK Midlands climate conditions. The conducted research is supported by an experiment made by De Montfort University. This consisted of seven photovoltaic-thermal collectors and a novel very shallow geothermal heat exchanger, supplying a heat pump used to heat a small house. The detail mathematical model of the system was formulated, and parametric analyses were conducted via simulation. Parametric analyses were carried out by assuming two dwelling types, one new and one refurbished, and by varying the number of the solar collectors and the size of the novel very shallow geothermal heat exchanger (1.5 m deep). Additionally, two potential system configurations and two locations of geothermal heat exchanger had been assumed (the one to be exposed and the other to be beneath the dwelling).

The important aspects of the research were: a) to determine the parameter which influence the systems energy performance and to define the energetically better system configuration, b) to identify the heat and electricity independence of the system from conventional energy sources, c) to examine the metrics in which the energy evaluation of the systems can be based on and d) the potential reduction of greenhouse gases emissions against a natural gas boiler-based system and a ground source heat pump system. Within the current work, no economic evaluation of the system has been conducted.

The results analysis has shown that the higher ratio of generated to consumed electricity is the index which illustrates the system with the best energy performance. This ratio is a valid approach only if the auxiliary heat required by the systems is added to the consumed electricity, by being assumed to be offered via electricity. By contrast, the seasonal performance factor, which is used widely, was diagnosed as an unappropriated metric to describe the energy performance of the systems. Additionally, the concept of the specific productivity was used to identify improvements on the performance of the systems caused by parameters variation.

Based on evaluation made via the studied metrics, the topology with direct use of solar heat was found to get lower efficiency than this without direct use. As regards the heat autonomy of the systems, this was found to be up to 83% for the new dwelling and 73% for the refurbished one. Similarly, the electricity offered by the photovoltaic-thermal collectors achieved a self-sufficient stage for most schemes paired with the new dwelling. However, the system paired with the renovated building did not manage to get more than the 90% of its electricity to be offered by

the collectors. A potential solution for greater power coverage from the solar energy may be a more efficient photovoltaic-thermal technology. Though, the key role of the system heat coverage was found to be the size of the geothermal heat exchangers and the area of the solar collectors. Hence, for a totally geothermal system paired with the new dwelling, the fractional heat coverage was estimated to be between 0.33 and 0.69 for the smallest geothermal heat exchanger of 16 and the largest one with 40 borehole heat exchangers (1.5 m deep), respectively. By adding 20 PVTs on the larger geothermal heat exchanger, the factional heat coverage was increased to 0.83 and to 0.70 for the smallest number of borehole heat exchangers. Likewise, the refurbished dwelling with only 16 borehole heat exchangers was found with 0.31 heat coverage and with 0.55 for the largest geothermal heat exchanger. By adding 20 PVT collectors on both borefields the heat coverage was increased to 0.65 and to 0.74 for the smaller and the larger geothermal heat exchanger, respectively.

It was found that higher energy performance can be obtained when the geothermal heat exchanger is exposed, instead of being placed beneath the new dwelling. The superiority of the geothermal heat exchanger to be installed at an uncover space instead of being placed beneath the dwelling applies to all the investigated configurations and sizes of the system. Thus, the largest system with 20 PVTs was estimated with ratio between the generated to consumed electricity of 1.9 for the exposed location, against the ratio of 1.5 which was found for the exchanger to be covered by the dwelling. Similarly, for the smallest array of 4 PVTs, the ratio was estimated to be 0.26 and 0.22 for the exposed and the covered by the dwelling choice accordingly.

Lastly, the investigated system was found with lower carbon emissions than the natural gas boilers system at all the investigated configurations and for both dwelling types. The gas boiler system was estimated to release 1509.7 kg CO_2e year^{-1} and 3050.9 kg CO_2e year^{-1}, when it is installed in the new and the refurbished dwelling accordingly. With the new dwelling, all configurations with more than 12 PVTs were found capable to decarbonize in total the emissions from the natural gas boiler system, while for the energy renovated dwelling the fraction emission savings were estimated up to 0.8. Also, the proposed system was estimated less emissive than the conventional ground source heat pump system for PVT arrays with more than 4 collectors and with more than 8 collectors for the new and the refurbished dwelling, respectively.

Publications associated with this research

Sakellariou, E. I. et al. (2019) 'PVT based solar assisted ground source heat pump system: Modelling approach and sensitivity analyses', Solar Energy, 193, pp. 37–50.

Sakellariou, E. and Axaopoulos, P. (2018) 'An experimentally validated, transient model for sheet and tube PVT collector', Solar Energy, 174, pp. 709–718.

Sakellariou, E. Wright, A. Oyinlola, M., (2019). Solar and Geothermal Energy for Low-Carbon Space Heating and Energy independence, in: Proceedings of the International Conference on Energizing the SDGs through Appropriate Technology and Governance. Leicester (UK). pp. 141–152.

Oyinlola, M. et al. (2019). Thermal Analysis of an Earth Energy Bank, in: Proceedings of the 16th UK Heat Transfer Conference (UKHTC2019) 8-10 September 2019, Nottingham. UKHTC2019-193.

Contents

List of figures

List of tables

Nomenclature

ACH	air changes per hour [-]
CBR	collectors to borehole heat exchangers ratio [$m^2\ m^{-1}$]
COP	coefficient of performance [-]
c_p	specific heat capacity [$J\ kg^{-1}\ K^{-1}$]
D	diameter [m]
E	electricity [kWh]
E_{AUX}	auxiliary energy used by the system [kWh]
$E_{heat\_recovery\_unit}$	electricity consumed by ventilation heat recovery unit [kWh]
E_{HP}	electricity consumed by the heat pump [kWh]
E_{pumps}	electricity consumed by the circulation pumps [kWh]
E_{PVT_u}	electricity delivered to the power grid by the PVTs [kWh]
$f_{sav.emis}$	fractional carbon emission savings [-] (equation 3.2)
GUE	gas utilization efficiency [-]
L	length [m]
M	mass flow rate [$kg\ s^{-1}$]
n	number of PVTs [-]
P	power [W]
PER	primary energy ratio [-]
Q	heat [kWh]
Q_{aux_syn}	the portion of the auxiliary heat with is covered by the synchronized PVT power generation [kWh]
Q_{cond}	heat pump's condenser delivered heat [kWh]
Q_{ev}	heat pump's evaporator inlet heat [kWh]
Q_{HP_syn}	the heat pump's electricity offered directly from PVT collectors (synchronized consumption and generation) [kWh]
Q_{solar_dir}	solar heat used directly by the system [kWh]
RHF	renewable heat fraction [-]
RPF	renewable power fraction [-]
SC	storage capacity [$m^3\ m^{-2}$]
SPF	seasonal performance factor [-]
SPF*	seasonal performance factor without considering the electricity generated by PVTs [-] (equation 3.3)
SP_{PVT_el}	PVTs' electric specific productivity [$kWh\ PVT^{-1}$] (equation 3.5)
SP_{PVT_heat}	PVTs' heat specific productivity [$kWh\ PVT^{-1}$] (equation 3.4)
SP_{sys_heat}	system heat specific productivity [$kWh\ PVT^{-1}$] (equation 3.6)
T	temperature [K]
T_{b_s}	mean soil temperature near borehole [K]
T_{s_und}	undisturbed ground temperature [K]
V	volume [m^3]

Subscripts

a	ambient
Avail	available
Bor	borehole
Deliv	delivered
G	ground
HP	heat pump
in	inlet
out	outlet
S	system

Acronyms

BHE or U-BHE	borehole heat exchanger or U-shaped borehole heat exchanger
DHW	domestic hot water
DMU	De Montfort University
DST	duck ground heat storage model
EEB	earth energy bank
ETC	evacuated tubes solar Collector
EU	European union
FPC	flat plate collector
GHE	geothermal heat exchanger
GHGs	greenhouse gases
GSHP	ground source heat pump
HCR	heating to cooling ratio
HP	heat pump
NG	natural gas
PCM	phase change material
PHE	plate heat exchanger
PV	photovoltaic panel
PVT	photovoltaic thermal collector
RES	renewable energy sources
SAGSHP	solar assisted ground source heat pump
SAHP	Solar assisted heat pump
STESS	solar thermal energy storage systems
TESS	thermal energy storage systems
UK	United Kingdom

Greek letters

ε	plate heat exchanger's effectiveness [-]
λ	thermal Conductivity [W m^{-1} K^{-1}]

Chapter 1. Introduction

1.1. Motivation

Nowadays, among the humanity's greatest challenges is that of climate change. Greenhouse gases emissions and especially of CO_2 is accused for global warming effect. Worldwide a huge action takes place with the aim of reducing the anthropogenic carbon emissions, which are produced mainly by the fossil fuels consumption. It is worth mentioning that, along with the greenhouse gases produced by the consumption of fossil fuels, lots of other pollutants are released. Pollutants like the oxides of Nitrogen NO_x, oxides of Sulphur SO_x and the unburnt hydrocarbons contaminate the environment (Markides, 2013). Globally, the acknowledgement of the situation and the proposed actions have been set via the Paris Agreement (UNFCCC. Conference of the Parties (COP), 2015). This protocol is implemented via intergovernmental organizations, such as the United Nations (UN, 2015), provide guidance for national measures against the atmospheric pollution. In the European Union (EU), actions have been made with the purpose of reducing the CO_2 emissions. The EU's objectives are to increasing the utilization of renewable energy sources (RES) and to improve systems' energy efficiency (Commission, 2020). Also, the UK has set a national target to achieve lower carbon emissions by 2050, compared to the level recorded in 1990. This legislation has come in to force in 2019 via the amended act of 2008 (HM UK Parliament, 2008).

In practice, greenhouse gases emissions released during the operation of the systems can be decreased by improving the energy efficiency of systems or by utilizing environmentally friendly energy sources. It is essential to improve system's energy efficiency firstly and then to find the best sustainable way to cover the demand effectively and efficiently. Nevertheless, the choice of the energy source remains a multi-objective topic with financial, social and geopolitical aspects. As regards the energy sources which can be used to reduce the emissions are RES and nuclear power. For the fraction of the load covered by alternative energy sources, no carbon emissions are released to the atmosphere. It is worth saying that, the above discussion refers to the emissions released from the operation of the systems and not the embedded or corelated emissions of the systems.

Up to now, a country's energy system cannot be totally based only on RES. The difficulties of energy storage and the stochastic energy conversion from RES are few of the boundaries for

their greater penetration in the system. Nevertheless, for systems designed for houses and up to district size systems consisted of several homes (Sibbitt *et al.*, 2012), RES may provide a substantial portion of the heat and power demand. In the EU, the 25.4% of the total energy consumption goes to domestic sector (EUROSTAT, 2015) and from that the 64.7% offered for space heating and the 14.5% for domestic hot water (DHW). The need for more environmentally friendly energy sources and the substantial energy consumption on households, combine a fertile ground for RES based heating systems.

Based on the argument deployed above, engineers and researchers must assist the policy makers to develop the future's energy systems around three pillars: sustainability, affordability and energy security (de Gouw *et al.*, 2014). With the present work, an investigation regarding the energy independence from fossil-fuels and electricity for a single-family dwelling takes place. Though, the energy autonomy may benefit all three aspects in which the future energy systems should be based on. The implementation of RES as a solution for energy independence can be amplified by establishing power and heat smart grids, which are capable to operate efficiently by managing the energy among the production, the consumption and the storage side (Yang *et al.*, 2017; Rad and Fung, 2016).

1.2. Focus of this study

Heating systems in residential buildings or dwellings consume conventional and/or renewable energy sources. The conventional energy sources used for space heating are mainly fossil fuels like natural gas, LPG and oil. As regards the alternative energy sources which can be used to provide heat in buildings, those are mainly solar energy, shallow geothermal energy and ambient energy (through air). However, electricity can be used as a space heating energy source, but this is not a good practice, since electricity is a superior form of energy and should be reserved for more efficient applications (motors and lighting).

An efficient method to utilize the renewable energy sources for space heating is through heat pump devices. Heat pumps operate in accordance with the second law of thermodynamics, via the exergy concept. In more detail, the operation of the heat pumps is based on the Carnot thermodynamic cycle (Moran and Shapiro, 2006). The thermodynamic cycle which describes the heating mode of the heat pump is illustrated schematically by Figure 1.1: the heat is absorbed from point 1 to point 2, and then work is added from point 2 to point 3, then delivers the total heat amount enclosed by points 3 to 4. In practice, the absorbed heat designated between the

points 1 and 2, originates from a renewable energy in low temperature (lower than the temperature required by the heating load). Then, by adding work, the temperature along with the pressure increases and by that, the heat can be transferred to the load. Thus, an available energy source with relatively low temperature can be used as a heat source for the system. As it can be seen in Figure 1.1 and as described above, the delivered heat is significant more than the consumed work on the system. It can be concluded that, by added work usually via electricity on a heat pump device, a substantial heat can be delivered by utilizing available RESs. It turns out that heat pump devices can obtain heat efficiency higher than 100%, and this is the greatest benefit of utilizing these devices.

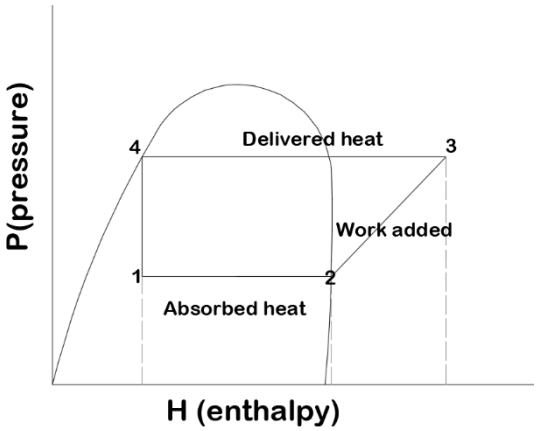

Figure 1.1. Heat pump's theoretical Carnot thermodynamic cycle for heating operation.

Systems like solar assisted ground source heat pump (SAGSHP) can utilize solar and shallow geothermal energy with the aim to heat a building and/or to provide DHW (Figure 1.2). Contrary to conventional ground source heat pump (GSHP) (Sarbu and Sebarchievici, 2014), or solar assisted heat pump (SAHP) (Ozgener and Hepbasli, 2007) systems, SAGSHP systems have the advantages of utilizing more than one renewable energy resource. Also, the benefit of resourcing and store the solar energy into the ground for later use, the system can be more energetical autonomous.

With the aim to specify better the focus of this study, Figure 1.3 illustrates the classification of the most widely used heat pump systems. In particular, the classification is about systems with electric drive heat pump devices and the three mostly used configurations: the air-source systems (ASHP), the ground source systems (GSHP) and the solar source systems (SAHP). It is worth saying, that an alternative energy source for a heat pump device can be heat (heat driven) (Hepbasli *et al.*, 2009), with the performance factor of these devices to be lower than the electric driven ones. Also, all branches above the aforementioned systems can be decomposed further

to more specific type of components. For instance, flat plate collectors may use liquid or air as heat carrier or may be covered with a transparent surface or to be uncovered. From Figure 1.3 a major outcome can be derived: the investigated type of the heat pump systems are combination of geothermal and solar systems. Also, a the SAGSHP system can be built by any combination of the solar and geothermal-source system (Nouri, Noorollahi and Yousefi, 2019). Taking the opportunity of illustrating this graph (Figure 1.3), the specific type of system which the research is interested in is a PVT based with a very shallow borefield. More information about both components can be reached in section 4.1 and 4.2 respectively for PVTs and the borefield.

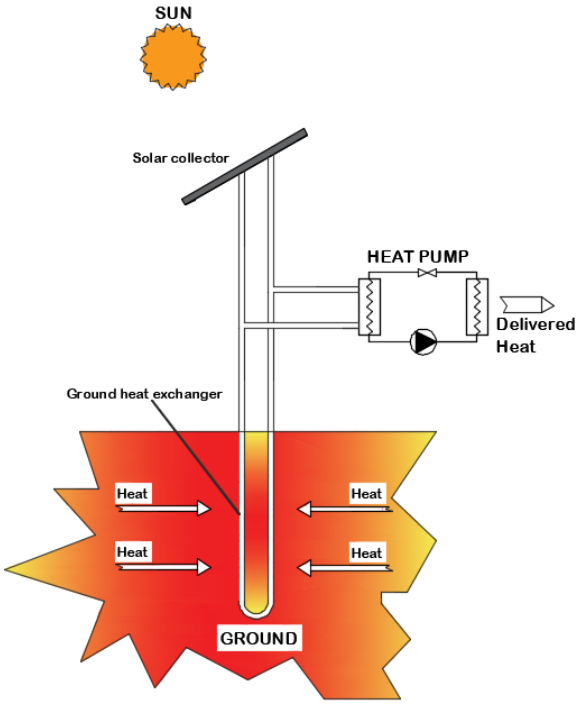

Figure 1.2. Schematic representation of the SAGSHP system's main components.

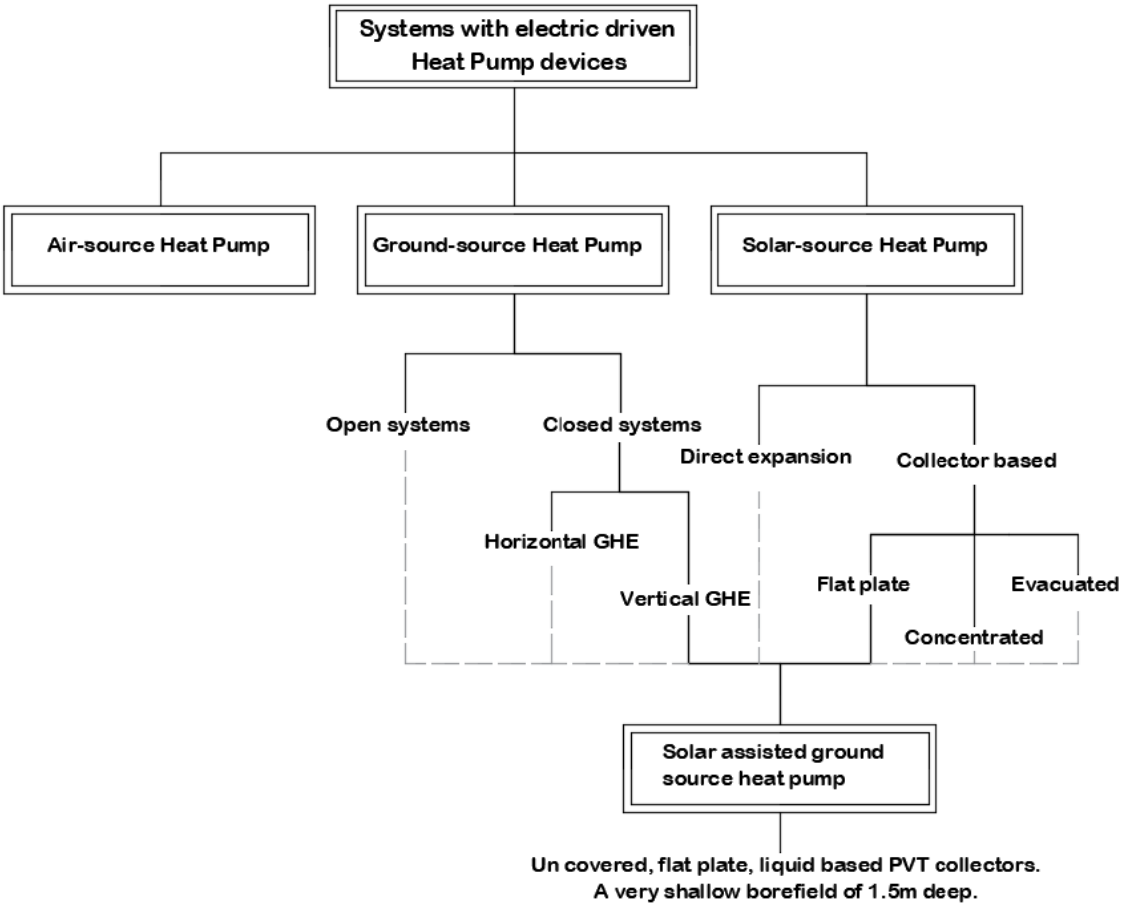

Figure 1.3. Classification of the mostly used systems paired with electric driven heat pump devices.

SAGSHP systems are comprised of solar and geothermal subsystems (Figure 1.3), which form the energy conversion side. The produced heat can be utilized for space heating and/or domestic hot water for buildings, but it can be used for other thermal processes as well (agricultural sector). Also, SAGSHP systems which are equipped with PVT collectors are attractive solution due to their ability of cogenerating heat and power. The generated power in many cases is capable of covering in total the electricity consumed by the system.

SAGSHP is not a new technology, back in 70s, Metz (Metz, 1980) made the first known attempt to investigate this type of system. Since then, more researchers have been involved in SAGSHP systems technology, while interest in this field is continuously growing. As regards the current scientific literature, this can be easily separated into two categories: a) the built SAGSHP systems (experiments) and b) the theoretical studies conducted via simulation. The grouping may go on by dividing the built systems (a) to these which are made for occupied buildings and to the pure experimentally conducted for the parametric analysis of the systems.

A real living condition SAGSHP system was built in Savoy-France (Trillat-Berdal, Souyri and Fraisse, 2006), with flat plat solar collectors (FPC) and a borehole heat exchanger (BHE) as its main characteristics. The system's performance was recording for eleven months and the system's seasonal performance factor (SPF) was calculated at 3.35. Also, the results shown that the parasitic energy along with the control strategy are crucial aspect for the system's performance. A PVT based SAGSHP system with homocentric vertical BHE installed in a occupied dwelling was investigated by Bertram et al. (2012). Along with the PVTs a PV was installed in order to obtain a comparison between the PVT's to PV's energy yield. After two years of data collection, the results showed that electric output from the PVT system outperform the PV systems output by 4%, while the system's SPF was calculated at 4.2. Experimental system like this illustrated by Yang et al. (2015), was made to compare the performance of SAGSHP with GSHP system, for diverse operational strategies. The results showed that the SAGSHP system demonstrated higher heat performance than the GSHP, while the operational mode which sets the solar heat to be stored into the soil during the day for evening used, found suitable for residential consumption profiles.

In literature, there are numerous studies made by computer-based simulation, with a variety of investigation topics. Bakker et al. (2005) made a work with the aim to evaluate the addition of the PVT collectors on a GSHP systems, for weather conditions of the Netherlands. The model was formulated in TRNSYS (Solar Energy Laboratory University of Wisconsin-Madison *et al.*, 2009) and an experimentally validated PVT collector was used. The PVTs found to offer the 96% of the consumed electricity and the 17% of the system's heating needs. Another theoretical study was conducted by Fine et al. (2018) with MATLAB for three building types in Toronto Canada. The buildings were characterized by different heat to cooling ratio. As regards the parametric analysis was made by varying only the area of the solar collectors with the purpose to find the energetically and financially optimum for each case. The results showed that for heating to cooling ratio of 1.2, there is no need for addition of solar collectors. A study made to compare SAGSHP systems for 8 European climates zones was conducted by Carbonell et al. (2014) by utilizing the POLYSUN simulation platform (Solaris, 2012). Via the results, the Alpes region was estimated as the ideal climate for SAGSHP systems implementation, with cold winter and substantial solar irradiation during the heating season.

As regards the current work, it was inspired by a PVT based SAGSHP system, which was installed at the De Montfort University (DMU) Leicester campus. The system's main characteristics were

the 7 PVT collectors connected hydraulically in series and the novel very shallow (1.5m) borefield. The experimental set-up and the performance analysis of the system have been published by Naranjo-Mendoza et al. (2019). With the DMU's experiment as starting point, the present research aims to shed some light on the system's feasibility by conducting parametric analyses. Giving that, a parametric analysis can be executed via experimentation or theoretically through computer passed simulation. Nevertheless, experimental based parametric analyses require further capital investment and is not feasible due to extended time in order to obtain useful results (up to several years for each parameter changed[1]). Therefore, the system's mathematical model was found as the appropriate solution for conducting parametric analyses and feasibility studies.

The existing system was source of data for components model validation and its layout offer guidance regarding the system's model formulation in TRNSYS simulation platform. With regards to the parametric analyses, were conducted by varying the amount of the PVT collectors and the geothermal heat exchanger (GHE) size. The variation pattern of the components took place for two different system layouts and two types of single-family dwellings, one newly built and the other energetically renovated. For the whole set of investigations, weather data for Birmingham were considered as representative city for the UK's Midlands. The choice of Birmingham is made because it is a good starting point, as it is representative of English climate. Also, Birmingham is the closest city to Leicester with available data, where the DMU's experiment was conducted. Local climate conditions and energy prices can strongly affect the design and performance of solar and geothermal systems. Although beyond the scope of the present study, future work can extend to other climates where similar effects are expected (Emmi, Zarrella, De Carli, *et al.*, 2015; Girard *et al.*, 2015; Ramos *et al.*, 2017). The energy evaluation of the systems was made by introducing new metrics like the specific heat productivity and load fractional coverage by renewables (section 3.5). Regarding the carbon emissions, the SAGSHP system was compared with a GSHP and a natural gas boiler (NGB) system via the fraction of CO_2e emission savings (subsection 3.5.5). Also, the carbon emissions of the SAGSHP system will be evaluated against the results obtained for a PVT heating system (Herrando, Markides and Hellgardt, 2014; Herrando *et al.*, 2018) and a hybrid solar PVT based

[1] The mean soil temperature assigned to a GHE has transient response on the system's year to year operation which cannot be evaluated within a year period. This transient period was found to cease after 3-4 years for all scenarios, with the soil mean annual temperature to enter in a monotony.

system (Ramos *et al.*, 2017). Although the emissions of the SAGSHP system and the emissions of the PVT based systems were not assessed under the same heating load and consumption profile, the present comparison aims to offer a wider view of the released CO_2 levels caused by similar technologies. The NGB system is chosen as the currently favourable system used to provide space heating and DHW to a dwelling. As regards the choice of the GSHP systems, these are heat pump systems currently installed in the UK, thus it is pertinent to compare this with the SAGSHP systems. Finally, the work targets to introduce a modelling approach and the applicable metrics as a holistic methodology which can be implemented for SAGSHP systems analysis worldwide.

1.3. Research Aims and objectives

By conducting a critical review of the literature on SAGSHP systems technology (Chapter 1), the knowledge gaps were identified. Thus, by bearing in mind the studied literature and DMU's system, the research questions were formulated:

a) What is the influence of solar collection area and GHE's size on the system's energy performance?
b) Does the direct use of solar heat benefit the system energetically?
c) What are heat and power fractions covered by RES for different levels of dwelling energy efficiency? The first to be built according to current regulations for new dwelling and the second as an energy renovated house.
d) What metric (s) can be used to evaluate energetically the PVT based SAGSHP systems?
e) Is the proposed SAGSHP system less carbon emissive than a system fired by natural gas (NG), or a conventional GSHP system? Also, what are the emissions of the SAGSHP system compare to other well-established solar heating technologies, like the PVT heating systems and the solar assisted heat pump systems?

The target of this thesis is to fulfil the literature gap by answering the research questions, thus based on that, the thesis aim is established:

What is the energetic performance and the carbon footprint of the proposed SAGSHP system for low-rise buildings in a UK's space heating dominated province?

Being driven by the established aim, six objectives have been set and listed below. These objectives can be grouped to the preliminary (1 to 4) in terms of preparing the ground for the feasibility studies and the 5 which is the tool for the systems evaluation.

1. Analyse data from DMU's experiment and use part of those data for component validation. It may be preferable to validate the system as a whole, but the operation of the experiment was partially recorded.
2. Build an uncovered, flat plate, liquid based PVT collector and conduct additional experimentation. The aim behind this objective is to validate a new PVT's dynamic model and utilize this for simulations.
3. Formulate the mathematic model of the systems on the simulation platform with the aim to obtain acceptable accuracy between the real system and the model.
4. Develop the methodology along with the set of metrics needed for the energy evaluation of the systems. To find the correct index which allows us to compare the greenhouse gases emissions made by different systems.
5. Conduct parametric analyses via system's mathematic model with the aim to answer the research questions.

1.4. Methodology, computer-based simulations

To answer the above questions, a mathematic model based on the experimentally investigated PVT-SAGSHP system was built in TRNSYS software. In the reviewed literature, TRNSYS was found to be the dominant platform for SAGSHP systems analysis. In order to create a valid tool, further experimentation was conducted regarding the uncovered, flat plate, liquid based PVT collector (Sakellariou and Axaopoulos, 2018). In what follows for convenience, for the uncovered, flat plate, liquid based PVT collector, the term PVT of PVT collector will be used. Except if a different type of PVT collector is implicitly stated. With the experimental data a new validated 1D dynamic model for PVTs was created and built on the simulation platform. Other investigators have developed dynamic models of sheet-and-tube PVT collectors based on similar principles, which have been successfully validated against data from outdoor tests, confirming that the inclusion of the collector's dynamics can in some cases be important (Guarracino *et al.*, 2016, 2019). Also, data from DMU's experiment were used to verify the Hellström's Duct Ground Heat Storage (DST) model (Hellström, 1989). As regard the heat pump (HP), a new hybrid model was developed, which is depended on manufacturers tabulated data (EN 14511) and on energy availability provided by the solar and the geothermal system (Sakellariou *et al.*, 2019).

The parametric analysis of the systems was conducted for two types of house, one newly built according to modern standards (L1A) (HM Government. Ministry of Housing & Communities & Local Government, 2016) and a refurbished one according to standards for energy renovated

dwellings (L2A) (HM Government. Ministry of Housing & Communities & Local Government, 2010). The two dwelling types had the same geometry with two storeys and total living area each of 120m^2. Also, the two buildings had the same orientation and location (Birmingham, UK).

Regarding the main part of the parametric analysis, it took place on the energy production side, by varying the PVT collectors' quantity from zero up to 20 and the BHEs from 16 up to 40 accordingly. The maximum numbers of PVTs and BHEs have been indicated by the dwelling's available roof and ground floor area, respectively (section 3.1). In order to conduct this parametric analysis a new index was introduced which indicates the ratio between the collectors and the BHEs (CBR). Also, another aspect which found to influence the systems energy productivity is the storage capacity (SC). Principally, the SC illustrates the ratio between the available heat storage volume and the energy harvesting equipment.

About the topology of the systems two scenarios were tested: a) the PVTs to supply heat only via the GHE and b) the PVTs to supply heat both ways, directly to DHW tank and to GHE. Also, regarding the newly built dwelling, two locations regarding the GHE installation was considered: a) the GHE to be exposed without any insulation and b) the GHE to be beneath the house. About the refurbish scenario, the GHE was investigated only for the exposed location due to practical reasons (it cannot easily be placed beneath the building, while this is already built). Finally, the carbon emissions of the SAGSHP systems were compared with these of GSHP and NG fired heating systems, for all the above-mentioned variations of the system. Additionally, the carbon emissions of the SAGSHP system are evaluated against the emissions which have been estimated for other well-developed solar technologies, such as the PVT heating systems (Herrando, Markides and Hellgardt, 2014; Herrando *et al.*, 2018) and the SAHP system (Ramos *et al.*, 2017).

1.5. Structure of thesis

The dissertation is deployed in seven chapters. Following this introductory Chapter 1:

In Chapter 1, a critical review on the current literature is conducted. The scientific work is listed and analysed regarding the existing experimentally based systems and those which have been evaluated via computer-based simulations. Also, information regarding the systems interconnection (topology) is extracted, along with utilized components (solar collectors and GHE type). The potential energetic benefits of solar collectors' addition on the ground loop are illustrated. Finally, the main gaps on current knowledge are highlighted and listed.

In Chapter 3, the methodology used is illustrated by overview the all process with the need to support the choice of simulation-based experiments against the physical experimentation. The SAGSHP system experiment which was constructed by DMU is described with the need to bound the current work with previous efforts. Problems and difficulties which were faced during the research are listed along with their solution. Within this chapter some important information regarding the utilized simulation environment (TRNSYS) are shown. Also, the two investigated system topologies are analysed along with their control flow chart. At the end of this chapter, the metrics deployed for the energy evaluation of the systems are offered and explained with adequate detail.

In Chapter 4, the subcomponents of the SAGSHP system are specified, along with their technical data and the used parameters. The validation of the GHEs with experimental data is shown with the achieved accuracies. Also, the GSHP system and the natural gas boiler-based system are illustrated and their topology is shown (A comparison regarding the carbon emissions of these two systems and the SAGSHP system is placed in Chapter 7). In general, this chapter provides technical information about the utilized components, PVTs, GHE, dwellings and heat pumps.

In Chapter 5, the results for the new dwelling are illustrated and discussed. The chapter is split into two sections: one dedicated to the heat analysis and the other to the electric output evaluation. Each section ends with a summary with the major finding. The simulation results are analysed with the energy metrics illustrated in Chapter 3.

In Chapter 6, the results for the results dwelling are illustrated and discussed. Similarly to Chapter 5, the chapter is split into two sections: one dedicated to the heat analysis and the other to the electric output evaluation. Each section ends with a summary with the major finding. The simulation results are analysed with the energy metrics illustrated in Chapter 3.

In Chapter 7, the investigated SAGSHP heating systems are compared regarding the carbon emissions with a natural gas fired heating system and a GSHP system. The discussion regarding the results is taking place along with the important information derived from the analyses.

In Chapter 8, the main results are emphasized, also the findings and the established aim are bridged. Suggestions regarding the systems implementation are proposed as solutions for more environmentally friendly heating systems. Finally, ideas regarding future works are listed and explained.

Chapter 2. Critical review of the literature

In this chapter the existing literature is reviewed and analyzed with the aim to obtain the up-to date knowledge on the technology and to identify the work's potential contribution. At the beginning, SAGSHP systems are defined with the scope to establish the foundations for the systems' investigation. Then, the reviewed scientific material is separated in two main categories: the experimental built systems; and the theoretical simulation-based studies. Along with the analysis, the technical and environmental aspects of the SAGSHP systems are analyzed and illustrated. At the end, the identified gaps in the literature are showed and matched with the research questions and aims.

2.1. Principles of solar assisted ground source heat pump systems

It is pertinent, to offer a wider view of the renewable energy technologies used as heating systems and then to focus on the analysis of SAGSHP systems. Roughly, the renewable energy technologies which are used for heating systems can be split into two groups, these which operate with heat pump and these which does not. Solar energy is the main source which can be used for heating applications without the use of Carnot engine (without heat pump)[2]. The capability of the solar collector to provide solar heat within the direct utilizable range of temperatures is the key point (30 – 80 ^{o}C (Kalogirou, 2004)). In many cases, the solar energy can be stored during summer with the objective to provide heat in winter when the demand is substantial (long-term) (Braun, Klein and Mitchell, 1981; Argiriou, 1997). Solar systems are a mature technology and so far many design method have been developed (Lunde, 1979; Okafor and Akubue, 2012; Guadalfajara, Lozano and Serra, 2015). An interest type of solar systems is this with PVT collectors (Axaopoulos and Fylladitakis, 2013; Herrando *et al.*, 2018). The peculiarity of PVT is that can coproduce heat and power form the same collector. Although the thermal efficiency of PVTs is lower that this of conventional flat covered collectors (Zondag, 2008), PVT based solar systems can be used in space heating dominate climates and by that to displace a substantial amount of conventional energy sources (Herrando, *et al.*, 2019). Various PVT collector types exist, spanning a range thermal and electrical module efficiencies, with

[2] Another renewable energy source for space heating it can be the deep geothermal energy (Agemar, Weber and Schulz, 2014), but this is not widely abundant.

different expected system-level performance (Herrando, Markides and Hellgardt, 2014; Herrando *et al.*, 2018; Herrando, Ramos and Zabalza, 2018) and corresponding module prices (Herrando and Markides, 2016).

Heating systems equipped with heat pump (mainly electric driven) can primarily be grouped in three types; the air source, the solar assisted and the ground source heat pump systems (Figure 1.3). The air source heat pump systems make used of the heat contained in the atmosphere, which is in relatively low temperature 0 – 10 ^{o}C, and via the refrigeration cycle the temperature increases to useful level (Bertsch and Groll, 2008; Hepbasli and Kalinci, 2009; Staffell *et al.*, 2012). Similarly, solar assisted heat pump systems utilized solar energy (Ji *et al.*, 2009; Stojanović and Akander, 2010; Wang *et al.*, 2017). The solar energy can be store for later usage or it can be absorbed from the collector via the refrigerant's direct expansion (Molinaroli, Joppolo and De Antonellis, 2014). Lastly, the shallow geothermal systems have the advantage to absorb heat from the ground at relatively stable temperatures (J. Lund, B. Sanner, L. Rybach, R. Curtis, 2004; Alkan, Keçebaş and Yamankaradeniz, 2013; Morrone, Coppola and Raucci, 2014). The mean temperature of the soil at 10 – 15 m below the surface of the ground is constant all year round, and its value approaches the mean ambient air temperature. This is a positive aspect for shallow geothermal systems, since during winter the air temperature is lower than the mean annual value, and that entail available heat stored in the soil which can be used via a heat pump.

The combined design of a GSHP systems with a solar system creates a SAGSHP system, which is a renewable energy technology. The solar and geothermal energy are system's heat sources, while in most cases electricity is required for heat pump's compressor and the circulation pumps. From early studies of solar energy as a potential energy source for space heating and domestic hot water (DHW), researchers tried to find a way of combining solar system with heat pumps (Anderson, Mitchell and Beckman, 1980). One of the first attempts to harness solar energy for space heating is described by Givoni (1977) for MIT's solar house, built in 1939. It took almost 40 years to start the investigation on SAGSHP systems and again from the USA researchers like Metz (1980) who have tried to shed some light on the topic. Metz did a pioneering work with one of the first known SAGSHP systems. The experimental objectives were to evaluate the system feasibility and to create a model with the purpose of conducting parametric analysis. Since then, more researchers have been involved in solar assisted heat pump systems technology, while interest in this field is continuously growing.

A review work on solar assisted heat pumps SAHP systems was done by Ozgener and Hepbasli (2007). In their study, SAGSHP systems are considered as a particular SAHP system type and the potential for Turkish market is discussed briefly. Marx et al. (2014) focused on the solar thermal energy storage systems (STESS) and the influence of the heat pump on systems efficiency. They concluded that the use of the heat pump does not always improve the system's efficiency, but it is able to partially enhance the solar collector heat productivity. In the SAHPS area, a comparative work was done by Chandrashekar et al. (1982) for seven Canadian cities with distinctive climate. The results showed that SAHP systems are capable of covering a significant portion of building's energy demand and in most of locations.

Similarly, to SAHP systems, many review works on GSHP field have been done, but the solar assisted influence on the systems feasibility is not the major topic investigated. In more detail, Zhu et al. (2014) did a review on GSHP systems with soil based thermal energy storage systems (TESS). In their work, a discussion on systems which are equipped with heat pump takes place, but not in detail and are mixed with the TESS. Similarly, a review work based on GSHP system is done by Qi et al. (2014), where SAGSHP systems are investigated as a hybrid type of GSHP system. Furthermore, the work of Sarbu & Sebarchievici (2014) is a review of GSHP systems with an analytical perspective and the SAGSHP systems' depiction is as a particular GSHP type.

A SAGSHP system is a complex system in terms of control, energy management and component sizing due to its combined character. The difficulty in systems design is also related to the large number of solar collectors and GHEs technologies available. Also, the correct matching of the utilized components is crucial for the choice of system's layout and applied control strategy. Therefore, every SAGSHP project to date has been built with site-specific method, due to the market's immaturity and lack of standardized approaches.

To avoid any misinterpretation and to clarify further the term of SAGSHP system, the solar assisted part is referred to thermal energy addition and not to electricity assistance. In the literature, works like (Franco and Fantozzi, 2016) refer to PV systems paired with a GSHP systems via net-metering scheme, while (Jradi, Veje and Jrgensen, 2017) refer to PVs which drive the heat pump to store thermal energy into the soil. The aforementioned systems are solar assistive regarding the power consumption, but they are not defined as solar assisted GSHP systems due to not including solar heat input in their configuration.

In regions where space heating is the dominant operation mode for GSHP systems, the ground temperature is annually reduced (You *et al.*, 2016). The temperature of the heat transfer fluid exiting the GHE is directly related to the soil's temperature and with decreased soil temperature, the heat pump's performance gradually drops. Also, the low soil temperature may result to heat pump's inlet brine temperature be lower than its operational limits and by that to disrupt system's operation.

A viable solution on the annual soil temperature reduction due to imbalance heat loads may be the addition of solar collectors (Nicholson-Cole, 2012b; Eslami-nejad *et al.*, 2009a; Emmi, Zarrella, Carli, *et al.*, 2015) on GSHP systems. Studies like the one conducted by Fine et al. (2018), show that the Heating to cooling load ratio (HCR) is a decisive parameter for solar field sizing and for ratios close to 1.2 HCR does not requires solar heat enhancement. Other potential solutions may be an oversized GHE or the utilization of a heat driven heat pump (Wu *et al.*, 2013) with the aim to reduce the heat absorbed from the ground. In what follows the review, we are going to study the SAGSHP systems with the solar collectors' area and GHE's size variation as potential solution on the temperature imbalance issue.

2.2. Greenhouse gases

It is believed that the high concentration of greenhouse gases (GHGs) in the atmosphere is mainly responsible for the global climate change effect. With Kyoto protocol six GHGs are defined as the reason for the greenhouse effect (GHE) (Prins and Rayner, 2008). These six GHGs are released via natural processes up to a certain low level, but nowadays are emitted in excess by human activities and mainly by fossil fuels consumption. Thus, via Kyoto protocol and as continues with the Paris agreement (ŻYLICZ, 2015), the manmade GHGs emissions are constrained with the aim to decelerate or to cease the global warming and keep it below 2 K.

Systems based on electric driven heat pumps can deliver heat 2 to 6 times greater than the consumed electricity. Nevertheless, the consumed electricity is usually imported from the power grid and has been generated by a mix of primary energy sources. The primary energy mixture (RES, Nuclear, Coal, Natural Gas) and power system energy efficiency (η) are factors which influence the grid's GHGs intensity. Therefore, for the environmental impact assessment, the indirect emissions released during the energy conversion at the power plants are used. Based on that, EU has set a benchmark which ensures that an electric driven heat pump system

decarbonizes the consumed electricity if a SPF_{H2} is greater than 2.5 (European Parliament, 2013) (Figure 3.11).[3]

Throughout the existing scientific work, the carbon emissions about the conventional GHSP systems are mainly studied and not the SAGSHP systems. One exception to the rule, is the experimental work done for SAGSHP system installed on a refurbished house in Germany (Loose and Drück, 2014). The SPF was calculated at 3.46 which show an environmentally friendly systems giving that the grid intensity was 0.56 kg CO_2e kWh^{-1}. The system was found to be feasible according to the IEA Task 44/ Annex 38 with annual average Global Worming Potential (GWP) of 0.153 kg CO_2e kWh^{-1}.

A new design tool for GHSP systems has been deployed by Nagato et al. (2006). Authors were aiming to offer a method to be suitable for energetic, economic, and environmental studies. A case study made during that work, showed that a house based GHSP system in Sapporo (Japan) is capable of reducing the carbon emissions by 2038 kg CO_2e annually, compared to natural gas-based system. Equal magnitude on annual carbon reduction was found in a study made by (Blum *et al.*, 2010) for a southwest region of Germany. The work was based on 1105 applicants who installed GSHP systems via a subsidy program. The results from collected data showed that the average annual emissions were reduced by 1810 kg CO_2e per system contrary to a gas boiler system.

2.3. Systems layout classification

In the literature, almost every research work and SAGSHP installed system is based on a site-specific configuration and components choice. The impact of the topology used and control strategy on system's efficiency is difficult to determine at the design stage. Moreover, the solar collectors and GHEs types, along with the system set point temperatures (in which deliver heat) and demand profile influence the choice of system's topology. Therefore, the need for a more standardized approach regarding the systems' layout and control is a crucial aspect.

The energy demand of the SAGSHP system was found to be primarily the domestic space heating and hot water, while in a few systems the energy have been used for an agricultural purpose (Ozgener and Hepbasli, 2005b; Mehrpooya, Hemmatabady and Ahmadi, 2015). Regarding the

[3] The SPF_{H2} considers all the electricity consumed by the system in order to deliver the heat at the load, except the auxiliary heat consumption and the circulation pumps of the load.

heat pump's energy source, electricity dominates the market with some exceptions like (Busato, Lazzarin and Noro, 2013) with a heat driven heat pump, while a mixture of 30% Propylene-Glycol and 70% water was found to be the most common heat-transfer fluid.

In Europe, research programs like the IEA Task 44/ A38 (D'Antoni, Fedrizzi and Sparber, 2012) try to create the common ground for wider penetration of the solar assisted systems on the market. According to T44/A38, some of the classification criteria can be the type of heat demand, the heat pump's energy source and the system's topology. The work described by D'Antoni et al. (2012), categorizes the solar assisted systems in three types: a) the in-series connection, in which solar system deliver heat to the load via the heat pump only, b) the parallel concept, where the solar system works independently from heat pump and c) the mixed connection, in which the solar system is capable of delivering heat directly at the load or via the heat pump.

Researchers like Kamel et al. (2015) via their review work are in line with the task 44 results. Three types of SAHP systems configuration have been proposed by Kamel et al. (2015): a) in parallel, when an air source heat pump operates in parallel with a solar system, b) in series, when the solar system can supply the load directly or via a heat pump and c) dual-sourced, when the heat pump's heat source is solar energy and ambient air. These configurations refer to the way which systems supply the building with energy (demand side), and not on the interconnection among the subsystems (heat conversion side).

With the aim to define the SAGSHP systems further, the geothermal and solar energy should both contribute heat to the heat pump. In other words, the direct or the indirect stored solar heat and geothermal energy should be heat pump's evaporator inputs. With the indirect solar heat, the portion of the energy stored into the ground and later used by the GHE is defined. Therefore, the Task 44 via (D'Antoni, Fedrizzi and Sparber, 2012) and (Kamel, Fung and Dash, 2015) layout classifications are not the best way to illustrate the SAGSHP systems interconnection and a new approach is required. In other words, the investigated systems may have a mix of two energy sources before entering the heat pump, which is not definable in both illustrated methods.

In order to obtain a coherence between the layout classification of the systems and the above-mentioned issues, a new way of classification is proposed and illustrated by Figure 2.1 and Figure 2.2. In Figure 2.1 and Figure 2.2 the interconnection between solar field and GHE and heat pump

is shown, while arrows depict the energy flow among systems components. In both configurations, the solar collectors' array can be connected also directly to the heat load, as this is depicted by the dashed line. The direct solar energy utilization is related to solar collector type and systems operation temperature.

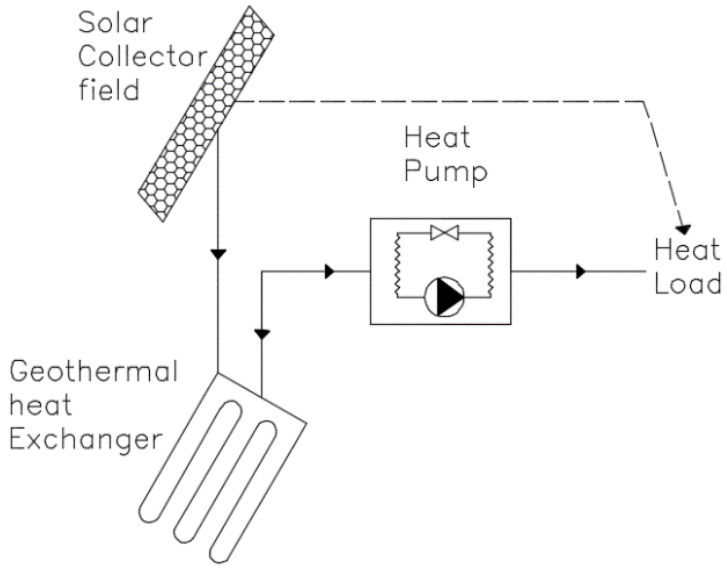

Figure 2.1. SAGSHPS in-series layout.

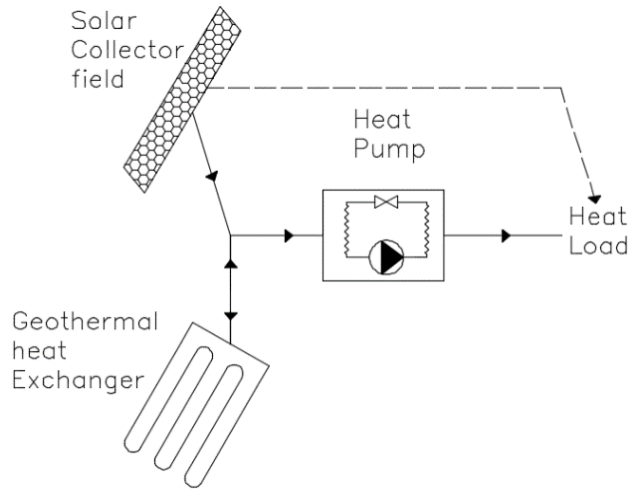

Figure 2.2. SAGSHPS in-parallel layout.

During the heat pump's operation, the two topologies have different energy flow strategy. Regarding the in-series topology, solar heat is used only when solar irradiance is high enough to overcome the control barrier (differential thermostat) and set the system in on mode. Whilst,

in-parallel connection, solar and geothermal energy are independent energy suppliers, while the ability to supply the heat pump's evaporator simultaneously is an advantage.

2.4. Existing solar assisted ground source heat pump systems

The majority of SAGSHP existing systems, which are described by the open literature, are installed in Asia and Europe. The purpose of installed systems is split equally between experimental and real living conditions-based systems. Experimental based systems are made for parametric analyses and are not installed in occupied residences.

In the literature, a variety of components are utilized for SAGSHP systems implementation. Regarding the solar collectors, all the market's available and some retrofitted collectors are chosen and installed. Contrary to solar collectors' variety, GHEs are mainly divided into two categories the horizontal and the vertical configurations (Florides and Kalogirou, 2007). As derived from the review, the majority of GHEs are found to be U-type BHE (66% of the total installed systems) and is followed by the horizontal type (22%), which includes all the GHE installed close to ground's surface and influenced directly by the ambient conditions. The BHEs are installed vertically from few meters to the depths greater than 100 m. The horizonal GHE are installed in trenches at depth between 1 to 2 m. In many cases, more than one BHE can be installed in an array which is called borefield. The GHE together with its assigned soil volume formulates the earth energy bank (EEB). Therefore, each of the stated terms can be used to describe part or the whole geothermal loop.

The types of solar collectors which were found to be utilized on SAGSHP systems, can be distinguished in three main categories: the flat plate collectors (FPC), the evacuated tube collectors (ETC), and the concentrated parabolic collectors (CPC). As regards the PVT collectors, these can be found in any of the above type of collectors, or with totally innovated concepts like this of (Herrando, Pantaleo, et al., 2019; Herrando, Ramos, et al., 2019). The heat transfer fluid of the collectors can be air or liquid and the collectors can be covered with transparent surface or uncovered. Additionally, the PVT collectors can be made by polycrystalline, monocrystalline, and amorphous PV cells. Finally, Figure 2.3 summarizes the energy performance as well as cost information for a wide range of commercially available PVT collectors, as reported in (Herrando, Markides and Hellgardt, 2014) and (Herrando and Markides, 2016). Extended information about the solar collectors and especially the PVTs can be found in (Kalogirou, 2004; Charalambous *et al.*, 2007; Zondag, 2008).

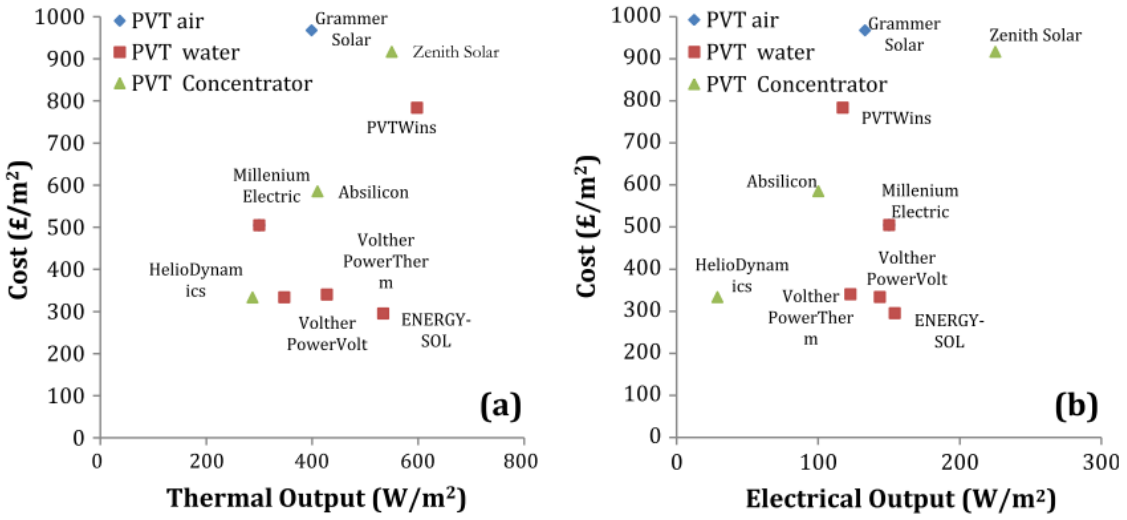

Figure 2.3. Summary of the commercially available PVT collectors: the heat transfer mean is air (blue diamond), water-liquid (red square) and the concentrated PVT collectors are designated by a green triangle. The figure is adopted from (Herrando and Markides, 2016).

An important device on SAGSHP systems analysis is the heat pump, which mostly refers to an electrically driven heat pump, with the R22 being the widely used refrigerant. Finally, the majority of systems are equipped with fan-coils or underfloor heating systems with few exceptions which employ heat radiators (Loose and Drück, 2014; Bakirci *et al.*, 2011; Stojanović and Akander, 2010).

2.4.1. Experimental SAGSHP systems

Of the 22 systems reviewed in this study, 11 are built as experimental installations, with the aim to assist SAGSHP systems feasibility studies. Moreover, most of the experimental based systems are built in China as part of the country's effort to increase the solar energy diffusion in the space heating and DHW market. The experimental based installations are focused on investigating control strategies along with the comparison among other types of heat pump systems. The main aims and results from the experimental based studies are summarized in Table 2.1.

*Table 2.1. Experimental based studies[4]*indicates that the work has also a simulation part, **Based on illustration needs*

Source	Aims	Results**
(Xi *et al.*, 2011)	To compare four different energy management strategies	The most efficient was found to be the parallel operation mode of the solar and geothermal subsystems.
(Wang *et al.*, 2009)*	To evaluate the systems efficiency. Therefore, four different control modes were set regarding the energy flow for space heating and cooling.	From 15-day data collection, the system's and heat pump's COP were calculated to 3.75 and 5.27 respectively.
(Yang, Sun and Chen, 2015)	A comparative work between the GSHP and SAGSHP systems for diverse evaluation based on three operational strategies.	SAGSHP system was found to be the most efficient while the mode with the solar energy to be stored into soil via the BHE during daytime for evening consumption was found to fits better on a residential energy demand profile.
(Dai *et al.*, 2015)	To evaluate SAGSHP systems via different operational modes and energy management among system's components.	The in-series connection of the solar collectors with the GHE was the most efficient.
(Bi *et al.*, 2004)	To evaluate the SAGSHP feasibility against the SAHP and the GSHP.	The GSHP system was more efficient than the joined operation of solar and ground source heat pump.
(Bakirci *et al.*, 2011)	To evaluate SAGSHP systems for cold and high-altitude places.	SAGSHP systems were found to be an effective mean for space heating in cold climates with high annual solar irradiation.
(Esen, Esen and Ozsolak, 2017)	To evaluate the coil shaped horizontal GHE in vertical and horizontal position.	The experimental results were utilized for system's model formulation. The system's SPF was found at 2.88 for the spiral loop be installed flat and at 2.34 for vertically.
(Verma and Murugesan, 2017)	To evaluate a built SAGSHP system for India's climate.	The solar system contributed to increase the COP by 23% and this had a vital role on systems feasibility.
(Stojanović and Akander, 2010)	An SAGSHP experimental system was built for ENDOHOUSING concept in Sweden as a pilot project.	The system's SPF for 2007 was calculated to 2.09 and the SPF_{HP} to 2.85.
(Yang, Zhang and Liang, 2018)	With a SAGSHP system built in a University campus, a parametric analysis was conducted.	The parallel operation of the geothermal and solar system found to be the most efficient with 3.61 COP and 51.5% solar system efficiency.
(Naranjo-Mendoza *et al.*, 2019)	The experiment was conducted with the aim to evaluate the systems operation.	The system may be a solution for a very efficient Dwelling. The heat pump's seasonal COP was calculated at 2.51 after 19 months of operation.

[4] During the literature review, a variety of energy performance factors were traced. Many works utilize the COP (Coefficient of Performance) and other the SPF (seasonal performance factor). There is no homogenic use of metrics, therefore in what follows the metric proposed by the sources is used to illustrate the results.

2.4.2. Review on systems based on real living conditions

Installations like the one described by Nicholson-Cole (2012a) have showed that a SAGSHP systems can be a retrofit solution for space heating and DHW. After the first two-years of operation, the system became inefficient due to soil's imbalanced discharge and small solar collectors' area. Therefore, more solar collectors were added (Nicholson-Cole, 2012b) and the system's COP improved from 2.6 to 4.4. A research focused on a newly built detached house equipped with SAGSHP was conducted by Wang et al. (2010). The system's objectives were to supply the house with space heating, cooling and DHW. Therefore, the soil's heating-charging period by the solar collectors was set not to conflict with the heat pump's space cooling operation mode. After two years of operation, the heat pump's COP was calculated at 4.29.

In Savoy-France (Trillat-Berdal, Souyri and Fraisse, 2006), a SAGSHP system's operation was recorded for eleven months. The results showed that the COP_S and COP_{HP} reached up to 3.35 and 3.75 respectively. The authors also highlight that the control strategy along with the parasitic energy are crucial aspects about the systems feasibility. In addition, the system's solar fraction was calculated to be 0.68 and the 34% of this portion was injected into the soil via the BHE. As second part of their work (Trillat-Berdal, Souyri and Achard, 2007), a TRNSYS model was built in order to evaluate the systems feasibility.

One of the six investigated systems built with WPSol project was illustrated and analyzed (Loose and Drück, 2014). The SAGSHP system was innovated regarding the solar collecting area which was made by aluminum tiles and the GHEs which were shaped as baskets. System's responsibility was to provide space heating and DHW in a single-family house (five persons) located in Bavaria (Germany). The system found capable of achieving SPF of 3.46 and was more environmentally friendly than systems fired with NG and Oil.

One of the approaches which employ PVTs as solar collectors was described by Bertram et al. (Bertram, Glembin and Rockendorf, 2012). A PVT based SAGSHP system with three homocentric BHEs was installed for a dwelling in Frankfurt. Along with the PVTs a PV was installed in order to conduct a comparison between the PVT's to PV's electricity yield. After two years of data collection, the results showed that the PVT managed to overperform of PV by 4%, while the SPF_S was calculated at 4.2 and the SPF_{HP} at 4.5. Another pilot work based on PVT utilization was done by Wright et al. (2014), which describe a newly developed house based on zero carbon emission restriction. The SAGSHP system was equipped with PVTs and a novel very shallow borefield. The

GHE was placed underneath the dwelling in order to constrain the heat losses, but there was insufficient monitoring to determine system performance.

Regarding the large-scale projects, it is difficult to completely rely on the SAGSHP concept, and back-up energy systems required. The necessity for back-up systems and the complex design make large systems to distinct from single dwelling size systems. The first solar assisted storage system with aquifer in Germany was analyzed by Schmidt & Muller-Steinhagen (2004). The system was built to supply space heating and DHW to a newly constructed district with 108 apartments with total heating area 7000m^2. After four years recorded data, the systems obtained a solar fraction of 0.49. Moreover, a SAGSHP system installed on a University campus was investigated by Liu et al. (2016), the COP_s was estimated, from energy bills, to be between 2.97 and 3.09. Then, a TRNSYS model was formulated to further investigate the system's feasibility on transient season (autumn and spring).

A SAGSHP system installation at a school in the north of Italy was illustrated by Busato et al. (2013). The system was equipped with a gas fired absorption heat pump along with a solar collector array and a borefield, while further evaluation via TRNSYS was conducted. By analyzing two years recorded data, the gas utilization efficiency (GUE) was calculated to be 1.773, while 35.7% of the energy demand was covered by solar and geothermal energy. The GUE is defined as the ratio of energy output to energy provided by the gas in a gas fired absorption heat pump.

To summarize the review on existing SAGSHP systems, the uniqueness of each system, along with the lack of long period data, make the conclusion difficult. No line can be drawn regarding the optimum topology, components used or implemented control strategy. The interest in SAGSHP systems is growing rapidly as can be observed from the conducted studies and is justified by relatively high systems' efficiency. In many cases, simulations are being used to investigate systems modifications or to estimate their efficiency through feasibility studies.

2.5. Installed Systems Analysis

In the literature, almost all the SAGSHP systems were found to have particular features regarding their topology, components used, design strategy, etc. By keeping in mind the above conclusion, an analysis based on the main systems' characteristics was conducted. In more detail, the relation among the systems' topology, use components and GHE length to collectors' area, with the efficiency is defined. The current investigation is based on Table 2.2, which summaries the key parameters from analyzed SAGSHP systems.

According to Table 2.2, twenty-two installed SAGSHP systems have been investigated. As universal information of the average values derived from data, the SAGSHP systems are capable to achieve, an average COP_S of 3.18 and COP_{HP} of 3.75. The average difference between the system and heat pump efficiencies, was calculated to 16%. This portion belongs to missed efficiency and to parasitic energy, thus a more sophisticated control strategy, with components to be sized for optimum operation may reduce this gap.

Table 2.2. Installed SAGSHP systems (experimental and real-living conditions)
**indicate that the system is also theoretically evaluated*
***Indicate that the value is calculated as SPF*

Location	**COP_S**	**COP_{HP}**	**Type of collectors and area**	**BHE type and length (m)**	**Layout type**	**Source**
Tianjin China	-	2.78	FPC / 5m^2	Spiral Horizontal 60m	not provided	(Bi *et al.*, 2004)
Rostock Germany	4.5	4.1	FPC / 980m^2	Aquifer 30m deep	In-parallel	(Schmidt and Muller-Steinhagen, 2004)
Savoy France	3.35-3.75	-	FPC/ 12m^2	U-BHE 2x90m	In-parallel	(Trillat-Berdal, Souyri and Fraisse, 2006); (Trillat-Berdal, Souyri and Achard, 2007)*
Izmir Turkey	-	-	FPC / 1.82 m^2	U-BHE 50m	In-series	(Ozgener and Hepbasli, 2005a)
Tianjin China	5.27		FPC / 25m^2	Dual U-BHE 50m	In-parallel	(Wang *et al.*, 2009)*
Sandviken Sweden	2.09**	2.85**	uncovered FPC / 42.5m^2	Horizontal area 52m^2	In-parallel	(Stojanović and Akander, 2010)
Turkey	2.8**	3.2**	FPC	U-BHE 2x53m	In-series	(Bakirci *et al.*, 2011)
China	-	4.57	ETC / 13.6m^2	U-BHE 5x21m	In-series	(Xi *et al.*, 2011)
Frankfurt Germany	4.2**	4.5**	PVT 39m^2	Homocentric BHE 3x75m vertical	In-series	(Bertram, Glembin and Rockendorf, 2012)*
North Italy	GUE 1.47		FPC/ 50m^2	U-BHE 6x125m	In-parallel	(Busato, Lazzarin and Noro, 2013)

Location	COP_S	COP_{HP}	Type of collectors and area	BHE type and length	Layout type	Source
Dalian China	3.54-4.93		ETC / 10.4m^2	U-BHE (9x50+1x25+ 1x75)m	Mixed	(Dai *et al.*, 2015)
Elazığ Turkey	2.34-2.88	2.91-3.55	FPC	Horizontal at 2m deep 2x15m coil shaped	In-parallel	(Esen, Esen and Ozsolak, 2017)*
Leicestershire UK	-	-	PVT/ 38m^2	Shallow in 1.5m deep with 56 x U-BHE type	In-series	(Bateson, 2014)
China	4.29		FPC/ 50m^2	Dual U-BHE 12x50m	In-series	(Wang *et al.*, 2010)
Nottingham UK	4.4-4.8		Mixed	U-BHE (2x48)	In-series	(Nicholson-Cole, 2012a)
Nanijing China	2.67	-	ETC	U-BHE 2x30m	Mixed	(Yang, Sun and Chen, 2015)
Tianjin China	2.97-3.09		ETC /1500m^2	U-BHE 580x120m	In-parallel	(Liu, Zhu and Zhao, 2016)*;(Zhu, Wang and Liu, 2015)
Roorkee India	2.37-2.47-2.51		CPC	Shallow at 3.5m and deep 8.5m	In-series	(Verma and Murugesan, 2017)
Yangzhou China	3.61		FPC/27.75 m^2	U-BHE (2x8x80)	In-parallel	(Yang, Zhang and Liang, 2018)*
Bavaria Germany	3.46**	3.77**	Alum-tiles 35m^2	4 basket-shaped (shallow)	In-parallel	(Loose and Drück, 2014)
Leicestershire UK	-		PVT / 10.5m^2	Shallow in 1.5m deep with 16 x U-BHE type	In-series	(Naranjo-Mendoza, Greenough and Wright, 2018); (Naranjo-Mendoza *et al.*, 2019)

SAGSHP system highest COP_S and COP_{HP} are found at 4.29 (Wang *et al.*, 2010) and at 5.74 (Dai *et al.*, 2015) respectively, while the lowest COP_S and COP_{HP} are found to be 2.09 (Busato, Lazzarin and Noro, 2013) and 2.51 (Verma and Murugesan, 2017) accordingly. Meanwhile, an even lower COP_S of 1.47 (Busato, Lazzarin and Noro, 2013) for a heat driven HP was found, but heat driven heat pumps cannot be compared with the compressor based systems due to their limitation for

high COP and different energy source. Finally, the measurements' and COP_S calculations' uncertainty are found as average values between 6.81% (Xi *et al.*, 2011) and 7.6% (Bakirci *et al.*, 2011) respectively.

2.5.1. Topology

Based on analysis which takes place on section 2.3, a SAGSHP system can be built with a series or parallel layout. Data from Table 2.2, show that the installed systems are almost equally built with both layouts. In more detail, the two configurations are consisted from nine systems in series and ten systems in parallel topology, while two systems are found to be installed in mixed configuration and one is undefined. The systems with mixed configuration were built to investigate the topology's impact on feasibility (ability to change configuration). Moreover, the in-series topology has an average COP_s of 3.76 and COP_{HP} 3.90, while the in-parallel option is 2.82 and 3.58 respectively. Finally, it is important to mention that, the above performance data are indicative, and it is not capable to draw any conclusion regarding the relation of topology and efficiency due to non-uniform systems set-up.

2.5.2. Solar collectors' area to GHE Length ratio

This section illustrates the potential relations between the solar collecting area with GHEs' length, using the ratio (CBR) (m^2 m^{-1}), based on finding listed in Table 2.3. knowing only the length of a GHE does not characterize its thermal properties, the comparison is only indicative. Furthermore, another useful metric for systems evaluation is the storage capacity (SC), which depicts the ratio of the heat storage volume per energy harvesting equipment. Due to lack of data from the literature, in current state only the CBR is illustrated, and the SC is going to be defined and illustrated analytically in the "Methodology" Chapter 3.

Table 2.3. Indicative outlet temperature and efficiency for various types of solar collectors. (Zondag, 2008), ;(Hossain *et al.*, 2011)*;*(Kalogirou, 2004)*;*(Sakellariou and Axaopoulos, 2017) **Thermal efficiency*

Solar collector groups	Indicative outlet temperature range (°C)	Indicative efficiency
Uncover PVT* and solar collector	10-50	0.50*
Covered Flat Plate Collectors FPC	30-80	0.80
Evacuated Tubes and Concentrated Parabolic solar Collectors ETC and CPC	For ETC 50-200 and for CPC 60-240	For ETC 0.82

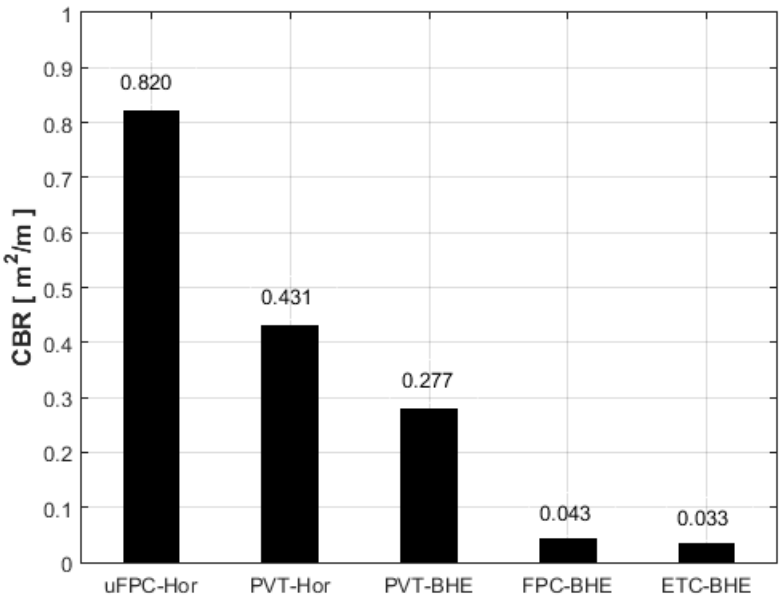

Figure 2.4. The ratio of solar collectors' area to GHE length for a variety of pairs, derived from Table 2.2. Where: FPC flat-plate solar collector, uFPC uncovered solar collector, PVT photovoltaic and thermal solar collector, ETC Evacuated Tubes solar Collector, Hor Horizontal GHE and all GHE installed above 3m deep in the ground, BHE Borehole Heat Exchanger (U or Homocentric type).

In Figure 2.4, the findings are shown regarding the pair of the GHE with the used solar collectors. The investigated solar collectors can be split in three groups regarding their ability to offer useful heat with particular range of outlet temperature and efficiency. Table 2.3 lists the indicative outlet temperatures and efficiencies for various types of solar collectors. Therefore, in Figure 2.4, solar collectors capable of producing higher temperatures, such as the evacuated tube, are able to recharge the soil's temperature for a larger BHEs (0.033 m^2/m), contrary to PVTs which their ratio is 13 times larger. Moreover, the higher the temperature stored or transferred from collectors to GHE, the higher the heat losses from the soil to the surround. Thus, low temperature systems are more likely match with a shallower GHE due to soil's influence from the ambient conditions. Finally, the BHE tend to be paired with ETC or flat plate collectors, while the horizontal and shallow GHEs are found to match with PVTs and uncovered collectors. The term 'shallow' in this analysis defines GHEs with depth less than 3m. Finally, the results illustrated in Figure 2.4 and analyzed above are in line with the results obtained via a study made by Reda (2015).

2.6. Literature review on theoretical approaches

The main experimental studies are categorized and summarized above, while Table 2.4 lists the theoretical approached research works with their basic objectives and results.

*Table 2.4. Summary of simulation-based projects *indicates that the work is based on an existing system, **Based on paper's illustration needs.*

Region	Major work Objectives**	Outcomes**	Method	Source
Zurich Switzerland	To investigate the LowEx concept with an innovated PVT based SAGSHPS.	The SFP_S estimated to 6.0	TRNSYS	(Baetschmann and Leibundgut, 2012)
Bialystok (Poland) Bolzano (Italy) Chengde (China) Kaunas (Lithuania) Montreal (Canada) Stockholm (Sweden)	To evaluate the SAGSHPS against the GSHPS for six distinctive cold climate zones.	The solar collector's addition obtained a positive effect on efficiency for all studied systems. A substantial reduction of BHE required length due to solar collectors' contribution on the system is estimated.	TRNSYS	(Emmi, Zarrella, De Carli, *et al.*, 2015);(Emmi, Zarrella, Carli, *et al.*, 2015)
Beijing China	The major aim was to design the systems in order to stop the HP's operation during transition seasons.	The proposed strategy can reduce the electricity consumption by 20.8%.	TRNSYS	(Si, Okumiya and Zhang, 2014)
Canada	To quantify the impact of the solar collectors' addition to GSHPS and illustrate a method for BHE length calculation for SAGSHPS.	The lowest energy consumption was the scenario with separated solar and ground sourced systems.	TRNSYS	(Eslami-nejad *et al.*, 2009b)
Montreal Canada	An approach to analytically model and validate a double U-BHE for SAGSHP with two separate circuits.	SAGHSPS does not have any great potential to reduce the consumed energy, but the great benefit is this of BHE length reduction.	-	(Eslami-Nejad and Bernier, 2011)
Harbin China	To examine an analytic model of the SAGSHPS with phase change material as additional storage for eight different operation modes.	The phase change material managed to improve the SAGSHP system's COP from 3.03 to 3.28.	MATLAB	(Han *et al.*, 2008)
Canada	To study the feasibility of SAGSHPS for six Canadian cities.	By adding 6.81m^2 of solar collector the required GHE length reduced by 15%.	TRNSYS	(Rad, Fung and Leong, 2013)

Region	Major work Objectives**	Outcomes**	Method	Source
Lund Sweden	To qualify the advantage of using solar collectors on a GSHP and the best design strategies.	For BHE deeper than 100m the operational sequence does not significant influences the COP_S.	TRNSYS	(Kjellsson, Hellström and Perers, 2010)
Shanghai Jiao Tong University China	The work's aim was to study the SAGSHPS feasibility for the Green Energy Lamp.	The solar collector addition on the GSHPS managed to reduce the consumed electricity by 26.1%.	TRNSYS	(Thorshaug Andresen and Li, 2015)
Beijing China	To evaluate the operation of the SAGSHPS for 20 year-period.	The SAGSHPS after a 20year simulation found to overperform the GSHPS by 26.3%.	TRNSYS	(Xi, Lin and Hongxing, 2011)
Qingdao China	To evaluate the alternative operation between the SAGSHP, SAHP and the GSHP.	The SAGSHPS found more efficient from GSHP by 14.5% and 10.4% with and without buffer tank respectively.	-	(Yang, Shi and Dong, 2006)
Canada	To illustrate a new energy storage strategy in Boreholes Thermal Energy Storage.	The low temperature concept managed to increase the solar collectors' efficiency by 35% and the storage losses were reduced substantial.	TRNSYS	(Chapuis and Bernier, 2009)
Netherland	To study the impact of the PVTs on the GSHP system.	PVT fulfill the 96% of the consumed electricity and the 83% heat extracted from the ground.	TRNSYS	(Bakker *et al.*, 2005)
Tianjin, China	A comparative work related to compare different SAGSHPS performance against the GSHPS and hybrid proposed SAGSHPS.	A SAGSHP and a GSHP systems cooperate in order to balance the air-conditioning in a large-scale project.	TRNSYS	(Wang *et al.*, 2012)
Korea	To investigate the ability of Fuzzy Control technique against the on-off control.	With the Fuzzy Logic control the system's efficiency was increased by 18.3% contrary to the on-off control.	Fuzzy control	(Putrayudha *et al.*, 2015)
Frankfurt Germany	To evaluate the long period effect of PVTs on Heat Pump's inlet temperature.	Improvement on the SPF_S by 0.56 and the consumed electricity reduced by 15%.	TRNSYS	(Bertram, Glembin and Rockendorf, 2012)*
Cardiff UK	A mathematic model is developed in order to analyze the systems' operation under various scenarios.	The daily system's COP was estimated to 5.	MATLAB	(Foulds, Abeysekera and Wu, 2017)

Region	Major work Objectives**	Outcomes**	Method	Source
Tianjin China	To intensify the possibility of energy storage on transient seasons. To find the effect of solar energy storage on systems performance.	The results shown that is feasible for the SAGSHPS to store energy and meet the demand on autumn.	TRNSYS	(Liu, Zhu and Zhao, 2016)*(Zhu, Wang and Liu, 2015)
Savoy France	To evaluate the system's configuration economically. Energetically and environmentally.	Determine the optimum configuration for the system.	TRNSYS	(Trillat-Berdal, Souyri and Achard, 2007)*
Europe	To compare the SAGSHPS against GSHPS for 19 European cities.	The SAGSHPS have better feasibility on cold climates with high solar irradiation.	Excel	(Girard *et al.*, 2015)
Tianjin China	To investigate the systems performance for longer period.	The buffer tank managed to increase the systems efficiency, while the suggested volume to collectors' area ratio estimated to 20-40 L/m^2.	Visual Basic	(Wang *et al.*, 2009)*
Europe	To compare the use of SAGSHPS against a GSHPS for 8 European climates.	The ideal climate for SAGSHP estimated to be this of the Alpine region.	Polysun	(Carbonell, Haller and Frank, 2014)
Finland	To evaluate the control strategy for a variety of paired components.	The efficiency of the systems in different topologies found to be related with the operational and external system's temperature.	TRNSYS	(Reda, 2015)
Montreal Canada	An approach to analytically model and validate a double U-BHE for SAGSHP with two separate circuits.	SAGHSPS does not have any great potential to reduce the consumed energy, but the great benefit is this of BHE length reduction.	-	(Eslami-Nejad and Bernier, 2011)
India	To find the optimum collectors' area and BHE length.	The Taguchi method found to be more reliable than Utility method for SAGSHPS design.	Taguchi and Utility methods	(Verma and Murugesan, 2014)

Region	Major work Objectives**	Outcomes**	Method	Source
Toronto Canada	Borefield simplified nodal model was created with the aim to conduct parametric analyses on three type of buildings.	The energetically optimum collectors' area was not the same with the financial optimum. Also, for buildings with heating to cooling ratio close to 1.2, there is no need for solar collectors' addition.	MATLAB	(Fine *et al.*, 2018)
Belluno Italy	A comparative simulation was done with the aim to identify, if the solar or geothermal energy is most efficient for a heat driven and an electric power heat pump system.	The simulation's results shown that the mixed source system is the most efficient for both cases, heat and electric driven HP.	TRNSYS	(Busato, Lazzarin and Noro, 2015)*
Emmerthal Germany	A comparative discussion took part regarding the HP's operation and performance under varying operation conditions.	The results shown that the HP's evaporator flow rate does not influence significantly the COP_{HP} contrary to the T_{source} which found to be more important. High T_{source} drops the HP's Exergetic coefficient. The dynamic operation of the HP should be considered.	TRNSYS	(Pärisch *et al.*, 2014)
Stockholm Sweden	A multiparametric analysis was made with the aim to illustrate the influence of the PVTs addition on the energetical and economical aspect of a GSHP system, for a large multi-family building.	The results showed that with the PVTs addition on the GHSP system, a reduction of 18% on the GHE length can be obtain, along with spacing drop among them at 50% and all that by maintaining an equivalent SPF with the initial GSHP system.	TRNSYS	(Sommerfeldt and Madani, 2019)

2.6.1. Available software

Regarding the studies listed in Table 2.4, TRNSYS (Klein, 2010) software dominates the researchers' preference, while a second group of projects is based on systems investigation via mathematical analysis or alternative software. In more detail, from the twenty-seven investigated research works, nineteen of these utilize TRNSYS (70%) and the minor portion is comprised by a variety of methods. Finally, just few works were found to be partly validated via

experimental data for existing systems (Si, Okumiya and Zhang, 2014; Rad, Fung and Leong, 2013; Pärisch *et al.*, 2014).

2.6.2. Comparative simulations

Works like Girard et al. (2015) and Carbonell et al. (2014) evaluate SAGSHP systems performance against GSHP systems for a variety of European regions. SAGSHP systems were found to be suitable for cold climates with high annual solar irradiation, where the dominant thermal load must be space heating. The locations which are matched with (Girard *et al.*, 2015) and (Carbonell, Haller and Frank, 2014) works' results, are the Alps region, and the mountains across the north Mediterranean sea. Additionally, Girard et al. (2015) concluded that for the highest latitude (Bergen 60.30^{o}N), a COP_S of 5.8 and 4.4 for SAGSHP and GSHP were achieved respectively, while for the most southern location (Granada 37.18^{o}) the figures were 4.3 and 5.1 correspondingly. Finally, Carbonell et al. (2014) concluded that the SAGSHP system outperforms the GSHP when the energy demand is relatively large.

Rad et al. (2013) compared solar assisted and conventional GSHPs for six Canadian cities, while Emmi et al. (2015) compared the systems for six distinctive cold zones. Regarding Rad et al. (2013) outcomes, Vancouver had the greatest feasibility among the investigated cities, while the solar collectors found to devastate the systems efficiency during the space cooling season for all cases. Contrary to (Rad, Fung and Leong, 2013), Emmi et al. (2015) predict that the solar collectors' addition on the systems will increase the systems efficiency by 10% for all locations. Also, in their second work (Emmi, Zarrella, Carli, *et al.*, 2015) a significant reduction (70-80%) on BHE length was estimated due to heat injection in the ground. The above results are in line with Kjellsson et al. (2010) simulation work. They conclude that by adding solar collectors on a GSHP system has a positive effect. The solar collectors work beneficial by increasing the average ground temperature, and decreasing the electrical energy consumed by reducing the heat pump operation time, which resulting in extra reduction on the net heat extraction from the ground.

Eslami-Nejad & Bernier (2011) compared SAGSHP systems and conventional GSHP systems for two different GHE types, the first was a conventional singly U-BHE and the second was a double U-tube BHE. The second BHE design was based on the idea to operate with two separated heat removal fluids cycles, one for charging from solar system and the other for the heat removal from the ground. The twenty-year simulation results, based on Canadian climate data, showed that the SAGSHP system has low potential to save electricity. The results showed only 3.5% and

6.5% reduction for first and second scenarios respectively. However, the significant benefit was 17.6% and 33.1% less BHE length for the two scenarios respectively.

Moreover, a TRNSYS simulation work, based on a Green Energy Lab SAGSHP system was conducted by Thorshaug Andresen & Li (2015). The results showed that, if solar collectors are installed with the GSHP, the system's electrical energy consumption will be decreased by 26.1%. Moreover, the COP_{HP} was estimated to 4.5 for solar assisted and 4.2 for the conventional GSHP system. Furthermore, Xi, Lin, et al. (2011) found that after a twenty-year simulation, the SAGSHP system efficiency improved by 26.3% compared to a conventional GSHP system. Finally, Yang et al. (2006), performed a simulation for an innovative SAGSHP system with a buffer tank, where the COP was estimated to be 14.5% and 10.4% higher than the GSHP, with and without buffer tank respectively.

2.6.3. Control Strategy and energy management

In the literature, many simulations have been conducted on the SAGSHP systems' energy management and optimization. A strategy which can utilize the stored energy from the GHE directly for space heating is proposed by Q. Si, M. Okumiya, & X. Zhang (2014) and Thorshaug Andresen & Li (2015). It is estimated that the proposed strategy can reduce the annual consumed electricity by 20.8% (Si, Okumiya and Zhang, 2014). Nevertheless, the soil temperature has to be relatively high in order to be applicable directly on the heating mean, also the proposed method matches more on transition season with mild weather and available solar irradiation. Furthermore, Kjellsson et al. (2010) proposed a strategy which consumes the solar energy during summer to fulfill the DHW demand and in winter to be used as a ground's recovery energy source. The proposed method is in favor with soil's natural recovery technique during the non-heating season and the direct utilization of the solar energy.

Eslami-nejad et al. (2009b) conducted a simulation study, firstly to quantify the impact of the addition of solar collectors on a GSHP system, and secondly to evaluate the energy efficiency for a novel SAGSHP system. As part of their initial investigation, a BHE with two independent U-type tubes sharing the same borehole was proposed. The lowest energy consumption scenario was found with separate solar system for DHW, and GSHP system for space heating. Although in Canada heating is dominant, the demand for space cooling in summer is also substantial. Hence, the solar system loses its ability to recharge the ground temperature due to opposing operation with the heat pump. A second work based on the proposed BHE was conducted (Chapuis and Bernier, 2009), with the basic idea to maintain a low storage temperature for two reasons; firstly

to mitigate the storage heat losses, and secondly to improve the solar collectors' efficiency. The outstanding outcomes regarding the low storage temperature concept were that the collectors' efficiency increased by 35% while the storage heat losses dropped substantially.

Han et al. (2008) formulated a mathematical model of a SAGSHP system combined with phase change material (PCM) for additional energy storage. The system's operation was split in eight modes, while the parallel topology Figure 2.2 was chosen. Via simulations, the systems with the integrated PCM gave the higher COP with 3.28, compared to 3.03 and 2.16 for SAGSHP and GSHP systems respectively.

Finally, an alternative approach was used by Putrayudha et al. (2015) based on Fuzzy Control technique applied on a SAGSHP system. The results showed that the Fuzzy Control technique managed to increase the systems efficiency by 18.3% contrary to the on-off strategy. Although the proposed control system achieved better results than the conventional on-off, the site-specific dependency and the high initial cost investment are the main drawbacks for its implementation.

2.6.4. Economic studies

Regarding the financial investment for a SAGSHP system, a few research studies have been done. Rad et al. (2013) and Girard et al. (2015) conducted an in-depth financial comparison between the solar assisted and the conventional GSHP systems. Girard et al. (2015) found that the payback period for the most north region (Bergen, Norway) of Europe is 8.5 years, contrary to most south one (Granada Spain) which is 23 years. Moreover, Rad et al. (2013) concluded that SAGSHP systems are slightly more expensive than the GSHPs. Lastly, Bakker et al. (2005) did an investigation regarding the PVT's installation cost on a SAGSHP systems against FPC and PV together for the same energy annual yield. The results showed that PVTs' cost is slightly increased (6%) contrary to flat plate collectors and PV together, meanwhile the required installation area for PVTs estimated 25% less than the combined solution.

N. Sommerfeldt and H. Madani (2019), found that, if PVT collectors are connected in-series with the borefield (for a large multi-family building), a reduction on the size of the GHE can be achieved, compared to a GSHP system. The decreased system's physical size, contrary to a GSHP system can be translated into a reduction on initial capital investment to buy the land for the building and the system installation. Additionally, via the analysis, the PVT-GSHP system was

estimated as a less economic feasible contrary to a GHSP paired with PV array, and depends on the land price to determine which of two is more suitable for the location.

Finally, (Busato, Lazzarin and Noro, 2015) did a comparative work in order to found the most economically viable system with the lowest primary energy ratio (PER, energy imported divided by the energy demand) for a north Italian province. The results showed that the combine operation of solar and geothermal energy is the most efficient and economically viable. It is proposed that for a SAGSHP system with a fixed budget, the GHE can be sized in order to not let the temperature drops lower than -2^{o}C to enter in the HP's evaporator, and the remaining capital to be used for installing solar collectors.

2.7. Discussion

Regarding the existing systems, almost all were found to be installed with a unique pair of solar collectors and GEHs. Most systems were designed for dwelling sized loads, while few systems have been installed to service large buildings or districts (Busato, Lazzarin and Noro, 2013);(Liu, Zhu and Zhao, 2016); (Yang, Zhang and Liang, 2018). Moreover, the installations reviewed are split between Europe and Asia with China to be the most active country. Meanwhile, the system layout is separated between the in-parallel and the in-series connection of the solar collectors with the GHE (2.5.1). System topology plays a significant role on the system's efficiency and control strategy, while the ratio of the required GHE to solar collectors' area LAR can be a design parameter but only related to a specific energy demand, components pairing, environmental conditions and soil thermal properties.

According to data from the existing systems, the SAGSHP systems are capable of achieving maximum COP_S of 4.29 (Wang *et al.*, 2010) or SPF_S of 4.2 (Bertram, Glembin and Rockendorf, 2012), while the lowest value was recorded for COP_s to be 2.09 (Stojanović and Akander, 2010). The ratio of COP_s between the most efficient to the least is therefore 2.20 which depicts the differences on the equipment choices and control strategies among the designers. Moreover, from data analysis an average portion of 16% efficiency drop was found to be related with system's parasitic energy. This efficiency drop can be reduced by selecting more efficient circulation flows and pumps and using a simple layout with less electrically driven valves.

From the investigated SAGSHP systems, the most interesting combination of components was found to be that of PVT based systems (Bateson, 2014; Bertram, Glembin and Rockendorf, 2012). Due to PVT's ability to cogenerate electricity and heat, a SAGSHP system equipped with PVTs

can be a good solution for energy efficient buildings. Moreover, the PVT's absorber decrease the cell's temperature and as a consequence the electricity yield is increased compared to a conventional PV panel, especially, for locations with high annual solar irradiation (Bertram, Glembin and Rockendorf, 2012; Sakellariou and Axaopoulos, 2015; Sakellariou and Axaopoulos, 2017). Furthermore, for a given annual electricity and the heat yield, the required PVT installation area is substantially smaller than the area from the combined installation of solar collectors and PV panels (Rad, Fung and Leong, 2013). Additionally, the generated electricity from PVTs in some cases can be used for self-consumption (Schwarz *et al.*, 2018). Finally, the uncovered PVT is ideally paired with systems based on summer GHE's soil heat recovery schedule with shallow GHE (Loose and Drück, 2014; Reda, 2015).

The energy management and the control strategy are among the topics which are discussed in both experimental and simulation-based studies. From the existing systems research, works like (Yang, Sun and Chen, 2015; Dai *et al.*, 2015; Verma and Murugesan, 2017) illustrate the effect of the operation mode on the system's performance. The need for harvesting the sun during the daytime and consuming the stored heat via the GHE at night is shown, while this tactic is suitable for sunny days with cold nights. Also an approach is to use the solar heat for DHW on summer, while in winter the solar field can be used to increase the soil's temperature or to provide heat on the HP (Loose and Drück, 2014; Kjellsson, Hellström and Perers, 2010). The above approach is enhanced by two facts, firstly the natural soil's temperature recovery during summer and the secondly the heat loss which is applied as penalty on the stored heat.

Theoretical based studies are more suited for investigating different control strategies. Simulations like (Reda, 2015; Si, Okumiya and Zhang, 2014; Kjellsson, Hellström and Perers, 2010; Han *et al.*, 2008) are done to evaluate the best energy management for a variety of SAGSHP system configurations. The convenience to investigate alternative scenarios along with a variety of configuration are characteristics of simulation-based works. Unfortunately, it is difficult to draw any conclusion regarding the optimum control strategy and the energy management due to the wide variety of layouts and component combinations.

The initial investment for a SAGSHP systems was found to be slightly higher than that required for a conventional GSHP (Bertram, Glembin and Rockendorf, 2012; Rad, Fung and Leong, 2013). The relative studies are influenced by system topologies, energy demand and locations, while there are studies which illustrate the energy demand interaction with systems feasibility (Carbonell, Haller and Frank, 2014). The reduction on the required GHE size was found to be the

normalizer for the initial cost investment between the SAGSHP and GSHP systems (Emmi, Zarrella, Carli, *et al.*, 2015). Based on comparative simulation studies, solar assisted systems perform better than conventional GSHP for almost all locations where the space heating is the dominant operation. Except Canada due to substantial cooling loads during summer which engages the HCR as decisive criterion for SAGSHP systems implementation (Fine *et al.*, 2018).

TRNSYS and a variety of software have been employed by researchers to conduct feasibility studies on SAGSHP systems. In line with the existing systems, the theoretical approaches are split between Asia and Europe with Canada as a minor third part. The major drawback for SAGSHP systems penetration in the Canadian market was found to be the dual operation of the HP, for cooling and space heating (Eslami-nejad *et al.*, 2009a; Chapuis and Bernier, 2009). The cooling mode conflicts with the solar heat injection during summer, therefore a more sophisticated layout for direct use of solar heat during this period is required.

The theoretical approaches are mainly based on systems investigation using TRNSYS (70%) while the remainder is split among a variety of software. TRNSYS was found to be the optimum tool for SAGSHP systems investigation, with existing components (TYPES) and useful toolboxes. Although TRNSYS was found to be a reliable tool for systems feasibility study, no work have been made to validate the predictions against real SAGSHP systems' data (Report, Engineering and Station, 2001). Furthermore, the alternative approaches are well developed analytically and can be used for system's first stage design, but again the validation of the methods found is yet to be done (Report, Engineering and Station, 2001; Raab, Mangold and Müller-Steinhagen, 2005).

Theoretical approaches, which are devoted to evaluate the SAGSHP systems for a variety of locations (Bakirci *et al.*, 2011; Emmi, Zarrella, De Carli, *et al.*, 2015; Girard *et al.*, 2015; Carbonell, Haller and Frank, 2014; Reda *et al.*, 2015) conclude that the investigated systems are more efficient for cold regions with high annual solar irradiation. Furthermore, for cold climates the SAGSHP systems over-perform compared to the GSHP systems, whilst a significant reduction of the BHE length was estimated (Emmi, Zarrella, De Carli, *et al.*, 2015). Finally, the reduction on the required GHE length in SAGSHP system of 15% to 80% is also estimated by (Chapuis and Bernier, 2009; Rad, Fung and Leong, 2013; Eslami-Nejad and Bernier, 2011; Emmi, Zarrella, Carli, *et al.*, 2015) and is related to the ground's energy enhancement by solar heat.

2.8. Gaps in knowledge

This chapter has shown that the main gap in the literature is a dedicated and specialized design method for SAGSHP systems, in other words, a universal way to handle the design procedure. The diversity of components, interconnections, applied control, weather climates and many other aspects constrain the design method formulation. A unified method will be assisted in order to assess the feasibility of project like the DMU's experimental one (section 3.4).

A design method calculates the required system size (collectors' area, BHE length) for a specific fraction of the heating load coverage. Some design methods which have been established for solar and geothermal systems are the f-Chart (Solar Energy Laboratory University of Wisconsin-Madison *et al.*, 2009) and the ASHRAE method (ASHRAE, 2011) respectively. With the f-Chart, along with the system sizing, a draft system configuration is imposed for method's validity. Regarding the ASHRAE method, the sizing part is the objective, while the system configuration is not suggested explicitly.

From the absence of the dedicated method the question listed below have been derived:

a) What is the influence of solar collection area and GHE's size on the system heat and power productivity?
b) What can be the configuration (interconnection) which benefits the most energetically the system?
c) What can be the heat and power fraction covered by RES for different levels of dwelling energy efficiency? The first to be built according to current regulations for new dwelling and the second as an energy renovated house.
d) What metric (s) can be used to evaluate energetically the PVT based SAGSHP systems?
e) Is the proposed SAGSHP system less carbon emissive than a system fired by natural gas (NG), or a conventional GSHP system? Also, what are the emissions of the SAGSHP system compare to other well-established solar heating technologies, like the PVT heating systems and the solar assisted heat pump systems?

The above list of questions sets a problem difficult to be solved due to many unknow parameters. Things becomes worse by having many potential pairings between solar collectors and GHE. Some universal lines have been drawn about the pairing aspect (subsection 2.5.2) but nothing to corelate the whole set of questions and by having not evaluate the systems' efficiency for the specific choice.

Through the research questions deployed above, the research main aim is set: What is the energetic and environmental performance of SAGSHP systems for low-rise buildings in a UK's space heating dominated province? With the research aim being stated, the objectives illustrated in section 1.3 have been created. It is worth mentioning, that an alternative aim can be the creation of a design method for SAHSHP system, but this attempt will need more than three years to be accomplished. Therefore, with the current work, an effort has been made to deliver a methodology which can be used for SAGSHP systems analysis, giving that the technology has many peculiarities.

The following chapter proposes a methodology which is utilized in order to conduct the proposed research. In Chapter 3 the whole process is overviewed and a brief discussion on what is followed takes place. The reasons for the choices made regarding the simulation environment and the overcame difficulties are illustrated. Finally, the Grasmere St. system is analyses with the need to offer a deeper understanding regarding the system's modeling approach and operation principals.

Chapter 3. Research methodology

In this chapter the used research methodology is overviewed, along with collected information from DMU's SAGSHP system experiment. The adopted research method has been deployed with the purpose of answering the research questions stated in section 1.3. Following the current layout of the methodology used, there are also dedicated subsections for in detail analysis of every aspect. Also, further particular description of the utilized components and their experimental validation is given in the next Chapter 4. In sections 3.3, a summary of the utilized simulation platform is provided, while in section 3.2, the two SAGSHP system topologies are illustrated along with their operational procedure. The last section 3.5, the metrics for the systems' energetic assessment are illustrated and analyzed. Following the Chapter 3 and Chapter 4 which are the methodology and the detailed analysis of the subsystems, the remain part of the Thesis responds to the research questions aim. The last Chapter 8 summarizes the main research findings and research ideas for future works are proposed.

3.1. Overview of the research methodology

Parametric analyses via simulation were conducted, with the purpose of answering the research questions stated in section 1.3. In accordance with the research aim and questions, these were:

- two system topologies
- two different locations for the installation of the GHE.
- two dwellings, with equal geometry but different heat demands.
- twenty-four pairs of PVT arrays with borefields.

The aim behind the above listed variations of parameters is to assist in answering to the research questions. Thus, the first research question (a, *what is the influence of solar collection area and GHE's size on the system's energy performance?*), can be answered by varying the size of the PVT arrays and borefields with twenty-four different pairs (last bullet in the above list). The second research question (b, *does the direct use of solar heat benefit the system energetically?*) is going to be answered by evaluating two different system topologies (first bullet). As regards the third research question (c, *what are heat and power fractions covered by RES for different levels of dwelling energy efficiency?*), this is built around the two types of dwellings considered for the analysis (third bullet). Nevertheless, the type of dwelling (new or refurbished) is a basic

characteristic for the parametric analysis, thus each dwelling type is tested against all the listed parameters on the above bullet points list (Figure 3.4).

All simulations have been carried out for Birmingham, West Midlands (UK), by utilizing annual weather data from Metronome (TMY2). The choice of Birmingham was made because it is in Midlands which is representative of English climate. Also, the Meteonorm' s data are available in TRNSYS for Birmingham, which is the closer city to Leicester, where the DMU's experiment was conducted. Also, the UK's Midlands are characterized as a space heating dominated province, and that matches with the established research aim. Finally, by considering that the DMU is in Midlands, the achieved results can be used directly by space heating systems designers and by that to contribute to the local development.

The energy flow diagrams for the two investigated system topologies are illustrated by Figure 3.1 for system A and with Figure 3.2 for system B. System A topology is the one used for the DMU's SAGSHP experimental system. System B differs from system A interconnection by having direct use of solar heat for DHW needs. Detailed analysis of the two systems is given in section 3.2, along with the utilized control procedure.

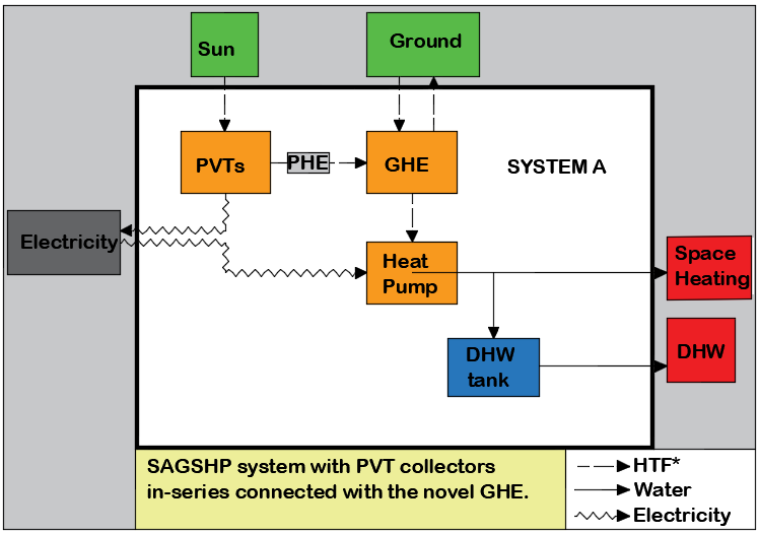

*Figure 3.1. System A energy flow diagram. *HTF: heat transfer fluid*

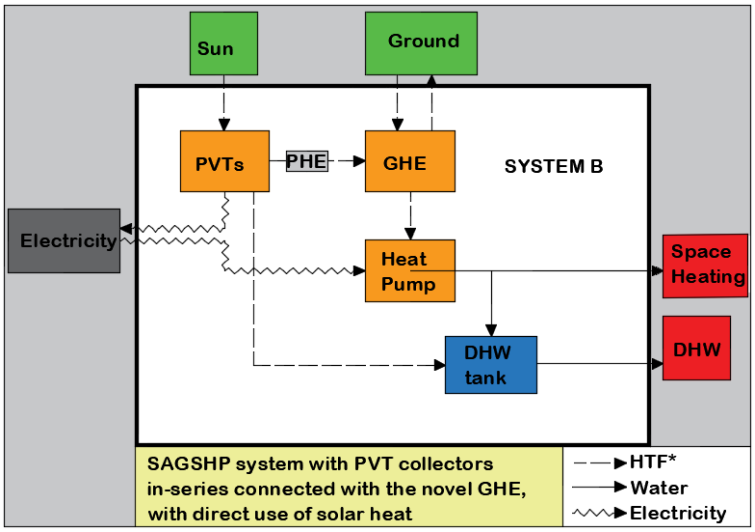

*Figure 3.2. System B energy flow diagram. *HTF: heat transfer fluid*

As regards the GHE installation, two possible locations are decided: exposed (E) and the beneath the dwelling (B). In Figure 3.3, the two GHE installation positions are depicted in relation to the dwelling. As it can be seen, the exposed choice leaves the EEB totally uncovered to the environmental conditions. In contrast to the exposed EEB location, the position beneath the house isolates the upper part of the EEB from the atmospheric conditions. Lastly, only the new dwelling is investigated for both locations, while for the refurbished, only the EEB with the exposed location is considered. All the details about the GHE size and installation are documented in section 4.2.

The studied SAGSHP systems are investigated by being connected to a low-rise dwelling, located in Birmingham, in the UK. The building is considered to be a two storey dwelling with 120 m^2 living area. Two scenarios have been created: the first one sets is for the dwelling built in accordance with the England L1A (HM Government. Ministry of Housing & Communities & Local Government, 2016) building regulations for new domestic building and the second one as a refurbished solution in accordance with L2A regulations (refurbishment) (HM Government. Ministry of Housing & Communities & Local Government, 2010). The two dwellings have the same geometry, but different space heating demand. To what follows, the dwelling built with L1A will be called new (N) and the one built with the L2A will be called refurbished (R). Also, on top of the space heating demand, the SAGSHP system is responsible to provide DHW on daily bases, regardless of the type of the dwelling. The space heating and DHW demand are set as the SAGSHP system heating load, and in section 4.4 the important information is shown.

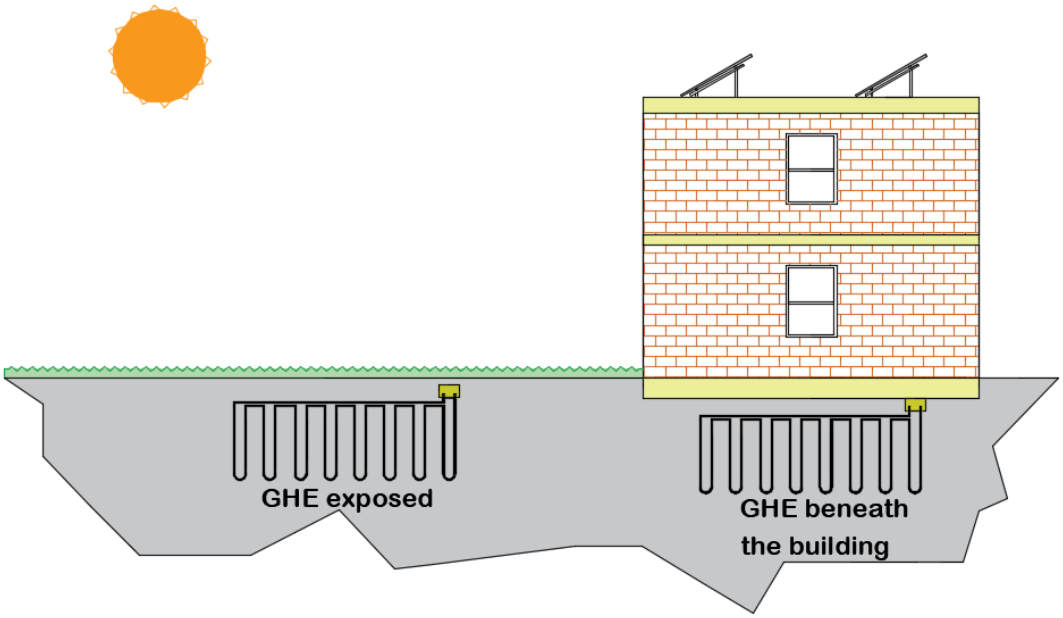

Figure 3.3. Depiction of the GHE installation for the two investigated locations: the exposed and the beneath the building.

For every simulation scenario, the number of PVTs varies from 0 to 20 with string of 4 collectors connected hydraulically in series. Similarly, the BHEs number starts from 16 and increases up to 40, by creating four borefield sizes of 16, 24, 32 and 40 BHEs. The maximum number of the collectors has been indicated by the available dwelling's roof area, with the aim to avoid shading effects a substantial spacing among PVT rows is needed. Thus, only two rows of 10 PVTs each can be installed on the roof, by considering the inclination of 30 degrees. As regards the BHEs, the minimum number is set equal to this of the DMU's experiment, while the maximum of 40 BHEs is set to not go over the dwelling's ground floor area.

According to the above parameters analysis, six system scenarios can be set. In Table 3.1 the created systems are listed along with their acronyms. Therefore, the A and B system type are evaluated for both dwelling types (new and refurbished). Also, only for the new dwelling, both EEB locations are considered.

Table 3.1. System simulation scenarios with their acronyms.

Topology	**EEB exposed**		**EEB Beneath the Building**
System A	New Dwelling (A_NE)	Refurbished Dwelling (A_RE)	New Dwelling (A_NB)
System B	New Dwelling (B_NE)	Refurbished Dwelling (B_RE)	New Dwelling (B_NB)

Therefore, for every system scenario, 24 simulations (6 PVT scenarios by 4 borefields) have been executed, with 10-year simulation span and 1-hour simulation time step. Figure 3.4 illustrates the available choices of the parametric analyses carried out for both dwelling types. All be above mentioned systems were formulated in TRNSYS simulation platform. The simulation starting time was set to be the 1st of September, by assuming the system to be installed and commissioned within the summer. Basic information regarding the utilized simulation software are written in section 3.3, along with the supporting reasons of the current choice. It is important to note that, the simulations took 35 min on average with a personal computer equipped with 1.8 GHz CPU and 8 GB RAM. This simulation time restricted the number of simulations carried out, thus for the system with topology B, the investigated borefields were limited to be the 16 BHEs and 40 BHEs (this limitation was found to provide the required information about the systems behavior). Finally, for every simulation, energy balance calculations of the system were executed with the aim to identify the accuracy achieved. Thus, the convergency deviation found to not exceed the 2% in any run, with the tolerance convergency index to be set at 1%.

With the results derived from simulations, the energetic evaluation of the systems was conducted. The systems energy analysis was based on:

- renewable heat fraction (RHF). The fraction of the heating load covered by RES
- renewable power fraction (RPF). The faction of the system's electricity covered by RES
- system heat specific productivity (SP_{sys_heat}). System's annual heat productivity per collector.
- PVTs heat specific productivity (SP_{PVT_heat}). PVTs' annual heat production per collector.
- PVTs electric specific productivity (SP_{PVT_el}). PVTs' annual electric generation per collector.
- seasonal performance factor (SPF). The ratio between the delivered heat by the system, to the electricity consumed in the system.

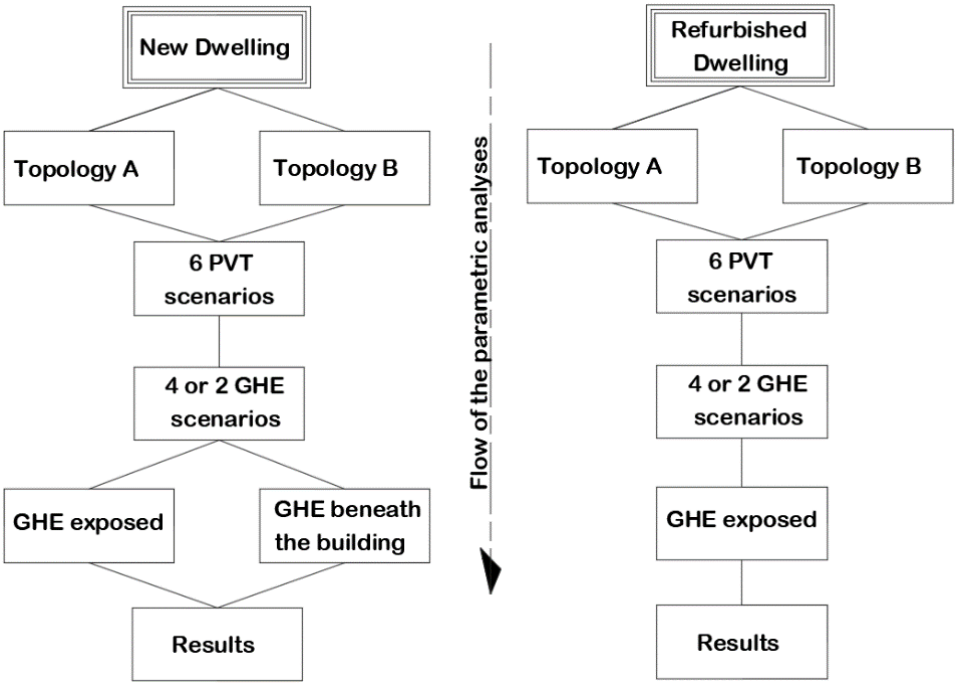

Figure 3.4. Flow chart of the parametric analyses carried out, for both dwelling types.

All the above energy metrics are illustrated and analysed with details in section 3.5, along with the alterations required to fit in with every system topology. The point behind the pluralistic choice of energy metrics is to obtain a spherical knowledge about the systems energetic behaviour, and to evaluate the metrics usability (research question d).

Following the energy analysis, all the six SAGSHP systems scenarios were compared regarding the carbon emissions with a GSHP and a NGB system (research question e and f). The analysis was made by considering the fraction of carbon emission saved (subsection 3.5.5) by utilizing the SAGSHP or the GHSP system against the NGB system. The GSHP system was used as the benchmark to the performance obtained by the SAGSHP systems parametric analyses. The GSHP system is designed in accordance with the ASHRAE procedure (ASHRAE, 2011), and all the followed process is covered by the subsection 4.5.1. Similarly, the system based on the natural gas boiler is illustrated with details in sub section 4.5.2.

3.2. Systems topology and operation analysis

In the current subsection, the two system topologies stated in the Overview of the research methodology subsection 3.1 are analyzed. The important aspects of these two types of system

topology is the applied control and the hydraulic connection of components. Therefore, for both topologies the emphasis is given to the system's layout, control strategies and to the operation flow chart. The interaction between the operation procedures (flow chart) with individual components of the system is shown in Chapter 4 for every subsystem.

It is essential to illustrate all the engaged parameters to the control procedure. These important parameters are three: a) the PVTs outlet temperature (T_{out_PVT}), stands for the temperature of the heat transfer fluid at the collectors outlet, b) the mean soil temperature near borehole (T_{b_s}), is the average soil temperature just outside the BHE wall (the mean from all BHEs) and finally and c) is the temperature at the bottom of the DHW tank (T_{tank}), illustrates the mean temperature at the bottom of the DHW tank.

3.2.1. System A

As it is shown by Figure 3.5 for system A, PVT collectors absorbs solar energy which part of it convert to heat and electricity. The solar heat is delivered only to the EEB in where may be stored or directly utilized by the heat pump. In case of no solar heat available, the heat pump absorbs heat form the EEB. The system's operation process is depicted by Figure 3.6 which illustrates the control flow chart for system A. The illustrated flow chart should be read together with Table 3.2, in which the system's control actions are shown for every operation mode.

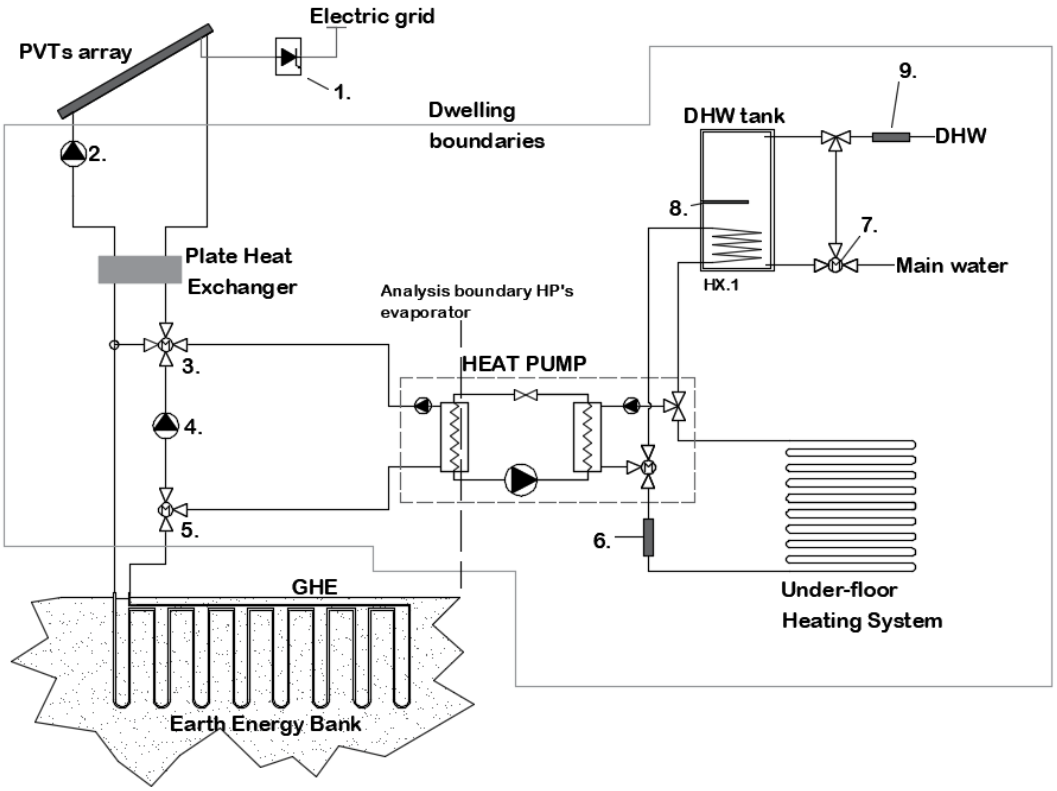

Figure 3.5. System topology for layout A. 1. DC to AC inverters, 2. Solar system pump, 3. Four-way deviator, 4. Solar-soil charging pump, 5. Three-way deviator, 6. Space heating auxiliary heater, 7. Temperature control valve, 8. DHW tank electric heater, 9. DHW auxiliary heater.

The system's control process is responsible to provide the necessary actions for the operation of the space heating system. The space heating system in comprised of the solar and geothermal system and ends on the heat pump. All the control actions descripted by the flow chart in Figure 3.6 and Table 3.2, aim to activate system's specific component. The proposed control process shows low complexity, and that makes the system more reliable, while it can be easily implemented by control devices, such as a programmable logic control (PLC) unit.

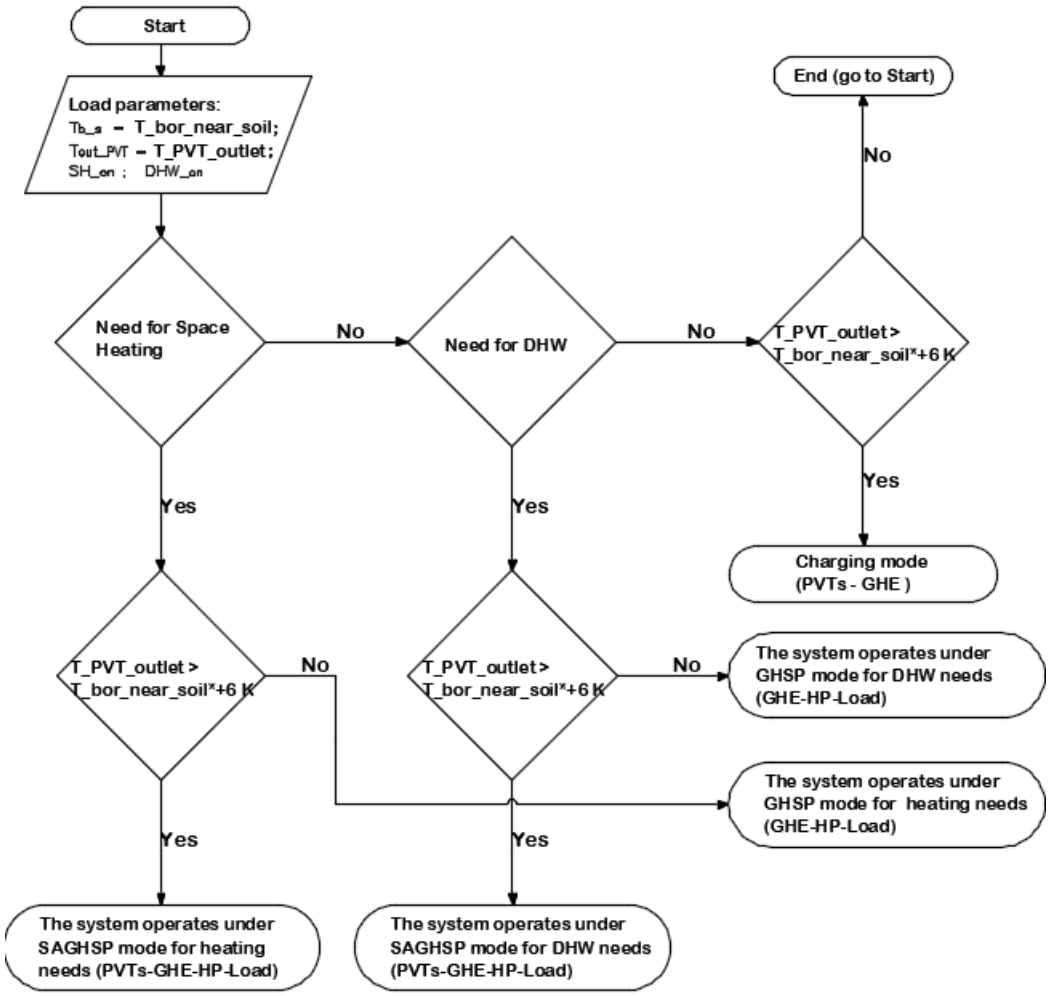

Figure 3.6. Control flow chart for system A.

Table 3.2. Description of operation modes for layout A.

Operation mode	Description	Control
PVTs-GHE-HP-Load	Heat pump supplies the load by employing the GHE and PVTs. The solar heat from PVT collectors is used as additional source to the geothermal.	Deviation valves 3 and 5 (Figure 3.5) are switched to drive the HP's flow rate via the GHE and the PHE. Pump 2 is turned on to gather solar heat. Pump 4 is bypassed.
GHE-HP-Load	The heat pump supplies the load by utilizing only the EEB available heat. Solar irradiance is not capable to increase the T_{out_PVT} over the set limit of 6^{o}C higher than the T_{b_s}.	Deviation valves 3 and 5 (Figure 3.5) are switched to drive the HP's flowrate via the GHE and bypass the PHE and pump 4.
PVTs-GHE	Solar heat is stored on the soil via the GHE. No need for space heating or DHW. PVTs' outlet temperature 6^{o}C higher than the T_{b_s}. This mode is also applied when the evaporator's (HP) inlet temperature raised above 25^{o}C. This last circumstance found to be activated no more than six times per year for an hour.	Deviation valves 3 and 5 (Figure 3.5) are switched to drive the pump's 4 flowrate via the PHE to the GHE and bypass the Heat Pump. Pump 2 is turned on to enable the solar system.

3.2.2. System B

Objectively, the difference between system A (Figure 3.5) and B (Figure 3.7), is the direct use of solar heat. The additional part in System B is that: the PVT collectors are capable of providing solar heat to the DHW tank directly via extra piping and a second immersed heat exchanger (HX.1). The operation principals of the systems with B topology alter from these with A topology by prioritizing the solar heat utilization for DHW needs (Figure 3.8). By neglecting the operation of the direct use of solar heat, the rest of the control procedure is equal to this of A system. Based on the alternative use of solar and geothermal systems, potentially, the DHW needs and space heating demand can be covered at the same time by different subsystem. Therefore, system B can be transformed to a solar-DHW system working in parallel with a GHSP system, or it can operate as a SAGSHP system as system A does.

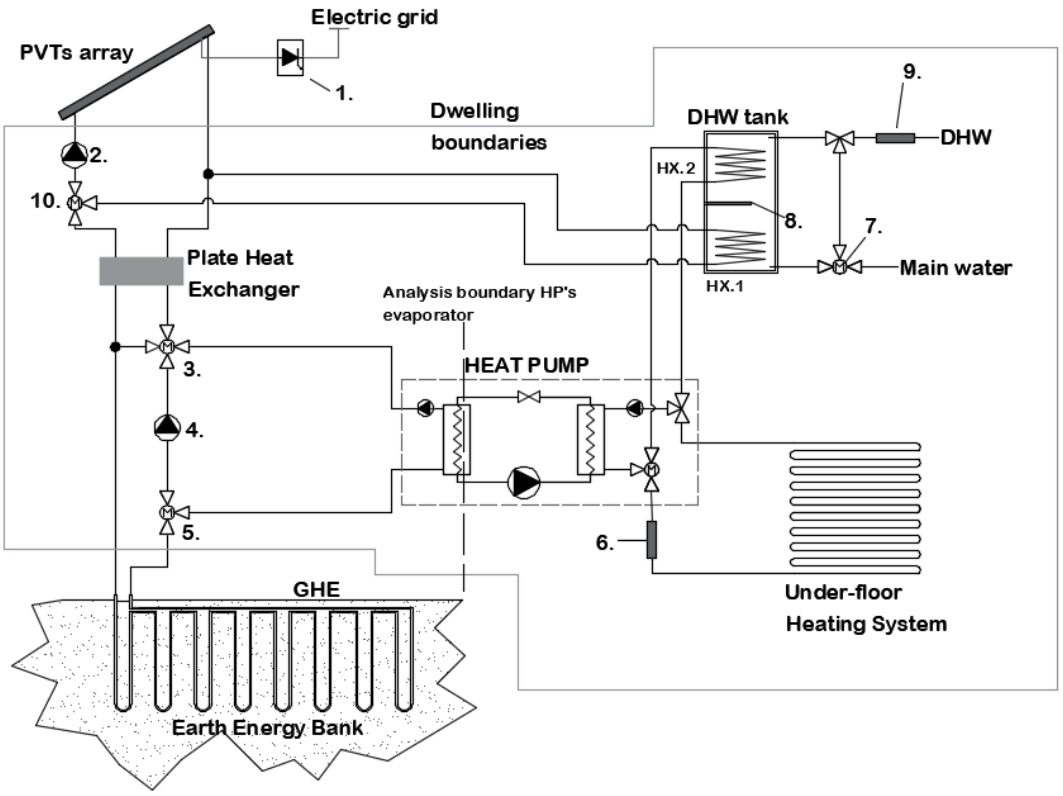

Figure 3.7. System topology for layout B. 1. DC to AC inverters, 2. Solar system pump, 3. Four-way deviator, 4. Solar-soil charging pump, 5. Three-way deviator, 6. Space heating auxiliary heater, 7. Temperature control valve, 8. DHW tank electric heater, 9. DHW auxiliary heater, 10. Three-way deviator for DHW.

Table 3.3. Description of operation modes for layout B.

Operation mode	Description	Control
PVTs-Tank	The solar heat from PVTs is used directly to heat up the water in the DHW tank. This mode can be applied simultaneously with "PVTs-GHE-HP-Load" or "GHE-HP-Load".	Deviation valve 10 (Figure 3.7) is switched to drive the solar heat directly into the DHW tank. Pump 2 is turned on.
PVTs-GHE-HP-Load	Heat pump supplies the load by employing the GHE and PVTs. The solar heat from PVT collectors is used as additional source to the geothermal.	Valves 3 and 5 (Figure 3.7) are switched to drive the HP's flow rate via the GHE and the PHE. Pump 2 is turned on to gather solar heat. Pump 4 is bypassed.
GHE-HP-Load	The heat pump supplies the load by utilizing only the EEB available heat. Solar irradiance is not capable to increase the T_{out_PVT} over the set limit of 6°C higher than the T_{b_s}.	Deviation valves 3 and 5 (Figure 3.7) are switched to drive the HP's flowrate via the GHE and bypass the PHE and pump 4.
PVTs-GHE	Solar heat is stored on the soil via the GHE. No need for space heating or DHW. PVTs' outlet temperature 6°C higher than the T_{b_s}. This mode is also applied when the evaporator's (HP) inlet temperature raised above 25°C.	Valves 3 and 5 (Figure 3.7) are switched to drive the pump's 4 flowrate via the PHE to the GHE and bypass the Heat Pump. Pump 2 is turned on to enable the solar system.

A closer examination on the system B operation reveals that the water in DHW tank can be heated up by the PVTs and the heat pump simultaneously. This decision is taken with the aim to reduce the system's electricity consumption. In more details, the DHW should be delivered at 50 °C, and by utilizing only the PVTs for this purpose is more likely an auxiliary amount of energy to be needed (the used PVTs are not capable of heating up the DHW at 50 °C). Therefore, it is preferable to have the heat pump to supply the supplementary heat required for the DHW consumption. However, the whole attempt is based on the temperature stratification of the water in the tank, by assuming the heat pump to heat up the upper part (directly utilized by the user) and PVTs' heat supply, to be benefited by the colder bottom layer of water in the tank (Figure 3.7).

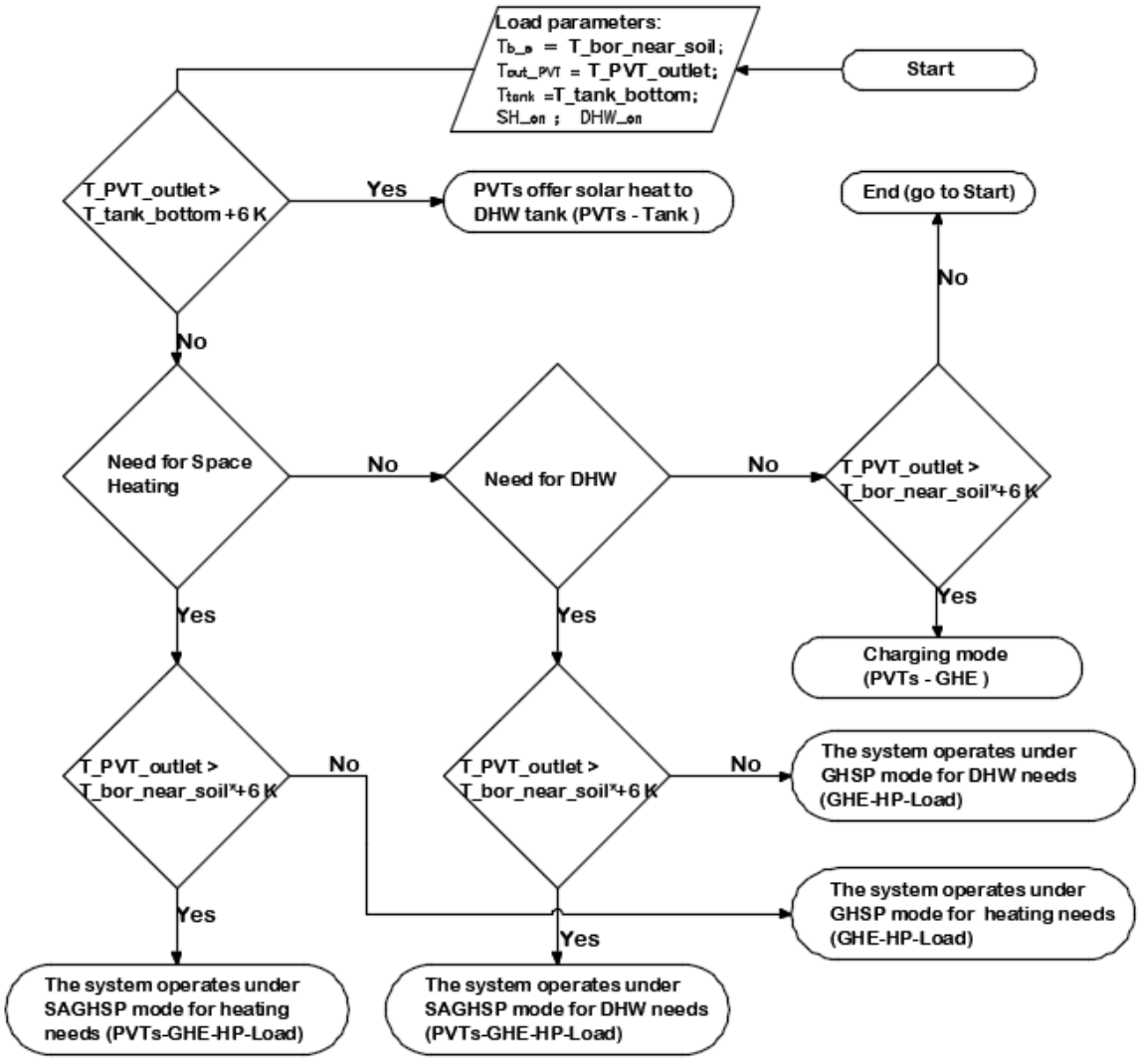

Figure 3.8. Control flow chart for layout B

3.3. Simulation platform

For the research needs, the transient energy system simulation tool (TRNSYS) was used (Solar Energy Laboratory University of Wisconsin-Madison *et al.*, 2009). The TRNSYS has been developed by the university of Wisconsin, as a graphically based platform mostly suitable for thermal and electrical systems simulation. The software is made up of two parts: the first one is the engine (kernel) which interfaces all systems variable and via iterative processes executes the simulation, the second part is the components (called TYPEs) library. It is important to emphasize on TRNSYS characteristic to perform simulations with convergency simulation time steps. In other words, kernel moves on from step to step by having achieve an acceptable convergency via iterations on the results. This is deemed highly important for systems where large heat inertias are used by the TYPEs.

TRNSYS is an open software in which the user may create its own TYPE (components) or modify the existing. The new components can be created with FORTRAN programing language or alternatively by C or C++. The user must compile the new TYPE and to create a dynamic link library (DLL) file. The DLL is required from windows operation software in order to resource information about the TYPE's nature.

The key reasons for the choice of TRNSYS as the simulation tool are:

- The open source environment, which offers the capability to build new TYPEs or to adjust the existing.
- TRNSYS is an excellent choice for complex energy system with heat inertia. In our case the EEB, the DHW tank and the house are characterized by heat inertia.
- All components are read by the kernel simultaneously. This offers extra accuracy on the results.
- TRNSYS found to be used from the majority of researcher and practitioners working in the field of solar and geothermal systems. During the literature review the vast majority of the research works was carried out with TRNSYS.

It is worth noting the issue faced about to use FORTRAN during the research time. As it is stated above, new TYPEs can be created by writing the script in FORTRAN and compile that with the aim to extract the DLL. FORTRAN is an old programming language with the new version to be incompatible with older applications, while during the research time the current version of TRNSYS (17) was not equipped with programming language (TRNSYS 18 has an embedded one).

The solution of purchasing the new TRNSYS 18 release was quoted to be 1.100€ and this amount of money was out of research budget. The only available FORTRAN found for free was the Compaq visual FORTRAN 6 (CVF 6), but XP windows operation environment was a requirement. Therefore, all new TYPEs and the changes on the existing TRNSYS library TYPEs were made by CVF 6 in XP windows. Then, the DLL created by CVF 6 compiler in XPs, was transfer to a device with windows 10 and TRNSYS 17. Therefore, all the script writing work was made by CVF 6 and all the simulations were carried out with TRNSYS 17 in windows 10 operation environment.

3.4. The SAGSHP system experiment conducted by DMU

It is pertinent to illustrate the trial made by DMU, in order to offer an overview of the experimental system. As it is already stated in the introduction Chapter 1, the current research project has been triggered by an installed SAGSHP system located at DMU's campus in Leicester, UK. The system was placed near by the Engineering school building (Queens Building) on Grasmere St. The system was installed to provide space heating and DHW to a dwelling owned by the university. Also, the system was designed empirically by the Institute of Energy & Sustainable Development (IESD) members and Caplin Homes commercial company. Finally, the scope of the DMU experiment was to provide data for models' validation and to offer an intuition regarding the phenomena governing the applied technology.

The DMU's experimental system was installed in a partly refurbished terrace house with shared (partly) walls on both sides. The two-storey building was unoccupied and it was used by the university as a crime scene for forensic science lectures. The building was erected at the end of 19th century and by the refurbishment new double glassing windows along with attic insulation have been installed. Though, the dwelling found to suffer by infiltration and heat losses via the uncovered walls. Regarding the space heating mean, an underfloor system was installed on the ground-floor in the two larger rooms, while for the DHW, a tank with 200 L volume was installed.

In Figure 3.9, the DMU's SAGSHP system top view is shown and by Table 3.5, the subsystems details are listed. As it can be seen, the GHE was place in an empty space, but was on the top and side thermally insulated (Table 3.5). Also, on the dwelling roof, 7 PVT collectors (Solar Angel, 2016) (Table 3.4) were installed along with one PV[5], with the aim to compare the power productivity between the two technologies. The type of PVT collectors was uncovered, flat plate,

[5] The PV panel was a similar panel used for PVTs, but with the absorber not to be placed side.

with sheet and tube absorber, as for the heat removal medium this was 30/ 70 % ethylene-glycol with water by weight. Additional information about the solar loop can be found in Table 3.5 . The heat pump heating capacity was rated at 3 kW_{TH} (Table 3.5). Finally, with Figure 3.10, the DMU's experimental system topology is illustrated. As it can be seen, the PVT collectors are in series connected hydraulically with the GHE (Figure 2.1), via a plate heat exchanger (PHE). According to the reviewed literature, the half of the built systems have been connected hydraulically with the same way (subsection 2.5.1).

Table 3.4. PVT collector specifications (Solar Angel, 2016).

PV Output (Wp) (Polycrystalline)	250	Frame material	Aluminium
Thermal Output (Wp)	648	Insulation material	Polymer foam
Gross collector area (m2)	1.607	Connections	22mm Compression
Aperture area (m^2)	1.552	Max. operating pressure (KPa)	600
Absorber area (m^2)	1.501	Pressure tested to (KPa)	1500
Dimensions (mm)	1630 x 986 x 35	Pressure drop (mBar) @ 2.5 l/min	50
Weight – empty (kg)	25	Max System Voltage (V)	1000
Liquid content (l)	0.82	Voltage at max power (V)	30.4
Glass (low iron)	3.2 mm	Current at max power (A)	8.1
Stagnation temperature (°C)	78.9	Over current Protection Rating (A)	12
Absorber material	Aluminium	Snow and Wind Loading (max Pa)	6600

The experimental system was set with the major scope to collect knowledge and experience regarding the SAGSHP systems. Therefore, three data acquisition systems were installed to record the system's important variables, while the environmental data were provided by the DMU's meteorological station. In more detail, the earth energy bank (EEB)[6] soil and heat removal fluid temperatures were recorded by the National Instruments *cDAQ system*, the main system's temperatures and flow rates by *VBUS* and the *Sunny Portal* gathers all the data about the PVT power generation. More information about the data collecting systems can be found in (Naranjo-Mendoza *et al.*, 2019) and (Naranjo-Mendoza, Greenough and Wright, 2018).

Based on data collected from June of 2016 until December of 2017 (20 months), Naranjo-Mendoza et al. (Naranjo-Mendoza *et al.*, 2019) did the first energy evaluation of the DMU's SAGSHP system. According to the analysis, the heat pump's seasonal performance factor (SPF) was found to fluctuate between the 2.01 and 3.58, with a mean value of 2.51. Additionally, important aspects like the soil volume expansion due to low temperatures[7] and the evaporator inlet beyond the operational limits are some of the issues which were identified needing further

[6] The EEB is the geothermal heat exchanger's assigned volume of soil.
[7] In porous materials like is the soil, their volume may expand in low temperature due to ice formation.

study.

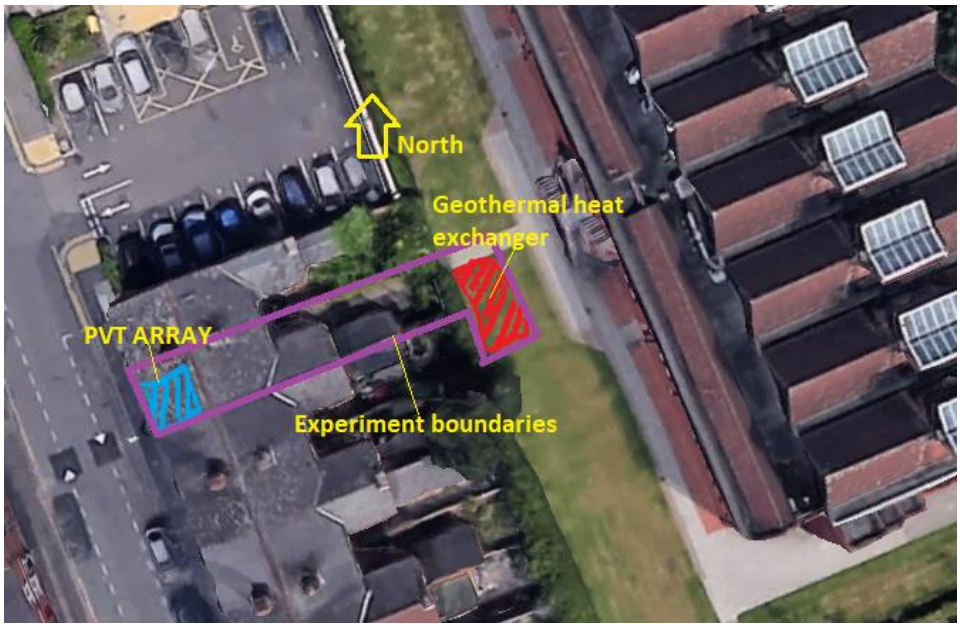

Figure 3.9. DMU's SAGSHP experimental system top view.

Table 3.5. DMU's SAGSHP system subsystems summary.

Subsystem	Analysis
PVTs and PV (solar loop)	The 7 PVTs were hydraulically connected in series, and electrically via individual optimizers to the DC-AC inverter which injects the electricity to the power grind. A temperature differential thermostat controls the operation of the solar system, the system provides heat to the ground loop when the PVTs' outlet temperature is 6 K higher than the soil temperature (near BHEs' wall). Along with 7 PVTs, a conventional PV panel was installed with the purpose to evaluate the potential benefit of greater electricity yield of installing PVT against a PV. All PVTs and the PV were installed on the housetop with the same azimuth and Inclination angle, 54^{o} and 34^{o} respectively.
Geothermal heat exchanger GHE (ground loop)	The GHE was a very shallow one with an array of 16 vertical short BHEs of 1.5m deep, which are connected in series. The GHE was installed 0.55m below the ground surface and was thermally insulated by polyurethane on the top and Celotex on its four sides, the bottom was open. The soil mass which actually influence the GHEs' thermal behavior is 60 m^3. The GHE was installed between the PVT array and the heat pump. The heat removal medium for both solar and ground loop was a mixture of 30/70% ethylene-glycol with water by weight.
Heating system-Consumption	The heart of the heating system was the Heat Pump, with maximum heating capacity of $3kW_{TH}$. The heat pump was a liquid to liquid one with Coefficient of Performance *COP*, from 2.9 to 4.5. The space heating mean was an underfloor coil, and a tank of 200 L was installed for DHW needs. Unfortunately, no data regarding the heat consumption have been collected, thus the system's measurement stop at the heat pump power consumption.

In brief, the operation of the systems is: when the outlet temperature of PVT collectors is 6 K (ΔT) higher than the soil temperature the pump No 2 (Figure 3.10) operates. If there is a need for space heating or domestic hot water, the heat pump's embedded circulation pump is responsible to curry the heat from the PHE via the EEB to the evaporator. If the ΔT is lower than 6 K and the system demands heat, the energy is extracted only from the EEB. If there is not a heating demand and the ΔT is higher than 6 K, pumps No. 2 ad No. 3 operate with the aim to store solar heat into the EEB. As regards the generated electricity by PVTs, this is injected to the power grid via power inverters.

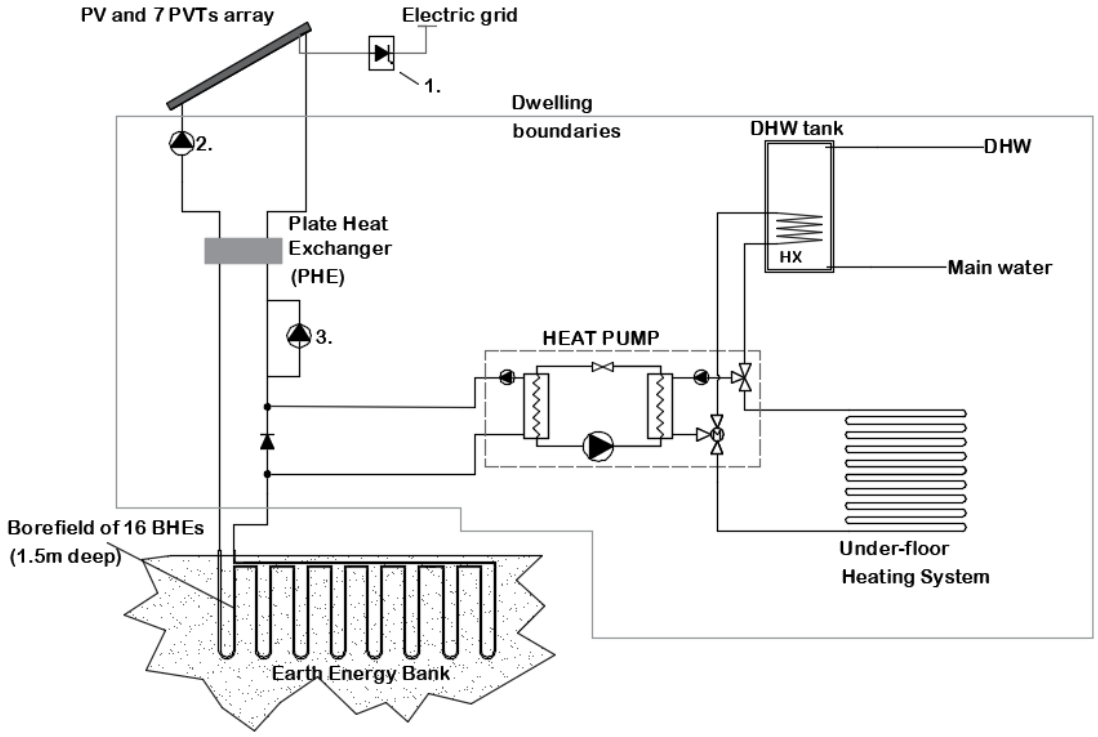

Figure 3.10. DMU's SAGSHP system topology. 1. DC to AC inverters, 2. Solar system pump, 3. Solar heat charging pump.

3.5. Metrics for energetic and greenhouse gasses emission assessment

Metrics are needed for systems' feasibility studies. In this section, the metrics used are demonstrated, defined and explained, with the aim to establish a common ground with the existing and future works.

3.5.1. Seasonal Performance Factor (SPF)

A widely used metric which assesses the energy performance on heat pump-based systems is the seasonal performance factor (SPF) and mathematically is expressed via equation 3.1. The

SPF index indicates the ratio of what you offer in terms of electricity (consumed energy) and what you get as delivered heat (condenser outlet). In order to be precise, the consumed electricity (denominator) in equation 3.1, potentially can be delivered by another form of energy like the heat for a heat driven heat pump, but in the current study only electrical powered compressors are used and in what follows will be only that way (in practice, the vast majority of heat pumps are powered by electricity).

The above paragraph can usefully summarized by EU's standard EN15316-4-2 (section 3.1.18 of (Cen *et al.*, 2006)) where:

"SPF is the ratio of the total annual energy delivered to the distribution subsystem for space heating and/or domestic hot water to the total annual input of driving energy (electricity in case of electrically-driven heat pumps and fuel/heat in case of engine-driven heat pumps or absorption heat pumps) plus the total annual input of auxiliary energy"

$$SPF = \frac{Heat\_delivered}{Electricity\_consumed} \qquad 3.1$$

With European's Parliament Decision, four different boundaries of measuring the SPFs with the increased electric consumptions inputs have been set (Figure 3.11)(European Parliament, 2016). The SFP_{H1} is the closest to heat pump's manufacturer steady state operation values as can be found by EN15411 and considers only the device's electricity consumption (compressor, control, pumps if any). With the SPF_{H2}, along with the Heat Pump's electricity the engaged pumps for heat transportation back-and-forth from RES are added. The SPF_{H3} further includes all the additional heat made by electricity which is required to cover the demand (auxiliary heat) and the electric apparatus used for heat transfer procedures. Finally, via SPF_{H4} the whole of electric inputs is added in equation 3.1 denominator, including consumption made by the heating system (fans, pumps).

It is important to be mentioned that, the SPF_{H4} does not reflects much information about the utilized heat and its aim is to assess the heating production system. In other words, the heating systems' efficiency is not considered, and the analysis stops on the delivered heat at the building or in the DHW tank. The metric does not illustrate how efficient is used the delivered heat, for instance, if the dwelling effectively consumes the delivered heat. If the numerator's delivered

heat in equation 3.1 is replaced by the end-user[8] utilize amount an extra SPF can be established. This SPF_{H5} will combine the heating production and end-user final useful heat. Though, in the present case, the SPF_{H4} is adequate metric to evaluate the SAGSHP system by knowing that the efficiency of the heating load is out of set research questions and aim.

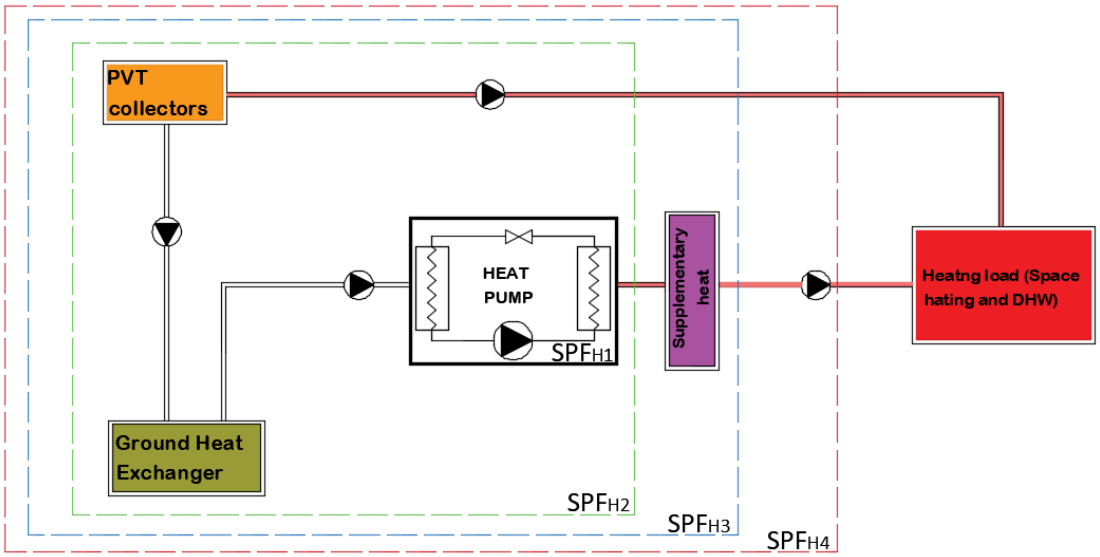

Figure 3.11: The four SPFs boundaries as these have been set by EU decision (European Parliament, 2016).

By calculating the SPF, information about the system's thermal performance can be obtained. Nevertheless, the SPF ratio neither indicates the systems efficiency nor tracks any component with low performance. In other words, a high SPF can be achieved by a large PVT array or a large GHE which operates inefficiently, but due to its size is capable to offer substantial heat in order to increase the system's performance. Considering this limitation, a new energy assessment method for SAGSHP systems was developed. The new metric is based on specific productivity concept and is defined below (subsection 3.5.2). Thought, with the need to maintain a consistency with the current literature, the SFP will be used as a system's performance metric. It is vital to mention that, SPF can be derived from experimental data or calculated via simulation process, in what follows SPF will be calculated always from simulation results. Finally, another solution to illustrate the systems holistically, thermally, and electrically, may be the exergy efficiency – analysis, which is out of the work's aims.

The SPF_{H4} will be used for systems' thermal evaluation with the aim to have a common approach

[8] The end-user energy is the actual delivered by taking into the account the heat transfer efficiency from the operation fluid to the space heated or to the used DHW.

for both SAGSHP system configurations. Equation 3.2 is the general relation which describes the SPF_{H4} for both solar assisted and conventional GSHP systems. On the numerator, the Q_{solar_dir} is included for the case where direct use of solar heat occurs (system B), otherwise is only the heat delivered by the heat pump. The denominator is the electricity balance, between the consumed by the system (via the power grid) and generated by the PVT. In this study, the calculated value from equation 3.2 is the average SPF_{H4}, by utilizing the total 10 years heat and electricity amounts from simulation results.

$$SPF_{H4} = \frac{\sum_{i-year}^{10} (Q_{cond} + Q_{Solar\_dir})_i}{\sum_{i-year}^{10} (E_{HP} + E_{pumps} + E_{Aux} - E_{PVT\_u})_i} \quad 3.2$$

Implementation of equation 3.2: The nominator includes the heat delivered to the heating load via the condenser (Q_{cond}) and the direct utilized solar heat (Q_{solar_dir}). The denominator is comprised of the balance between the electricity consumed by the heat pump (E_{HP}), the parasitic energy (E_{pumps}) and the auxiliary energy (E_{AUX}), against the electricity delivered to the power grid by the PVTs (E_{PVT_u}). To the majority of systems, on the denominator the E_{PVT_u} is excluded from the calculations. Therefore, along with the SPF_{H4}, a second index without the electricity delivered by PVTs will be illustrated (SPF^{*}).

3.5.2. Specific productivity (SP)

With the need to evaluate the system's energy harvesting side, specific productivity (SP) is used as a diagnostic tool for heat or electricity aspects. The specific productivity indicates the annual energy production per installed unit or corelated units (such as solar collectors with BHEs). In this study, two boundaries have been set for specific productivity estimation, the PVT collectors (SP_{PVT}) and the heat absorbed by Heat Pump via the evaporator (SP_{sys_heat}).

Regarding the PVT collectors, the specific productivity is focused on the heat (SP_{PVT_heat}) and power (SP_{PVT_el}) generation. These two metrics are expressed by equations 3.3 and 3.4 for heat and power respectively, while are used to express the mean annual value out of 10-year simulation period (where n is the number of PVT collectors).

$$SP_{PVT\_heat} = \frac{\sum_{i=1year}^{10} Q_{PVT\_i}}{n \cdot 10_{years}} \quad 3.3$$

$$SP_{PVT\_el} = \frac{\sum_{i=1year}^{10} E_{PVT\_i}}{n \cdot 10_{years}} \quad 3.4$$

With regard to the system's specific productivity (SP_{sys_heat}), the absorbed heat by the heat pump's evaporator and the directly utilized solar heat are entered to the calculations (equation 3.5). The evaporator's inlet energy may potentially be provided by the solar or the geothermal subsystem or even from both. Therefore, a useful index to clarify the SP_{sys_heat} is the ratio between the PVT Collectors and the BHEs (CBR). This index is useful to identify any potential correlation between the installed components count and size with the coverage of the heat demand. A second useful index is the storage capacity (SC), which illustrates the ratio of the storage soil volume per solar collector area ($m^3\ m^{-2}$). The SP_{sys_heat} metric has been used to evaluate the results from a SAGSHP system parametric analysis (Sakellariou *et al.*, 2019). The index found useful to identify system energy efficiency improvements resulted by parameters variation.

$$SP_{sys\_heat} = \frac{\sum_{i=1year}^{10} (Q_{ev} + Q_{Solar\_dir})_i}{n_{CBR} \cdot 10_{years}} \quad 3.5$$

More on CBR ratio, this can be illustrated as dimensionless index, or it can be expressed in units of $m^2\ m^{-1}$ (subsection 2.5.2). In our case, the division will take place between collectors and boreholes with standard area and length respectively. Since a PVT collector has fixed area and the BHE have fixed length, for convenience the CBR will be expressed without units (PVT per BHE). But the transition between the two illustrational ways can be made easily by knowing the PVT collector area and the BHE length. It is worth saying that, both indexes, the CBR and the SC, are illustrating the correlation between the solar and the ground system. But the first is indicates to illustrate the ratio between the collectors and BHE influence, while the second index show how the fraction between the size of EEB with the area of collectors influence the energy performance of the system.

3.5.3. Renewable Heat Fraction (RHF)

The Renewable Heat Fraction (RHF) indicates the portion of the total heat demand covered by RES. In other words, it shows the system's heat independence from conventional energy sources

and can hold values from 0 for no RES contribution up to 1 for 100% RES dependence. Figure 3.12, shows the composition of the energy consumed by the system for space heating and DHW needs. Part 1 representing the RES offered as heat to the system and with parts 2 and 3 is the heat pump electricity consumption and the auxiliary heat (in our case the additional energy is provided by electricity). Also, by gathering the portions 1 and 2 (Figure 3.12), the heat pump's delivered heat (condenser) is defined. Based on this representation, with equation 3.6, the RHF can be calculated as mean value from the 10-year simulation span. There are three important notes regarding the equation 3.6: a) the Q_{solar_dir} represent any direct use of solar heat, b) the Q_{HP_syn} stands for the compressor's electricity offered directly from PVT collectors (synchronized consumption and generation) and c) the Q_{aux_syn} represents the portion of the auxiliary heat with is covered by the synchronized PVT power generation. Finally, the RHF is consisted of three contributors: the contribution of the heat from the evaporator, the contribution from the direct solar heat, and the contribution added by the synchronized operation of the system with the generation of electricity. Each of the mentioned contributors defines a fraction which is derived by keeping fixed the denominator of equation 3.6 and place on the numerator the corresponding term (Q_{ev}, Q_{solar_dir}, Q_{syn}).

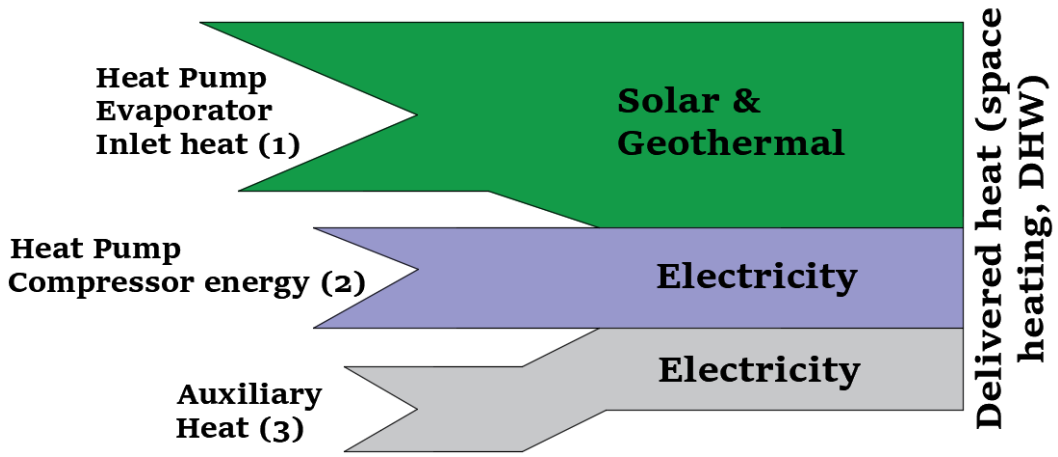

Figure 3.12. SAGSHP system delivered heat mixture.

$$RHF = \sum_{i-year}^{10} \left[\frac{Q_{ev} + Q_{solar\_dir} + Q_{HP\_syn} + Q_{aux\_syn}}{Q_{cond} + Q_{aux} + Q_{solar\_dir}} \right]_i \qquad 3.6$$

3.5.4. Renewable Power Fraction (RPF)

In this work, the PVT collectors is assumed to be connected via net-metering scheme with the local power distribution grid. The investigation is based on the energy aspect and not on the financial balance between the power consumption and generation. Therefore, the system's electrical side can be evaluated with equation 3.7 which calculates the renewable power fraction (RPF). As regards the equation 3.7, the nominator is the PVTs' delivered on the power meter electricity and the denominator gathers all the system's power consumptions. The RPF potentially can hold values from 0 for no PVTs contribution to more than 1 for electricity overproduction by PVTs. Due to fractional nature of index, the analysis will be carried out up to RPF value of 1.

$$RPF = \sum_{i-year}^{10} \left[\frac{E_{PVT\_u}}{E_{HP} + E_{pumps} + E_{aux} + E_{heat\_recovery\_unit}} \right]_i \qquad 3.7$$

An important note about equation 3.7. The systems' energy assessment takes place on the boundary set as SPF_{H4} classification (Figure 3.11). Therefore, the delivered energy is the utilized value and not the end-used received. In other words, the system's energy performance is calculated on the energy delivered at the underfloor space heating system and at the immersed heat exchanger (DHW tank), and not at the final useful heat. In that way, any energy consumed outside the SPF_{H4} boundaries is excluded from the calculations. As an exception, with the need to consolidate any related electricity consumption to the space heating system, the energy consumed by the ventilation heat recovery unit is included (installed only with the new dwelling and not with the refurbished one). Thus, the electricity corelated with the ventilation heat recovery machine is inserted in the equation 3.7 denominator, as part of the space heating procedure ($E_{heat\_recovery\_unit}$). Electricity for other uses such as lighting and appliances are not included by definition.

3.5.5. Fraction CO_2e-emission saving ($f_{sav.emis}$)

According to the EU's Directive 2009/28/EC (European Parliament, 2016), a heat pump system is considered as RES if can operate with SPF_{H2} greater than 1.15/η, where η is the efficiency of the power generation and transition system.[9] The EU has set the electrical system efficiency to be 45.5% for all State members by accepting an average until the 2020 (European Parliament,

[9] By aiming to decarbonize the emissions caused by the primary energy

2013). With the electrical system's efficiency to 45.5%, a heat pump system should operate with SPF_{H2} greater the 2.5 in order to be considered as RES. However, for the environmental assessment of PVT based SAGSHP systems, the $SPF_{H2} > 2.5$ is not a difficult aspect due to PVT ability to cogenerate heat and power. The generated electricity from PVT collectors can decarbonize a substantial portion of emissions. By bearing in mind that the SPF_{H2} should be greater than 2.5 for a RES system, a benchmark has been established for SAGSHP systems evaluation.

There is a need for a metric which can compare carbon emissions between different space heating systems. This requirement can be fulfilled via the $f_{sav.emis}$, which indicates the fraction of carbon emissions which were prevented by using SAGSHP system against a natural gas boiler (equation 3.8) (in our case). In equation 3.8, the numerator is the electricity balance between the generation and consumption in the SAGSHP system, while the denominator states the emissions due to gas consumption. The results from the fraction emission saving are presented in Chapter 7, where the comparison of SAGSHP systems with a conventional GHSP and a gas boiler heating system takes place. Finally, for systems environmental impact assessment, the boundaries defied as SPF_{H4} in Figure 3.11 are used.

$$f_{sav.emis} = 1 - \frac{\sum_{i-energysource} [(E_{consumed\_i} \cdot GWP_{e\_i}) - (E_{generated\_i} \cdot GWP_{e\_i})]_{SAGSHP}}{\sum_{i-energysource} [(Q_{consumed\_i} \cdot GWP_{e\_i})]_{GasBoiler}} \quad 3.8$$

Implementation of equation 3.8: With the fractional carbon emission saving the two SAGSHP systems A and B, along with the GSHP system are compared with the NGB heating system. For both SAGSHP systems, the CO_2e emissions made by electricity consumed in the heat pump, circulation pumps and as auxiliary energy are considered. As regards the GSHP system, the only carbon emissive activity is the electricity used by the heat pump, since the circulation pumps is assumed to be embedded in the device. For all investigated systems, in the denominator are placed the total CO_2e emissions caused by the natural gas boiler-based system (4.5.2). Therefore, the emissions made by the CH_4 consumption and by the electricity (circulation pump) are added.

Chapter 4. Systems model and validation

Preparatorily, important information about the system have to be stated. As the heat transfer fluid for both solar and geothermal loop, it is assumed a mixture of 30% by 70% ethylene-glycol with water by weight. The utilized specific heat capacity was set to be 3.72 kJ kg^{-1} K^{-1} and the density at 1035 kg m^{-3} (Incropera *et al.*, 2007a). Similarly, for the dwelling's heating loop, water was used with specific heat capacity of 4.185 kJ kg^{-1} K^{-1} and density 1000 kg m^{-3}.

It is worth noting the weather conditions which were considered for the systems analysis. Table 4.1 shows the monthly total horizontal solar energy per square metre and in Figure 4.2, the annual fluctuation of ambient along with the mains water temperature are presented. The illustrated data are taken from Meteonorm in TMY2 format and formulated to monthly values. Additional to the presented figures, the mean annual wind speed was found to be 4.32 m s^{-1}, while the mean ambient temperature was estimated to be 9.01 ^{o}C.

Finally, the model formulation and validation have been published in Solar Energy scientific journal (Sakellariou *et al.*, 2019)

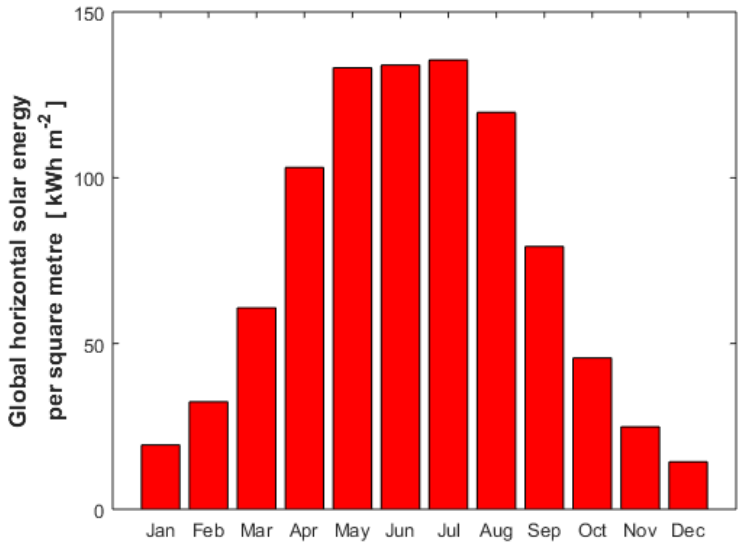

Figure 4.1. Global horizontal solar energy per square meter for Birmingham. Taken from Meteonorm TMY2.

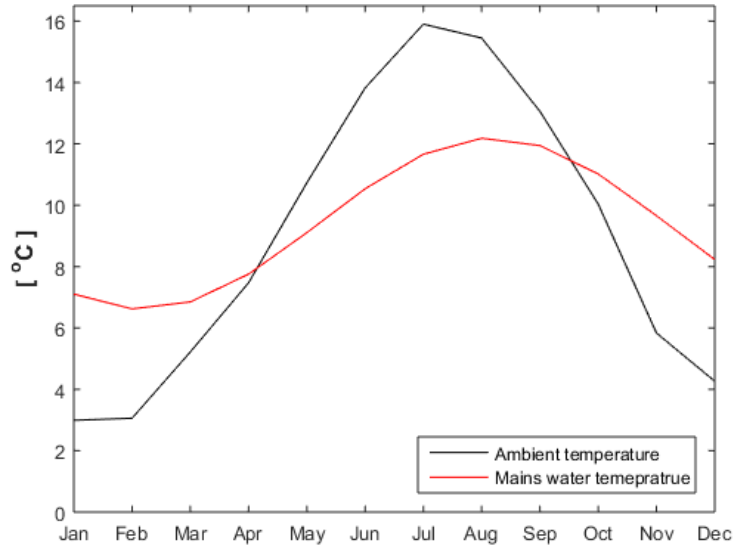

Figure 4.2. Ambient and mains water temperature for Birmingham. Taken from Meteonorm TMY2.

4.1. Solar subsystem

The solar subsystem (or solar loop) is consisted of the components listed in Table 4.1, along with the TRNSYS TYPE utilized for their model.

Table 4.1. Solar subsystem components along with the TRNSYS TYPE utilized or created.

Component	Notes	TRNSYS TYPE
PVT collector	New validated analytic transient model	New TYPE created
Power modulation system	DC to DC converters and DC to AC inverter	No need for TYPE, calculations on the results
solar circulation pump	Solar pump, Figure 3.5 {2}	TYPE 114
EEB heat charging circulation pump	Charging pump, Figure 3.5 {4}	TYPE 114
Piping system with the thermal insulation	The exposed to ambient conditions	TYPE 709
Plate heat exchanger (PHE)	With fixed effectiveness (ε)	New TYPE created

As stated in the methodology overview section 3.1, the electricity generated by PVTs is injected to the power grid. For the current analysis, the power losses from PVTs to the electricity meter device are set to be fixed at 10 % overall. It was assumed, each PVT to be equipped with a DC to DC power converter and all the converters supply the DC to AC inverter. This configuration was chosen for tackling the PV string process which arises by varying the array of collectors.[10] Thus, the power losses are caused by the converters (4%), the inverter (4%) and joule losses in copper cables (2%), hence 10% overall.

The solar circulation pump is sized for every PVT array scenario with the aim to increase the flow rate of the fluid by 200 kg h^{-1} per 4 PVTs. The soil heat charging circulation pump (Figure 3.5 {4}), remains with constants fluid flowrate for all system configurations. Also, the solar pump was constrained to operate only during the day, with the aim to avoid the sudden turn on and off due to lack of substantial ambient energy. The parametric analyses were conducted with the PVT array to vary from 0 to 20 collectors, by increasing with strings of 4 collectors. The maximum count of 20 PVTs was chosen in order to be substantial space for installation with free stand mounted racks on the roof of the dwelling. For each PVT string of 4 collectors, 8 m of insulated

[10] The number of panels in series connected in order to obtain the optimum inverter input voltage.

pipes are installed (exposed to ambient conditions), while it is assumed a fixed inclination of 30^{o} with south facing orientation. The pipes dimensions and thermophysical properties were fixed for all arrays, with inner diameter at 0.024 m, outer diameter at 0.027 m, made of copper with 0.016 m foam insulation with 0.03 W m^{-1} K^{-1} thermal conductivity.

As regards the PHE, this was sized to provide an effectiveness (ε) of 0.7 for all simulation schemes. That was achieved by assuming that the heat charging circulation pump operates with equal mass flow rate to the one provided by the embedded pump in the heat pump (Figure 3.5). All the above stated parameters were equal for both system configurations (A or B), while in Table 4.2 are listed all the related to solar loop values of parameters for all simulation schemes.

Table 4.2. Solar subsystem values of parameters. Where the exponents 1 is for the new dwelling values and the 2 states the refurbished related values.

	Solar Pump		**Charging pump**				**Piping**
PVTs	**Power [W]**	**Flow rate [kg h^{-1}]**	**Power$^{(1)}$ [W]**	**Power$^{(2)}$ [W]**	**Flow rate$^{(1)}$ [kg h^{-1}]**	**Flow rate$^{(2)}$ [kg h^{-1}]**	**length [m]**
0	0	0	0	0	0	0	0
4	20	200	45	60	900	1290	8
8	25	400	45	60	900	1290	16
12	30	600	45	60	900	1290	24
16	40	800	45	60	900	1290	32
20	50	1000	45	60	900	1290	40

The major component of the solar subsystem is the PVT collectors. Therefore, for the research needs, a new transient model was created and validated via experimental data (Sakellariou and Axaopoulos, 2018). The important to use transient validate models of solar collectors for computer based simulations can be highlighted by numerus studies (Bilbao and Sproul, 2015; Guarracino et al., 2016, 2019). Up to now, the available analytic PVT model in the literature are based on the Hottel and Whillier analysis (1955) for flat plate collectors and as this was adjusted for PVTs later by (FLorschuetz, 1979). In contrast with analytical PVT models, there is a pluralistic approach as regards the numerical available models, with increased complexity which makes their implementation a difficult aspect. For SAGSHP system study, an analytic model is preferable for conservation of the simulation time. Although, numerical solutions are suitable for collectors' performance analysis and optimization. The only disadvantage of the existing PVT models is the lack of considering the absorbers heat inertial. This aspect interacts dynamically with the other components and influences the PVT array outlet temperature. Thus, additional experimentation was conducted with the aim to validate a dynamic model which includes the

absorbers heat inertia (Sakellariou and Axaopoulos, 2018). The model is based on fin-heat transfer analysis concept (Incropera et al., 2007b) and the analytic solution of the collector's energy balance first order differential equation, with respect to the heat inertia of the absorber. Further reasons for this attempt where: to gain intuition on the utilized model, the lack of experimental data from the DMU's trial and to create a validated TRNSYS TYPE (fully capable for parametric analysis, thermal and optical).

Table 4.3. PVT collector parameters (Sakellariou and Axaopoulos, 2018)

Basic data	**Value**
PVT total area (m^2)	1.65
PVT absorber plate area (m^2)	1.58
Packing factor (-)	0.9
Azimuth angle, γ (degrees)	0
Inclination, β (degrees)	30
Electrical data	
Cell type	p-Si
PVT peak power (W_e)	235
Nominal electrical efficiency (%)	14.3
Temperature Power coefficient (K^{-1})	-0.0046
Thermal data	
Number of raisers	8
Centre to centre distance between raisers (m)	0.12
External raisers diameter (m)	0.008
Internal raisers diameter (m)	0.006
Absorber aluminium sheet thickness (m)	0.0005
Back side thermal insulation thickness (m)	0.03
Back side thermal insulation conductivity (W m^{-1} K^{-1})	0.04

Driven from the need to validate the new model, an uncovered, flat plate, liquid based PVT collector was built by using a PV panel joined with a plate and sheet absorber (Table 4.3). The new model is based on 1st order differential energy balance equation of the collector which solves analytical and calculates the absorber plate mean temperature. The whole process takes place via iterations, while the validation with experimental data was conducted in MATLAB. The model's analysis was based on three characteristic days regarding the weather conditions: the first day illustrates mild weather conditions until the evening where the sun gave away to the sporadic rain and strong winds (Figure 4.4), the second day was a sunny day (Figure 4.6) and the third was with fully transient ambient conditions (Figure 4.8). The three above days where used to validate the simulation results of the new PVT model. The new PVT transient model found capable of estimating the collector outlet temperature (T_{PVT_out}) with accuracy between 0.6% and 2.06% RMSD. As regards the power generation, the prediction of the model was varying from 4.15% to 5.05% RMSD. The measurements uncertainty study can be reached on the

published paper (Sakellariou and Axaopoulos, 2018). Finally, for the current research needs, the model's equations were written with FORTRAN along with the iterative procedure with the aim to create a DLL for TRNSYS.

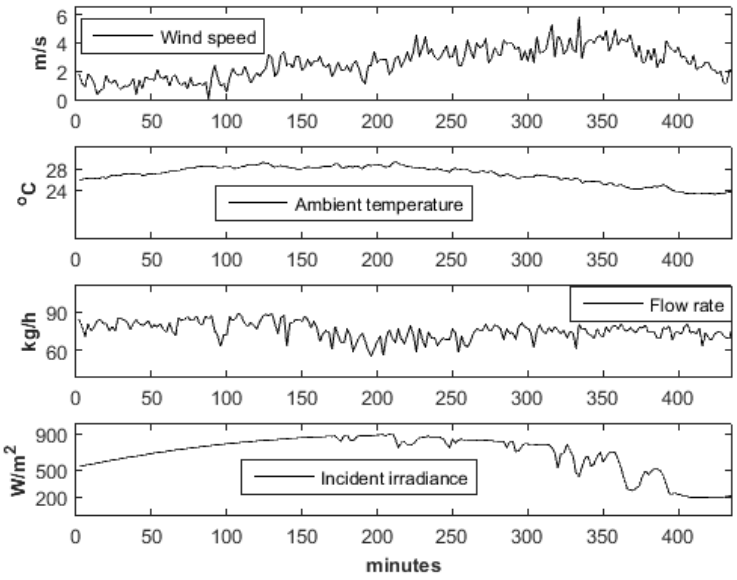

Figure 4.3. Experimental conditions on 02/05/2018

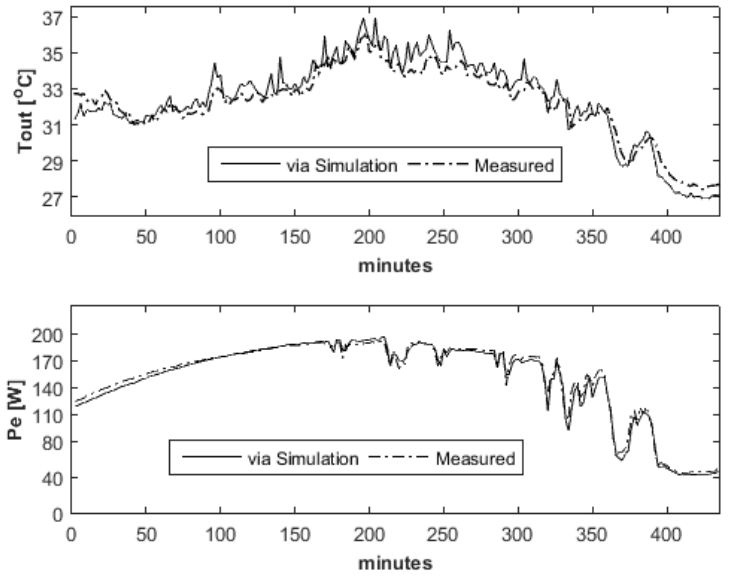

Figure 4.4. Comparison between the simulation results and measured value for T_{out} and P_e, on 2/05/2018 (Sakellariou and Axaopoulos, 2018)

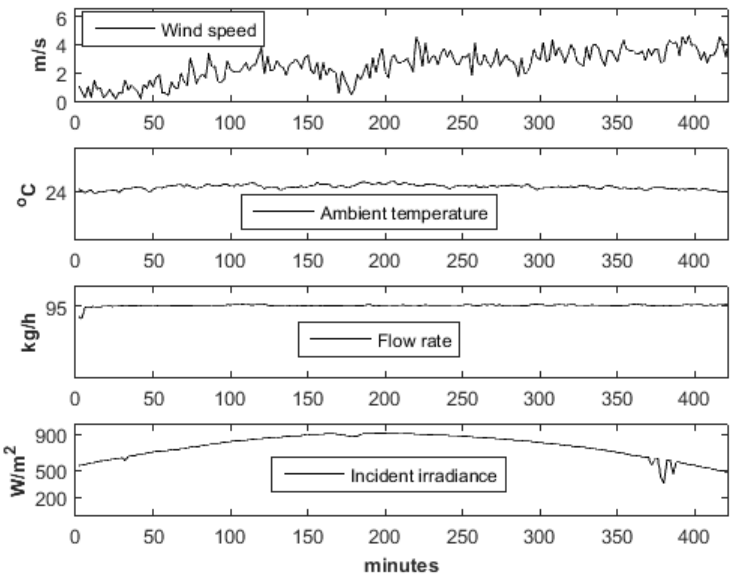

Figure 4.5. Experimental condition on 09/05/2018

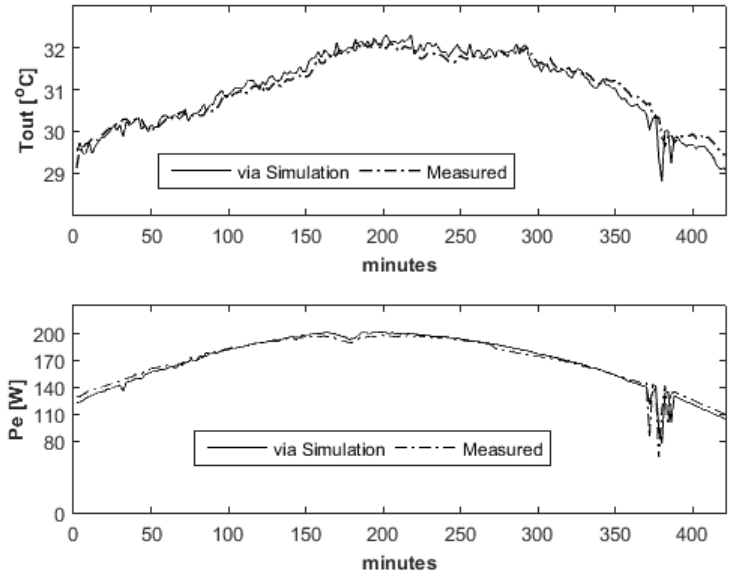

Figure 4.6. Comparison between the simulation results and measured value for T_{out} and P_e, on 9/05/2018 (Sakellariou and Axaopoulos, 2018)

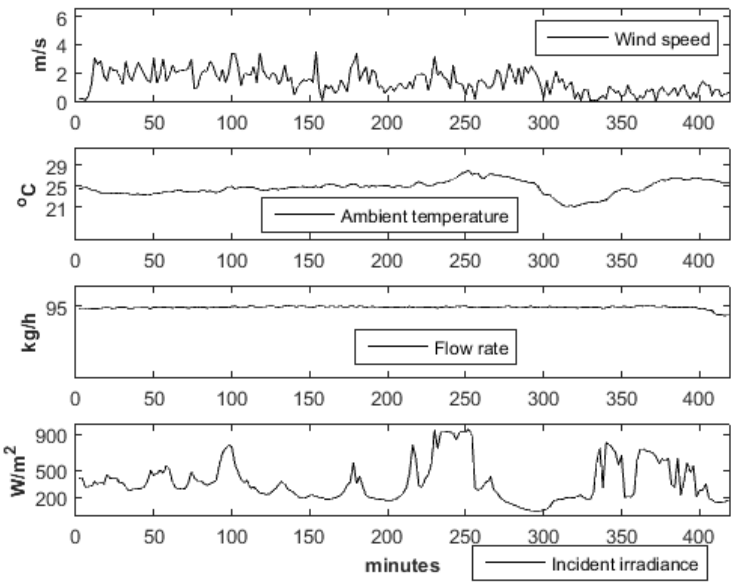

Figure 4.7. Experimental condition on 24/05/2018

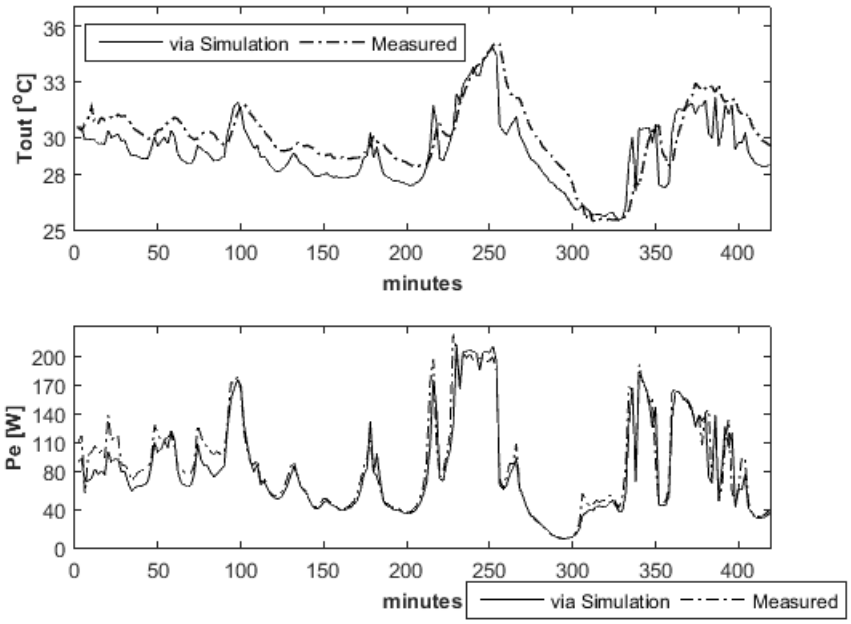

Figure 4.8. Comparison between the simulation results and measured value for T_{out} and P_e, on 24/05/2018 (Sakellariou and Axaopoulos, 2018)

4.2. Geothermal sub system

The geothermal subsystem is comprised by the GHE which is assembled with BHEs (borefield) and the assigned to the borefield soil which formulates the EEB. In this section, the transition from the experimental borefield to this used for the SAGSHP system studies, is done by illustrating the DMU's GHE and then the modeling procedure. The experimental GHE was a novel very shallow borefield formulated by 16 BHEs of 1.5 m long. Perimetrically to the GHE, cemental walls of 0.15m thick were built and inside of that thermal insulation material was placed (the soil volume (V_{EEB}) inside these walls defines the EEB). The EEB was not closed neither insulated on the bottom. The mean spacing among BHEs was 1.5 m and the layout of the borefield is shown by Figure 4.9. The EEB was buried 0.55m below the ground. The insulation was place on the EEB to resemble the installation conditions of EEB being place underneath the dwelling, and to evaluate the impact of this on the heat storage losses. Finally, with Table 4.4, the thermophysical properties of the borefield and EEB are illustrated.

Table 4.4. Parameters and thermophysical properties of the borefield and EEB.

Parameter	**Value**
V_{EEB} (m^3)	47
N_{bor} (BHE number)	16
L_{bor} (m)	1.5
D_{bor} (m)	1.5
Soil thermal conductivity (W m^{-1} K^{-1})	1.5
Soil (clay) specific heat capacity (kJ m^{-3} K^{-1})	2400
Soil diffusivity (m^2 day^{-1})	0.054
Borehole radius (m)	0.075
Outer Radius of Pipe (m)	0.02
Inner Radius of Pipe (m)	0.018
Pipes center-to-center half distance (m)	0.045
Pipe Thermal Conductivity (W m^{-1} K^{-1})	0.33
λ_g (W m^{-1} K^{-1})	0.9
Insulation thickness (top & sides) (m)	0.18
Insulation thermal conductivity (W m^{-1} K^{-1})	0.021
Brine specific heat (kJ/kg K)	3.72
Brine density (kg m^{-3})	1035

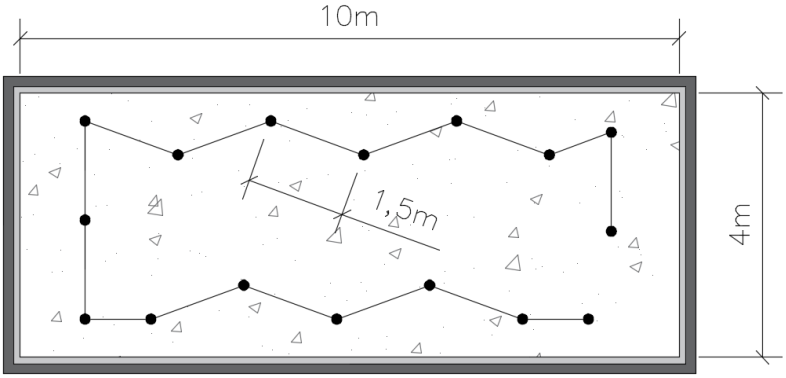

Figure 4.9. DMU's experimental EEB with the borefield (GHE) layout.

In order to model the experimental borefield, the TYPE 557 from TRNSYS was utilized. This is based on Hellström's duct ground heat storage model (DST) (Hellström, 1989) and the temperature of the soil is estimated via superimposing two numerical and one analytical calculation. The heat inertial of the heat removal fluid is consider as function of length in piping and not explicitly function of time. The heat inertia of BHE's grout is neglected. The main difference between the real GHE and the modeling approach is that the DST model sets the borefield cylindrically and symmetrically arranged (Figure 4.10), while the experimental GHE was a rectangular (Figure 4.9). The parameters which were used in order to validate DST model against data are listed in Table 4.4.

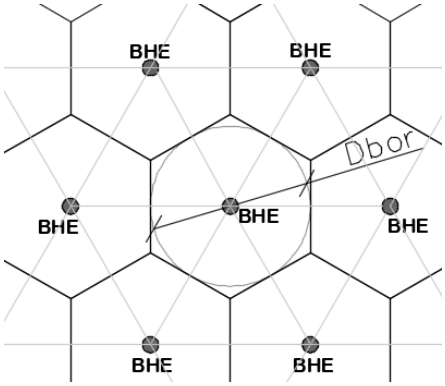

Figure 4.10. DST model allocated hexagonal volume for each BHE (Sakellariou et al., 2019).

For the GHE validation, experimental data of 3500 hours from 6/06/2016 to 28/10/2016 were used. Experimental measurements were taken at 15 minutes interval and then averaged to get hourly values via MATLAB. An uncertainty study was conducted for the experimentational measured parameters and can be found in (Naranjo-Mendoza *et al.*, 2019). Regarding the inputs of the DST model, the GHE's heat transfer fluid inlet temperature and flowrate were used from

experimental measurements, while the ambient temperature (T_a) was obtained from DMU's campus meteorological station. The T_a was set as the boundary condition for the GHE ground surface which is a valid approach for low-rise vegetation (Naranjo-Mendoza *et al.*, 2018), while the initial soil temperature was set to be 12.9 ^oC.[11]

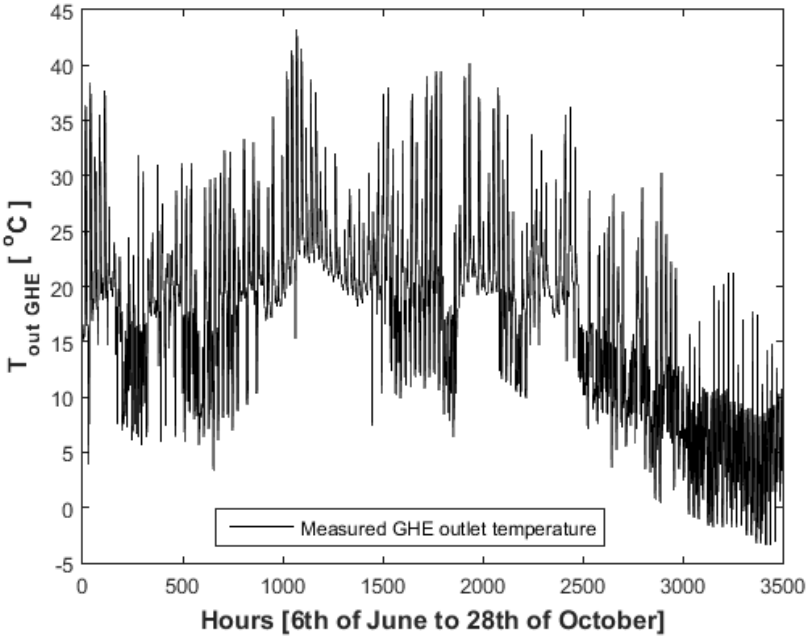

Figure 4.11. Measured GHE's heat transfer fluid outlet temperature during the period 6th of June until the 28th October (Sakellariou et al., 2019).

[11] It is the soil's undisturbed temperature found from DMU's experimental measurements for 1st of September at depth of 2m.

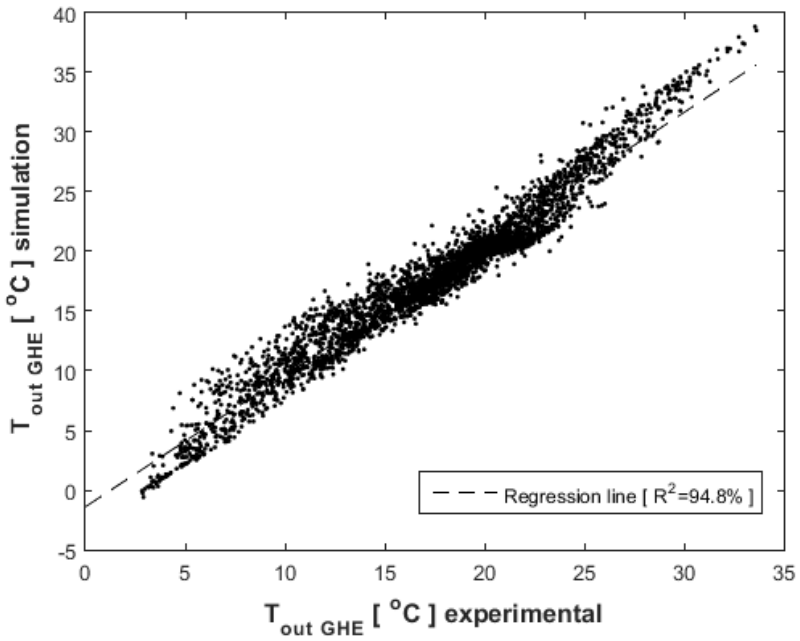

Figure 4.12. Comparative depiction between the simulation results and experimental data for T_{out_GHE} (Sakellariou et al., 2019).

By utilizing the parameters which are shown in Table 4.4 and the experimental measurements, a simulation in TRNSYS with DST model was executed. The GHE's fluid outlet temperature (T_{out_GHE}) (Figure 4.11) was set as the compared parameter. According to the results published by Sakellariou et al. (Sakellariou *et al.*, 2019), a good agreement with measured values was achieved, with RMSD to be 4.43%. Furthermore, Figure 4.12 shows the regression line comparing measurements and simulation results.

As it is already mentioned in section 3.1, during the parametric analyses the borefield gets four sizes and two positions (Figure 3.3). Across the analysis, the BHE dimensions does not change, fixed length (L_{BHE}) and borehole diameter (D_{BHE}). The parameters which alters among simulation schemes are the number of the installed BHEs (N_{BHE}) and V_{EEB}. According to the DST model (Hellström, 1989), the relation which links the number of N_{BHE} with the V_{EEB} is the equation 4.1.

$$V_{EEB} = L_{BHE} \cdot N_{BHE} \cdot \pi \cdot (0,525 D_{BHE})^2 \qquad 4.1$$

As regards the EEB's two potential locations, the exposed one is assumed without any insulation but be buried 0.55 m beneath the surface of the ground. With additional simulations it was found that EEB thermal insulation constrains the natural heat recovery process of the soil and reduces the system's efficiency. The results from these additional simulations are in line with the observation made by (Naranjo-Mendoza *et al.*, 2019) during the experimental data analysis,

regarding the role of the insulation on the EEB. The second potential location of the EEB is to be placed beneath the dwelling (0.02 m below the ground floor slab). For the second scenario, the boundary conditions between the EEB and the dwelling are set to be the mean soil temperature at the top and the mean outer temperature of ground-floor respectively.

During the parametric analysis, the GHE was given four sizes 16, 24, 32 and 40 BHEs. The maximum number of 40 BHEs is derived from the fixed distance among them and from the building's footprint. It is assumed that the EEB should not go over the land area covered by the dwelling. But with the smaller borefields a mismatch between the EEB upper surface and the dwelling footprint exists. This is solved by assuming a very thin layer of insulating material. This is important in order the heat transfer process which is taking place underneath the building to be conducted. If the insulation layer was not entered, the ambient air temperature will be the boundary condition of the GHE and not the dwelling ground slab outer temperature, for the area left uncovered by the EEB. In Table 4.5, the values of the EEB parameters used for simulations are listed, along with the chosen configurations of the BHEs. It is important to be mentioned that derived borefield configurations are influenced by TYPE 557 for numerical solution-stability reasons.

Table 4.5. Volume of the EEB along with the borefields configuration for every simulation scenario.

BHEs	V_{EEB} [m^3]	Borefield configuration (In series BHEs x parallel strings)
16	47.0	16 x 1
24	70.0	12 x 2
32	98.5	16 x 2
40	116.5	10 x 4

4.3. Heat pump

Based on the research needs, two heat pumps were required with different heat capacity, one for the new dwelling and one for the refurbished one. The utilized heat pumps were Brine to Water made by VAILLANT, a well-known German manufacturer. The two heat pump capacities were chosen according to the available devices in order to much as possible as can be with the maximum space heating load derived from dwelling study. Since there is no design procedure for the studied SAGSHP system, the before mentioned heat pump sizing approach can be considered as an action of investigation.

The chosen heat pumps have embedded both circulation pumps, the one for the ground loop and the other for the heating loop. Thus, the electricity consumed by the heat pump includes

the electric compressor and both circulation pumps. In Figure 4.13 the heat pumps operation envelope is shown, outside these temperatures the operation stops for safety reasons.

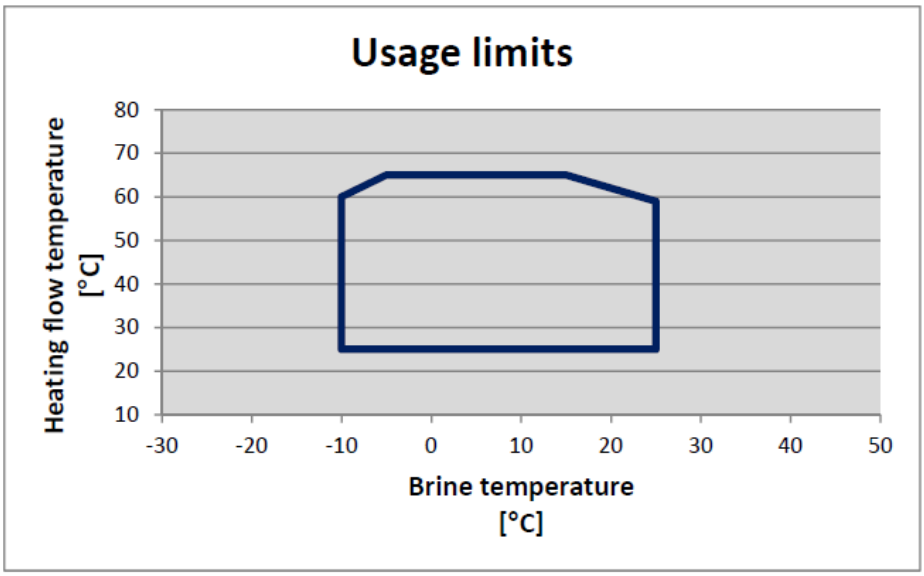

Figure 4.13. Heat pump (VAILLANT, VWF 87/4) operations envelope, adopted from (VAILLANT, Report, 2010).

In order to model the Heat Pump, a new TYPE for the device was built with TRNSYS. The need for the new model has been derived by the improper modelling solution offered by TRNSYS for the investigated system. The available in TRNSYS heat pump model TYPE 919, is based only on normalized data sourced by the manufacturer's performance test (EN 14511). This solution reads the inlet temperatures and estimates the heat delivered and the power consumption. But, the model assumes a certain heat amount to be offered by the soil Q_{ev} (equation 4.2), however, due to luck of design procedure is not currented to be available in the EEB. Therefore, a hybrid new model was developed, which is based partially on performance data according to EN 14511 and partially to the evaporator's absorbed heat. The new modelling approach has been published by (Sakellariou *et al.*, 2019).

The performance data of the heat pump were obtained and normalized in order to be capable to be utilized with any heat capacity and power consumption. The normalized data derived from the VWF 87/4 VAILLANT model and used for both heat pumps (Table 4.6). Regarding temperature operation limits of the heat pump (Figure 4.13), the evaporator accepts brine with temperature from -10°C to 25°C and the condenser delivers water with temperature as low as 25°C up to 65°C.

*Table 4.6. Normalized performance data of VWF 87/4 VAILLANT brine to water heat pump. For temperatures above the 55°C, the model extrapolates linearly the derived values (VAILLANT, Report et al., 2010). * The indicated COP is for the heat pump used on the refurbished dwelling (4.8kW heat capacity).*

Capacity	Power	T_{in_cond} (°C)	T_{in_ev} (°C)	COP*	Capacity	Power	T_{in_cond} (°C)	T_{in_ev} (°C)	COP*
0.78	0.77	25	-10	3.47	1.19	0.85	40	10	4.80
0.89	0.73	25	-5	4.18	1.30	0.85	40	15	5.24
1.00	0.70	25	0	4.90	1.33	0.83	40	20	5.49
1.11	0.68	25	5	5.60	1.36	0.83	40	25	5.62
1.18	0.67	25	10	6.04	0.79	1.07	50	-10	2.53
1.27	0.67	25	15	6.50	0.90	1.05	50	-5	2.94
1.33	0.67	25	20	6.81	1.00	1.03	50	0	3.33
1.36	0.67	25	25	6.96	1.09	1.00	50	5	3.74
0.77	0.77	30	-10	3.43	1.20	1.00	50	10	4.11
0.88	0.73	30	-5	4.13	1.31	1.00	50	15	4.49
0.99	0.70	30	0	4.85	1.35	1.00	50	20	4.63
1.09	0.68	30	5	5.50	1.36	1.00	50	25	4.66
1.17	0.67	30	10	5.99	0.78	1.10	55	-10	2.43
1.26	0.67	30	15	6.45	0.89	1.08	55	-5	2.83
1.32	0.67	30	20	6.75	1.00	1.07	55	0	3.20
1.36	0.67	30	25	6.96	1.09	1.03	55	5	3.63
0.77	0.83	40	-10	3.18	1.20	1.03	55	10	3.99
0.88	0.83	40	-5	3.64	1.31	1.02	55	15	4.40
0.98	0.83	40	0	4.05	1.35	1.02	55	20	4.54
1.08	0.87	40	5	4.26	1.36	1.00	55	25	4.66

The heat pump's model requires as inputs the evaporator (T_{in_ev}) and condenser (T_{in_cond}) inlet temperatures along with the heat offered by the GHE and the solar system. An operation command is also needed in order to turn the heat pump to on and off.[12] The heat pump model is equipped with two input which define if the operation command comes from the space heating thermostat or from the DHW thermostat. In case of the space heating need, the heat pump regulates the outlet temperature of the condenser not to over the 31°C. This temperature found to not cause a floor surface temperature higher than 27 °C, which is the upper limit for under-floor space heating systems. As regards the parameters which are required for the model of the heat pumps, these are listed in Table 4.7.

[12] One operation command for the space heating mode and one operation command from the DHW mode. Both commands are offered by the thermostats assigned for each system. The heat pump delivers heat at 31 °C for the space heating and at 60 °C for the DHW.

Table 4.7. Parameters and values of the heat pumps used for both dwelling types.

	Heat pump used value for both dwellings	
Parameter	**New**	**Refurbished**
Nominal heat capacity (Q_{cond_no})	3.00 kW_{TH}	4.80 kW_{TH}
Nominal power consumption (P_{HP_no})	0.78 kW_e	1.40 kW_e
Evaporator Flow rate	900 kg h^{-1}	1290 kg h^{-1}
Condenser Flow rate	576 kg h^{-1}	920 kg h^{-1}

The procedure for the new heat pump model is as follows:

1. The T_{in_ev} and T_{in_cond} are used to estimate, via linear interpolation from normalized performance data, the HP condenser heat (Q_{cond}) and the consumed power (P_{HP}).
2. With the estimated Q_{cond} and P_{HP}, the evaporator's absorbed heat (Q_{ev}) can be calculated via equation 4.2. Then with the calculated Q_{ev} and equation 4.3, the evaporator's outlet temperature T_{out_ev} can be found.
3. Based on T_{out_ev} calculated from equation 4.3, the available heat from GHE and solar system are summed in order to find the total available heat Q_{ev_avail} which enters the evaporator.
4. Then, the estimated Q_{ev_avail} is added on the P_{HP} in order to end up with the heat pump's delivered condenser heat Q_{cond_deliv}. As explained already, the evaporator heat is estimated implicitly through performance data. The estimated Q_{ev}, is a theoretical value based on the operational conditions applied during the test (EN14511). In real systems, the GHE or the solar systems may not be capable of delivering the required amount of heat. Therefore, the delivered energy by the geothermal and the solar system is utilized to complete the calculation. Also, if the Q_{ev_avail} is greater that the Q_{ev}, then the estimated value of Q_{ev} is used for calculation.
5. Finally, by utilizing the Q_{cond_deliv} in equation 4.4, the condenser's outlet temperature can be estimated T_{out_cond}.

$$Q_{ev} = Q_{cond} - P_{HP} \qquad 4.2$$

$$T_{out\_ev} = T_{in\_ev} - \frac{Q_{ev}}{\overset{o}{(mCp)}_{ev}} \qquad 4.3$$

$$T_{out\_cond} = T_{in\_cond} + \frac{Q_{cond\_deliv}}{\overset{o}{(mCp)}_{cond}} \qquad 4.4$$

At the time of the DMU's experimental data analysis conducted by Naranjo-Mendoza et al. (2019), a problem detected regarding the inlet temperature of the evaporator, the values found to be above the device's operation envelop. During simulations, this issue was traced no more than three time per year. The heat pump was set to wait for the next simulation time step in order to start again the operation, while for the experimental device an acknowledgement-action was required by the occupants. The simulation time step was set to 1 hour and that cease the PVT to BHEs sub-hour dynamic operation, the heat inertia is included on the delivered energy but with the mean temperature. Through the experimental data analysis (Naranjo-Mendoza *et al.*, 2019) was found that the inertia of the BHEs is an important aspect for the system operation. In real conditions, the above mention issue can be solved by installing a small buffer tank (30-40 L) between the borefield and the evaporator and/ or temperature control valve, these modifications can compensate any dynamically risen temperature of the brine entering evaporator.

4.4. Heating load

The role of the SAGSHP system was to provide space heating for the dwelling and to cover the DHW demand. Regarding the space heating two schemes were set, the dwelling to be built in accordance with the regulations for new domestic building L1A and the dwelling being refurbished in line with L2A regulations. Both dwelling scenarios share the same building dimensions and layout, as illustrated by Figure 4.14. It was assumed that, the building was two-storey one with the total living floor area of 120 m^2 and was occupied by a four-member family. Under-floor space heating system was installed in the total heated area of 120 m^2, while each floor was considered as a thermal zone heated up to 20 ^oC (mean air temperature). The space heating thermostat was set to operates with ± 1.5 ^oC dead band, which means at 21.5 ^oC turn-off the heat pump and at 18.5 ^oC turn-on the heat pump. The relative humidity in the dwelling did not influence the operation of the thermostat, which was taken to be based totally on mean air temperature of the two thermal zones. In other words, the conform conditions (temperature and humidity envelop) were excluded from the current analysis, as the aim of the research was to evaluate the SAGSHP system. Finally, for both dwellings, it was assumed that were built in Birmingham, Midlands, UK.

In Table 4.8 are listed the minimum heat insulation requirements and the maximum permittable infiltration according to building regulations. For both dwellings, the ground floor level shapes the first thermal zone with 156 m^3 air volume and the second one consists the second thermal

zone with 144 m^3 air volume. For both dwellings the windows were estimated to obtain a U-value of 1.4 W m^{-2} K^{-1} and the g-value 0.63 (in accordance with L1A). For the dwellings model, TRNSYS TYPE 56 was utilized by inserting the building's description file created by the TRNbuild. The TRNbuild is a peripheral software of TRNSYS in which the user can formulate the building (detentions, orientation, wall U-values and all the important aspects). Regarding the TYPE 56, it is a dynamic model which accounts the solar gains and internal gains. The under-floor heating system was modeled by creating an active layer on the TRNbuild platform. For both systems A or B, the space heating auxiliary energy was assumed to be offered after the heat pump's condenser outlet, by setting the water to reach the 31 °C (subsection 4.3). Also, it was assumed that, the additional energy was supplied via electricity consumption.

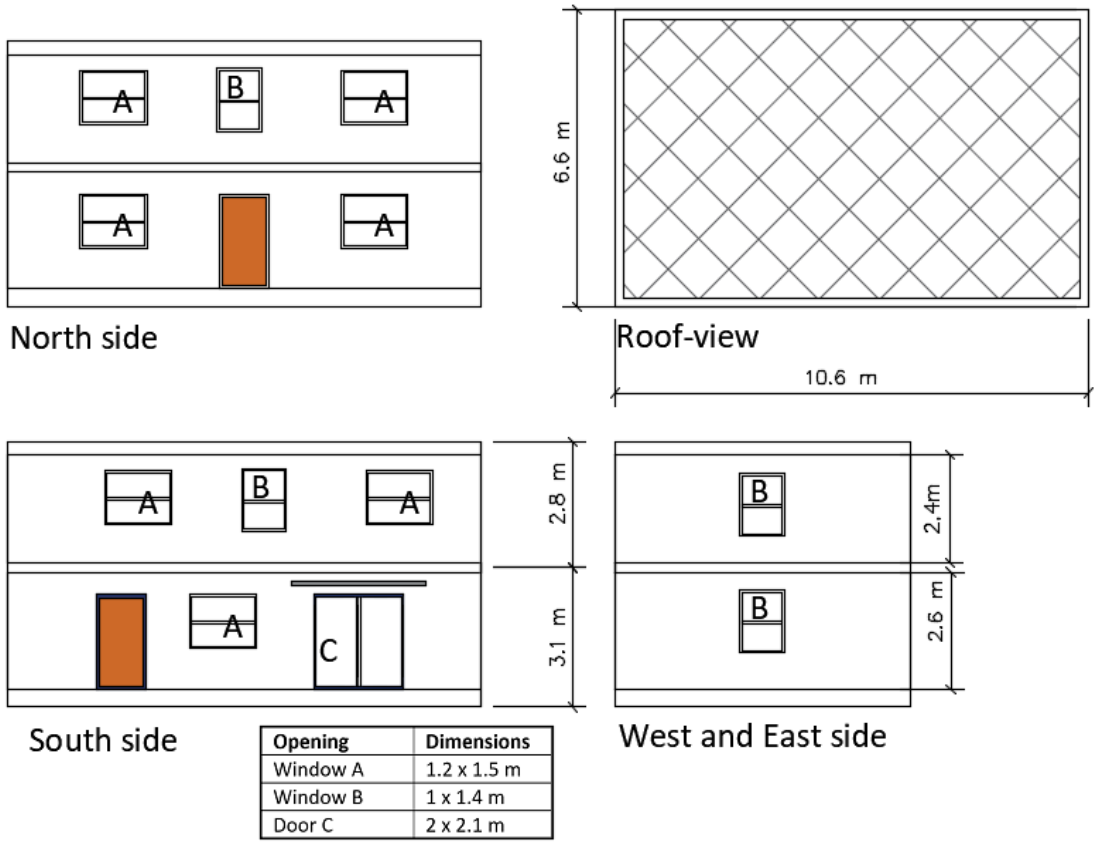

Opening	Dimensions
Window A	1.2 x 1.5 m
Window B	1 x 1.4 m
Door C	2 x 2.1 m

Figure 4.14. Dwelling's external dimensions and layout.

The internal heat gains were simplified by accounting limited number of those (Table 4.9). The simplicity of the internal heat gains was related to the research questions and aim, which was about to investigate the space heating system and not the dwelling's heat performance. In the current study, the dwellings are used as a dynamic heat loads which are models in acceptance detail for purpose of the simulations.

Table 4.8. Minimum U-values and maximum infiltration requirements for the new and refurbished dwelling.

Dwelling	Ground floor [W $m^{-2} K^{-1}$]	External walls [W $m^{-2} K^{-1}$]	External roof [W $m^{-2} K^{-1}$]	Permissible ACH [air changes per hour]
New with L1A	0.13	0.18	0.13	5 $m^3 h^{-1} m^{-2}$
Refurbished with L1B	0.25	0.30	0.18	1 to 2 ACH

By assessing the heat demand for the new dwelling via TRNSYS, this was found to be 3522 kWh_{TH} per year in total. The maximum heat load was estimated at 2.17 kW_{TH}. The ACH index was set to 1, from which the 0.2 was caused by infiltration and the 0.8 by mechanical validation with heat recovery capability. It was assumed that, the mechanical ventilation was capable to recover the 80 % of the heat from the extracted air. Also, for the mechanical ventilation and the heat recovery mechanism, 173 kWh_e of electricity was consumed per year. In Table 4.10, the utilized U-values and the synthesis of the dwelling's external surfaces are listed.

Table 4.9. Internal heat gains for both dwellings, new and refurbished.

TYPE	Internal Gains
Occupants – persons	4 by 150 W (sensible and latent heat) light work, seated (EN ISO 7730) • 20:00 to 08:00 – 4 persons • 08:00 to 15:00 – 1 person • 15:00 to 20:00 – 3 persons
Oven	• 06:00 to 08:00 – 600 W (sensible and latent heat) • 11:00 to 12:00 – 2000 W (sensible and latent heat) • 17:00 to 18:00 – 1000 W (sensible and latent heat)

As regards the refurbished dwelling, the ACH was set to 1.2 and it was assumed to be a result of infiltration in total. The heating demand was estimated via TRNSYS to be 9740 kWh_{TH} per year and the maximum heat load requirement to be at 4.07 kW_{TH}. The refurbished house was not equipped with mechanical ventilation and heat recovery system. The used U-values of dwelling's outer walls are listed in Table 4.11.

Table 4.10. External surfaces U-values and synthesis for the new dwelling.

Component	U-value [W m^{-2} K^{-1}]	Layering Analysis			
		External layer [m]	Insulation [m]	Internal layer [m]	Total width [m]
External walls	0.174	Combined brick (0.2)	Polyurethane (0.1)	Gypsum- board (0.02)	0.35
Ground floor	0.130	steel reinforced concrete slab (0.15)	Polystyrene Expanded (0.28)	Grout with the active layer embodied - pipes (0.09)	0.525
External roof	0.123	steel reinforced concrete slab (0.15)	Polyurethane (0.15)	Gypsum- board (0.02)	0.32

Table 4.11. External surfaces U-values and synthesis for the refurbished dwelling.

Component	U-value [W m^{-2} K^{-1}]	Layering Analysis		
		External layer or additional material [m]	Existing structure - Internal side [m]	Total width [m]
External walls	0.288	Polystyrene Expanded placed externally (0.07)	Internal brick (0.12) + Mineral-wool (0.02) + air (0.02) + external brick (0.12)	0.35
Ground floor	0.132	Polystyrene Expanded (0.28) + Grout with the active layer embodied - pipes (0.09)	steel reinforced concrete slab- boundary layer with the ground (0.15)	0.52
External roof	0.175	steel light-reinforced concrete slab (0.15) + Polystyrene Expanded (0.20)	steel reinforced concrete slab (0.15)	0.40

In order to verify the method used for the dwellings model, a comparison with the Design Builder (Energy Plus) took place. The refurbished dwelling was used with both simulation platforms, and the heat demand was estimated. In Figure 4.15, the simulation results from both methods are compared, and the discrepancy between them was estimated to be 1.37% of standard deviation. With TRNSYS the annual heat demand was estimated to be 9740 kWh_{TH} and for the Design Builder at 9606 kWh_{TH}. Based on the results, it can be concluded that there is nothing significant missing from the model of the dwellings.

With regard to the DHW consumption, 35L per person per day at 50°C was assumed (Energy Monitoring Company, 2008). The profile of DHW usage is shown in Figure 4.16, while the adopted consumption pattern was adapted from the widely used f-Chart method (Duffie and Beckman, 2013). The total annual heating demand for the DHW was estimated to be 2528 kWh_{TH}, by assuming the water entering the tank to be the temperature of the mains and to be delivered for consumption at 50°C. Lastly, in case of the water exiting the tank in lower temperature than the set one (50°C), an electrical fast heater was responsible to supply the remaining part (Auxiliary heat for DHW).

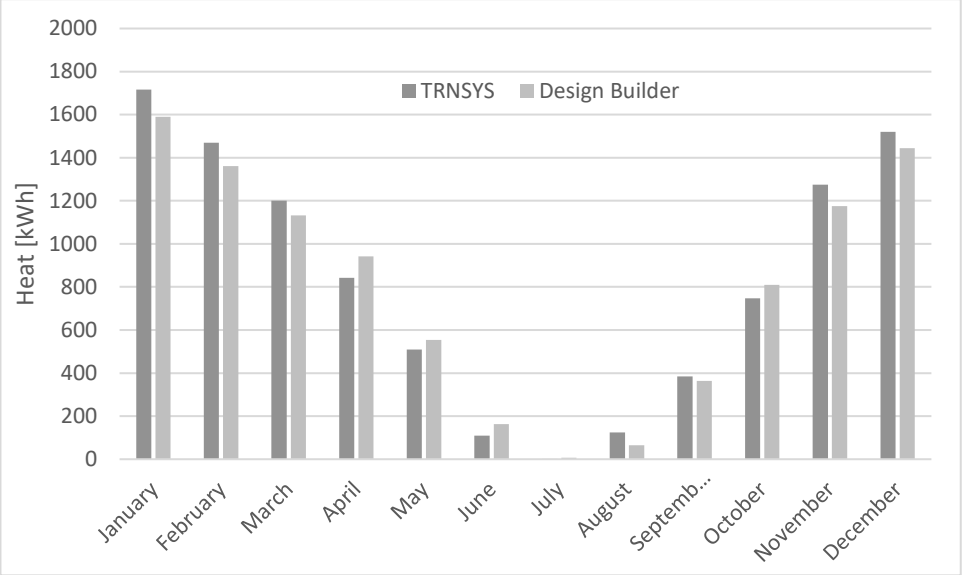

Figure 4.15. Monthly heat demand estimation by using TRNSYS and Design Builder (Energy Plus).

A DHW tank with 200 L capacity was installed and modelled with TYPE 60. Also, the tank was equipped with one embedded heat exchanger for the system A (HX1, Figure 3.5) and two heat exchangers for system B (HX1 & HX2, Figure 3.7). The stratification of water in the tank was model by assuming 5 layers with equally volume. The tank was cylindrical with internal dimensions of 1 m high and 0.5 m diameter. Both merged heat exchangers were assumed to have 10 m length with internal pipe diameter of 0.018 m and external pipe diameter of 0.02 m. Additionally, the heat exchangers were made from copper, while were equipped with 40 fins per meter of 0.024 m diameter. The dimensions of heat exchanger entail to 0.25 m of the tank's height as an installation requirement (with 6.3 revolutions of the pipe). For system A, the heat pump offers the heat to the heat exchanger place at the bottom of the tank, while on system B, the heat pump offers the heat at the tank's upper part. The configuration of the pipes which entering and exiting the tank, are shown in both systems layouts by Figure 3.5 and Figure 3.7.

The tank it was assumed to be insulated with heat loss coefficient of 0.6 W m^{-2} K^{-1}, the losses was set to be between the in the tank water temperature (at every layer) and the ground floor mean air temperature (by assuming that the tank is installed on the ground floor). Also, the main water enters the tank at 0.05 m above the bottom and exits at 1 m. Finally, the thermostat was set to measure the tank's upper thermal stratified layer and from there to evaluate the DHW needs. The thermostat was set to operate at 50 °C, with the dead band of ±3 °C.

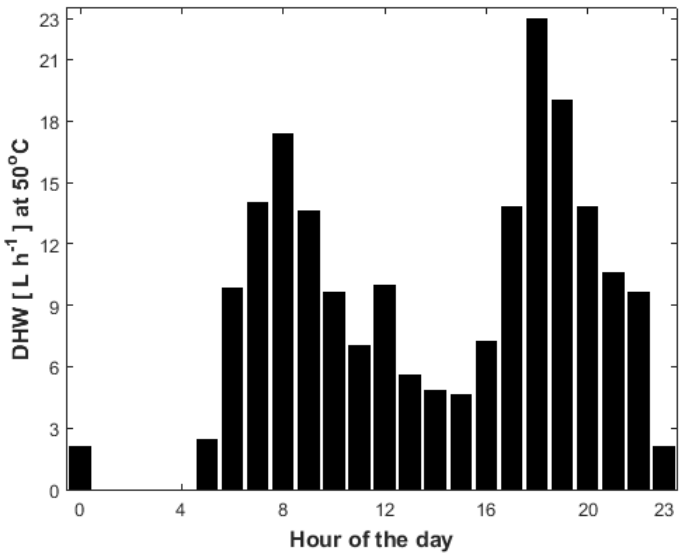

Figure 4.16. DHW daily consumption profile.

4.5. Ground source heat pump and natural gas-based systems

This section provides information regarding two space heating systems which are compared regarding the carbon emissions with the SAGSHP system in Chapter 7.

4.5.1. Ground source heat pump system

For both dwellings, the new and the refurbished, a U shaped BHE (U-BHE) was sized with the ASHRAE method, as this was proposed by (Philippe *et al.*, 2010). The method superimposes four solutions related to heating load with the aim to estimate the required length of the borefield or the borehole. Also, the loads are considered to be extracted from the soil: as the peak load (q_h), as the highest monthly ground load (q_m) and the average yearly ground heat load (q_y).[13] The correlation between the ground load and the space heating load is achieved by entering the

[13] The q_h is used two time with two different thermal resistance, the R_b (BHE's effective thermal resistance) and the R_{6h} (Soil's effective thermal resistance corresponding to a 6 h load).

nominal COP of the heat pump. For calculations, all the thermophysical properties used for the experimental borefield (DMU's) are adopted for U-BHE length estimation (Table 4.4). Also, the undisturbed ground temperature (T_{s_und}) is required, thus was estimated via equation 4.5 (Badache *et al.*, 2016), where T_{a_mean} is the mean annual ambient temperature[14]. Thus, the T_{s_und} was estimated to be 13.09 °C by accepting the T_{a_mean} to be 9.01 °C for Birmingham. Based on calculations, the length of U-BHE for the new dwelling was estimated to be 27m and for the refurbished 53m. Additional U-BHEs lengths, the assigned soil volume was estimated to be 276 m^3 and 553 m^3, for the new and refurbished dwelling respectively. This allocated soil volume was calculated by assuming a radius of 2 m from the center of the U-BHE (this is used for mean soil temperature estimation). The utilized heat loads and COP are listed in Table 4.12, the heat loads have been derived by processing the data offered via TRNSYS for the space heating demand study.

$$T_{s\_und} = 17.898 + 0.951 \cdot T_{a\_mean} \qquad 4.5$$

Table 4.12. Heating loads used for U-BHE length estimation for both dwellings.

Parameter	New dwelling	Refurbished dwelling
q_h	2172 W	4073 W
q_m	1065 W	2332 W
q_y	401 W	1112 W
COP	3.5	3.5

It is important to be mentioned that, the topology of the GHSP system alters from this of SAGSHP system only at the energy harvest side. In other words, from the heat pump and to the right (Figure 3.5), the GSHP system remains the same with the SAGSHP system (by aiming not to change the heating system). The heat pump device used for the SAGSHP systems is utilized also for the GSHP, though, the only control needed for the GSHP system operation is the two thermostats, one from the space heating and the other for the DHW tank. Lastly, the only conventional energy source needed for the operation of the GSHP system is the electricity consumed in the heat pump.

For the GSHP system's modelling needs, data from Beier et al. (2011) used to validate the TRNSYS TYPE 557. The offered data are based on experiment conducted via a sandbox and offer the BHE dimensions along with the sand's thermophysical properties. The parameters and

[14] All temperatures are entered in Kelvins.

properties used by (Beier, Smith and Spitler, 2011) where entered to TYPE 557. Then a simulation was executed in TRNSYS. In Figure 4.17, the simulation results are contrasted with the experimental data, while the GHE outlet temperature was set as the comparative value. As it can be seen from the results, the available data illustrate an interruption on the supplied fluid after 500th min of operation. In this instance the TYPE 557 cannot follow the measurements, because the BHE heat inertia is not considered on its calculations. Though, the simulations for both dwelling were conducted with 1-hour simulation time step, thus the effect of the BHE heat inertial does not significantly influence the results. Finally, the RMSD% between the results and the offered data was estimated to be 0.75% (the value is estimated only for the flowrate existing time). It can be concluded that, TRNSYS's TYPE 557 can be used to simulate single BHE with acceptable accuracy.

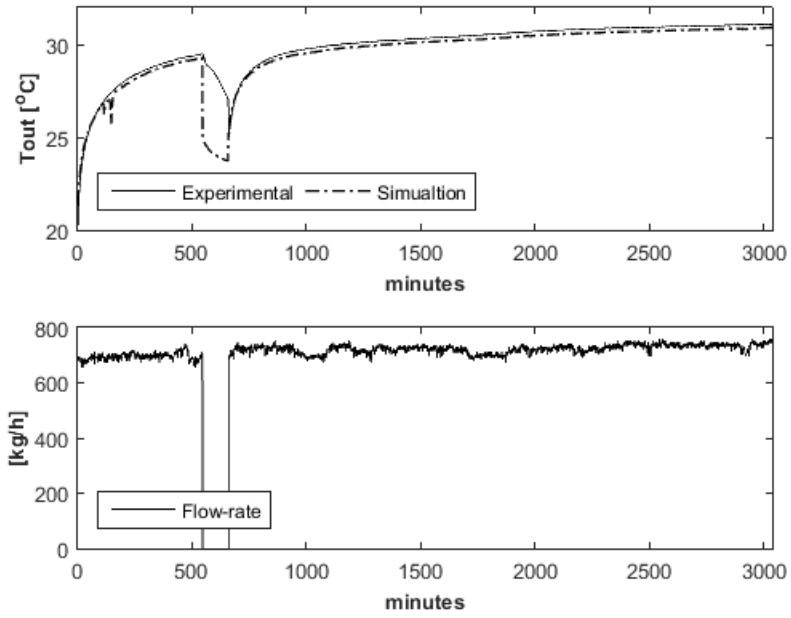

Figure 4.17. GHE outlet fluid temperature comparison between data resourced by (Beier, Smith and Spitler, 2011) and TYPE 557.

4.5.2. Natural gas boiler-based system

The energy flow of the natural gas boiler (NGB) based system is shown in Figure 4.18. The NGB system consumes natural gas and electricity for the circulation pump (is the right side of the gas boiler in Figure 4.18). The system was based on a conventional gas boiler without heat recovery system via the exhaust gas condensation; thus, the water was driven at the underfloor space heating system without any additional equipment. For the simulation need, TRNSYS TYPE 700 was used, with two set point temperatures: one at 31 ^{o}C for the space heating system and the

other to be at 60 °C for DHW. The nominal thermal efficiency of the boiler was set to be 94 % (fixed), and it was resourced from VAILLANT's domestic product (ecoTEC).

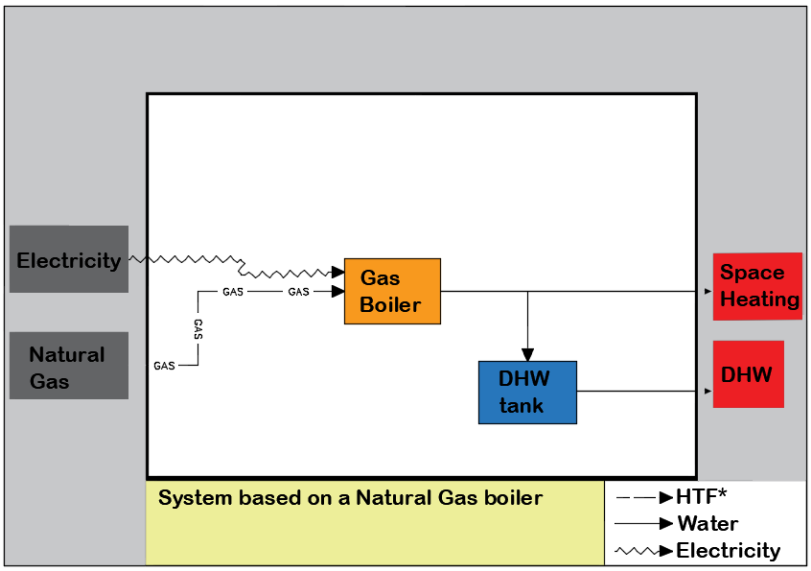

*Figure 4.18. System based on natural gas boiler. *HTF: heat transfer fluid*

Chapter 5. Results evaluation for the new dwelling

This chapter is split into two sections, the one dedicated to the evaluation of the results from heat perspective (5.1) and the second section evaluates the electric output of the systems (5.2). The first four subsections of the first section 5.1 illustrated and discuss the results from the evaluation of the energy performance metrics, while the 5th (5.1.5) summarizes the findings of the section. The metrics used for the heat output evaluation are: a) the RHF, which depicts the system's heat fraction supplied by renewable energy (subsection Renewable Heat Fraction (RHF) 3.5.3), b) the system's heat productivity, which shows the annual renewable heat production per PVT collector (subsection 3.5.2), c) the PVT heat productivity, which illustrates the annual heat production of the collectors (subsection 3.5.2), and d) the SPF_{H4} (subsection 3.5.1). The second section 5.2 contains three sub sections. The first two subsections are dedicated to the discussion on the electric results, while the last subsection summarizes the results of the section 5.2 and provides additional discussion. The electric output evaluation (first two subsections of section 5.2) is split in two subsections (metrics): one for the PVTs' electric specific productivity (SP_{PVT_el}) (5.2.1) and the second for renewable power fraction (RPF) (5.2.2).

In Table 5.1, all simulation schemes are listed and described along with their used acronymic name (also see Figure 3.4). Information about the simulation scenarios can be found in section 3.1, in where the utilized research procedure is summarized. Additionally, a more specified description about the two system topologies (A and B) can be reached via section 3.2.

Table 5.1. All simulation schemes along with their acronymic names and description for the new dwelling.

SAGSHP system acronymic name	Description
A_NE	System built with A topology (A, without direct use of solar heat), in the new Dwelling (N) and with the GHE exposed (E)
B_NE	System built with B topology (B, with direct use of solar heat), in the new Dwelling (N) and with the GHE exposed (E)
A_NB	System built with A topology (A, without direct use of solar heat), in the new Dwelling (N) and with the GHE beneath the building (B)
B_NB	System built with B topology (B, with direct use of solar heat), in the new Dwelling (N) and with the GHE beneath the building (B)

5.1. Heat output evaluation for the new dwelling

5.1.1. New dwelling renewable heat fraction

The first indicator is the system's renewable heat fraction (RHF) (subsection 3.5.3). With the RHF, the heat demand which has been covered by renewables is depicted, while is an explicit way to identify the system's heat independence from convectional energy sources. In Figure 5.1, the RHF is plotted for the new house and for system A with the EEB being exposed , this scenario has the acronymic name A_NE (Table 3.1 and Table 5.1). The parametric analysis is done by varying the quantity of PVT collectors from 0 to 20 and the BHEs from 16 to 40 (section 3.1).

The results plotted in Figure 5.1 shows that the A_NE system's RHF to vary from 0.45 to 0.79, with the lower value for the system without PVTs and 16 BHEs, and the highest for the system with 40 BHEs paired with 20 PVTs respectively. The non-PVT scenarios stands for a pure geothermal based system, and as it can be seen in Table 5.2, the non-PVT systems' RHF hold values from 0.45 to 0.69, for the smaller and bigger borefield respectively. Also, the listed results (Table 5.2) illustrate that the A_NE system's RHF depends more on the size of the PVT array for small borefields. Therefore, the greatest increase of 0.25 RHF (from 0.45 to 0.70) is found for the system equipped with a borefield of 16 BHEs paired with 20 PVT collectors. In contrast the largest borefield, obtained a RHF gain from the non-PVT to 20 PVTs of 0.1. Also, by enlarging the PVT array a non-proportional improvement of RHF is caused. For instance, for the system with 24 BHEs, by adding the first 4 PVTs an improvement of 0.09 RHF is made, but with the next PVT array of 8 collectors the improvement dropped to 0.04 RHF.

Table 5.2. System's A_NE achieved RHF.

	RHF			
PVTs	**16 BHE**	**24 BHE**	**32 BHE**	**40 BHE**
0	0.45	0.56	0.65	0.69
4	0.57	0.65	0.70	0.74
8	0.62	0.69	0.73	0.76
12	0.66	0.71	0.75	0.77
16	0.68	0.73	0.77	0.78
20	0.70	0.75	0.78	0.79

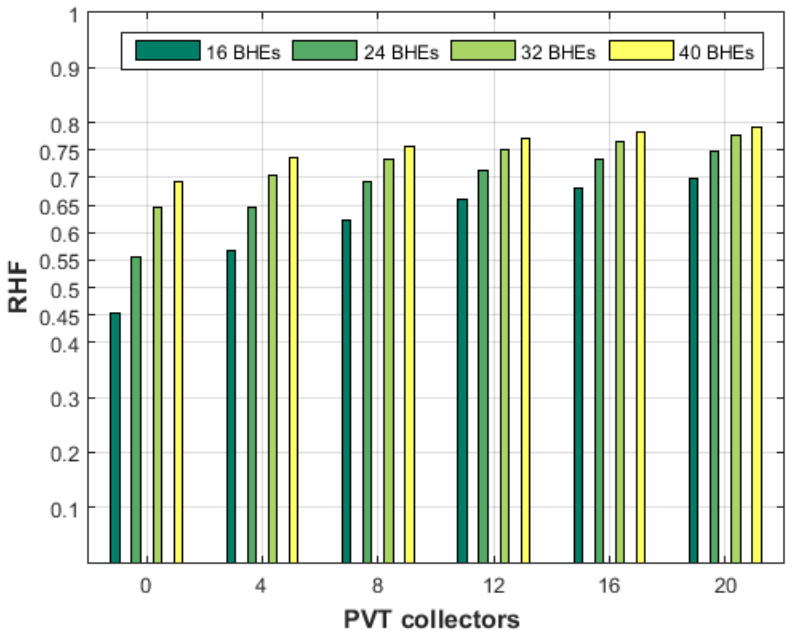

Figure 5.1. System A_NE renewable heat fraction (RHF) for parametric analysis of PVT collectors from 0 to 20 and for BHEs from 16 to 40.

The larger GHEs get better system heat independence against the smaller ones, due to more available heat offered via the soil which can be absorbed effectively by the increased number of BHEs, which means larger heat transfer area. In numbers, the GHE with 16 BHEs formulates an EEB of 46.76 m^3,at the same time, the GHE with 40 BHEs shapes an EEB's available volume at 116.90 m^3 (section 4.2). The larger EEB of 40 BHEs, has 2.49 times greater soil mass than the smaller one and 2.5 times more available heat transfer area (between the refrigerant and the soil).

The PVT collectors' higher contribution on the RHF with the smaller GHE of 16 BHEs is made due to the soil's dropped temperature: the soil temperature in the small GHE is lower than a larger one because it has lower heat capacity, therefore the heat absorbed by the heat pump reduces easily the ground temperature. With the soil temperature being reduced, the PVTs' critical irradiance is lower and therefore can operate more and offer more solar heat into the system. Also, a lower collectors' inlet temperature influence positively their thermal efficiency.

As it is evidently stated in the paragraphs above, the investigated SAGSHP system is benefited the most by the energy delivered from the soil rather the energy offered by the PVTs. This preference is developed due to the reasons listed below:

- The heat stored in the soil is all day available, unlikely the solar energy which is only during the day and it can be utilized under specific conditions (irradiance level, soil temperature, ambient temperature, need for heat demand etc.).
- From 1593 kWh / year of solar energy incidents on each PVT (section 4.1), only a small fraction is absorbed by the systems. The factors which constrain the larger heat absorption have been investigated and determined with additional studies (Sakellariou *et al.*, 2019). Namely, the PHE's effectiveness, along with the EEB's storage capacity and the BHE's effective heat resistance are the main reasons for this restriction.

By hypothesizing that the EEB is built below the dwelling's ground floor slab, Figure 5.2 illustrates the RHF achieved by A_NB system, for PVTs and BHEs quantity variation. By observing the Figure 5.2 and Figure 5.1, system A_NB shows higher dependence on the solar system than system A_NE. Also, in the case of the smallest borefield (16 BHEs) for A_NB system, the RHF is more than doubled from 0.33 to 0.68 by adding 20 PVTs (Table 5.3) on top of the borefield. Based on the listed RHF values in Table 5.3, the influence of the solar system on the RHF cease as the GHE enlarges.

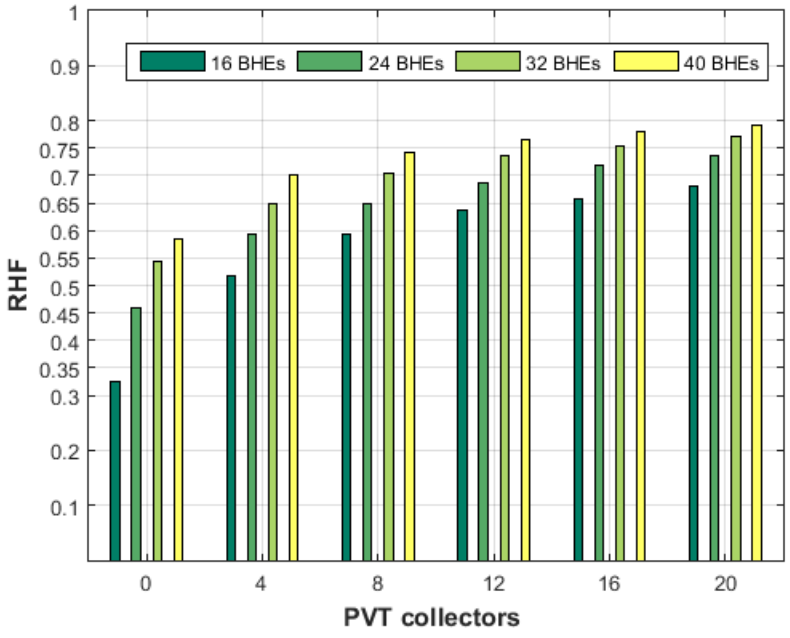

Figure 5.2. System A_NB renewable heat fraction (RHF) for parametric analysis of PVT collectors from 0 to 20 and for BHEs from 16 to 40.

Based on the results listed in Table 5.3, the A_NB system's lower and the higher heat dependencies are 0.33 and 0.79 respectively, for the system with 16 BHEs without PVTs and the one equipped with 40 BHEs and 20 PVT collectors. Also, the RHF increases rapidly when an array

of 4 PVT collectors is used by the system. The RHF elevation of 0.25, 0.14, 0.11 and 0.11 is estimated by adding 4 PVTs on the borefields of 16, 24, 32 and 40 BHEs respectively.

Table 5.3. System's A_NB achieved RHF.

	RHF			
PVTs	**16 BHE**	**24 BHE**	**32 BHE**	**40 BHE**
0	0.33	0.46	0.54	0.59
4	0.52	0.59	0.65	0.70
8	0.59	0.65	0.70	0.74
12	0.64	0.69	0.73	0.77
16	0.66	0.72	0.75	0.78
20	0.68	0.74	0.77	0.79

Table 5.4 lists the differences of RHF obtained by A_NE against A_NB system. Based on the listed RHF values (Table 5.4), system A_NE is capable of greater heat independence than system A_NB, for the majority of PVTs and GHEs pairs. The disparity is greater for non PVTs scenarios and reduces as the collectors' array is getting larger. The two systems obtain equally heat contribution for the borefield of 40 BHEs paired with PVT arrays larger than 8 collectors. Nerveless, with a wider perspective on the RHF disparities listed in Table 5.4, system with 0.01 to 0.02 difference may be considered equally capable for systems heat independence. By accepting this approach of up to 2% lower RHF, it may be concluded that systems with PVT array larger than 8 collectors, offer similar system's heat independence.

Table 5.4. Difference of RHF between the A_NE and A_NB system.

	RHF			
PVTs	**16 BHE**	**24 BHE**	**32 BHE**	**40 BHE**
0	0.13	0.10	0.10	0.11
4	0.05	0.05	0.05	0.03
8	0.03	0.03	0.03	0.01
12	0.02	0.02	0.02	0.00
16	0.02	0.01	0.01	0.00
20	0.02	0.01	0.01	0.00

According to the disparities between the two systems (Table 5.4), the largest values are shaped for the system without PVTs. With the aim to explain this phenomenon, we have to keep in mind that, the EEB for the A_NB system is located beneath the house, and at its center (section 4.2). Thus, by having the EEB above the house, the soil's natural heat recovery process is constrained by the building's footprint (Figure 4.14). Also, by installing the EEB at the center of the ground

floor slab, that causes longer distance to be covered by the heat from the uncovered regions in order to reach the GHE (section 4.2). This distance between the EEB boundaries and the uncovered by the building regions eliminates as the GHE grows. Unlikely system A_NB, the A_NE has its EEB being exposed without any barrier for the soil natural heat recovery process.

The next task is to compare system A topology with system B topology (section 3.2), for the new dwelling and the EEB being exposed. In Figure 5.3 the obtained RHF is shown for systems A_NE and B_NE, for borefield sizes of 16 BHEs and 40 BHEs. Also, Figure 5.3 shows the heat source mixture of the RHF for each scenario. The heat sources for system A, as this is analyzed in Metrics section (section 3.5), it can be the heat pump's evaporator heat and the heat offered by the synchronized power generation with the consumption (subsection 3.5.3). The additional heat source for system B, is the direct utilized solar heat for DHW needs (Figure 3.7).

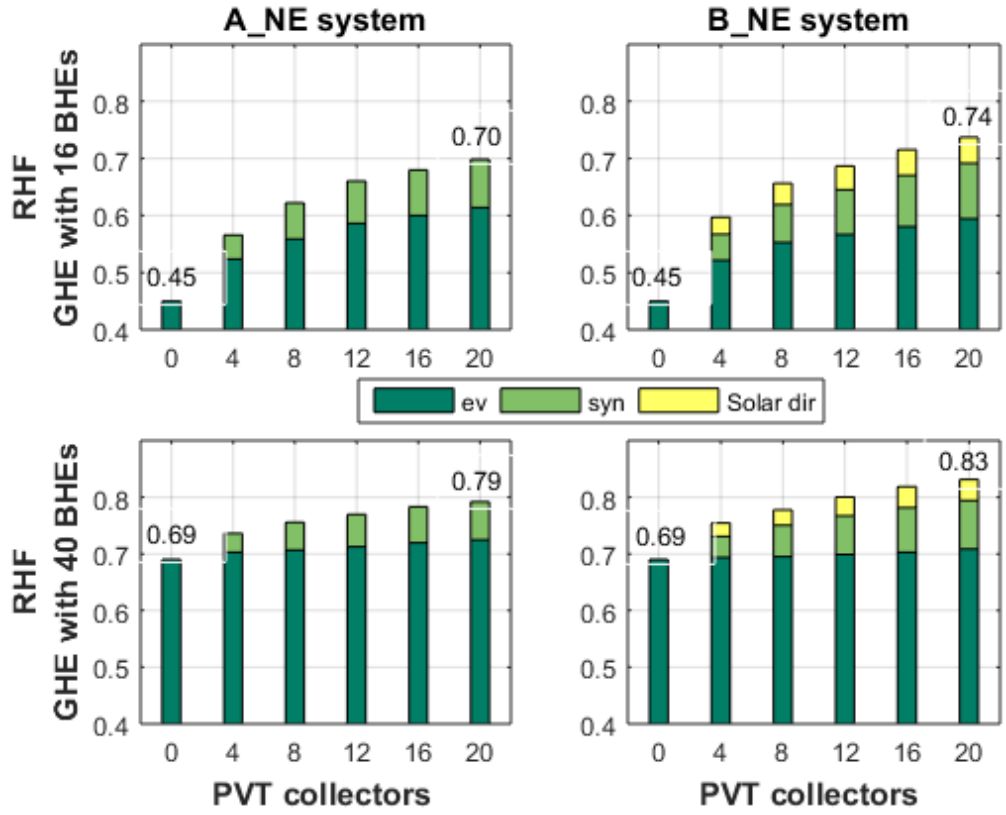

Figure 5.3. RHF comparison between systems A_NE and B_NE, for GHE sizes of 16 BHEs and 40 BHEs, along with the heat sources mixture. Where: ev- RHF corresponding to the evaporator syn- RHF corresponding to the synchronized power generation and consumption Solar dir- RHF corresponding to the directly used solar heat.

Based on the results, system B_NE obtain higher RHF in all scenarios compared with A_NE (Figure 5.3). The higher heat independence of 83% was achieved by the B_NE system, with the largest system's size, of 20 PVTs and 40 BHEs. This RHF best value of 0.83, is higher than the one estimated for A_NE system (0.79), by the fraction of 0.04. In Figure 5.3, the RHF for B_NE system grows as the PVT array is getting bigger and the GHE is getting larger, this trend is equal to the one identified for both systems A_NE and A_NB (Figure 5.1,Figure 5.2).

Table 5.5 lists the contribution of each heat sources to the RHF (3.5.3), and summarizes the gain made by system B_NE utilization instead of system A_NE. It is worth mentioning that, the scenarios with non PVTs, the RHFs are equally for the two systems due to the systems reformation to configuration A (no direct solar heat). Moreover, system B_NE with the 16 BHEs constantly gets higher RHF by 0.03 or 0.04 than system A_NE. About the B_NE system equipped with the borefield of 40 BHEs, the disparity on the RHF with the A_NE, increases gradually from 0.02 to 0.04, as the PVT array enlarges.

*Table 5.5. RHF mixture analysis, for systems A_NE and B_NE, and the gain made from system B utilization against system A. *SF is the fraction of the DHW needs covered by direct solar heat from PVTs.*

		RHF evaporator		**RHF synchronized**		**RHF direct solar**		**DHW SF* [%] for B_NE system**	**RHF gain made from B_NE instead of A_NE**
	PVTs	**B_NE**	**A_NE**	**B_NE**	**A_NE**	**B_NE**	**A_NE**		
GHE 16 BHEs	0	0.45	0.45	0.00	0.00	0.00	0.00	0.0	0.00
	4	0.52	0.52	0.05	0.04	0.03	0.00	7.2	0.03
	8	0.55	0.56	0.07	0.06	0.04	0.00	9.6	0.03
	12	0.57	0.59	0.08	0.08	0.04	0.00	9.6	0.03
	16	0.58	0.60	0.09	0.09	0.05	0.00	12.0	0.04
	20	0.59	0.61	0.10	0.09	0.05	0.00	12.0	0.04
GHE 40 BHEs	0	0.69	0.69	0.00	0.00	0.00	0.00	0.0	0.00
	4	0.69	0.70	0.04	0.03	0.02	0.00	4.8	0.02
	8	0.69	0.71	0.06	0.05	0.03	0.00	7.2	0.02
	12	0.70	0.71	0.07	0.06	0.03	0.00	7.2	0.03
	16	0.70	0.72	0.08	0.07	0.04	0.00	9.6	0.04
	20	0.71	0.72	0.09	0.07	0.04	0.00	9.6	0.04

To interpret this, a closer inspection on Table 5.5 is needed. It can be seen that, the heat provided directly by PVTs is constrained to figures below 5% of the total heating needs or 12% of DHW needs. This limitation is made by the apply control (Figure 3.8) and the used system's layout (Figure 3.7). The control, prioritizing the solar heat to be delivered to DHW tank, only if the water in the tank is 6 K lower than the PVTs' outlet. This condition is not widely formulated during the system's B operation, because the DHW tank is heated also by the heat pump. Therefore, the water in the tank is always in higher temperature, which demands an even higher

PVT outlet temperature in order to have solar heat transfer in the DHW tank. Thus, the PVT-tank operation mode (Table 3.3) is more likely to be skipped early morning, where the DHW needs are substantial (Figure 4.16) and the irradiance level is low and incapable to produce high PVT outlet temperature. Since the PVT-tank mode is skipped, then, there is no chance for PVTs to provide heat, because, now the heat pump is taking care of the DHW. On this problem, two potential solutions are offered and analyzed below:

1. A solution on the restriction of direct solar heat utilizability may be the installation of an additional DHW tank, in which the solar heat may be delivered without any interaction with heat pump operation. Then the new 'solar' tank may fulfill the DHW needs and mix the water with the one heated by the heat pump's tank. Therefore, only the additional heat is delivered by the heat pump. This modification increases the system's initial cost investment and operation complexity.
2. Another solution may be an alternative system control. The alternative system operation, potential sets only the solar heat to be delivered to the DHW tank by avoiding the heat pump's contribution. This operation mode is more effective by set the DHW tank charging period to be the summer, while for the rest of the year the system may operate with both heat sources for the DHW tank or as system A (without direct solar heat). The main drawback regarding this solution is that the remaining heat required by the water to reach the 50 ^{o}C is offer by electricity (in our case). Thus, even in the favorable instance of having 50% of the DHW needs be covered by solar heat, the remaining is made by electricity (or any other potential heat source). But the heat pump utilization is preferable from pure electricity due to higher coefficient of performance. In other words, with electricity, by offering 1 kWh someone gets 1 kWh of heat, unlikely the heat pump where with the 1 kWh_e, more than 2.5 kWh of heat can be delivered. As a conclusion, additional investigation on the temperature threshold above which the heat pump should operate for DHW needs is required. For instance, PVTs may be responsible to warm up the DHW tank water temperature up to 30 ^{o}C and after this point, the heat pump to supply the remaining heat.

As regards the comparison between the RHF caused by the heat pump's evaporator (Table 5.5, Figure 5.3), system B_NE is constantly lower by zero to 0.02 than system A_NE. This small reduction is made by the heat pump's reduced operation and from the lower solar heat offered to the soil due to direct use for DHW. The reduced heat pump's operation drops further the RHF provided by the synchronized power generation and consumption (Table 5.5). System B_NE

have two out of three parts of RHF slightly reduced against system A_NE, though has managed to obtain greater heat independence due to the direct solar heat contribution. More on that, the direct solar heat delivered to the DHW tank is increased as the PVT array is getting bigger. Since the PVT-tank mode (Table 3.3) is set to 'on', then, the delivered heat to the DHW tank is a matter of the available solar heat which increases as the PVT collectors are getting more.

In Table 5.5, the system equipped with the 16 BHEs found to operate favorable for direct solar heat utilization, due to its occasionally limitation to provide the DHW tank with heat. This heat pump's restriction to deliver heat, is derived by the small EEB and its limitation to maintain a soil temperature above critical level.[15] The small EEB has low heat capacity and thus easily the soil in its volume can drop by the heat absorbed for the system's needs. Regarding the critical soil temperature, this can be defined as the near boreholes soil mean temperature which does not drive the refrigerant entering the heat pump out of the operational limits.

Figure 5.4 depicts the comparison between system A and system B configurations, for the scenario of the GHE being buried beneath the building. According to the results illustrated in Figure 5.4, system B_NB is capable of higher heat independence than A_NB system for all equally sized systems. An improvement of the RHF found with the B system configuration especial for the smaller borefield of 16 BHEs. The greater difference of RHF between the two systems, is recorded to be the fraction of 0.04, for the pairs of 16 BHEs with 8,16 and 20 PVTs. The system B configuration achieved an RHF of 0.81 for the larger system of 40 BHEs and 20 PVTs. As it can be seen in Figure 5.4, the size of the PVT array influences the most the system with the small borefield by increasing the RHF from 0.33 to 0.72, for non PVT scenario to the scenario with 20 PVTs respectively. Similarly, the larger GHE of 40 BHEs is fount to improve its RHF by 0.22 between the two scenarios of not PVT and 20 PVTs.

In Table 5.6, the mixture of energy sources for each system are listed along with the gain on RHF made by B_NB against the A_NB. The reasons on which the B_NB system gets better RHF values than the A_NB are similar with the A_NE to B_NE debate. The different aspect about the B_NB system against the B_NE system, is that the GHE is beneath the house and that buffers the soil owned by the EEB from the ambient conditions. As is already stated above that, location of the EEB for B_NB system, adds a difficulty to the soil natural heat recovery. Based on the above issue

[15] Below that the fluid entering the evaporator is lower than -10^{o}C, thus is outside the heat pump's operation envelop, Figure 4.13.

and as it can be observed in Figure 5.5, the EEB's mean soil temperature drops when the GHE is installed beneath the house. Therefore, the EEB's mean soil temperature is lower at every PVT array for system B_NB than the system A_NB. The lower soil temperature regime established by B configuration, drives the heat pump to operate with reduced COP than the A configuration. Consequently, the electricity used by the device is increased in the case of B system against A system, and by having a wider need for electricity by the heat pump, potentially the synchronized part of the RHF increments.

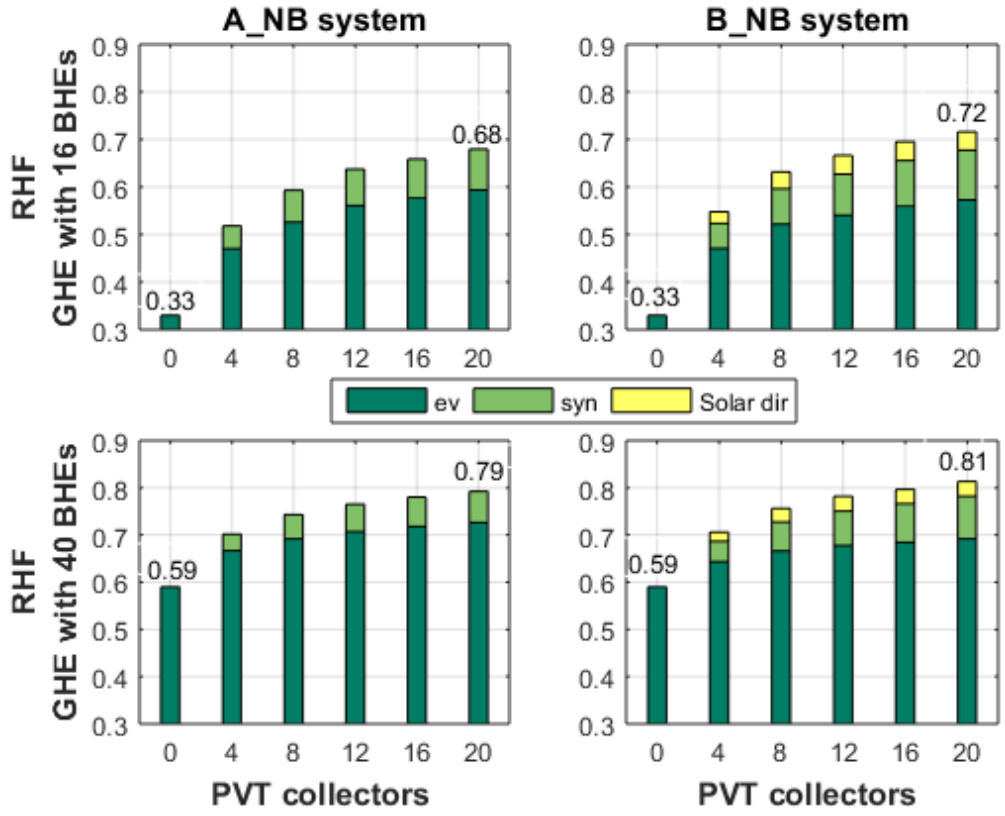

Figure 5.4. RHF comparison between systems A_NB and B_NB, for GHE sizes of 16 BHEs and 40 BHEs, along with the heat sources mixture. Where: ev- RHF corresponding to the evaporator syn- RHF corresponding to the synchronized power generation and consumption Solar dir- RHF corresponding to the directly used solar heat.

It is worth discussing the reasons for the small reduction of 2.4% on DHW SF, between the smaller to the bigger GHE (Table 5.6). In order to identify the reasons of this reduction, is needed a closer look on how the system with direct use of solar heat operates (Figure 3.7). As the system B control diagram illustrates (Figure 3.7), the water in the tank can be heated up by the PVT collectors and the heat pump. Since the heat pump can heat up the water in the tank, a higher water temperature regime is established. Thus, the raised water temperature is the barrier for broader direct utilization of the solar heat. By keeping in mind the above observation, it is

concluded that, a system equipped with large GHE is more likely to end up with a poor DHW SF, due to increased heat pump capability to cover the system's heat demand.

Table 5.6. RHF mixture analysis, for systems A_NB and B_NB, and the gain made from system B utilization against system A. *SF is the fraction of the DHW needs covered by direct solar heat from PVTs.

		RHF evaporator		RHF synchronized		RHF direct solar		DWH SF* [%] for B_NE system	RHF gain made from B_NE instead of A_NE
	PVTs	B_NB	A_NB	B_NB	A_NB	B_NB	A_NB		
GHE 16 BHEs	0	0.33	0.33	0.00	0.00	0.00	0.00	0.0	0.00
	4	0.47	0.47	0.05	0.05	0.02	0.00	4.8	0.03
	8	0.52	0.53	0.07	0.07	0.04	0.00	9.6	0.04
	12	0.54	0.56	0.09	0.08	0.04	0.00	9.6	0.03
	16	0.56	0.58	0.10	0.08	0.04	0.00	9.6	0.04
	20	0.57	0.59	0.10	0.09	0.04	0.00	9.6	0.04
GHE 40 BHEs	0	0.59	0.59	0.00	0.00	0.00	0.00	0.0	0.00
	4	0.64	0.67	0.04	0.04	0.02	0.00	4.8	0.00
	8	0.67	0.69	0.06	0.05	0.03	0.00	7.2	0.01
	12	0.68	0.71	0.07	0.06	0.03	0.00	7.2	0.02
	16	0.68	0.72	0.08	0.06	0.03	0.00	7.2	0.02
	20	0.69	0.73	0.09	0.07	0.03	0.00	7.2	0.02

From all the parts which are comprised the system, the EEB may illustrates a year to year dynamic behavior. As it is justified by Figure 5.5, the mean soil temperature reacts dynamically throughout the simulation ten-year span. The curves in Figure 5.5, belong to the EEB mean soil temperature for the scenario of the borefield with 16 BHEs. The smallest of GHEs, is potentially the worst-case scenario for systems sustainability studies. Based on that, most curves can be split in two sectors: a) the up to 4th year intense dynamic behavior and b) the post 4th year monotonic trend. We must acknowledge the fact that, the mean soil temperature does not provide much information about the annual oscillation of the soil temperature, but in our case offers the overall pattern. The annual soil temperature variation may potential illustrates, if the heat pump operates or not properly during the heating season. Though, in all investigated scenarios, most of the systems with 16 BHEs, have obtained a substantial RHF higher than 0.5 and the mean soil temperature does not show any dramatic reduction (Figure 5.5). The above substantiate that, most of the systems equipped with 16 BHEs, are capable to operate beyond the ten-year period without any substantial reduction on the heat provided to the system.

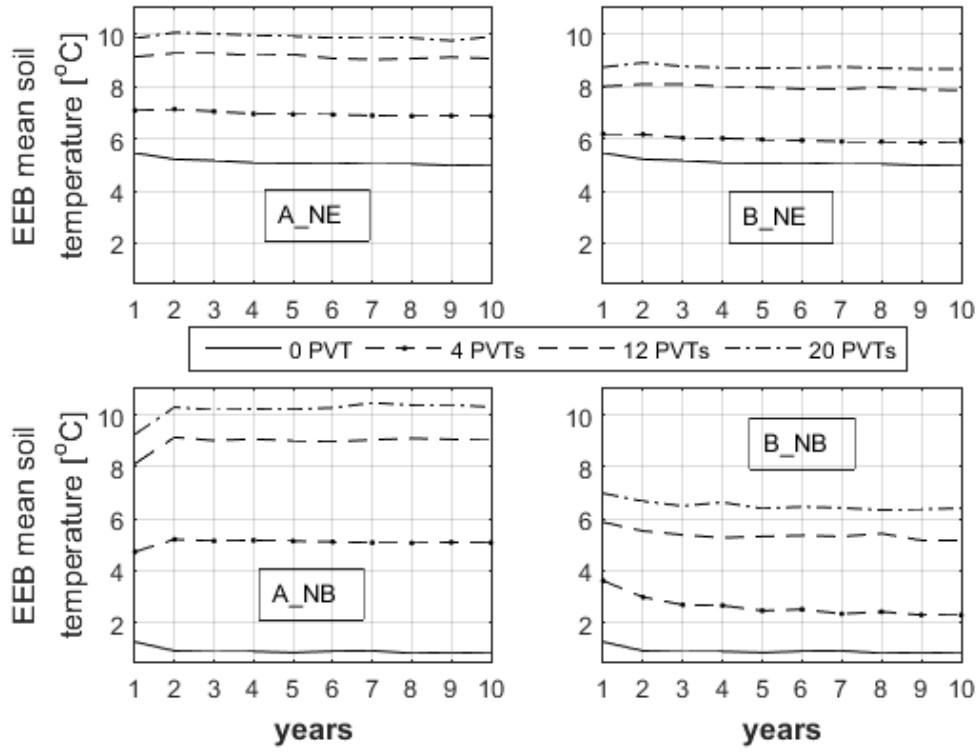

Figure 5.5. EEB mean soil temperature profile for the ten-year period. For all system which is installed at the new dwelling with the borefield of 16 BHEs.

The RHFs obtained by all systems used with the new dwelling are illustrated by Figure 5.6, for borefields of 16 and 40 BHEs paired with all investigated PVT arrays. Based on the results (Figure 5.6), system B_NE owns the higher RHF from all the investigated system with equally sizes PVT arrays and borefields. Also, the hierarchy among systems regarding the achieved RHF is stable until the PVT array of 12 collectors. With details, the B_NE is constantly through all scenarios the most capable and is followed by the B_NB, A_NE and as the last one the A_NB. Though, as already stated above, this order changes and splits the comparison into other two sections: this of the GHE with 16 BHEs and this with 40 BHEs. Regarding the small GHE, the B_NB system remains second until the PVT array of 4 collectors and then swifts to be the third. As regards, the largest GHE, the B_NB system gets slightly less RHF than the A_NE for the array of 8 PVTs and downgrades on the second position afterwards.

To sum up, the systems with the EEB being beneath the building are competitive when a larger PVT array is used, and by applying this configuration without or with small solar collecting area, causes dramatic reduction on RHF. Contrary to the systems with the EEB beneath the dwelling,

the exposed choice is less solar heat dependent and it can offer substantial portion of heat to the system with small PVT arrays.

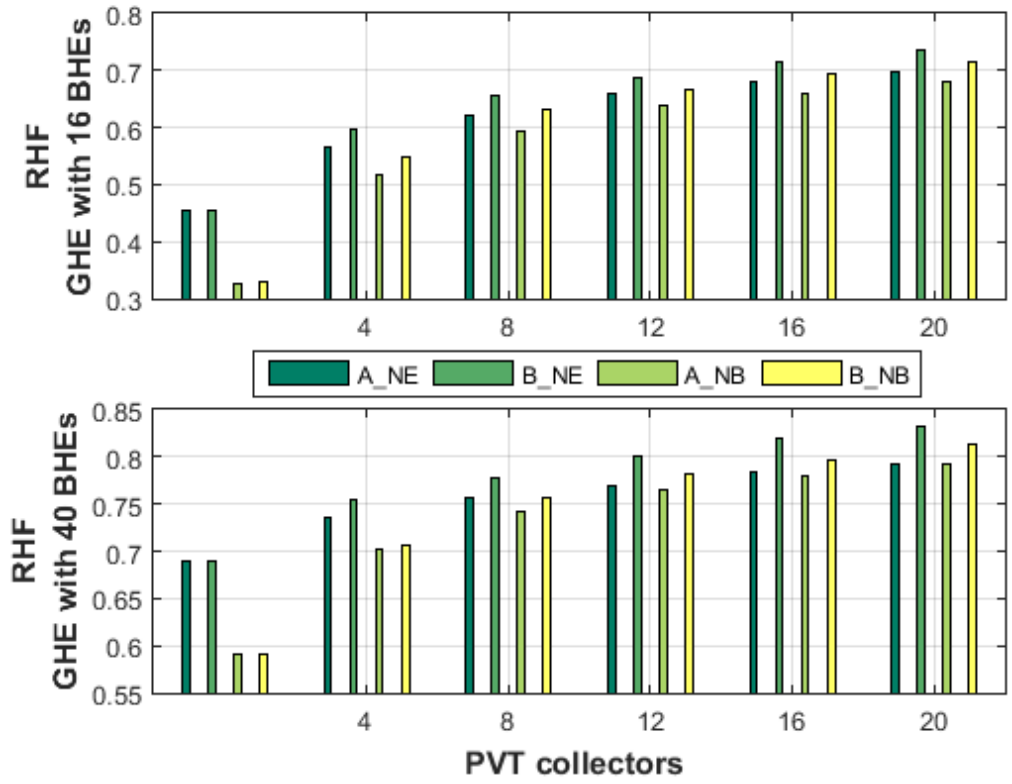

Figure 5.6. All systems RHF installed in the new dwelling, for borefields of 16 and 40 BHEs paired with all investigated PVT arrays (0 to 20 PVTs).

5.1.2. System's specific heat productivity for the new dwelling

As is already analyzed and illustrated in section of metrics, the specific productivity (SP), is a value which illustrates the offered energy per installed harvesting equipment (subsection 3.5.2). Based on that concept, Figure 5.7 visualizes system's SP (SP_{sys_heat}) for the A_NE simulation scenario and Figure 5.7 lists the achieved values.

As it can be seen in Figure 5.7, SP_{sys_heat} is influenced explicitly by the GHE size. For instance, the system with 4 PVTs, increases its SP_{sys_heat} with 403 kWh PVT^{-1} by enlarging the GHE from 16 BHEs to 40 BHEs. Also, the influence of the GHE size on the harvested heat, scales down as the PVTs quantity increases. Thus, for the group of bars plotted with the array of 20 PVTs, the discrepancy between the larger and the small GHE is 52.5 kWh PVT^{-1} (Table 5.7).

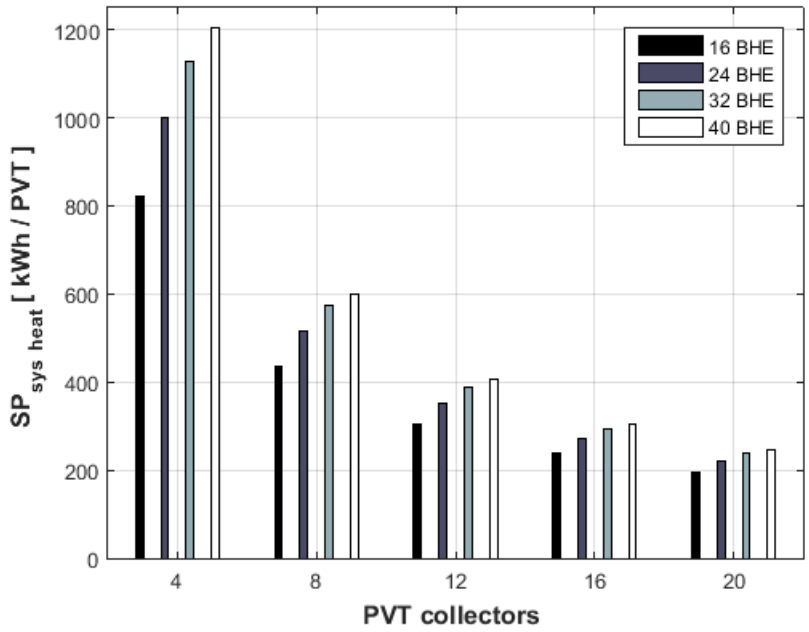

Figure 5.7. System's heat specific productivity for A_NE simulation scenario.

By observing Figure 5.7, someone can say that the most efficient system is this of 40 BHEs paired with 4 PVTs (1203.1 kWh PVT^{-1}), and the less efficient is the system of 16 BHEs with 20 PVTs (194.3 kWh PVT^{-1}). Based on the above statement about the most and the least efficient system, it can be concluded that: a large borefield paired with a small PVT can obtain higher SP than a smaller borefield paired with a larger PVT array. This statement is supported by Figure 5.8, which shows the SP_{sys_heat} as function of CBR (Collectors to BHE ratio, subsection 3.5.2). It can be seen in Figure 5.8 that, as the collectors to BHEs ratio increases, the system's SP drops.

In equation 3.5, the PVTs on the denominator are denoted with the CBR index. In order to answer the question: "What is the influence of the CBR on the systems SP?". The answer can be offered by observing the Table 5.7 at its first and its last column. Thus, by keeping the PVT fixed and traversing the row from left to right, the SP_{sys_heat} increments as the CBR decreases, because CBR is the PVTs / BHEs. Based on that, the CBR influencing the calculated SP_{sys_heat} similarly to the general trend described on the above paragraph.

Table 5.7. System heat SP Values for A_NE and A_NB scenarios.

		System SP [kWh PVT^{-1}]			
System	**PVT**	**16 BHE**	**24 BHE**	**32 BHE**	**40 BHE**
A_NE	4	820.3	1001.2	1126.2	1203.1
	8	436.5	515.8	574.1	601.1
	12	304.0	353.1	387.2	404.7
	16	237.8	272.3	293.9	305.6
	20	194.3	221.4	237.4	246.9
A_NB	4	726.2	948.3	1079.7	1206.7
	8	410.4	500.9	563.4	609.6
	12	297.1	350.7	383.7	409.8
	16	233.3	271.8	293.5	309.9
	20	192.8	220.9	237.6	251.4

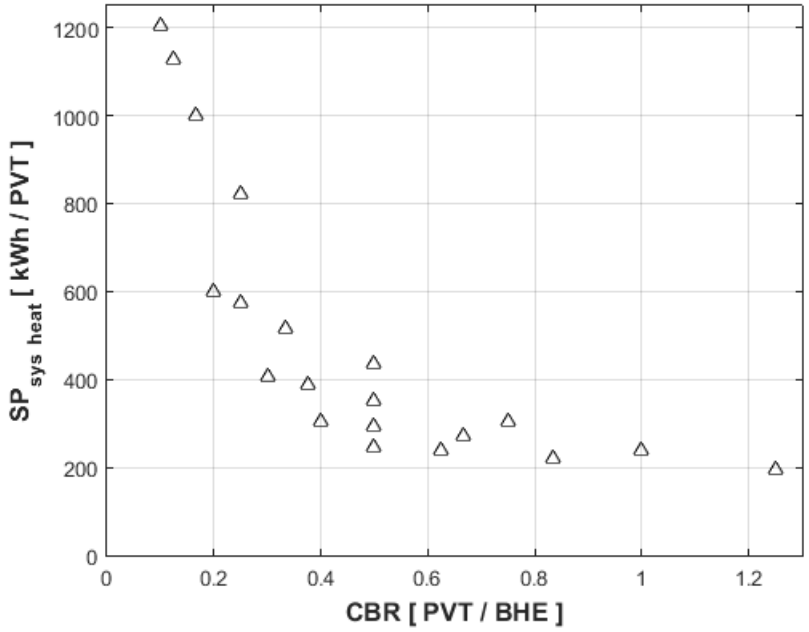

Figure 5.8. System's SP as function of CBR for A_NE scenario.

It is worth to be discussed, the contribution of each subsystem (solar-PVTs and geothermal-BHEs) on the heat harvested by the system. Based on results listed in Table 5.7, the borefield of 16 BHEs increases the heat used by the system from 3280 kWh to 3887 kWh by enlarging the PVT array from 4 to 20 collectors. Similarly, the borefield of 40 BHEs increases the offered heat from 4812 kWh to 4937 kWh by enlarging the PVT array from 4 to 20 collectors. In the case of the small GHE, the heat offered by the 16 additional PVTs is 607 kWh, likewise, for the larger GHE the heat added from the 16 extra collectors is 125 kWh. The above relatively small heat

contribution from the additional PVTs and the results illustrated in subchapter 5.1.1, conclude that, the GHE plays the key role on heat harvesting procedure. Thus, the size of GHE sets a minimum system SP and then is the PVTs which are responsible to elevate further this production and to recharge the EEB soil mass.

Table 5.8. System's SP as function of CBR and SC, for the A_NE scenario.

CBR [PVT / BHE]	SC [m^3 / m^2]	System SP [kWh PVT^{-1}]
0.10	19.42	1203.1
0.13	15.58	1126.2
0.17	11.67	1001.2
0.20	9.71	601.1
0.25	7.83	820.3
0.25	7.79	574.1
0.30	6.47	404.7
0.33	5.83	515.8
0.38	5.19	387.2
0.40	4.85	305.6
0.50	3.92	436.5
0.50	3.90	293.9
0.50	3.89	353.1
0.50	3.88	246.9
0.63	3.12	237.4
0.67	2.92	272.3
0.75	2.61	304.0
0.83	2.33	221.4
1.00	1.96	237.8
1.25	1.57	194.3

Having illustrated the relationship between the SP_{sys_heat} and the CBR, the remaining index which to discuss is the storage capacity (SC) (section 3.5). The SC depicts the ratio between the storage volume and the solar collectors' area. In our case, the storage volume is formulated by the EEB with the contained soil (

Table 4.5). The Table 5.8 illustrates the SP_{sys_heat} values as function of the CBR and SC. Based on the listed values, the CBR and the SC operate with opposite order. Contrary to what is analyzed above for the CBR index, the SC high values benefit the system's SP and the lower SC values reduce its efficiency. The preference to the bigger EEB is due to a larger volume contains higher heat capacity which can be used to store more solar heat, or the stored energy can be utilized directly. Also, in the current study, the EEB volume is linearly proportional to the BHEs quantity,

because the distance among BHEs is fixed. Thus, a bigger EEB contains more BHEs than a smaller one and consequently larger heat transfer area. Also, studies made by varying the distance among BHEs (Sakellariou *et al.*, 2019), showed that for a given PVT array and fixed CBR, the larger EEB volume would improve the system's SP. This enhancement was made due to larger assigned soil volume for every BHEs, which offers greater opportunities for solar heat storage.

Figure 5.9 illustrates the system's SP obtained by the A configuration with the GHE be installed underneath the dwelling. The highest SP_{sys_heat} value was achieved by the system with 4 PVT collectors paired with 40 BHEs (1206.7 kWh PVT^{-1}), and the lowest belongs to the system with 20 PVT and 16 BHEs (192.8 kWh PVT^{-1}). As regards the variation of collectors and BHEs, A_NB system is governed by similar trends as these of A_NE system discussed above. In general, the system efficiency increases as the GHE enlarges and the PVT array becoming smaller.

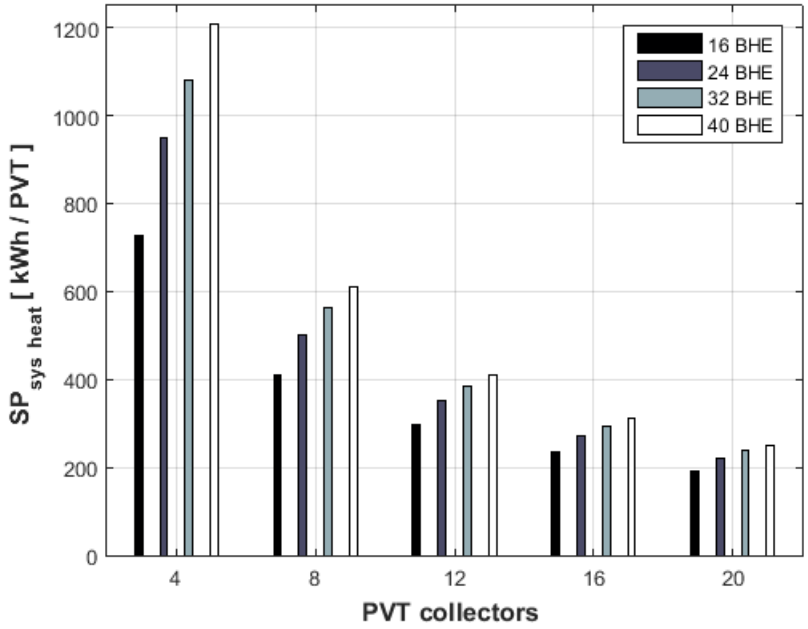

Figure 5.9. System's heat specific productivity for A_NB simulation scenario.

In Table 5.7, the SP_{sys_heat} values achieved for the A_NE and A_NB systems are listed. By comparing the SP_{sys_heat} values from the two systems, A_NB found less efficient than the A_NE at all system with PVT arrays of 4 and 8 collectors and borefield smaller than 40 BHEs. This discrepancy ceases at all remain pairs and the two systems establish a regime with equal efficiency. The A_NB lower efficiency at the small PVT arrays is caused by the poor soil temperature natural recovery, due to restriction imposed by the build. The difference between

the two systems is larger for the smaller GHE, because are placed on the center of the building footprint and that imposes additional difficulty to the soil temperature natural recovery. Based on the above trend and as is already analyzed for the A_NE system's RHF, a large PVT array deems to be important for A_NB system efficiency and viability.

The A_NB system's SP productivity as function of CBR is illustrated in Figure 5.10. As it can be seen in Figure 5.10, the A_NB system's efficiency depends on collectors to BHEs ratio similar to the A_NE does. Consequently, the SC follows the reversed trend as

Table 5.8 shows for the A_NE system. Bear in mind that, the CBR and SC ratios are equal values across all the studied scenarios, thus, the above argument is valid.

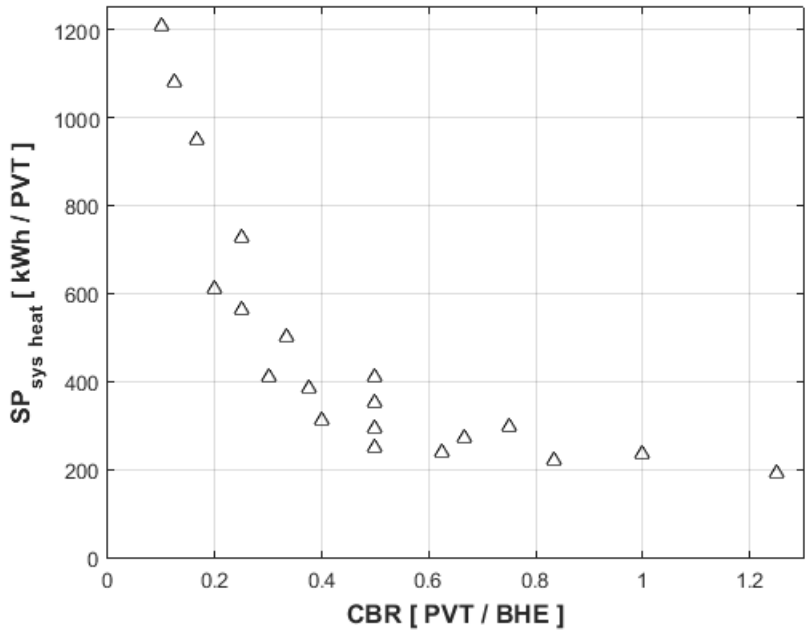

Figure 5.10. System's SP as function of CBR for A_NB scenario.

System's B SP_{sys_heat} performance is plotted in Figure 5.11 for both GHE topologies, against the A systems, for the borefield sizes of 16 and 40 BHEs. Based on the plotted results, both systems which are formed with the B topology type, share similar trend to this descripted for both A systems. The larger GHE is favorable for higher systems' efficiency along with the smaller PVT arrays. Also, as the collectors' quantity increases, the discrepancy among the borefield sizes reduces. Based on the results listed in Table 5.9, system B_NE owns the higher system SP of 1450.7 kWh PVT^{-1} and is followed by the B_NB with 1372.8 kWh PVT^{-1}, both case with 40 BHEs and 4 PVTs. The best achieved value SP_{sys_heat} (1450.7 kWh PVT^{-1}), moves over the upper limit set

by the A_NB system at 1206.7 kWh PVT^{-1} (Table 5.9). Therefore, with the same heat harvesting equipment of 40 BHEs and 4 PVTs, system B_NB obtained higher efficiency. It is important to link the B system's higher efficiency against A, with the RHF illustrated in subsection 5.1.1. As it can be seen through Figure 5.11 and Figure 5.6, the B_NE and B_NB improved system SP, reflects on the enhanced RHF against system A scenarios. Thus, the improved system SP drives the system to a higher RHF.

Table 5.9. System heat SP Values for all system scenarios, for the borefield of 16 and 40 BHEs.

Borefield	PVT	System heat SP [kWh PVT^{-1}]			
		A_NE	B_NE	A_NB	B_NB
16 BHEs	4	820.3	974.6	726.2	832.8
	8	436.5	524.9	410.4	479.7
	12	304.0	362.6	297.1	340.5
	16	237.8	283.2	233.3	263.2
	20	194.3	232.3	192.8	218.9
40 BHEs	4	1203.1	1450.7	1206.7	1372.8
	8	601.1	712.8	609.6	708.5
	12	404.7	476.5	409.8	473.5
	16	305.6	360.0	309.9	354.8
	20	246.9	290.0	251.4	288.9

By observing the results from Figure 5.11 and Figure 5.6 regarding the system SP and the systems RHF, it seems that the higher values of RHFs are obtained with rather poor heat SP. In detail, for the case of 0.83 RHF (B_NE), the harvest heat per installation unit was 290 kWh PVT^{-1} (40 BHES with 20 PVTs). But, the lower RHF of 0.6 was made by the highest system SP of 974.6 kWh PVT^{-1} (16 BHEs with 4 PVTs). The first system (0.83 RHF) owns a CBR of 0.5 and the second (0.6 RHF) has a CBR at 0.25. Thus, the improvement of the system's RHF may be promoted by increasing the system's SP, and the circumstances for better system efficiency offered by a low CBR.

As is justified by Figure 5.8, Figure 5.10 and Figure 5.12, the CBR plays a key role on the system heat SP, the lower the CBR the highest the system SP. Also, through the results plotted in the above figures, someone can say that the CBR has a consolidated influence on all the studied configurations. The conditions which act in favor of the high SP_{sys_heat} are: a) the adequate EEB storage (soil) volume and b) the GHE large heat transfer area per collector, which in our case is translated to more BHEs. Of course, as is already shown by (Sakellariou *et al.*, 2019), there are many aspect which can potential influence and improve the system's efficiency. These aspects may be the geometry and material content of the BHEs, the soil thermophysical properties, the

refrigerant flowrate, and outside the EBB, aspect like the plate heat exchanger effectiveness and many more.

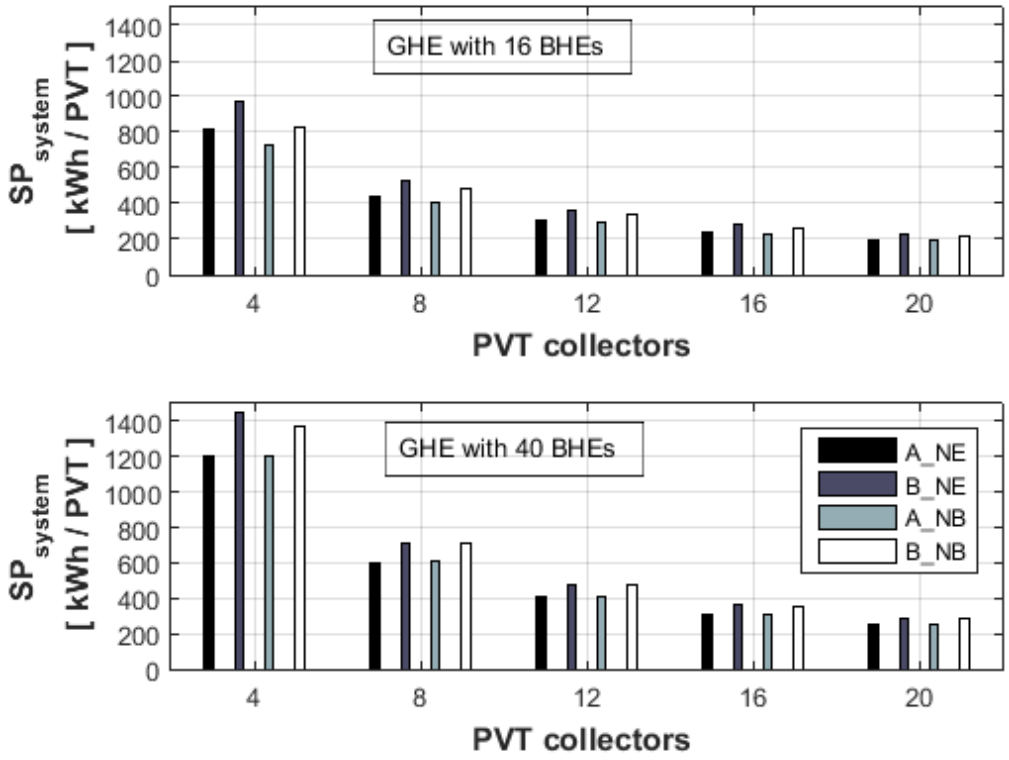

Figure 5.11.Systems' heat specific productivity for all simulation scenarios and for the borefield of 16 and 40 BHEs.

The two improving conditions of the heat SP stated on the above paragraph, may be established by incrementing the distance among BHEs regarding the storage volume aspect, and as for the enhanced heat transfer area (by keeping fixed the BHE's length and diameter), the solution may be a grout with higher thermal conductivity and the optimum distance between the polyethylene pipes (in the borehole) for the given pipe diameter.

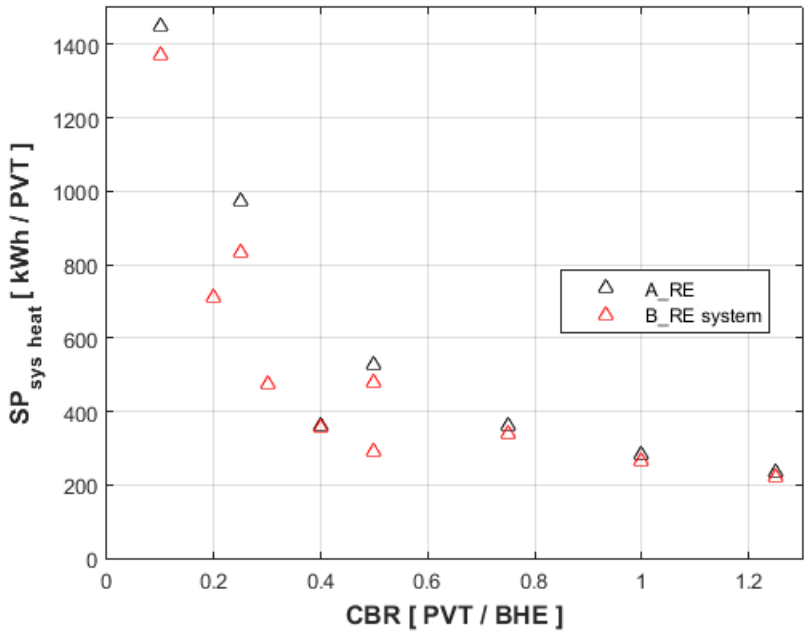

Figure 5.12. System's SP as function of CBR for B_NE and B_NB scenarios.

5.1.3. PVT specific heat productivity for the new dwelling

As it analyzed in section of metrics (3.5), the PVT specific heat productivity (SP_{PVT_heat}) depicts the solar heat offered per collectors per year. In other words, the SP_{PVT_heat} metric shows annual efficiency of the PVT collector, as a part of the investigated system. In order to set an upper limit, 1593 kWh of solar energy incident on each PVT collector annually, for the given orientation, inclination and for Birmingham (section 4.1). In this subsection, the analysis is made about a system's component and how the rest of the system influences its productivity. Therefore, is the reversed process of the system heat productivity.

In Figure 5.13, the SP_{PVT_heat} values are illustrated for A_NE system. According to the results, the PVT heat SP varies throughout all the investigated pair of PVTs and BHEs. The highest PVT heat SP was found to be 663.6 kWh PVT^{-1} for the system with 4 PVTs and 16 BHEs, while the lowest was at 525.5 kWh PVT^{-1} for the system with 20 PVTs and 16 BHEs accordingly (Table 5.10). Based on the listed in Table 5.10 values of the PVT heat SP, the array of 4 PVTs can offer equally heat regardless the GHE size. This trend of the equal SP continues for the borefields of 32 and 40 BHEs until the array of 12 PVT, and as someone can see, the systems of 32 BHEs and 40 BHEs paired with 12 PVTs obtain similar values. As the PVT quantity increase, a proportional rising discrepancy is appeared among SP_{PVT_heat} achieved for each borefield. The peak difference of

96.89 kWh PVT^{-1} is recorded between the system with 20 and 4 PVTs paired both with the larger borefield of 40 BHEs.

Table 5.10. PVT heat SP Values for A_NE and A_NB scenarios.

System	PVT	PVT heat SP [kWh PVT^{-1}]			
		16 BHE	24 BHE	32 BHE	40 BHE
A_NE	4	663.6	661.8	661.4	662.6
	8	617.8	621.8	627.8	626.6
	12	582.8	593.2	602.2	601.8
	16	552.2	571.5	578.7	581.9
	20	525.5	546.8	560.6	565.7
A_NB	4	703.7	718.5	717.7	713.1
	8	631.1	651.8	661.1	659.2
	12	581.4	597.4	612.5	612.3
	16	543.8	564.4	571.7	572.3
	20	515.7	532.5	542.9	543.1

The phenomena descripted in the above paragraph regarding the SP_{PVT_heat} relationship with the PVTs and BHEs quantity, can be explained by acknowledging the variation of the EEB's heat capacity with its BHEs content. Thus, the achieved PVT heat SP rises as the borefield enlarges. That happens because the larger GHE contains higher heat capacity and can store more solar heat than a smaller one. Additionally, the larger the EEB, the lower the mean soil temperature for a given PVT array, due to the bigger soil mass. And by having the EEB with lower mean soil temperature, the PVTs' outlet temperature can operate more frequently as a heat recharger (Table 3.2). As regards the scenarios where the systems attain similar SP, it seems to be due to PVT array size which cannot offer more solar heat. This can be easily proved by observing the array of 4 PVTs in Figure 5.13, the SP remains stable regardless the GHE size, thus it is no matter of greater storage volume. Consequently, as the PVT array enlarges, the storage capacity influences the SP, and as it can be seen with the 8 and 12 PVTs, the EBBs of 16 and 24 BHEs are these which restrict the utilized solar heat. Finally, it is important to highlight the heat load as one of the parameters which influence the solar heat utilization. A different heat load may cause alternative operation conditions and by that to let more or less solar heat to be utilized.

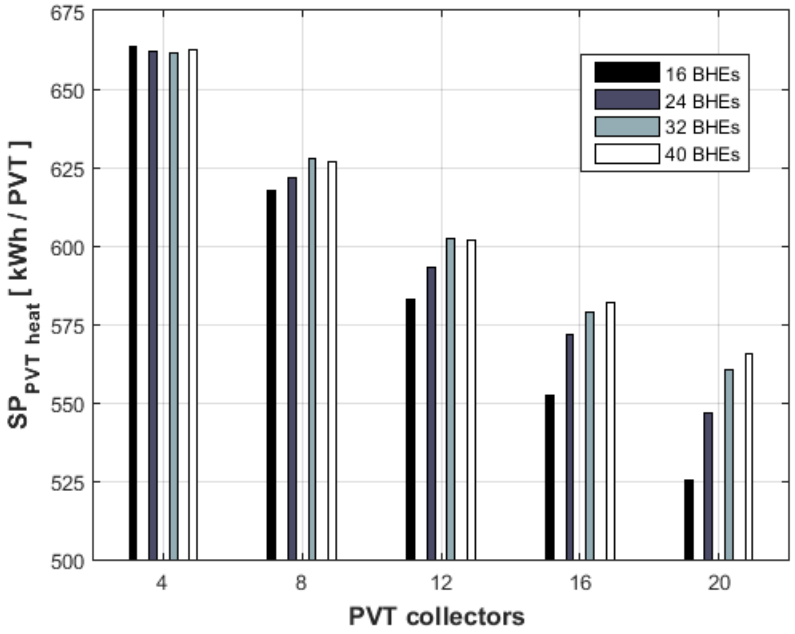

Figure 5.13. PVT heat specific productivity for A_NE system.

The results illustrated in Figure 5.14 and listed in Table 5.10, are about system's A_NB PVT heat SP. Based on the results, someone can say that, the values share similar trends with the values showed for the A_NE system. The main different on the results between the two systems is that the A_NB achieved higher SP_{PVT_heat} that the A_NE in most simulation scenarios. A_NB system's improved PVT heat performance is based on the EEB's lower mean soil temperature which is caused by the poor natural heat recovery (Figure 5.5). As it is analyses for A_NB system's heat SP, the soil owed by the EEB requires a portion of solar heat, with the aim to be recharged and to rebound its temperature. By having the EEB with low temperature due to poor natural soil heat recovery, preferable conditions for PVT greater heat production are shaped. The favorable conditions for PVTs greater heat production are due to easier achieved ΔT of 6 K (solar pump operation condition for soil recharging) between the collectors' outlet and the near to BHEs soil temperature. This temperature difference can be appeared frequently with lower EEB soil temperature.

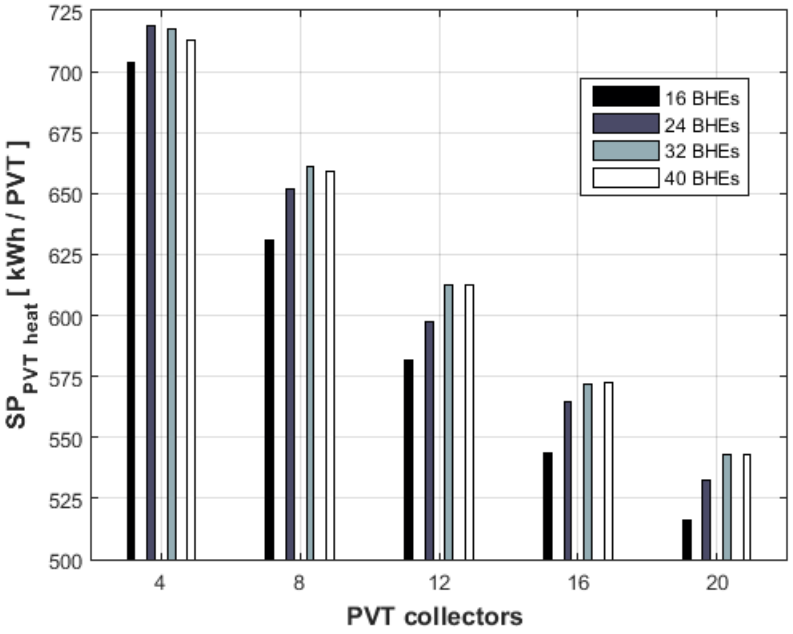

Figure 5.14. PVT heat specific productivity for A_NB system

As it is well known, the solar collector inlet temperature influences its efficiency. With the lower inlet temperature to operate favorable for higher efficiency, contrary to increased inlet temperatures which deteriorate its heat losses. In the current system, the PVTs' mean inlet temperature was found to not vary significantly from system to system with equal amount of PVTs and different EEB's volume. In other words, the variations of SP_{PVT_heat} illustrated in Figure 5.13 and Figure 5.14 among borefield sizes for equal sized PVT arrays, are caused mainly due to different EEBs' heat capacity.

With the aim to prove the above, Figure 5.15 shows the mean inlet temperature for PVT arrays of 4 and 20 PVTs paired with all investigated borefield. As it can be seen in Figure 5.15, for 4 PVT collectors the inlet temperature varies less than 0.5 K for all borefield, after the transitional period of the first three years. As regards the array of 20 PVTs, the variation amplitude increases slightly and remains less than 1 K, after the transitional period. Regarding the above observations, a useful question may by: "why the mean collectors' temperature does not follow the EEB size variation?". It was expected to obtain lower inlet temperature as the EEB enlarges, due to higher heat capacity and larger soil volume, for equally sized PVT arrays. In order to have lower PVTs' inlet temperature, the EEB's soil temperature should decreases as the soil mass grows. But as it is plotted in Figure 5.16, the mean soil temperature seems to be influenced more

from the PVT quantity rather the borefield. Therefore, in Figure 5.16, the two PVT arrays formulate two soil temperature regimes which are not influenced significantly by the EEB size. One can say that the two arrays obtain soil temperature conditions with less than 1 K variation.

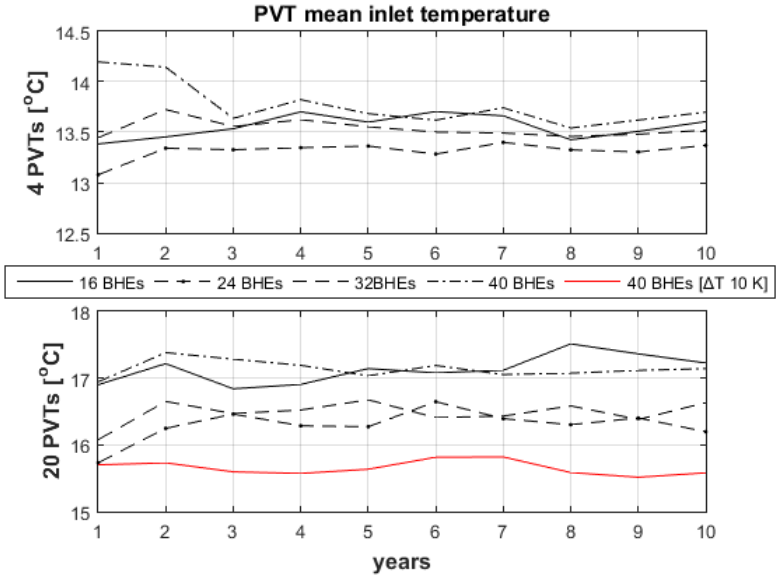

Figure 5.15. PVT collectors mean inlet temperature for the PVT arrays of 4 and 20 collectors for all borefield sizes and for A_NB system. The inlet temperatures are considered only when the solar pump operates.

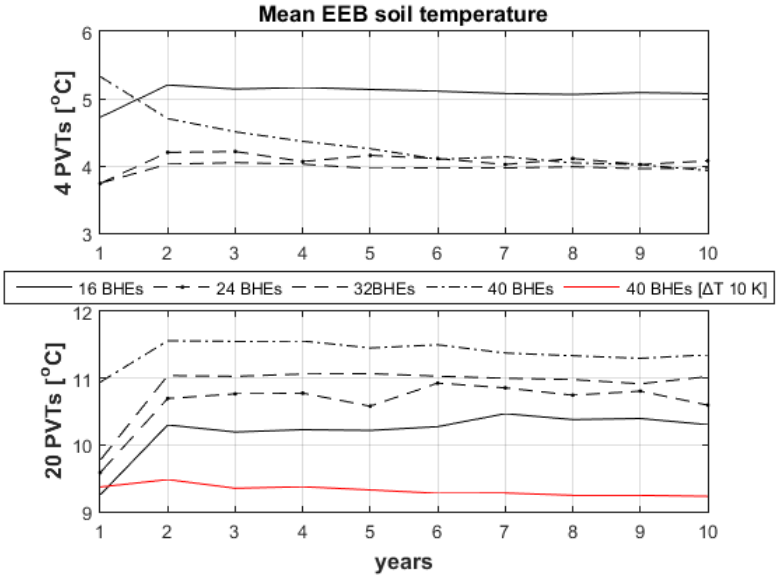

Figure 5.16. Mean EEB's soil temperature for the arrays of 4 and 20 PVTs for all borefield sizes and for A_NB system.

The second question derived from the observations illustrated in Figure 5.15 and Figure 5.16 can be: “why is the PVT quantity the factor which determines the mean soil temperature level?”. The answer is listed below:

- Let is assumed that the PVT inlet temperature is fixed for all simulation span.
- Also, the incident irradiance and the ambient conditions are not varying from year to year (due to TMY used), a certain annual value of solar heat is then delivered (also the heat load does not vary).
- Then, the annually harvested solar heat is also characterized by a PVT outlet temperature which follows a specific annually profile, as function of the environmental conditions and the fixed inlet temperature (as this assumed).
- By utilizing the solar heat with a specific annual temperature profile, the EEB’s soil temperature will follow this trend, to impose a fixed annual temperature variation.
- By accepting the above, there are two factors which can influence the solar heat utilizations: the plate heat exchanger’s PHE’s effectiveness (fixed) and the system’s control procedure. As it is already illustrated by Sakellariou et al. (Sakellariou *et al.*, 2019), an improved PHE effectiveness can increase further the soil temperature. As regards the system’s control, this is imposed by the ΔT formulated between the collectors’ outlet and the soil near boreholes temperature (Table 3.2). In the current system, the ΔT is fixed at 6 K, but by increasing this to 10 K, a new lower soil temperature can be achieved as it can be seen in Figure 5.16. Based on the ΔT of 10 K, the mean soil temperature dropped by 2 K.
- With fixed PVT outlet annual profile temperature, in the current state, the only barrier for mean soil variation is the control of 6 K ΔT, between the production and the soil. Therefore, for all EEBs, the solar energy is offered to charge the soil and to elevate its temperature up to a level where this is restricted by the applied ΔT. Regardless, the EEB size, the solar energy fills up the soil until the restriction of ΔT. Also, as bigger is the PVT array, the formulated soil temperature is higher, due to increment available solar heat. Bear in mind that, the ΔT is applied for the temperature near the BHE walls, thus, in bigger EEB the heat diffusion drops this near to walls temperature and increases further solar heat utilization.
- All the above-mentioned process is governed by a transient state up to 4^{th} first year (Figure 5.16). After that period, the system reaches a monotony and balances all the

procedure analyzed on the above bullets. As it can be seen, in this monotonic period, the assumption made for the PVTs fixed annual temperature is valid.

With Figure 5.17, the PVTs' heat SP is plotted for all system and for the borefields of 16 and 40 BHEs. Based on the results, the B_NE and B_NB system are capable of lower SP_{PVT_heat} than system with A configuration. This drop of high magnitude for systems B against systems A, is due to raised PVT inlet temperature. The elevated temperature is caused by the DHW tank in which the water is maintained in relatively high temperature (higher than the EEB's soil), thus the return from the tank fluid owns higher temperature. As it is well known, the collectors' high inlet temperature deteriorates the heat losses and increases the critical irradiance level. Similarly, the very low inlet temperature may not add more heat losses but decreases the collectors' outlet temperature. This is what happens with B_NB system, the soil temperature is way much lower than all the other system, and that causes a dropped inlet temperature (Figure 5.5). In order to escape from being confused, the lower inlet temperature increases the PVTs efficiency but drops the outlet temperature which is the criterion for solar heat utilization. Therefore, as it is analyzed above, the lower outlet temperature potential has lower changes to be absorbed by the system.

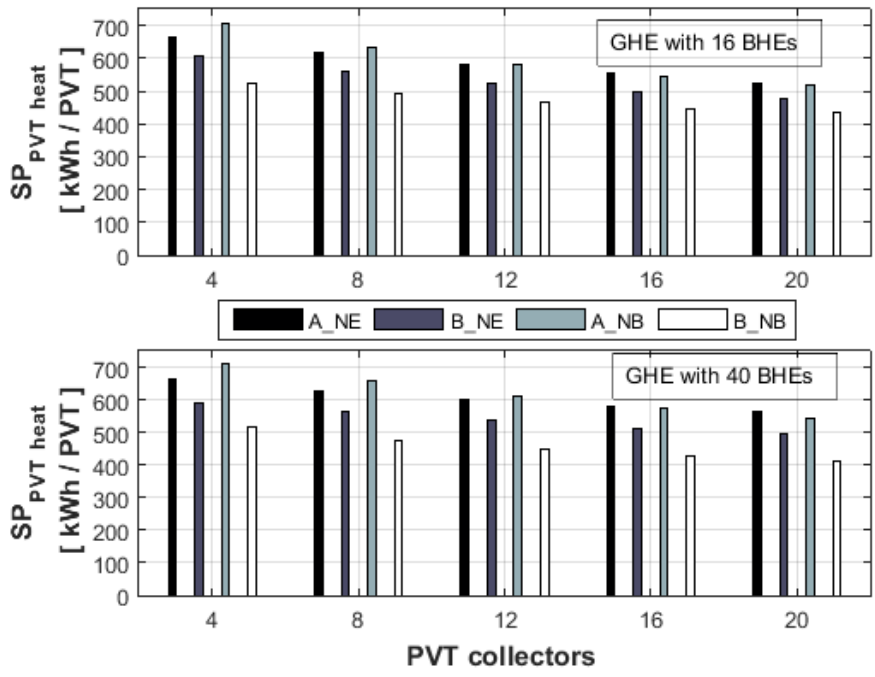

Figure 5.17. PVT heat specific productivity for all system and for borefield of 16 and 40 BHEs.

Table 5.11 lists the PVT heat SP values for all system and for the borefield of 16 and 40 BHEs. As it can be seen, the A_NB system is the most efficiency until the array of 16 PVTs which shifts with the A_NE. Systems B_NE and B_NB own the third and fourth posts throughout all the arrays and borefield respectively. The PVT collectors higher heat SP was recorded for A_NB system to be 713.1 kWh PVT^{-1}, and the lower is owned by B_NB system at 412.6 kWh PVT^{-1}.

Table 5.11. PVT heat SP Values for all system scenarios, with borefields of 16 and 40 BHEs.

Borefield	PVT	PVT heat SP [kWh PVT^{-1}]			
		A_NE	B_NE	A_NB	B_NB
16 BHEs	4	663,6	606,3	703,7	521,4
	8	617,8	560,2	631,1	490,5
	12	582,8	524,1	581,4	464,2
	16	552,2	496,2	543,8	443,8
	20	525,5	476,2	515,7	434,0
40 BHEs	4	662,6	589,0	713,1	514,5
	8	626,6	564,2	659,2	474,5
	12	601,8	535,4	612,3	447,8
	16	581,9	511,0	572,3	426,1
	20	565,7	496,5	543,1	412,6

The Figure 5.18 shows the PVTs' heat SP relationship with the SC. In Figure 5.18, the SP_{PVT_heat} increases as the SC grows, and after the value of 12 $m^3 m^{-2}$, the SP reaches a plateau (for systems A layout). The above mention trend is applied to all the investigated systems. For systems A, the PVT heat SP is influenced more from the SC than the systems with B layout. The mechanism in which the larger EEB volume benefits the solar heat utilization has been analyzed previously in this subsection. At this moment, one can say that after the critical value of 12 $m^3 m^{-2}$ (graphically estimated), the solar heat utilization is no more increased by increasing the EEB. This may be a useful optimum design strategy, to keep this ratio between the PVTs and BHEs (0.17 PVT / BHE) for the best solar heat productivity. The critical SC for the systems B layout is between 8 and 12 $m^3 m^{-2}$, and it seems totally acceptable a lower value, because the DHW tank plays also a heat storage role which is not include in this analysis.

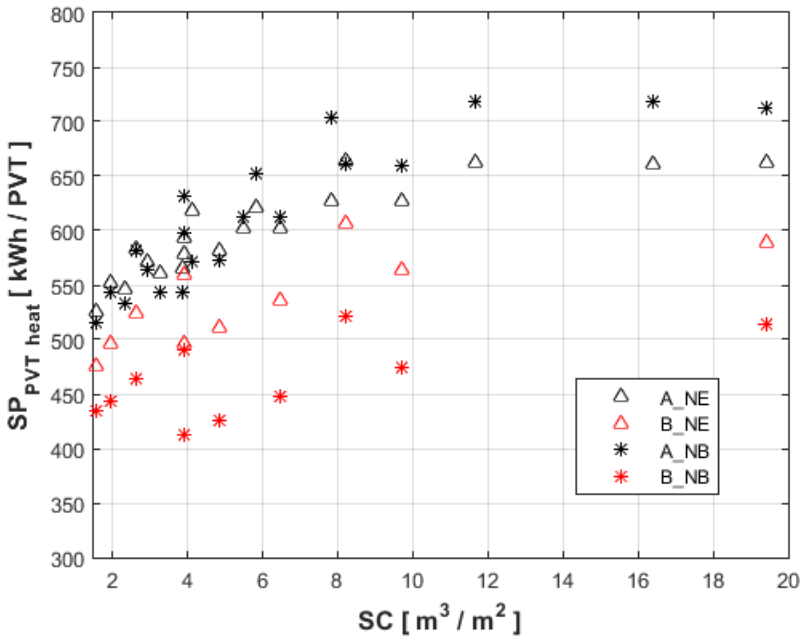

Figure 5.18. PVT heat SP for all systems as function of the storage capacity (SC).

5.1.4. Seasonal performance factor for the new dwelling

The systems seasonal performance factor (SPF), is the remaining metric in order to finish the new dwelling's heat analysis. SPF is the ratio between the heat delivered and the electricity used by the system (subsection 3.5.1). In the investigated system, PVTs offer electricity to the system and by that a substantial portion of the consumed energy is balanced. Based on equation 3.2, Table 5.12 lists the SPF calculated for the A_NE system. As it can be seen in Table 5.12, due to PVTs contribution to electricity consumption, the SPF increments after the array of 4 PVT, and literally obtains infinity value. The infinity value for the SPF can be interpreted as a system which can runs on its one energy supplies. In what follows, the SPF will be treated as the SPF_{H4} discussed in metrics subsection 3.5.1, for convenience the index is removed. With the index H4 on the SPF, all the electricity consumed by the space heating system is accounted, heat pump, circulation pumps and auxiliary energy (see equation 3.2 for details).

SPF is used widely to evaluate heat pump-based system's performance, but most of available systems are not equipped with cogeneration devices as PVTs. With the need produce a SPF with a broader use, the SPF^* is calculated and plotted in Figure 5.19. The SPF^* differs from the SPF on the fact that the electricity generated by PVTs is not included on the calculations (only the electrical consumptions are added). The above approach creates a SPF which illustrates the system performance as to be equipped with uncovered flat plate solar collectors instead of PVTs

(without the power generation part, but with the PVT's efficiency). As it can be observed in Figure 5.19, the SPF* increases as the borefield enlarges, and a secondary smaller increase of the SPF* occurs as the PVT array grows. The maximum SPF* of 3.04 and minimum of 1.46, have been obtained by the larger system consisted from 20 PVTs and 40 BHEs and by the systems without PVTs and 16 BHEs respectively (Table 5.13). By not considering the electricity balance on the calculation, the GHE's size seems to influence the most the SPF*. The influence of the GHE on the SPF* is stronger as the borefield is getting bigger and turns out to be weaker for smaller GHEs.

Table 5.12. SPF for A_NE system, calculated via equation 3.2.

	SPF			
PVTs	**16 BHEs**	**24 BHEs**	**32 BHEs**	**40 BHEs**
0	1.46	1.90	2.56	3.00
4	2.38	3.22	4.20	5.01
8	4.70	7.68	11.39	16.37
12	48.33	∞	∞	∞
16	∞	∞	∞	∞
20	∞	∞	∞	∞

By observing the SPF* results plotted in Figure 5.19 and listed by Table 5.13, systems with PVTs almost always have higher coefficients of performance than pure ground source based systems (0 PVTs). The only exception on the above trend, is the system equipped only with the borefield of 40 BHEs without PVTs. In this instance, the SPF* varies slightly through all the PVT arrays. As it can be seen in the results, the borefield of 40 BHEs gets the lower variation of SPF* values throughout all the simulation scenarios. This mainly happens due to substantial large EEB which can maintain a high soil temperature even without PVTs. But, by adding PVTs, the system needs to consume parasitic energy in order to utilize the solar heat. This aspect mitigates the benefits form the higher soil temperature created by the PVTs and balances the SPF*. For all other borefield sizes, the PVTs increase the mean soil temperature which consequently drive the heat pump to operate with higher COP, and that causes lower compressor's electricity consumption (the evaporator's inlet temperature is influenced directly by the EEB's soil temperature).

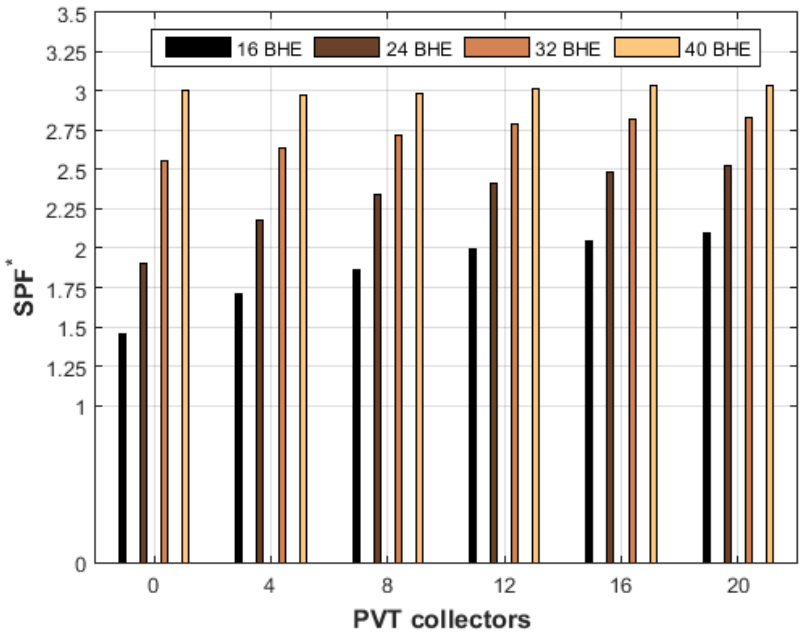

Figure 5.19. SPF for A_NE system. The electricity offered by PVTs is excluded from calculations in equation 3.2.*

Table 5.13. SPF for A_NE system.*

	SPF*			
PVTs	**16 BHEs**	**24 BHEs**	**32 BHEs**	**40 BHEs**
0	1.46	1.90	2.56	3.00
4	1.71	2.18	2.64	2.98
8	1.87	2.34	2.72	2.98
12	2.00	2.42	2.79	3.01
16	2.04	2.49	2.82	3.03
20	2.10	2.52	2.83	3.04

In Figure 5.20 the correlation of the SPF* with the CBR is illustrated for the A_NE system. In this figure, the blue marks show the systems without PVTs and the red marks depict the SPF with infinity value (Table 5.12). Based on the illustrated results, there is no explicit link between the CBR and the best SPF*. The higher SPF*are for CBR between 0.3 and 0.5, and that belongs to a PVT array of 12 and 20 collectors respectively paired with 40 BHEs. Following that, in Table 5.13, for the GHE of 40 BHEs paired with 16 PVTs to the array of 20 PVTs, there is a small drop in SPF*which is caused by more parasitic energy without the result of higher temperature. Also, by observing the Table 5.12 and Figure 5.20, systems which can be energetically self-sufficient, need a critical quantity of PVTs which decreases as the borefield enlarges. Thus, for borefield of 16 BHEs 16 and more PVTs required for a system which can run on its own energy supplies. Accordingly, for larger borefields of 24,32 and 40 BHEs, the systems become self-sufficient by

12 collectors. This mainly happens because a larger GHE maintains a higher mean soil temperature (more heat is stored in the EEB) which causes lower electricity consumption in the heat pump, and that decreases substantial the denominator of equation 3.2.

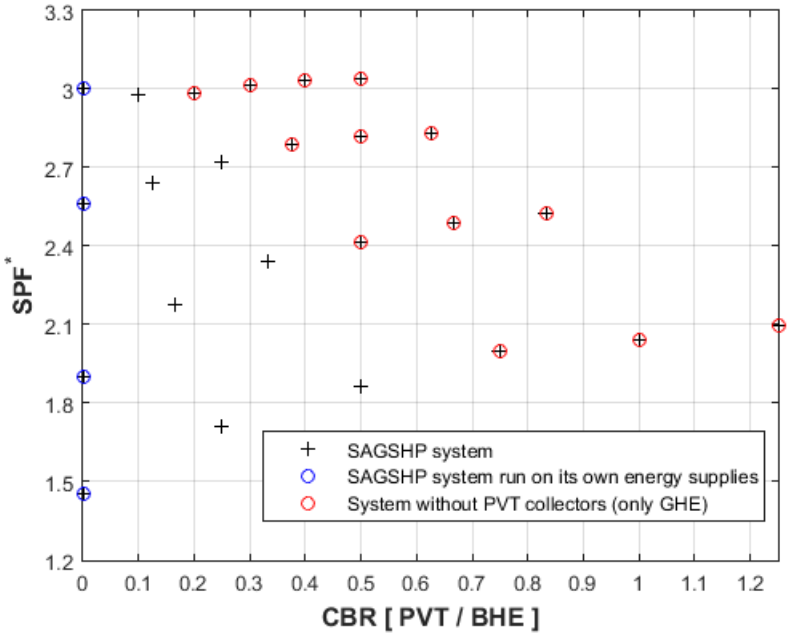

*Figure 5.20. SPF*for A_NE system as function of the CBR (Table 5.13).*

As regards the A_NB system, in Table 5.14 the values for the SPF and for SPF*are listed. As it can be seen by the values listed for the consolidated SPF, the A_NB system's performance is lower than system A_NE in all equally sized systems. In contrast with the A_NE, the A_NB requires more than 12 PVTs for the half of its borefield sizes in order to achieve a self-sufficient system. Also, for the totally geothermal energy system (without PVTs), the SPF is lower in all cases than the same system with the EEB being exposed (Table 5.12). The A_NB system's lower SPF against the A_NE, is caused by the poor natural soil heat recovery and the need of solar heat in order to rise the soil temperature. Therefore, the solar heat is offered not only to elevate the soil temperature but to mitigate the lack of the natural heat recovery process.

As it is plotted in Figure 5.21 and listed in Table 5.14, the SPF* gets values from 0.96 up to 3.07 for the system of 16 BHEs without PVTs and the system of 20 PVTs paired with 40 BHEs. Beyond these lower and higher SPF* values, the whole process follows the same trend with the A_NE system, improving its performance as the borefield enlarges and the PVT quantity increases, but with a more explicit way. The main difference between the two systems is that the A_NB show higher dependency on PVT quantity in order to rise the SPF*, contrary to A_NE which is matter

of the borefield size. As it can be seen in Figure 5.21, even the GHE of 40 BHEs is influenced by the PVTs count, and the achieved SPF*increases from 2.06 to 3.07 after the addition of 20 PVTs. This phenomenon illustrates that unlikely the A_NE system, the A_NB even in the larger borefield improves further its performance as the PVT quantity increases and it does not enter in a stagnation. The main reason for this continuously improved performance with the PVT quantity grow is due to the thirst soil for heat.

Table 5.14. SPF and SPF for A_NB system.*

PVT	16 BHE	24 BHE	32 BHE	40 BHE	
0	0.96	1.40	1.81	2.06	SPF
4	1.95	2.49	3.14	4.00	
8	3.87	4.96	7.35	11.47	
12	16.65	39.73	∞	∞	
16	∞	∞	∞	∞	
20	∞	∞	∞	∞	
0	0.96	1.40	1.81	2.06	SPF^*
4	1.45	1.81	2.18	2.62	
8	1.69	2.01	2.42	2.82	
12	1.85	2.17	2.61	2.95	
16	1.90	2.35	2.70	3.02	
20	1.97	2.43	2.79	3.07	

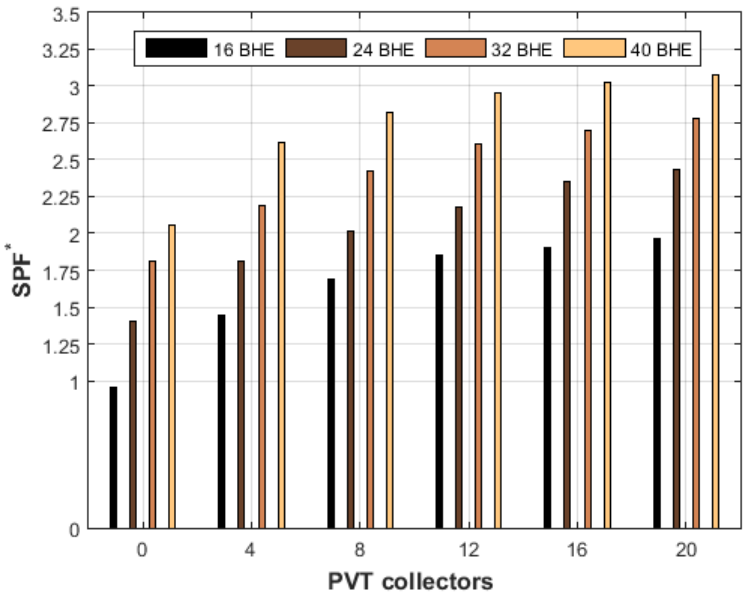

*Figure 5.21. SPF*for A_NB system. The electricity offered by PVTs is excluded from equation 3.2.*

With Figure 5.22, the A_NB system's SPF* is plotted as function of the CBR. Like Figure 5.20, in Figure 5.22 the blue marks show a 100% geothermal energy depended systems without PVTs and the red marks depict the values where the SPF is infinity. As a general observation, can say

that the SPF* higher values are formulated for CBR between 0.3 and 0.5, that means 1 PVT per 3 BHEs and 2 BHEs respectively. Also, for CBR lower than 0.3, the system cannot obtain be self-sufficient in energy with any borefield size.

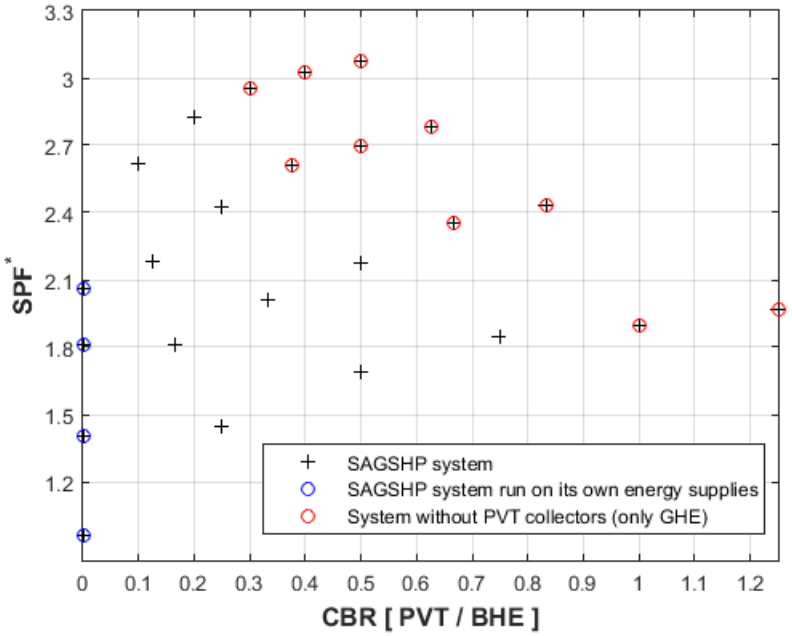

Figure 5.22. SPF* for A_NB system as function of the CBR.

Table 5.15. Values of SPF for all system with the new dwelling and for the borefields of 16 and 40 BHEs.

		SFP			
Borefield	**PVT**	**A_NE**	**B_NE**	**A_NB**	**B_NB**
16 BHEs	0	1.46	1.46	0.96	0.96
	4	2.38	2.30	1.95	1.99
	8	4.70	3.82	3.87	3.51
	12	48.33	8.40	16.65	7.52
	16	∞	∞	∞	∞
	20	∞	∞	∞	∞
40 BHEs	0	3.00	3.00	2.06	2.06
	4	5.01	4.26	4.00	3.43
	8	16.37	8.17	11.47	6.56
	12	∞	156.78	∞	37.28
	16	∞	∞	∞	∞
	20	∞	∞	∞	∞

In Table 5.15, the SPF values obtained from systems B and A layout are listed. Regarding the SPF for B_NE and B_NB systems are lower than both A configuration-based systems. This discrepancy is caused by the direct use of solar heat which results lower soil temperature than systems A configuration. Consequently, with lower evaporator's inlet temperature more electricity for the compressor is needed in order to cover the heat load. Between system B_NE

and B_NB, the first one show better performance, due to easily heat rechargeable EEB from the surrounding soil mass.

*Table 5.16. Values of SPF*for all system with the new dwelling and for the borefields of 16 and 40 BHEs.*

		SFP*			
Borefield	**PVT**	**A_NE**	**B_NE**	**A_NB**	**B_NB**
16 BHEs	0	1.46	1.46	0.96	0.96
	4	1.71	1.75	1.45	1.53
	8	1.87	1.91	1.69	1.77
	12	2.00	1.97	1.85	1.85
	16	2.04	2.03	1.90	1.92
	20	2.10	2.09	1.97	1.96
40 BHEs	0	3.00	3.00	2.06	2.06
	4	2.98	2.91	2.62	2.48
	8	2.98	2.89	2.82	2.67
	12	3.01	2.92	2.95	2.76
	16	3.03	2.93	3.02	2.77
	20	3.04	2.94	3.07	2.80

Table 5.16, the SPF* values for all systems installed in new dwelling and for borefields of 16 and 40 BHEs are listed, while Figure 5.23 illustrates the results graphically. Based on the results shown by Figure 5.23, the order of system SPF*, can be distinguished between the two borefield sizes. In details, for the borefield of 16 BHEs and for non-PVT to up to 8 PVTs, the B_NE holds the higher SPF* values and is followed in order by the A_NE, B_NB and A_NB system. For PVT arrays larger than 8 collectors, the systems are shaping two pairs with similar SPF*: the first group is the systems with the EEB being exposed which get the higher values and the second pair, with lower performance, are the systems with the EEB underneath the building. Also, as the PVT collectors' quantity increases the SPF*discrepancy among system drops. As regards the bigger borefield, up to the array of 12 PVTs, the A_NE system owns the highest values and after that the A_NB gets the first post. It seems that, after the system of 16 PVTs, the EEB's soil temperature increases further than the exposed scenario. This is confirmed by Figure 5.24, which show the EEB's mean soil temperature for systems A_NE and A_NB equipped with the borefield of 40 BHEs and for the arrays of 8, 12 and 16 PVTs. An equally magnitude sifting between systems B_NE and A_NB is taking place with the PVT array of 8 collectors (Figure 5.24). As it can be seen, the B_NE owns higher SPF*than the A_NB until the array of 8 PVTs, after that shifts to third place which remains there for the remaining configurations. The fourth post is owned by the B_NB system through all the PVT arrays paired with the larger borefield.

It is important to discuss further the Figure 5.24 and the mechanism which is revealed from this illustration of temperatures. As it can be seen, the A_NB has lower mean soil temperature than the A_NE for the array of 8 PVTs, this temperature profile is characterized also by a monotony of constant reduction. In contrast, system A_NE get higher soil temperature with the same equipment. But, both system with the array of 12 PVTs shape the similar mean soil temperature. That gives us the opportunity to say: there is a critical solar energy amount which compensates the lack of natural heat recovery mechanism and balances the soil temperature. Finally, after the array of 12 PVTs, the mean soil temperature for A_NB system grows further than A_NE by improving all the illustrated metric up to now. The A_NE system is not capable to rise further its temperature mainly because there are expedited heat losses through the EEB boundaries.

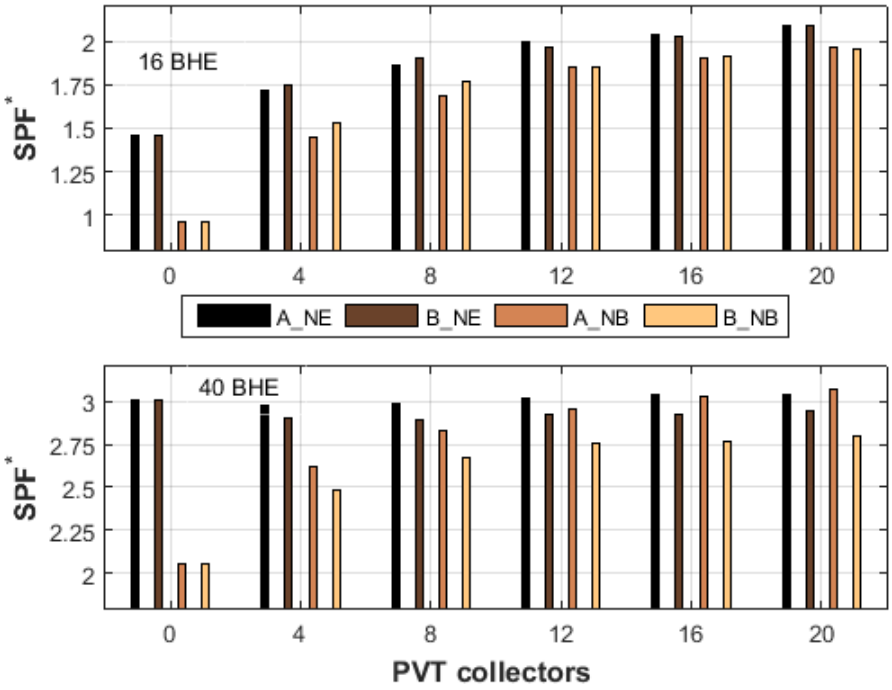

Figure 5.23. SPF*of all systems for the new dwelling for borefields of 16 and 40 BHEs.

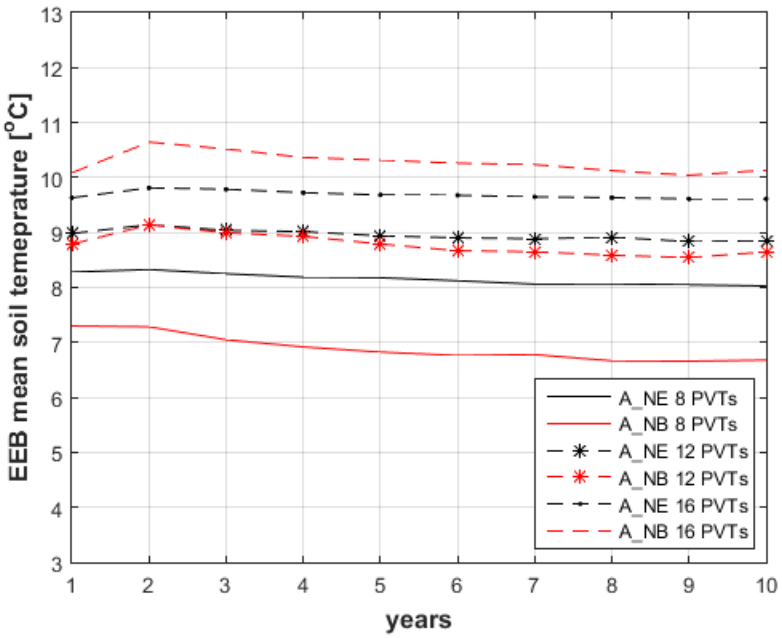

Figure 5.24. EEB's mean soil temperature for A_NE and A_NB system, for the borefield of 40 BHEs and for the arrays of 8,12 and 16 PVTs.

5.1.5. Results summary of the heat output evaluation

With Table 5.17, the higher and lower values of the four metrics presented in this section are listed, for the new dwelling. On the beginning of this summary, the universal outcomes from the parametric analyses are presented and then specified to each metric, important information is listed with dot points.

All the investigated systems (A_NE ,B_NE, A_NB, B_NB), interact similarly on the PVTs and BHEs variation. In other words, all systems follow the same trend of increase or decrease their values of the metrics with the variation of the system size (PVTs and BHEs).

The mean annual soil temperature of the EEB it can be distinguished in two periods: the fist which goes up to 4th year and is characterized as transient (Figure 5.5), and the second period which illustrates a monotony without sudden changes. The footprint of the dwelling was found to constrain the soil natural heat recovery mechanism, but for the larger borefield of 40 BHEs this phenomenon is eliminated. The direct solar heat utilized for the DHW needs was estimated to be up to 12% of the new. With the contacted parametric analyses, the mean soil temperature of the EEB was found to be highly related with the number of PVT collectors and the applied control of the system. Also, for the given system control, each PVT array shapes a mean soil temperature, regardless the borefield size (Figure 5.16).

Table 5.17. List of lower and higher values of heat evaluation metrics for all investigated schemes, new dwelling.

System		RHF	SP_{sys_heat} [kWh PVT^{-1}]	SP_{PVT_heat} [kWh PVT^{-1}]	SPF*
A_NE	higher	0.79	1203	664	3.04
	lower	0.45	194	526	1.46
B_NE	higher	0.83	1451	606	2.94
	lower	0.45	232	476	1.46
A_NB	higher	0.79	1207	719	3.07
	lower	0.33	193	516	0.96
B_NB	higher	0.81	1373	521	2.80
	lower	0.33	219	413	0.96

RHF: the highest value of 0.83 was achieved by B_NE system for the new building systems and at 0.74 for the refurbished systems.

- In general, the GHE imposes an initial RHF which increase further as the PVT array enlarges.
- The contribution of solar heat to RHF is greater for small borefields, while the phenomenon ceases as the number of BHEs increases. The main reason for this preference is the all-day long availability of the geothermal energy, contrary to the solar which is constrained by a number of factors like the level of the irradiance and PHE's effectiveness (Sakellariou *et al.*, 2019).
- With the EEB being installed beneath the building, the solar energy influences vitally the RHF. This solar heat dependence reduces as the number of BHEs increases.
- By injecting a critical solar heat amount in the EEB, the soil temperature balances with this of the EEB installed exposed. Thus, with the array of 12 PVT the A_NE and the A_NB get the same RHF and creating similar soil temperature regime (Figure 5.24).
- The higher RHF values for all systems have been obtained with 20 PVTs and 40 BHEs (20 PVTs with CBR 0.5 [20 $PVT_{0.5}$]).

System heat SP: the SAGSHP systems with 20 PVTs and 40 BHEs paired with the new dwelling, were found capable of harvesting from 1203 kWh PVT^{-1} (A_NE). For all systems and dwellings, the low values of the CBR (0.1 to 0.2) were found to benefit the heat SP.

- The system heat SP found to influence the RHF, because the renewable energy absorbed by the evaporator of the heat pump is the bigger portion of the RHF (Table 5.5).
- The system heat SP is Influenced more by the borefield size rather the PVT quantity.

PVT heat SP: the PVT heat SP was estimated between 476 kWh PVT^{-1} and 779 kWh PVT^{-1}, for the B_NE system with 20 PVT paired with 16 BHEs and for the A_RE with 4 PVT paired with 24 BHEs accordingly.

- The PVT heat SP rises with the larger soil volume, therefore small CBR values benefit the solar heat production (less PVT per BHE).
- The installation of the EEB underneath the dwelling is a positive aspect for the PVT heat SP. The natural heat recovery of the soil is constrained by the dwelling, thus the EEB shapes a lower temperature regime than this when the EEB being exposed. The lower mean soil temperature is prosperous ground for greater solar heat utilization.
- All the systems with the B layout (direct use of solar heat), were found with lower PVT heat SP from systems built with A layout. The reduction of the PVT heat SP was caused by the elevated temperature of the water in the DHW tank, which forces the PVT collectors to operate with higher inlet temperature and consequently a reduced thermal efficiency.
- For A topology systems built with new dwelling, it was found that for lower CBR value than 0.17 (or SC 12 m^3 m^2) the PVT heat SP does not improve further (Figure 5.18). Likewise, for systems with B topology and built with the new dwelling, the critical CBR values are between 0.2 and 0.17 (or 8 to 12 m^3 m^{-2}).

SPF: all systems built with the new dwelling reach the energy self- sufficient regime. With details, the A_NE becomes energy self-sufficient for all systems consisted of 12 and more PVTs, by excluding the configuration of 16 BHEs paired with the array of 12 PVTs. Similarly, the A_NB enters in the self- sufficient regime from the PVT array of 12 collectors, by excluding the borefields of 16 and 24 BHEs where larger arrays required. The B_NE and B_NB systems, both were entered in the energetically independent stage from PVT arrays larger than 12 PVTs and regardless the borefields size. The GHE size influence more than the PVT quantity the SPF, for both dwelling types.

- There is not a direct link between the SPF* and the CBR index, but higher CBR improve the SPF due to more PVTs and thus higher electricity generation.
- System with the EEB beneath the dwelling get lower SPF than these with the exposed EEB, because of the lower mean soil temperature and the higher parasitic energy. Additionally, systems with the EEB beneath the building, illustrate higher solar heat

dependency than these with the exposed EEB (which are influenced more by the GHE size).

- SPF values for B system topology were estimated to be lower than the A topology, due to direct use of solar heat which resulting to a dropped mean soil temperature. Thus, more electricity is needed from the heat pump to operate with lower COP and for more time.

5.2. Electric output evaluation of the new dwelling

5.2.1. PVTs' electric specific productivity for the new dwelling

PVT electric SP indicates the annual electricity generated per collector. As it can be seen in Table 5.18, the PVTs' yield varies slightly through all simulation scenarios for both systems A_NE and A_NB. For the A_NE system, the PVT electric SP fluctuates slightly from 240.6 kWh PVT^{-1} up to 242.3 kWh PVT^{-1}. As regards the A_NB system, the SP_{PVT_el} varies between 240.3 kWh PVT^{-1} and 242.8 kWh PVT^{-1} correspondingly. The highest disparity among the SP_{PVT_el} values illustrated in Table 5.18 remains below the 1% and the average electricity yield is estimated to be 241.7 kWh PVT^{-1}.

The reasons for PVT electric SP small variation during systems parametric analyses, as shown by Table 5.18, is caused by:

- During the analyses the inclination and the orientation of the collectors were fixed (section 4.1). Also, the annual environmental conditions were kept unchanged for all simulations.
- The PVTs flow rate was increased linearly by 50 L h^{-1} PVT^{-1}, thus the flowrate on which the fluid remove heat from every collector was not changed through simulations. Bear in mind (section 4.1) that, the PVT array scales up by strings of four collectors in series connected hydraulically, and therefore the solar pump ({2} in Figure 3.5) supplies fluid with flow rate 200 L h^{-1} per string. The above conditions buffer the PVTs power yield from changes applied to the system's size and established a constant in-pipe heat removal coefficient (section 4.1).
- The PVT inlet temperature is the only parameter left, which can influence the collectors plate mean temperature and consequently the PV cells efficiency. As it is proved in subsection 5.1.3, the inlet temperature does not fluctuate significantly with the systems' size variation. Because the EEB's mean soil temperature is regulated by the system's

applied control, the PHE and the number of PVTs in-series connected. By having the EEB's soil to be in similar temperature condition regardless the system size, the PVTs' inlet temperature is not influenced significantly (Figure 5.15).

Table 5.18. PVT electric SP for systems A_NE and A_NB.

		PVT electric SP [kWh PVT^{-1}]			
System	**PVT**	**16 BHE**	**24 BHE**	**32 BHE**	**40 BHE**
	4	242.2	242.3	242.3	242.3
	8	241.8	241.9	242.0	242.0
A_NE	12	241.5	241.6	241.7	241.8
	16	241.0	241.3	241.5	241.5
	20	240.6	240.9	241.3	241.3
	4	242.6	242.8	242.8	242.8
	8	242.0	242.3	242.3	242.3
A_NB	12	241.5	241.7	241.9	241.8
	16	240.9	241.3	241.4	241.5
	20	240.4	240.7	241.0	241.1

The only worth to be mentioned trend identified in Table 5.18, is the small drop in the power SP as the PVT array grows. This small reduction is linked to the ability owed by more PVTs to maintain a raised EEB's soil temperature (slightly higher than the smaller arrays), which sequentially offers a higher collectors inlet temperature, thus the PV cells efficiency reduces. Lastly, the higher power SP are achieved by the array of 4 PVTs paired with 40 BHEs and the lower values are derived by the array of 20 PVTs paired with 16 BHEs. The above-mentioned systems are characterized by CBR 0.1 and 1.25 for the highest and lower values of SP_{PVT_el} respectively. Therefore, someone can say that the SP_{PVT_el} variation as function of CBR, is governed by the same rules as the system and PVT heat SP (subsection 5.1.2).

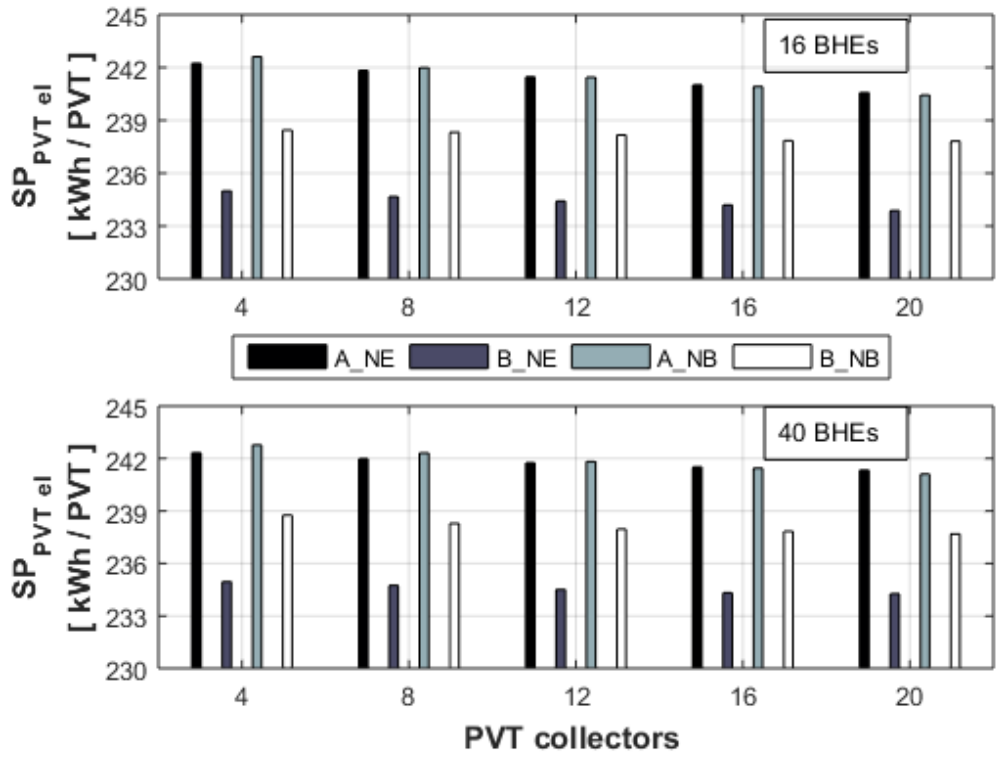

Figure 5.25. PVT electric SP for all systems paired with the new dwelling and for the borefield of 16 and 40 BHEs.

The power SP for all systems paired with the new dwelling and for the borefields of 16 and 40 BHEs are illustrated in Figure 5.25 and listed by Table 5.19 respectively. According to the results, systems A_NE and A_NB are the most capable for electricity generation with fractional different between the listed values. A substantial drop in SP_{PVT_el} was recorded for system with B topology against the values belong to the A type of systems. Therefore, system B_NB is in the third place with average reduction of 1.5% against A topology systems mean value and the last one is the B_NE with 3% lower power generation respectively. System's B_NB average SP_{PVT_el} was found to be 238.1 kWh PVT^{-1} with the small PVT arrays to obtain marginally higher values. As regards the system B_NE, the mean power generated per collector was 234.5 kWh PVT^{-1} with the PVT array size to not influence significantly the generation.

Table 5.19. PVT electric SP vales for all systems paired with the new dwelling and for borefield of 16 and 40 BHEs.

		PVT electric SP [kWh PVT^{-1}]			
Borefield	**PVT**	**A_NE**	**B_NE**	**A_NB**	**B_NB**
16 BHEs	4	242.2	235.0	242.6	238.5
	8	241.8	234.7	242.0	238.3
	12	241.5	234.4	241.5	238.2
	16	241.0	234.2	240.9	237.9
	20	240.6	233.9	240.4	237.8
40 BHEs	4	242.3	235.0	242.8	238.8
	8	242.0	234.7	242.3	238.3
	12	241.8	234.5	241.8	238.0
	16	241.5	234.3	241.5	237.8
	20	241.3	234.3	241.1	237.7

5.2.2. Renewable power fraction for the new dwelling

The renewable power fraction (RPF) depicts the portion of the system's electricity annual demand covered by the PVTs' delivered yield (subsection 3.5.4). Thus, Table 5.20 lists the power fraction for systems A_NE and A_NB, also values calculated higher than one are treated as the ratio between the delivered by PVT power and the consumption.[16] Among the power SP listed in Table 5.20, A_NE system found to obtain higher electricity independence than A_NB system to all equally sized system. Also, both systems found capable of establishing a self-sufficient condition on the half of the simulations scenarios. Thus, for the A_NE system's power self-sufficient starts with the array of 12 PVTs paired with more than 16 BHEs. Similarly, for the A_NB system, the power independence can be achieved with 24 BHEs and 12 PVTs.

As it can be seen in Table 5.20, the RPF rises as the PVT quantity increases and as the borefield size enlarges. By accepting that PVTs' electricity yield is not influenced much by the system's size (5.2.1), then the reasons for this improvement are: a) the higher inlet temperature of the evaporator which can formulated by the larger PVT arrays, b) bigger EEBs are capable of offering more heat without experiencing a substantial drop into the mean soil temperature (buffering the heat absorption from the heat pump) and c) with the larger system, the RHF is increased (Figure 5.1), thus less auxiliary energy is needed. For ostensive reasons, *Figure 5.26* is printed to illustrates the mixture of system's power consumption as function of the PVTs and BHEs quantity. In *Figure 5.26*, someone can see the reduction of the electricity used by the heat pump and the drop of the auxiliary energy as the system enlarges. Only the used parasitic electricity

[16] by definition a fraction cannot go over the value of one.

rises as the PVT array grows and that is due to the pumps with higher nominal capacity (Table 4.2).

Table 5.20. RPF achieved for A_NE and A_NB systems. The number in the parentheses state the ratio between the delivered electricity by PVT to the consumption.

		RPF			
System	**PVT**	**16 BHE**	**24 BHE**	**32 BHE**	**40 BHE**
	4	0.27	0.30	0.35	0.38
	8	0.57	0.65	0.71	0.76
A_NE	12	0.90	1.00	1.00 (1.08)	1.00 (1.14)
	16	1.00 (1.20)	1.00 (1.35)	1.00 (1.46)	1.00 (1.53)
	20	1.00 (1.52)	1.00 (1.69)	1.00 (1.82)	1.00 (1.91)
	4	0.25	0.26	0.29	0.32
	8	0.53	0.56	0.63	0.70
A_NB	12	0.84	0.89	1.00 (1.01)	1.00 (1.10)
	16	1.00 (1.12)	1.00 (1.27)	1.00 (1.39)	1.00 (1.51)
	20	1.00 (1.43)	1.00 (1.63)	1.00 (1.79)	1.00 (1.90)

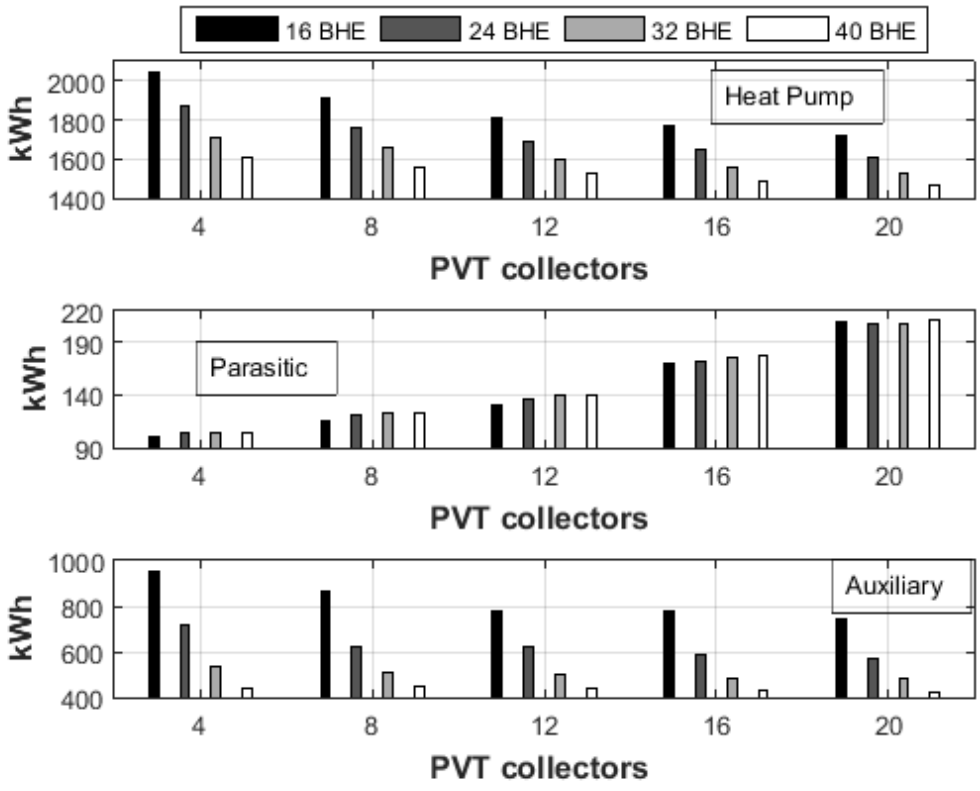

Figure 5.26. A_NE system's electricity consumption mixture as function of the PVTs and BHEs amount. Where: Heat pump-is the energy used by the device, Parasitic-is the electricity consumed by the circulation pumps, Auxiliary-is the energy used additional to the offered by the heat pump's condenser in order to cover the heat demand.

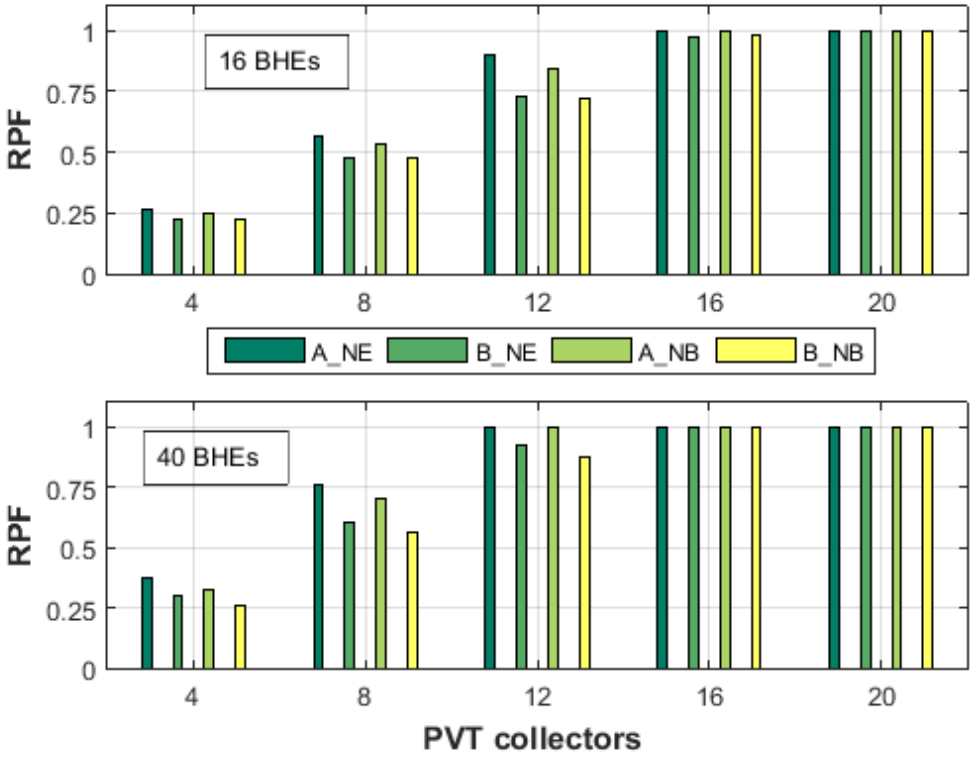

Figure 5.27. RPF achieved from all system as function of the PVT array and for the borefields of 16 and 40 BHEs.

Table 5.21. RPF values achieved from all system as function of the PVT array and for the borefields of 16 and 40 BHEs.

		RPF			
Borefield	**PVT**	**A_NE**	**B_NE**	**A_NB**	**B_NB**
	4	0.27	0.23	0.25	0.22
	8	0.57	0.48	0.53	0.47
16 BHEs	12	0.90	0.73	0.84	0.72
	16	1.00 (1.20)	0.99	1.00 (1.12)	0.99
	20	1.00 (1.52)	1.00 (1.24)	1.00 (1.43)	1.00 (1.23)
	4	0.38	0.30	0.32	0.26
	8	0.76	0.61	0.70	0.56
40 BHEs	12	1.00 (1.14)	0.92	1.00 (1.10)	0.87
	16	1.00 (1.53)	1.00 (1.23)	1.00 (1.51)	1.00 (1.18)
	20	1.00 (1.91)	1.00 (1.54)	1.00 (1.90)	1.00 (1.47)

With Figure 5.27 and Table 5.21, the RPF values for all system are illustrated and listed for the borefields of 16 and 40 BHEs. Based on the results, all systems installed with the new dwelling can reach a self-sufficient state with 16 PVTs and for both GHE sizes. Also, systems with A topology are the most productive and are followed by system B_NE and B_NB. The sequence of

the system regarding the RPF values follows the PVTs power SP. There is only an alteration between the B_NE with B_NB, regarding the RPF, B_NE system achieves higher values than the B_NB. In that case, the slightly increased mean soil temperature benefits the heat pump compressor which consumes less electricity.

5.2.3. Summary and further discussion of the electric output evaluation

In Table 5.22, the higher and lower values of the PVT electric SP are presented, for all systems considered for the new dwelling (Table 5.1). The average value of the SP_{PVT_el} for both systems A_NE and A_NB were estimated at 241.7 kWh PVT^{-1} (Table 5.19), with the higher disparity among the values to be 1%. Regarding the B topology, the average PVT electric SP of the systems is 236.3 kWh PVT^{-1} (N_NE and B_NB) and the disparity of the estimated values is 2% (Table 5.19). The small variation of SP_{PVT_el} among systems with the same topology (A or B) was caused by:

- Fixed inclination and orientation of the PVTs. By changing the inclination of the PVT collectors, the electricity yield is influenced directly.
- The flow rate for each PVT collector was kept constant through all the parametric analyses. Variation on the flow rate causes variation on the temperature of the photovoltaic cells', and consequently their electrical efficiency changes respectively.
- The small variation of the PVT inlet temperature, regardless the borefield size (subsection 5.1.3).

A small reduction of the PVT electric SP was identified for larger PVT arrays, due to their ability to maintain a slightly higher soil temperature than the smaller arrays, this condition consequently elevates the inlet temperature of the PVTs. There is not a strong link between the SP_{PVT_el} and the CBR index, but the power generation was influenced more by the system topology. Therefore, two groups can be classified, the systems with the A topology (Figure 3.5) and higher electricity generation, and the systems with the B topology (Figure 3.7) with lower capability for electricity production. The system B topology offers higher PVT inlet temperature than A topology, due to the relatively increase temperature of the water in the DHW tank. Consequently, the increased inlet temperature elevated the absorber's mean plate temperature, which drives the PV cells to operate with reduce efficiency. The mean PVT power SP for the B_NB systems was estimated to be 1.5% lower than the average value of both systems with A topology (A_NE and A_NB), while for the B_NE systems the reduction was at 3% respectively.

Table 5.22. List of lower and higher values of PVT power SP, for all systems.

System		SP_{PVT_el} [kWh PVT^{-1}]
A_NE	higher	242.3
	lower	240.6
B_NE	higher	235.0
	lower	233.9
A_NB	higher	242.8
	lower	240.3
B_NB	higher	238.8
	lower	237.8

The RPF is increase for all systems as the borefield enlarges and as the PVT quantity increases. The reasons for this trend are mainly:

- The higher inlet temperature of the evaporator formulated by the increase soil temperature (more PVTs and bigger EEB).
- With a bigger system, consisted of more PVTs and BHEs, the need for auxiliary energy is lower than a smaller system.
- Regarding the values of the RPF, all systems paired with the new dwelling can balance the consumption with the generation after the array of 16 PVTs, regards the borefield size. It is worth noticing that, the energy self-sufficient regime is formulated with equal size systems with these entering the infinity SPF (subsection 5.1.4). Therefore, the information delivered by the SPF regarding the electricity sufficiency of SAGSHP systems can be delivered alternatively by the RPF metric.[17]

With this chapter all the SAGSHP systems paired with the new dwelling are evaluated and compared with the aim to identify the higher energy performance. Based on the results illustrated in this chapter, all systems have achieved a RHF which is function of the PVTs' and BHEs' quantity, giving that the remaining parameters did not alter during the analysis. In that point is appropriate to remind that the RHF depicts the fraction of the heating load covered by RES (equation 3.6). Inductively, what remains from the RHF should be covered by the heat added via the heat pump's compressor and the amount of auxiliary energy. Both parts of the remaining heat have been assumed to be offered by consuming electricity, which may be imported from the power grid or produced by PTVs. Based on that, it turns out that the system with the higher

[17] This is based on the fact of making the denominator of equation 3.2 zero or negative, which means the PVT generation is greater than the system consumption.

RPF is the most energetically efficient. Because, the RPF is the ratio of the electricity generated by PVTs and the electricity consumed by the SAGSHP system (equation 3.7). In other words, the RPF indicates the proportion between the generated and consumed electricity of the system, but giving that the parameters are considered to be the same for all systems, the higher the RPF the higher the energy performance of the system.

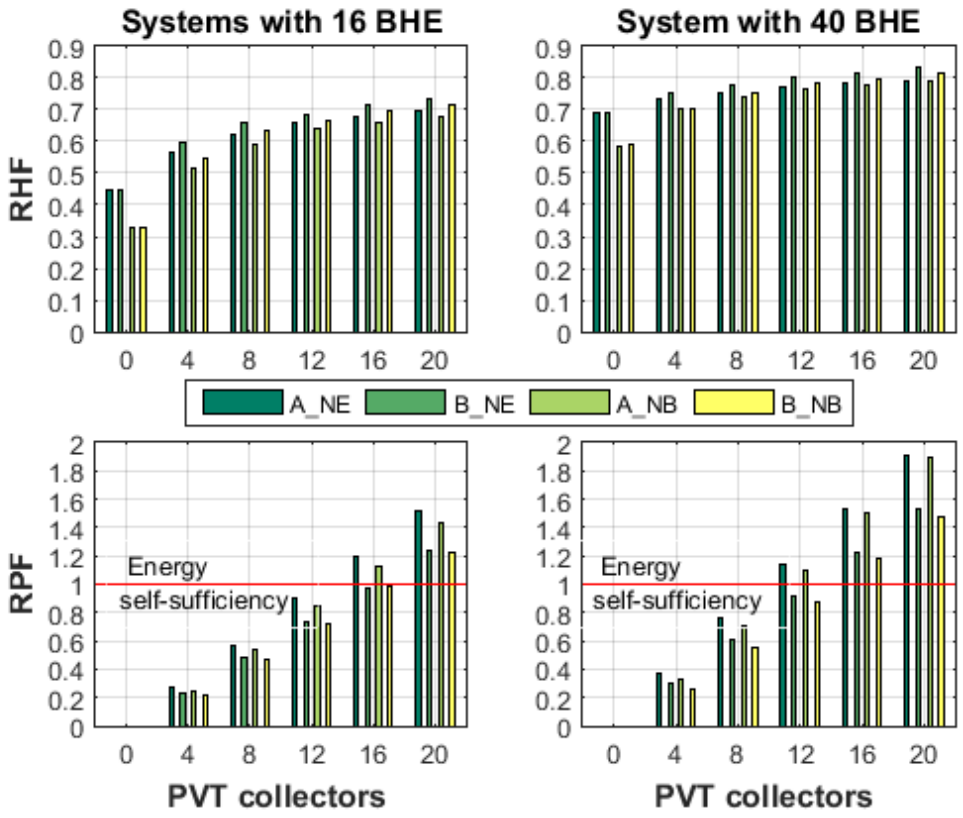

Figure 5.28. RHF and RPF for all systems built with the new dwelling and for borefields of 16 BHEs and 40 BHEs.

In Figure 5.28, the RHF and RPF are printed for all systems considered with the new dwelling and for the borefields of 16 and 40 BHEs. Based on the results, systems with A topology found to be energetically better than these with the B configuration (direct use of solar heat). The EEB location ends up being a second criterion for the energy efficiency, with the exposed choice to be the best solution against the beneath the building. Across all the schemes of systems illustrated by Figure 5.28, the A_NE gets the highest RPF and is followed with slightly lower value by the A_NB. As regards the systems B_NE and B_NB, these share the third and fourth position with substantial drop from systems with A topology. Finally, for the schemes without PVT collectors, the exposed arrangement benefits the most the energy efficiency of the system.

Because the RHF is made by 100% geothermal energy, and the exposed location is the most suitable for the natural heat recovery of the soil.

Nearly all of the reviewed research works, the SPF was utilized as the metric to evaluate the performance of the systems (Chapter 1, Table 2.1, Table 2.2,Table 2.4). In the current study, the achieved by systems SPF and SPF* were calculated and illustrated for all schemes. The SPF* is the version of the SPF which does not contain the generated by PVT electricity, thus the metric shows the ratio between the heat delivered and the electricity consumed by the system. But, as it can be seen in Figure 5.23, the SPF* does not follow the order of the RPF illustrated in Figure 5.28. Therefore, the most energetical efficient cannot be identified via the highest SPF*, due to not considering the power from PVTs. In contrast with the SPF*, the SPF (Table 5.15) includes the generated electricity by PVTs, thus the metric can follow the same order with the RPF. The limitation on this occasion is that the SPF illustrate values which may reach the infinity, though the SPF is a ratio which cannot get infinity values. To conclude, the SPF is the appropriate metric to evaluate the performance of SAGSHP systems which are equipped with heat and power generation devices, by acknowledging the limitation of getting infinity value under some instances.

Chapter 6. Results evaluation for the refurbished dwelling

6.1. Heat output evaluation for the refurbished dwelling

The analysis moves on to the refurbished dwelling with the EEB being exposed for both systems layouts, A and B (Figure 3.4). As regards the differences between the new and the refurbished house, this is based on the 2.76 greater space heating load of the renovated one against the brand new. In numbers, the above ratio of the annual space heating demand is 3522 kWh_{TH} and 9741 kWh_{TH}, for the new and the refurbished dwelling accordingly (the annual DHW needs is equal for both houses: 2528 kWh_{TH}). Therefore, in this chapter the system is tested under a substantial larger heating load than this considered in the section of the new dwelling. Lastly, the structure of the chapter follows the one used for the new dwelling (Chapter 5), with two sections, one for the heat and one for the electric output evaluation.

In Table 6.1, all simulation schemes are listed and described along with their used acronymic name (also see Figure 3.4). Information about the simulation scenarios can be found in section 3.1, in where the utilized research procedure is summarized. Additionally, a more specified description about the two system topologies (A and B) can be reached via section 3.2.

Table 6.1. Simulation schemes along with their acronymic names and description for the refurbished dwelling.

SAGSHP system acronymic name	Description
A_RE	System built with A topology (A, without direct use of solar heat), in the refurbished Dwelling (R) and with the GHE exposed (E)
B_RE	System built with B topology (B, with direct use of solar heat), in the refurbished Dwelling (R) and with the GHE exposed (E)

6.1.1. Refurbished dwelling renewable heat fraction

Figure 6.1 illustrates the RHF achieved by A_RE system's parametric analyses for the refurbished dwelling. Also, the values estimated for systems A_RE and B_RE are listed by Table 6.2. Based on the results, the system's heat independency varies from 31% to 74%. The system's RHF fluctuation as function of the borefield and PVT array size, follows similar pattern with this found for the A_NE system (Figure 5.1). In details, the RHF increases as the borefield enlarges and the

PVT array becomes bigger. Also, the GHE size turns out to influence more the system's RHF for the small arrays of collectors. Additionally, the array of 20 PVTs was found capable to elevate the RHF for the net borefield of 16 BHEs from 0.31 to 0.64 (16 BHEs with 20 PVTs). Accordingly, the borefield of 40 BHEs with 0 to 20 PVTs got a fractional rise of 0.18, from 0.55 to 74 respectively.

It should be noted that the highest value of 0.73 RHF for the A_RE system corresponds to 9078.7 kWh_{TH}, been provided by the SAGSHP system. However, system A_NE best RHF was found to 0.79, which corresponds to 4779.1 kWh_{TH} accordingly. Bear in mind that, both systems have equal size component (40 BHEs and 20 PVTs) and differ only at the heat pump capacity and at the space heating load. Based on that, the harvest heat was increased by 4300 kWh_{TH} between the two systems. The reasons for the above-mentioned improvement is discussed in subsection 6.1.3, where the analyses of the PVT heat SP take place.

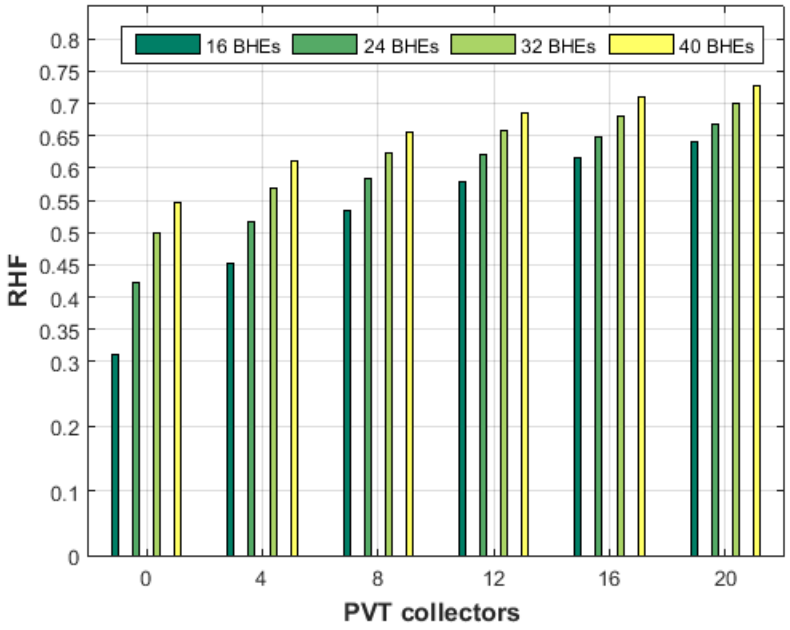

Figure 6.1. System A_RE renewable heat fraction (RHF) for parametric analysis of PVT collectors from 0 to 20 and for BHEs from 16 to 40.

The results for B system configuration with the EEB being exposed are illustrated by Figure 6.2 and the values are listed in Table 6.2. As it can be seen via the results, B_RE system has obtained a marginally higher RHF value than A_RE system of 0.01. Thus, B_RE system's heat independence is framed between 0.74 and 0.31 RHF. Also, the RHF values for B_RE system, illustrate an improvement in almost all the equal sized systems with the A_RE (Table 6.2). This trend is similar

with the one identified between the A_NE and B_NE systems (Figure 5.3), with the second one to achieve higher RHF than the first one. Therefore, the B system topology is capable of greater heat independence than A topology for equal sized systems (BHEs and PVTs). This conclusion governs all the systems investigated up to now regardless of the site EEB topology.

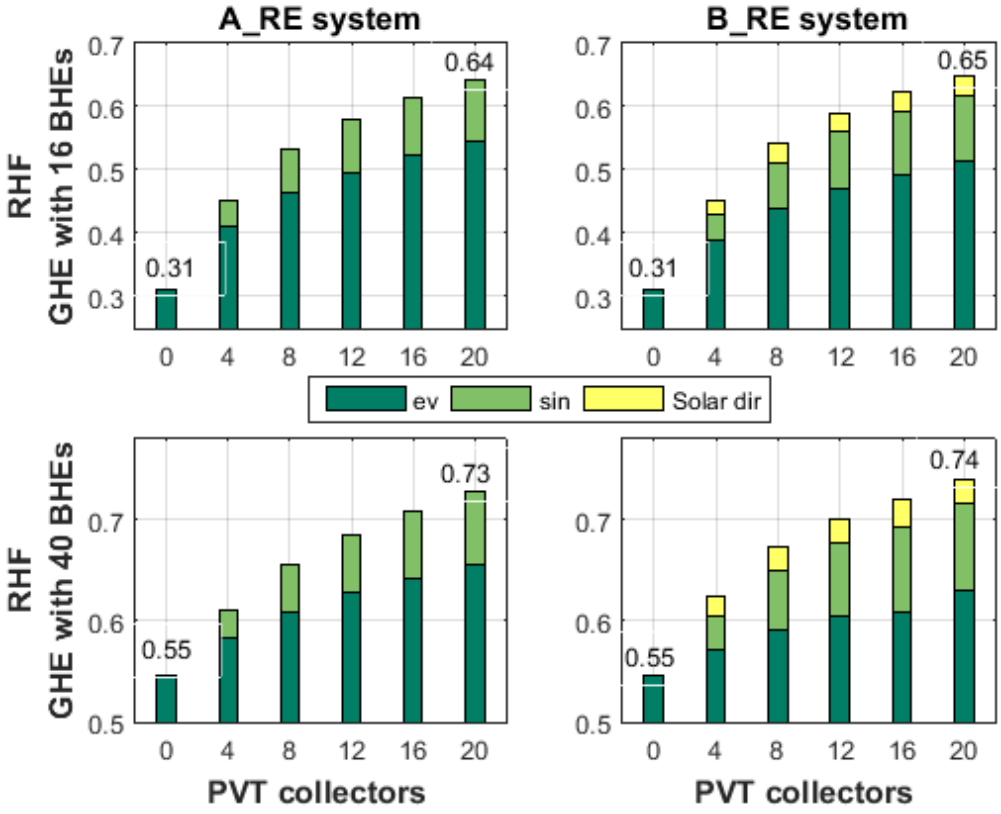

Figure 6.2. RHF comparison between systems A_RE and B_RE, for GHE sizes of 16 BHEs and 40 BHEs, along with the heat sources mixture. Where: ev- RHF corresponding to the evaporator syn- RHF corresponding to the synchronized power generation and consumption Solar dir- RHF corresponding to the directly used solar heat.

Table 6.2. System's A_RE and B_RE achieved RHF values.

	RHF					
	A_RE				B_RE	
PVTs	16 BHE	24 BHE	32 BHE	40 BHE	16 BHE	40 BHE
0	0.31	0.42	0.50	0.55	0.31	0.55
4	0.45	0.52	0.57	0.61	0.45	0.62
8	0.53	0.58	0.62	0.65	0.54	0.67
12	0.58	0.62	0.66	0.69	0.59	0.70
16	0.62	0.65	0.68	0.71	0.62	0.72
20	0.64	0.67	0.70	0.73	0.65	0.74

The RHF mixture for systems A_RE and B_RE is contrasted in Figure 6.2 and Table 6.3. The comparison between A_RE and B_RE system illustrate similarity with the debate made between systems A_NE and B_NE (Table 5.5). Giving that, the RHF mixture analysis for the refurbished dwelling-based system will be shorter than the one made for the new dwelling. The heat contribution of the evaporator is greater for the A_RE scheme than the B_RE. This difference is based on the directly used fraction of the solar heat, which consequently reduces the available EEB's heat. Following that, the EEB shapes a lower soil temperature regime, which drives the heat pump to operate less effective and with higher electricity consumption. This discrepancy, is illustrated by "RHF synchronized" column, where clearly the B_RE system gets higher values than the A_RE. As it is discussed in the following section 6.2, the PVTs' power generation does not varies much with the components quantity and systems' topology, thus the above statement is valid.[18] As regards, the direct solar utilization for the DHW needs, this was limited to values below 7.7% for the borefield of 40 BHEs and to 11.5% for the smaller one with of 16 BHEs.

Table 6.3. RHF mixture analysis, for systems A_RE and B_RE, and the gain made from system B utilization against system A. *SF is the fraction of the *DHW needs covered by direct solar heat from PVTs.*

		RHF evaporator		RHF synchronized		RHF direct solar		DWH SF* [%] for
	PVTs	B_RE	A_RE	B_RE	A_RE	B_RE	A_RE	B_NE system
GHE 16 BHEs	0	0.31	0.31	0.00	0.00	0.00	0.00	0.0
	4	0.39	0.41	0.04	0.04	0.02	0.00	7.7
	8	0.44	0.46	0.07	0.07	0.03	0.00	11.5
	12	0.47	0.50	0.09	0.08	0.03	0.00	11.5
	16	0.49	0.52	0.10	0.09	0.03	0.00	11.5
	20	0.51	0.54	0.11	0.10	0.03	0.00	11.5
GHE 40 BHEs	0	0.55	0.55	0.00	0.00	0.00	0.00	0.0
	4	0.57	0.58	0.03	0.03	0.02	0.00	7.7
	8	0.59	0.61	0.06	0.05	0.02	0.00	7.7
	12	0.61	0.63	0.07	0.06	0.02	0.00	7.7
	16	0.62	0.64	0.08	0.07	0.02	0.00	7.7
	20	0.63	0.66	0.09	0.07	0.02	0.00	7.7

6.1.2. System's specific heat productivity for the refurbished dwelling

With Figure 6.3, the estimated via simulations values of SP_{sys_heat} for A_RE system are illustrated as function of PVT collectors and BHEs. According to the results, the system heat SP decreases

[18] In other words, the synchronized offered heat was a product of greater electricity consumption and not from higher power generation from PVTs.

as the PVT array grows. Also, for systems with fixed PVTs quantity, the larger borefields benefits the SP_{sys_heat} which rise. Thus, for the array of 4 PVTs, the SP_{sys_heat} increase from 1343.3 kWh PVT^{-1} to 2532.3 kWh PVT^{-1} between the borefields of 16 and 40 BHEs respectively (Table 6.4). Also, the GHE size influences less the system's heat SP at the larger PVT arrays.

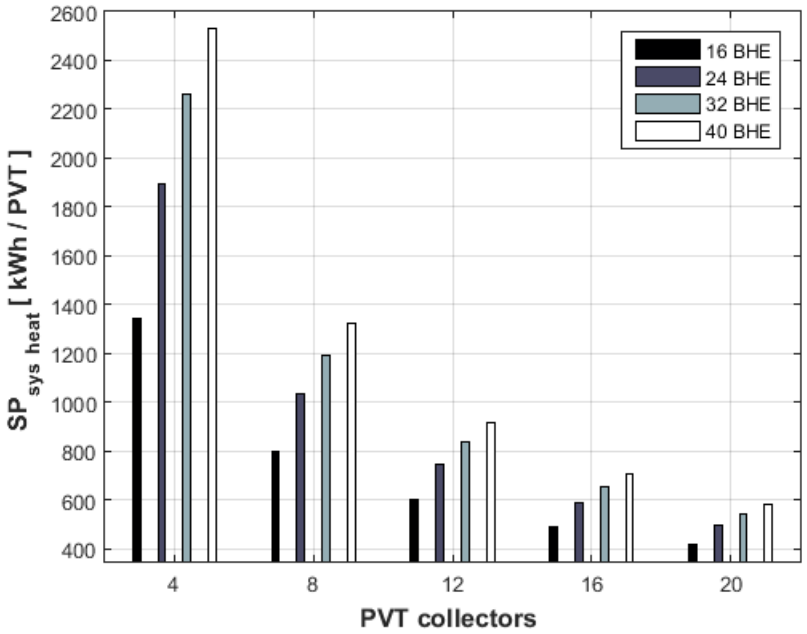

Figure 6.3. System's heat specific productivity for A_RE simulation scenario.

Table 6.4. System SP Values for A_RE and B_RE scenarios.

	System heat SP [kWh PVT^{-1}]					
	A_RE				B_RE	
PVTs	**16 BHE**	**24 BHE**	**32 BHE**	**40 BHE**	**16 BHE**	**40 BHE**
4	1343.3	1893.8	2261.2	2532.4	1397.1	2993.3
8	802.5	1035.3	1194.1	1325.0	844.0	1529.0
12	601.8	744.7	838.1	915.1	631.1	1035.3
16	489.6	591.4	656.8	707.5	510.2	783.0
20	419.4	497.9	545.8	582.7	429.1	639.0

In Figure 6.4, system heat SP is showed for A_RE and B_RE scenarios, and for GHEs with 16 and 40 BHEs. The B_RE system gets higher SP values than the A_RE, which is identical with the comparison between the A_NE and B_NE system (Figure 5.11). According to the results listed in Table 6.4 and Table 5.9, B_RE system's higher SP_{sys_heat} is two times bigger than the higher values achieved by the B_NE. With details, the best SP_{sys_heat} for the B_RE found to be 2993.3 kWh PVT^{-1}, while for B_NE the best SP was 1450.7 kWh PVT^{-1}. Following that, with equally sized systems

(B_NE and B_RE), the increased heat demand was the key factor which influence the most the heat productivity. It is to be noted that, the B_RE superiority against the B_NE system, is limited only to the greater heat productivity. Later, in electricity analysis section 6.2, it is revealed that the greater heat productivity has been produced by greater system's electricity consumption.

The contrast between system's A_RE and B_RE heat SP, reviles that B configuration obtains higher system heat SP than the A at all equal sized systems (BHEs and PVTs). The improved heat productivity is made from the direct use of solar heat which counts as a surplus on the heat delivered from the condenser. Also, the EEB is exposed and the natural heat recovery mechanism replaces easily the removed heat. This is justified by Figure 6.5, where the heat gains for B_RE system found to be higher than the values from A_RE system for all PVT arrays.

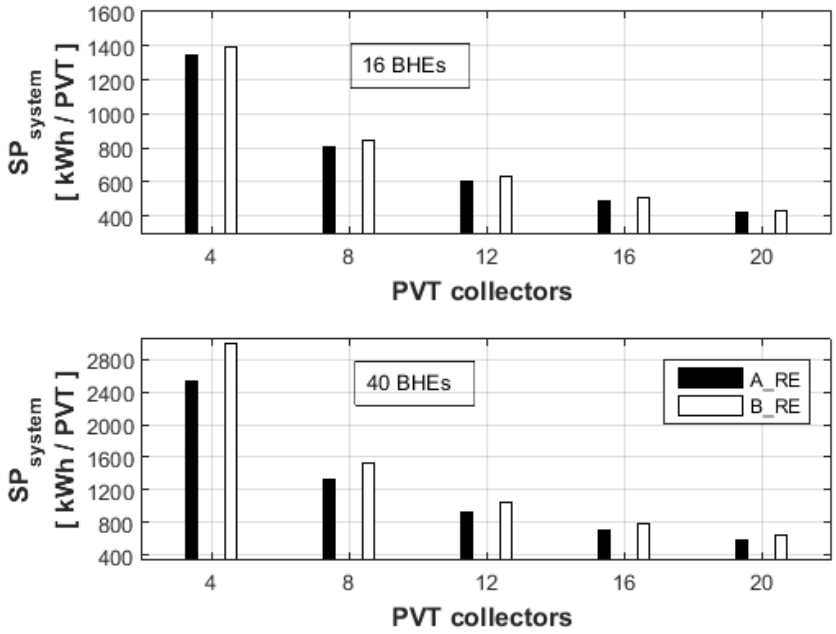

Figure 6.4. Systems' heat specific productivity for A_RE and B_RE simulation scenarios and for the borefield of 16 and 40 BHEs.

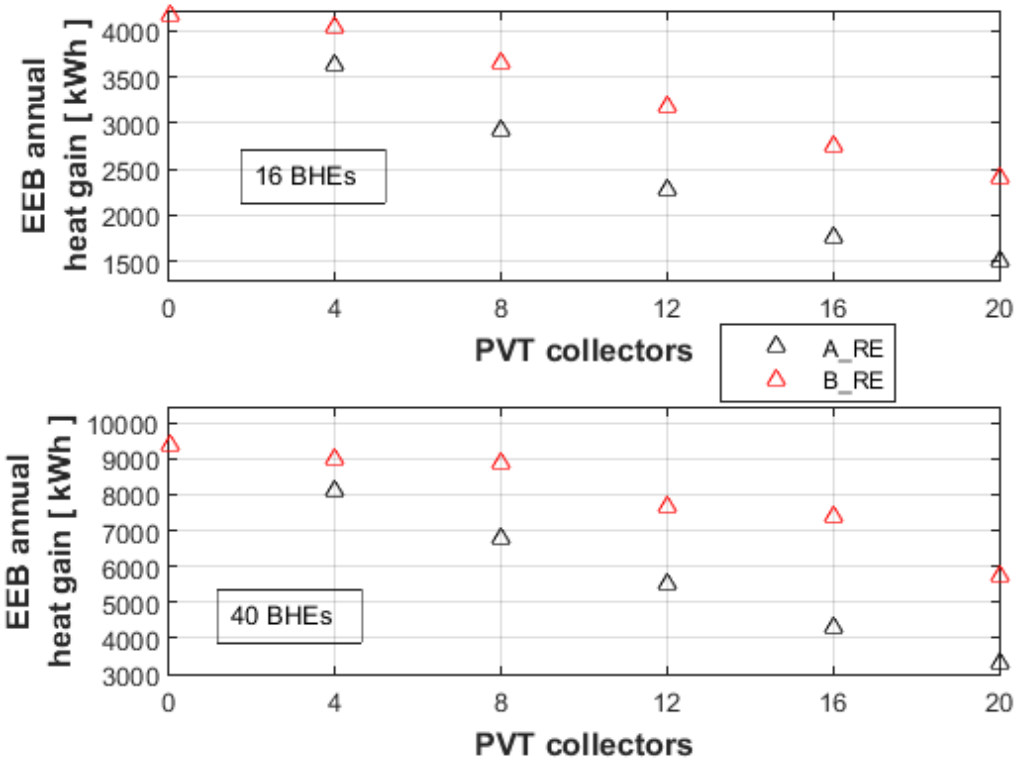

Figure 6.5. EEB annual heat gains as function of PVT array, for systems A_RE and B_RE, and for borefields of 16 and 40 BHEs.

In Figure 6.6, the relationship between the system heat SP with the CBR index is shown, for both systems paired with the refurbished house. As reflected from the results, the systems' SP drops exponentially as the CBR index increases. This phenomenon has been explained for systems paired with the new dwelling (Figure 5.8) and the reasons are the same. In general, the higher SP value is obtained with the lower collectors to BHEs ratio of 0.1 and the lower SP with the ratio of 1.25, which corresponds to 20 PVTs paired with 16 BHEs.

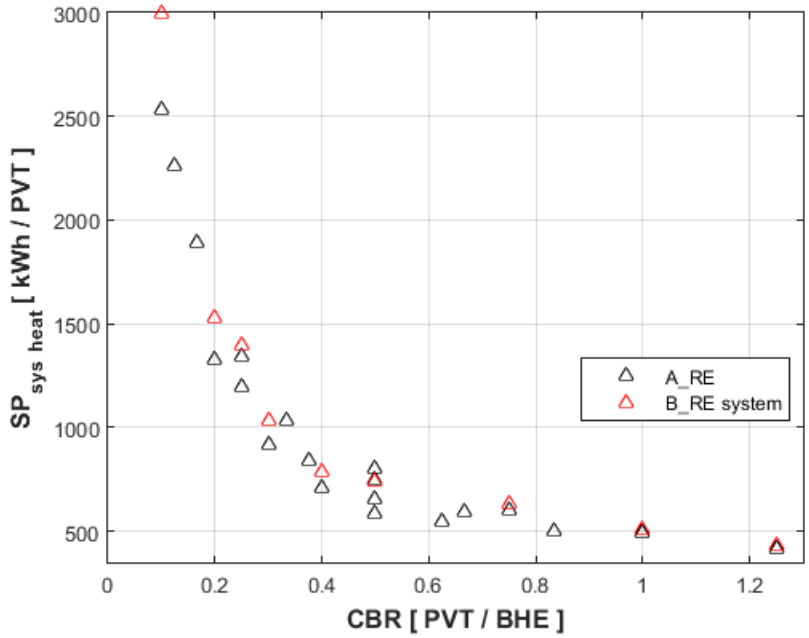

Figure 6.6. System's SP as function of CBR for A_RE and B_RE scenarios.

6.1.3. PVT specific heat productivity for the refurbished dwelling

As regard the PVT heat SP, Figure 6.7 illustrates the values achieved by A_RE system for PVT arrays and borefields size variation. In overall, the variation of SP_{PVT_heat} shows similar pattern with the one recorded for the A_NE system (Figure 5.13). As it is found in the results, system-topology A_RE is capable to obtain the highest PVT heat SP through all investigated systems. Specifically, the highest SP_{PVT_heat} for system A_RE was found to be 779.1 kWh PVT^{-1} (Table 6.5), and the second in order was estimated for A_NB system at 718.5 kWh PVT^{-1} (Table 5.10). Also, all the SP_{PVT_heat} values obtained for A_RE system are higher than all equal sized B_NB systems. The last statement allows us to talk about the A_RE favorable system conditions which cause higher solar heat productivity. The larger heating load than this of the system with the new house, absorbs more heat from the EEB which consequently decrease its mean soil temperature. As is already stated, the low soil temperature is beneficial to PVTs thermal efficiency, by offering a lower inlet temperature. Thus, the lower soil temperature regime found to benefit the most the greater PVT heat SP of the A_RE system.

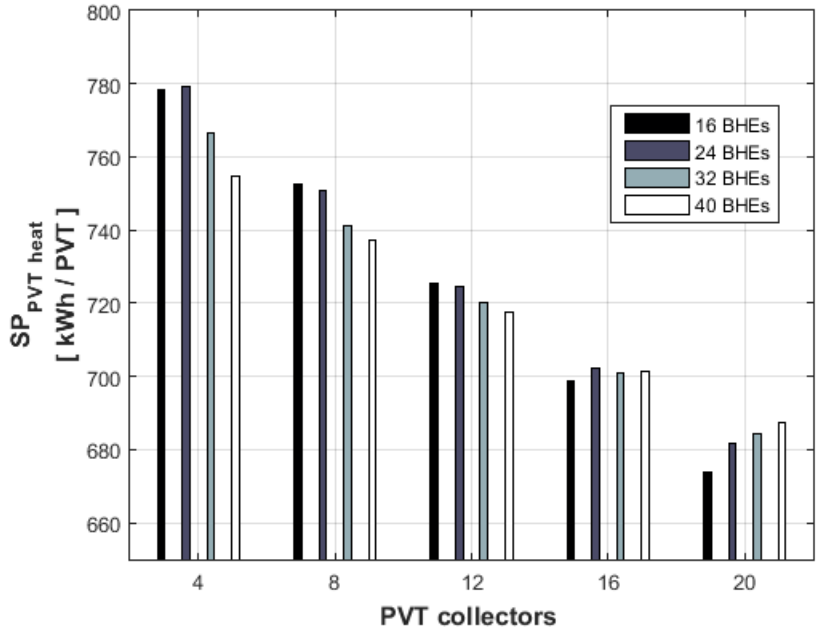

Figure 6.7. PVT heat specific productivity for A_RE system.

The SP_{PVT_heat} values of the System B_RE are lower than A_RE for all equal size systems (Table 6.5). This order is the same with the this recognized between the A_NE and B_NE systems, and is caused meanly by the elevated PVTs' inlet temperature and the relatively EEB's lower mean soil temperature (subsection 5.1.3). Both above mentioned conditions found to influence negatively the PVT collectors' thermal efficiency and utilizability. Regarding the achieved SP by the B_RE system, the borefield with 16 BHEs paired with 4 PVTs gets the highest value of 659.9 kWh PVT^{-1}.

Table 6.5. PVT heat SP Values for A_RE and B_RE scenarios.

	PVT heat SP [kWh PVT^{-1}]					
	A_RE				B_RE	
PVTs	16 BHE	24 BHE	32 BHE	40 BHE	16 BHE	40 BHE
4	778.4	779.1	766.7	754.8	659.9	649.7
8	752.7	750.7	741.0	737.4	632.6	626.4
12	725.5	724.7	720.1	717.7	610.6	607.0
16	698.9	702.2	700.8	701.5	585.6	570.3
20	673.8	681.5	684.3	687.3	568.0	573.6

Following this subsection dedicated on the refurbished dwelling, the harvested heat by the B_RE system is estimated more than two time greater than this needed for the new building. The extra

amount of energy needed to obtain the higher RHF of 0.74 for system B_RE is originated from the ground. As it can be observed in Figure 6.8, the soil is capable to offer substantial heat to the EEB. The EEB's heat gain drops as the PVT array grows, because the soil temperature elevates and that intercepts the heat entering the EEB. Therefore, the GHE can offer more heat that the amount which is enclosed by the EEB boundaries. Thus, it is technically correct to state that the geothermal heat available to be harvested is more than this owned by the EEB. Moreover, the main parameters which influence the above process are the ambient temperature, the undisturbed ground temperature and the rate in which the heat absorbed via the GHE. It is worth mentioning that, B_NE system becomes more solar depended than geothermal with 8 and more PVT (Figure 6.8). In contrast, B_RE system due to extended heating needs, absorbs more ground sourced heat and the solar energy becomes the first energy source only at the array of 20 PVTs.

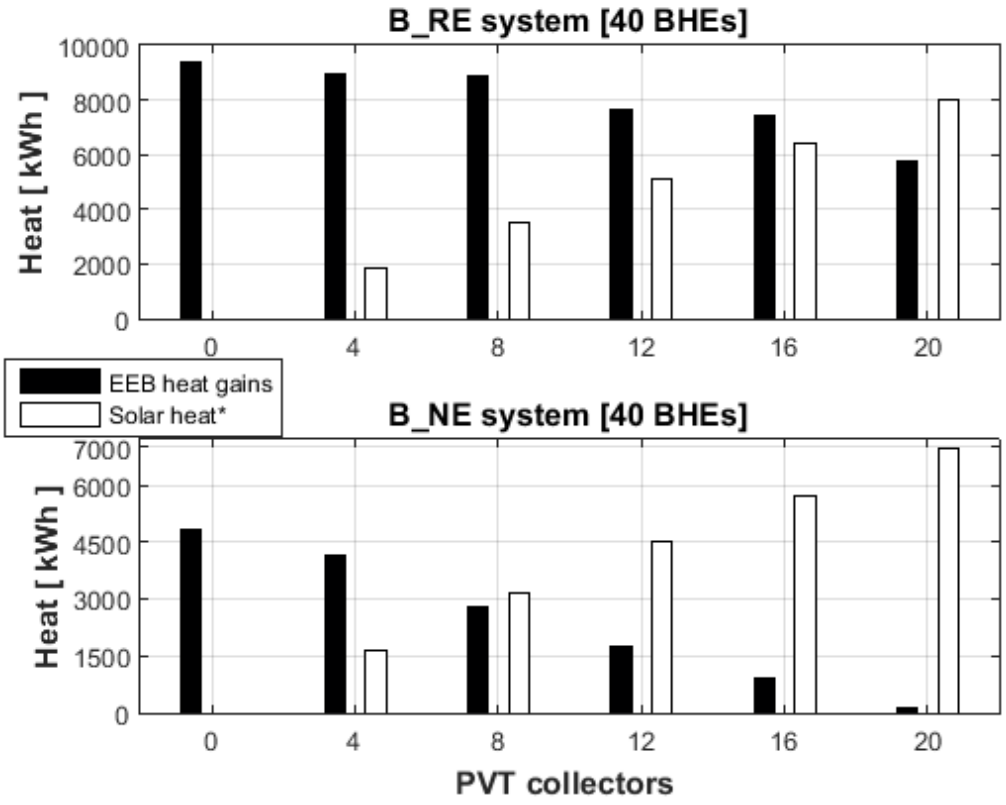

*Figure 6.8. EEB heat gains and Solar heat as function of PVT collectors for the borefield of 40 BHEs and for system B_RE and B_NE. * Is the amount of solar heat which is offered to the system after the PHE, plus the direct solar heat used for the DHW needs.*

In Figure 6.9, the PVT heat SP is plotted for A_RE and B_RE systems as function of the CBR index. The results indicate similar trend with all the investigated up to now systems. In other words,

the SP_{PVT_heat} influenced significantly by the CBR, with the larger assigned soil mass per PVT to benefit the SP. Therefore, the highest values are achieved for smaller than 0.3 CBR, with the highest one to be at the ratio of 0.1.

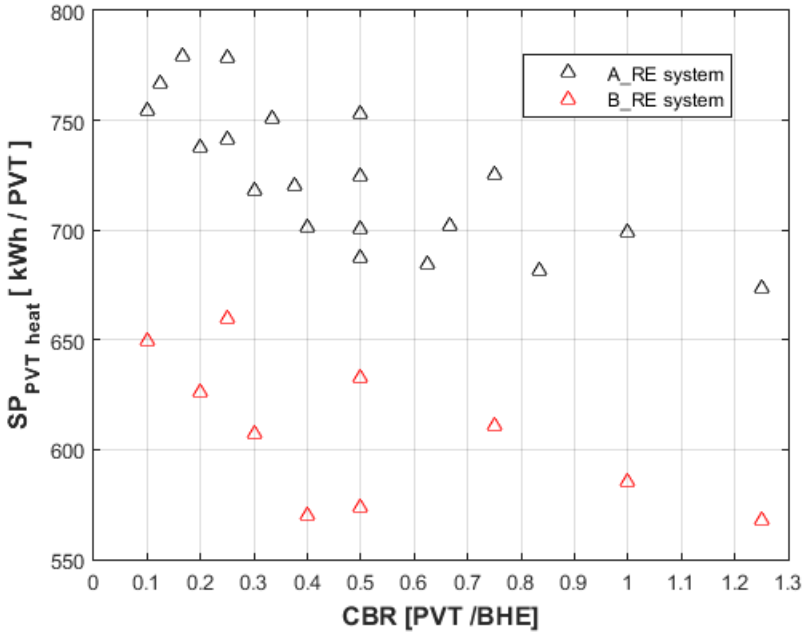

Figure 6.9. PVT heat SP for A_RE and B_RE systems as function of the storage capacity (SC).

6.1.4. Seasonal performance factor for the refurbished dwelling

In this subsection the analysis of the SPF is taking place for systems paired with the refurbished dwelling. In Table 6.6, illustrates the calculated SPF values for systems A_RE and B_RE. As it can be seen, the A_RE system got higher SPF values from B_RE system at all equal size system. The highest SPF for A_RE is calculated at 8.25 and the lowest at 1.04, which corresponds to systems with 40 BHEs paired with 20 PVTs and 16 BHEs with no PVT respectively. The highest coefficient for the B_RE system is found to be 5.49. From a winder perspective, someone can say that the SPF values are high at the majority of pairs, but are in lower magnitude than these calculated for the systems paired with the new dwelling (Table 5.15). In the current systems with the energy renovated house, no one configuration managed to reach the self-sufficient regime with infinity SPF.

As it is made for systems paired with the new house, the SPF*is calculated and listed in Table 6.7 for the refurbished dwelling-based systems.[19] According to the results, the highest SPF*belongs to A_RE system and is calculated to be 2.58, while the second in order value is for the B_RE system at 2.39. Additionally, the SPF*improves as the GHE enlarges and the PVT array grows. With a closer look at the results listed in Table 6.7 and illustrated by Figure 6.10, the coefficient increases almost linearly as the A_RE system becomes bigger. This pattern has been identified for system A_NE. It is worth to be mentioned, that all systems based on the new dwelling got higher SPF* than A_RE and B_RE. But by comparing the best values achieved by the A_NE with this of A_RE, the difference is 0.46 (for equal size systems). While for the B_NE and B_RE the discrepancy is risen to 0.60. Giving that B_RE and A_RE must cover two times higher heating load, the above drops on the performance may be characterized as acceptable.

Table 6.6. SPF for A_RE and B_RE systems, calculated via equation 3.2.

	SPF					
	A_RE				B_RE	
PVTs	16 BHE	24 BHE	32 BHE	40 BHE	16 BHE	40 BHE
0	1.04	1.39	1.69	1.90	1.04	1.90
4	1.51	1.82	2.09	2.38	1.43	2.27
8	1.98	2.35	2.67	3.01	1.84	2.72
12	2.51	2.96	3.42	3.92	2.26	3.29
16	3.36	3.80	4.49	5.37	2.79	3.94
20	4.61	5.09	6.46	8.25	3.64	5.49

*Table 6.7. SPF*for A_RE and B_RE systems.*

	SPF*					
	A_RE				B_RE	
PVTs	16 BHE	24 BHE	32 BHE	40 BHE	16 BHE	40 BHE
0	1.04	1.39	1.69	1.90	1.04	1.90
4	1.34	1.62	1.86	2.10	1.29	2.05
8	1.52	1.80	2.03	2.25	1.46	2.17
12	1.63	1.91	2.15	2.38	1.56	2.24
16	1.75	1.99	2.24	2.49	1.63	2.26
20	1.84	2.06	2.32	2.58	1.71	2.39

Figure 6.11 shows the SPF*relationship with the CBR for A_RE and B_RE system. The index CBR shows to be similarly related to the SPF*found for A_NE and B_NE system. This indicates that all

[19] The SPF* is calculated without considering the electricity from PVTs.

systems up to now respond with the same way on CBR variation. The highest values for both systems A_RE and B_RE are caused by CBR of 0.5, sequentially both systems' coefficient share the same monotony through all the configuration. The main alteration between systems A_RE and A_NE, is the steep rise of SPF* as the CBR increase from 0 to 0.5. This transition from 0 to 0.5 CBR shapes a plateau for the A_NE system (Figure 5.20). The higher inclination for A_RE system can be explained by observing the Figure 6.8. As it can be seen, the B_RE system requires both renewable energy sources to contribute, the solar and the geothermal, due to the large heat demand. Unlikely, with B_NE system, the geothermal heat part eliminates as the solar heat increases, that shows the system's sufficiency in energy sources.

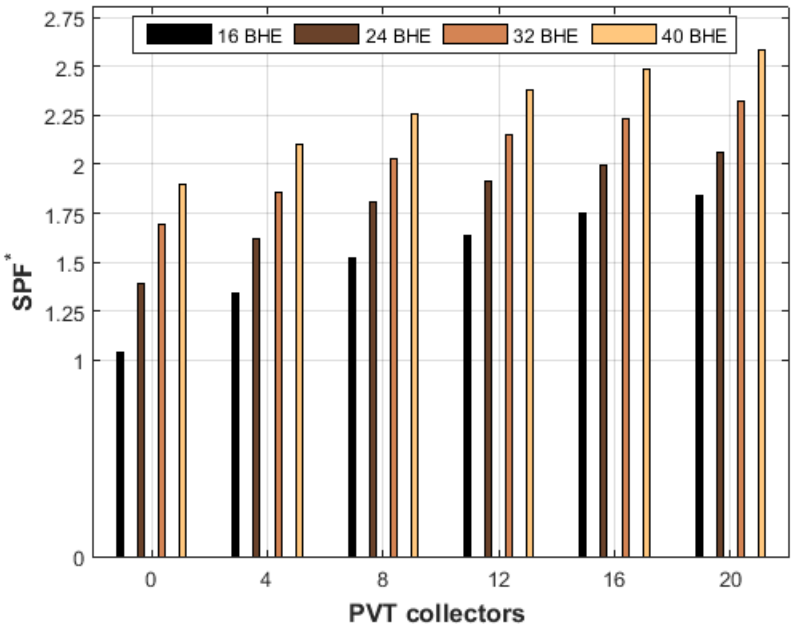

*Figure 6.10. SPF*for A_RE system. The electricity offered by PVTs is excluded from calculations via equation 3.2.*

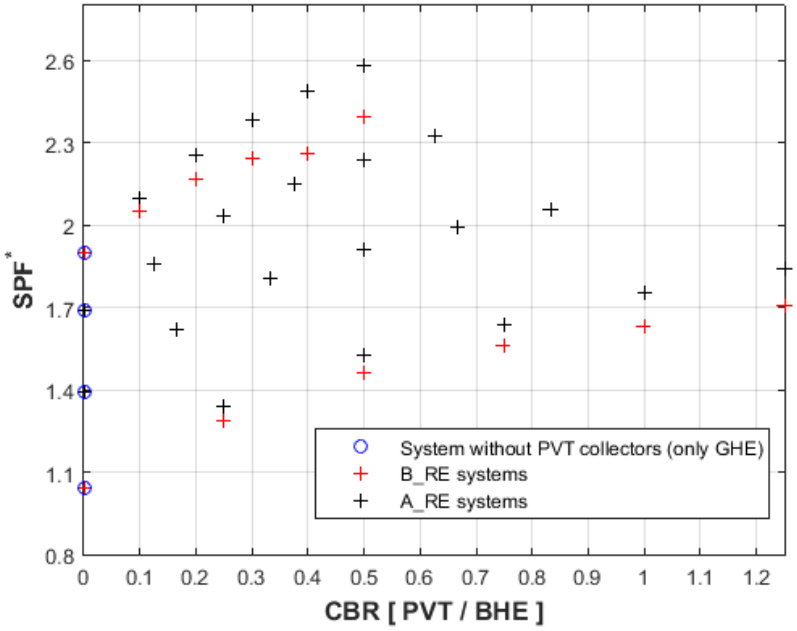

Figure 6.11. SPF*for A_RE and B_RE systems as function of the CBR.

6.1.5. Results summary of the refurbished dwelling's heat evaluation

With Table 6.8, the higher and lower values of the four metrics presented in this chapter are listed, for the refurbished dwelling. On the beginning of this summary, the universal outcomes from the parametric analyses are presented and then specified to each metric, important information is listed with dot points

Likewise to the analysis made for the new dwelling, the investigated systems (A_RE ,B_RE), interact similarly on the PVTs and BHEs variation. In other words, all systems follow the same trend of increase or decrease their values of the metrics with the variation of the system size (PVTs and BHEs).

A substantial amount of heat can be utilized by the system via the soil which surrounds the EEB. This mechanism is influenced by the: ambient temperature, the undisturbed soil temperature and the heat load (Figure 6.8). The heat gains of the EEB was the additional energy source to the solar one for the A_RE and B_RE systems. The systems with the refurbished dwelling were estimated to absorb 4300 kWh $year^{-1}$ more heat with renewable origins than these paired with the new building. For the renovated dwelling, the direct solar heat utilized for the DHW needs was estimated to be up to 11.5%.

Table 6.8. . List of lower and higher values of heat evaluation metrics for all investigated schemes, refurbished dwelling.

System		RHF	SP_{sys_heat} [kWh PVT^{-1}]	SP_{PVT_heat} [kWh PVT^{-1}]	SPF*
A_RE	higher	0.73	2532	779	2.58
	lower	0.31	419	674	1.04
B_RE	higher	0.74	2993	660	2.39
	lower	0.31	429	568	1.04

RHF: the highest value of 0.74 was achieved by B_RE system.

- In general, the GHE imposes an initial RHF which increase further as the PVT array enlarges.
- The contribution of solar heat to RHF is greater for small borefields, while the phenomenon ceases as the number of BHEs increases. The main reason for this preference is the all-day long availability of the geothermal energy, contrary to the solar which is constrained by a number of factors like the level of the irradiance and PHE's effectiveness (Sakellariou *et al.*, 2019).
- The higher RHF values for all systems have been obtained with 20 PVTs and 40 BHEs (20 PVTs with CBR 0.5 [20 $PVT_{0.5}$]).
- The B_RE system was found to be slightly more heat independent than the A_RE to all size systems. For the refurbished house, the system configuration did not influence significantly the heat independency of the system (Figure 6.2).

System heat SP: the SAGSHP systems with 20 PVTs and 40 BHEs paired with the refurbished dwelling, were found capable of harvesting up to 2993 kWh PVT^{-1} (B_RE). The B_RE system absorbed about 2.5 times more heat from the environment than the A_NE, with equal size system. Based on this observation, the heating load of the system it can be considered as key parameter which influences directly the system's heat SP.

- For all systems and dwellings, the low values of the CBR (0.1 to 0.2) were found to benefit the heat SP.
- The system heat SP found to influence the RHF, because the renewable energy absorbed by the evaporator of the heat pump is the bigger portion of the RHF (Table 5.5).
- The system heat SP is Influenced more by the borefield size rather the PVT quantity.

PVT heat SP: the PVT heat SP was estimated between 568 kWh PVT^{-1} and 779 kWh PVT^{-1}, for the B_RE system with 20 PVT paired with 16 BHEs and for the A_RE with 4 PVT paired with 24 BHEs accordingly (Table 6.5).

- The PVT heat SP rises with the larger soil volume, therefore small CBR values benefit the solar heat production (less PVT per BHE).
- All the systems with the B layout (direct use of solar heat), were found with lower PVT heat SP from systems built with A layout. The reduction of the PVT heat SP was caused by the elevated temperature of the water in the DHW tank, which forces the PVT collectors to operate with higher inlet temperature and consequently a reduced thermal efficiency.
- Unlikely to systems paired with the new dwelling, both systems A_RE and B_RE are not reaching any stagnation regime (plateau) as regards the CBR value (Figure 6.9). This illustrates that even higher PVT heat SP can be achieved with larger EEBs and/or borefields.

SPF: The A_RE and B_RE were found uncapable to enter in the energy self-sufficient stage, at all the PVTs and BHEs range. Regarding the SPF*[20], the values obtained by the systems of the refurbished dwelling, these are from 1.04 up to 2.58, both from A_RE system.

- The GHE size influence more than the PVT quantity the SPF.
- There is not a direct link between the SPF* and the CBR index, but higher CBR improve the SPF due to more PVTs and thus higher electricity generation.
- SPF values for B system topology were estimated to be lower than the A topology, due to direct use of solar heat which resulting to a dropped mean soil temperature. Thus, more electricity is needed from the heat pump to operate with lower COP and for more time.
- System built with the new dwelling were proved capable of higher SPF* than systems paired with the refurbished one. Whoever, this discrepancy between the dwellings remains in low level, with the A_NE to be more coefficient than the A_RE by 0.46 and the B_NE from the B_RE by 0.60 respectively (but the heat load is two time bigger for the refurbished dwelling).

[20] The PVT generated electricity is not entered on the calculation.

6.2. Electric output evaluation of the refurbished dwelling

The systems' electric output evaluation follows the pattern used for the heat analysis. Therefore, the section is split between the part dedicated to the new dwelling and to this for the refurbished one. In each part, two further analyses are conducted: one for the renewable power fraction (RPF) and the second for PVTs' electric specific productivity (SP_{PVT_el}). Both metrics are analyzed in metrics section 3.5

6.2.1. PVTs' electric specific productivity for the refurbished house

In Table 6.9, the SP_{PVT_el} values obtained by systems A_RE and B_RE are listed. As it can be seen, the A_RE system illustrate greater power SP than the B_RE system in all equal size systems. The average power SP for A_RE system is calculated to be 242.5 kWh PVT^{-1}, which is slightly higher than the one found for the A_NE system by 0.8 kWh PVT^{-1}. The higher energy generation for A_RE system against the A_NE system, was made by the lower EEB's soil temperature, due to extensive heat absorption from the heat pump. The highest power SP for A_RE is found to be 243 kWh PVT^{-1} for the array of 4 PVTs with 16 BHEs, and the lower was estimated at 241.9 kWh PVT^{-1} from the system of 20 PVTs paired with 16 BHEs. As regards the B_RE system, the mean power SP is estimated to be 234.5 kWh PVT^{-1}, which is 3.3% lower from the mean power SP of the A_RE system. As in all schemes with B topology, the return stream of the heat removal fluid from DHW tank carries high temperature which deteriorates the PV cells efficiency. Based on that, the B_RE system owns lower electric SP than the A_RE system. Finally, the A_RE system's electric SP shows fluctuation with less than 0.4%, among the listed values.

Table 6.9. PVT electric SP for systems A_RE and B_RE.

	PVT electric SP [kWh PVT^{-1}]					
	A_RE				B_RE	
PVTs	16 BHE	24 BHE	32 BHE	40 BHE	16 BHE	40 BHE
4	243.0	242.9	242.8	242.7	234.6	235.3
8	242.8	242.8	242.7	242.7	234.5	235.1
12	242.5	242.6	242.6	242.5	234.4	235.0
16	242.3	242.4	242.4	242.4	234.1	233.5
20	241.9	242.1	242.2	242.2	234.0	233.5

6.2.2. Renewable power fraction for the refurbished dwelling

According to the results illustrated in Table 6.10 and Table 5.21, the system installed with the refurbished dwelling has reduced electrical self-sufficient than systems paired with the new house. With details, the maximum RPF for A_RE is estimated to be 0.67 and for B_RE at 0.55. As

can be observed in Table 6.10, the RPF increases as the system size enlarges, this pattern is similar to the one identified for systems paired with the new dwelling.

Table 6.10. RPF achieved by A_RE and B_RE systems parametric analysis.

	RPF					
	A_RE				B_RE	
PVTs	16 BHE	24 BHE	32 BHE	40 BHE	16 BHE	40 BHE
4	0.10	0.11	0.11	0.12	0.10	0.11
8	0.23	0.23	0.23	0.24	0.20	0.21
12	0.34	0.34	0.36	0.38	0.30	0.31
16	0.46	0.47	0.49	0.52	0.41	0.42
20	0.58	0.59	0.62	0.67	0.52	0.55

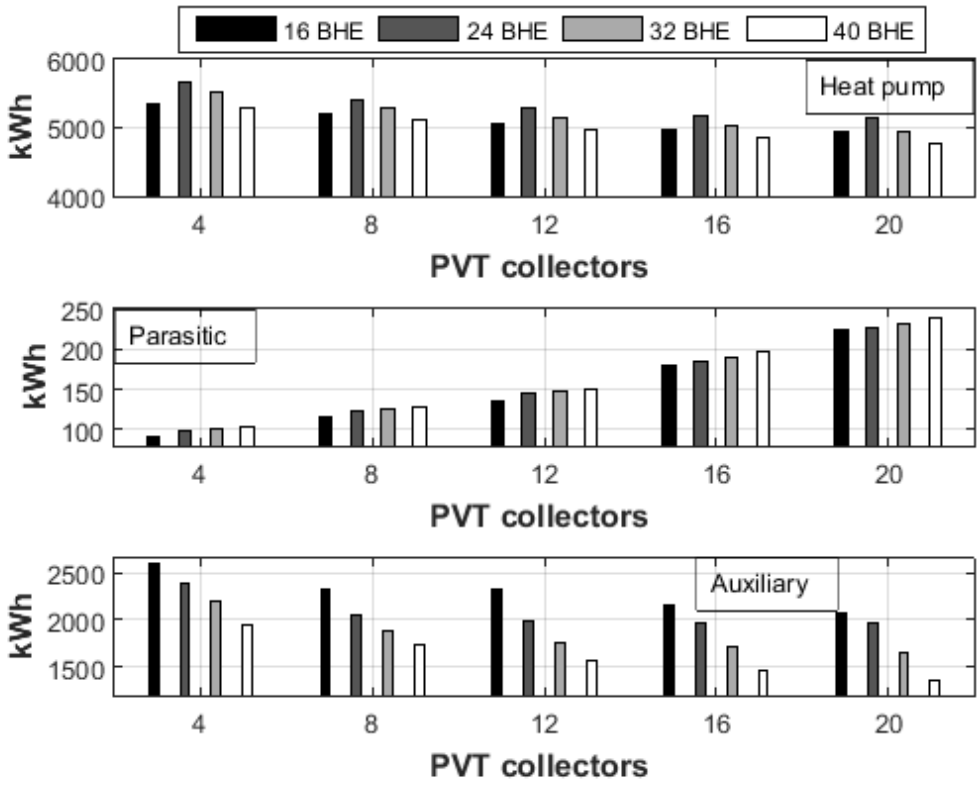

Figure 6.12. A_RE system's electricity consumption mixture as function of the PVTs and BHEs amount. Where: Heat pump-is the energy used by the device, Parasitic-is the electricity consumed by the circulation pumps, Auxiliary-is the energy used additional to this offered by the heat pump's condenser in order to cover the heat demand.

In the above section, the A_RE system's electric SP found without significantly fluctuation among the parametric scenarios (0.4%). On that bases, the system RPF is influenced more by the consumed electricity and not from the generated (because is fixed). In Figure 6.12, the A_RE system's electricity mixture of consumption is shown for all PVT arrays and borefield sizes. As it

can be seen, the auxiliary energy drops as the system enlarges. This can be linked to the increased RHF (Figure 6.2), where a larger system is capable of greater heat independence and thus less additional heat is needed. As regards the parasitic energy, this is increase due to pumps higher nominal capacity. Finally, the heat pump energy consumption can be split in two section: this with the borefields consisted of 24,32 and 40 BHEs and this of 16 BHEs. The first group of GHEs follows similar trend as the one descripted for the A_NE system (*Figure 5.26*), the energy consumption drops as the system enlarges. But the smaller borefield of 16 BHEs shows reduced electricity consumption than the larger one, and that does not follow the analysis made for the A_NE system. The borefield of 16 BHEs was not capable to maintain a soil temperature sufficiently high in order the condenser's inlet temperature to stay into the operation limits (section 4.3). Therefore, within the simulation period the EEB made from 16 BHEs cannot provide always the heat pump with heat and that causes reduction on the device's operation time, and consequently lower electricity demand.

6.2.3. Summary and further discussion of the electric output evaluation

In Table 6.11, the higher and lower values of the PVT electric SP are presented, for systems evaluated with the refurbished dwelling (Table 6.1). The average value of the SP_{PVT_el} for both systems A_RE and B_RE was estimated at 239.8 kWh PVT^{-1}, with the higher disparity among the values to be 4%. The small variation among achieved SP_{PVT_el} values was caused by:

- Fixed inclination and orientation of the PVTs. By changing the inclination of the collectors, the electricity yield is influenced directly.
- The flow rate for each PVT collector was kept constant through all the parametric analyses. Variation on the flow rate causes variation on the temperature of the photovoltaic cells', and consequently their electrical efficiency changes respectively.
- The small variation of the PVT inlet temperature, regardless the borefield size (subsection 5.1.3).

A small reduction of the PVT electric SP was identified for larger PVT arrays, due to their ability to maintain a slightly higher soil temperature than the smaller arrays, this condition consequently elevates the inlet temperature of the PVTs. There is not a strong link between the SP_{PVT_el} and the CBR index, but the power generation was influenced more by the system topology. Therefore, the systems with the A topology (Figure 3.5) and higher electricity generation, and the systems with the B topology (Figure 3.7) with lower capability for electricity production. The system B topology offers higher PVT inlet temperature than A topology, due to

the relatively increase temperature of the water in the DHW tank. Consequently, the increased inlet temperature elevated the absorber's mean plate temperature, which drives the PV cells to operate with reduce efficiency.

Table 6.11. List of lower and higher values of PVT power SP, for all systems.

System		SP_{PVT_el} [kWh PVT^{-1}]
A_RE	higher	242.9
	lower	242.5
B_RE	higher	235.3
	lower	234.5

The RPF is increase for both systems as the borefield enlarges and as the PVT quantity increases. The reasons for this trend are mainly:

- The higher inlet temperature of the evaporator formulated by the increase soil temperature (more PVTs and bigger EEB).
- With a bigger system, consisted of more PVTs and BHEs, the need for auxiliary energy is lower than a smaller system.
- The highest electricity independency for the A_RE system was estimated to be 0.67 and for the B_RE at 0.55 respectively. When the systems are paired with the refurbished dwelling, a substantial lower RPF can be caused against those pared with the new dwelling (Table 5.20). This is created by their extensive power consumption on the heat pump and to the increased auxiliary energy. Finally, the borefield of 16 BHEs found to be an inappropriate size for the heating load of the refurbished dwelling. The heat pump operation was restricted by the low inlet temperature of the evaporator.

With this chapter the SAGSHP systems paired with the refurbished dwelling are evaluated and compared with the aim to identify the most energetically efficient. As it is illustrated and explained in subsection 5.2.3, the renewable power fraction (RPF) is the proper metric which can be used to identify the system with the highest energy performance. In Figure 6.13, the RHF and the RPF are plotted for the borefields of 16 and 40 BHEs, for all PVT arrays and for both topologies (A and B). As it can be seen, the A_RE gets the highest values of RPF for all systems configurations, against the B_RE which illustrates a substantial drop. As regards the RHF, the B_RE system achieves slightly higher values than A_RE for all PVT arrays.

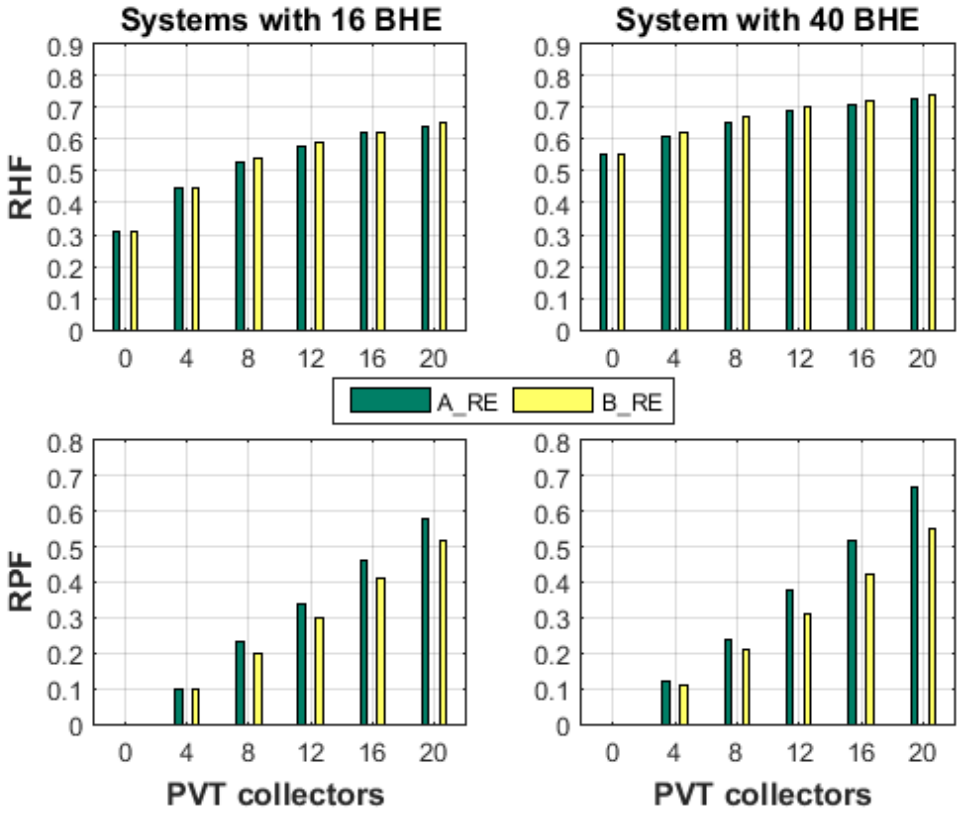

Figure 6.13. RHF and RPF for A_RE and B_RE systems and for borefields of 16 BHEs and 40 BHEs.

Chapter 7. Carbon emission comparison of the systems

In this section, a comparison is conducted regarding to greenhouse gasses emissions (GHGs) caused by the SAGSHP, GSHP and the NGB based systems (subsection 3.5.5). In more detail, the fractional GHGs emission savings (equation 3.8, f_{sav_emis}) achieved by utilizing the SAGSHP and GSHP system against the NGB system are estimated. The comparison between the SAGSHP system with the NGB system is taking place for all parametric analysis schemes of dwellings, number of PVTs, BHEs and layout types (A, B). The f_{sav_emis} achieved by GSHP system compared with this of NGB system and this is used as benchmark for all investigated SAGHSP systems. The conversion factors used for this analysis are 0.20428 kg CO_2e per kWh_{Th} for the natural gas, 0.2556 kg CO_2e per kWh_e and 0.0217 kg CO_2e per kWh_e for electricity and transmission-distribution of the electricity accordingly. All the conversion factors have been sourced from (UK-Gov, 2019) and reflect the average acceptable values for the UK. Finally, the current section is split in two subsections: the one dedicated to the new dwelling and the second one to the refurbished dwelling.

7.1. Greenhouse gasses emission comparison for the new dwelling

By utilizing the results from NGB system's simulation (subsection 4.5.2), annually 1509.7 kg CO_2e are emitted to the atmosphere, for the system installed with the new dwelling in Birmingham. The emissions for the natural gas boiler-based system are derived from 7334.0 kWh_{Th} offered by natural gas (527.6 kg of CH_4) and 41.3 kWh_e of electricity consumed by the circulation pump. As regards the GSHP system (subsection 4.5.1), the GHGs emissions are estimated to 582 kg CO_2e per year and are caused from 2098.8 kWh_e of electricity. Based on the results illustrated above, the GSHP system can reduce the GHGs emissions by the fraction of 0.61 against the NGB system.

In Figure 7.1 and in Table 7.1, the f_{sav_emis} values are illustrated for A_NE system against the NGB system. Based on the results, all investigated SAGSHP systems found to be less emissive than the system which consume natural gas. The results from the conducted parametric analysis for the A_NE system can be split in two domains, to this with the system equipped from non-PVT to up to 8 PVT collectors and to this with arrays larger than 12 PVTs. In the first group of systems with the small PVT arrays, the f_{sav_emis} rises proportionally with the borefield size and PVT quantity. As regards the second part of the results with larger PVT arrays, the emission savings are characterized by 1, which can be interpreted to a system without carbon emissions. The size

of the PVT array found to influence the most the carbon emission savings. As it can be seen, from the system with non-PVT and 16 BHEs and f_{sav_emis} 0.36, the addition of 4 PVTs entails an additional fractional savings of 0.22, though the addition of 8 BHEs causes only a fractional rise of 0.06. The PVTs' capability to cogenerate power and heat is the reason for their greater influence on system's carbon emissions. The delivered electricity can easily decarbonize the gas emissions which are caused by the natural gas, and to compensate the power consumption.

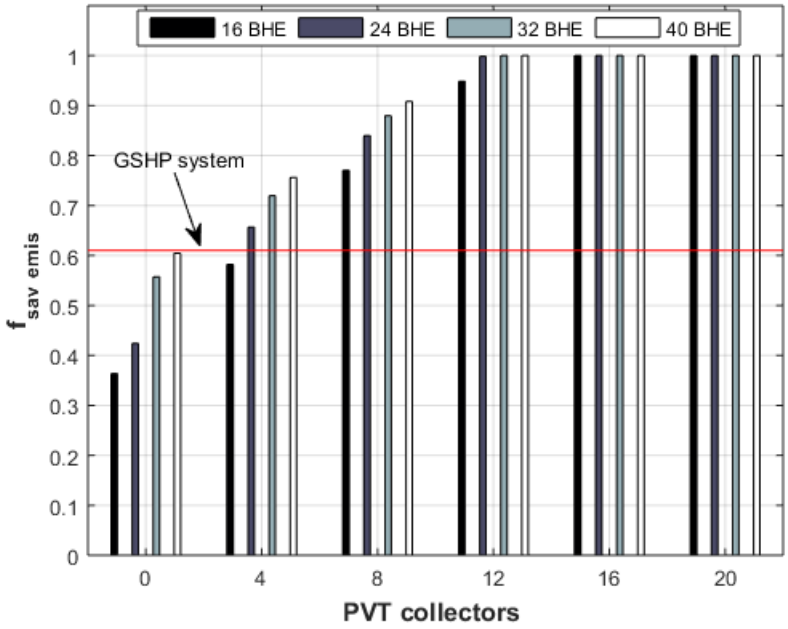

Figure 7.1. Fraction of GHGs emission savings for A_NE system from the use of natural gas boiler-based system.

Based on the results shown in Figure 7.1, the SAGSHP system is less emissive than the GSHP system in the majority of system sizes. The system with the net borefield of 40 BHEs misses gets slightly lower emission fraction savings than the GSHP system (are both 100% ground sourced systems). Regarding the array of four collectors, only the borefield of 16 BHEs is found with reduced emission saving fraction than the GSHP system. It must be noted as an important aspect for the current discussion, that the mean soil temperature declines annually by utilizing a conventional GHSP system only for space heating. This phenomenon can be seen in Figure 7.2, where the soil mean temperature in the vicinity of the U-BHE declines annually. The temperature drop of the soil may cause a dramatic rise on the energy consumed by the system, higher than this one used for the estimation of the emission fractional savings, also raises questions about the system viability. In contrast, as it is shown in Figure 7.2, the proposed

SAGSHP system shows greater resilience regarding the mean soil temperature, even in the extreme case without PVTs.

It is important to highlight that in Table 7.1, there are CO_2e emissions with negative value. The negative emission cannot hold any natural meaning, but it can be used to decarbonize other GHGs emissions caused by the dwelling's operation (electric devices and cooking). Alternatively, can be used by the power production company with the aim to compensate the pollution released during the energy generation process on the field.

Table 7.1. Annual GHGs emissions and fraction savings from SAGSHP systems against the NGB system, for all systems installed with the new dwelling.

		Annual GHGs emissions [kg CO_2e]				**f_{sav_emis}**			
BHEs	**PVTs**	**A_NE**	**B_NE**	**A_NB**	**B_NB**	**A_NE**	**B_NE**	**A_NB**	**B_NB**
16	0	960.5	960.5	1209.8	1209.8	0.36	0.36	0.20	0.20
	4	630.8	764.2	709.1	797.5	0.58	0.49	0.53	0.47
	8	346.8	494.7	401.5	508.1	0.77	0.67	0.73	0.66
	12	77.8	258.0	136.3	275.6	0.95	0.83	0.91	0.82
	16	-143.5	33.7	-89.5	29.7	1.00	0.98	1.00	0.98
	20	-378.4	-197.5	-327.0	-189.7	1.00	1.00	1.00	1.00
24	0	869.5		1047.8		0.42		0.31	
	4	518.1		660.9		0.66		0.56	
	8	242.0		358.6		0.84		0.76	
	12	2.2		88.4		1.00		0.94	
	16	-230.0		-186.3		1.00		1.00	
	20	-457.7		-428.1		1.00		1.00	
32	0	668.4		899.7		0.56		0.40	
	4	423.5		566.1		0.72		0.62	
	8	182.0		267.2		0.88		0.82	
	12	-56.5		-10.7		1.00		1.00	
	16	-284.2		-252.3		1.00		1.00	
	20	-507.6		-494.3		1.00		1.00	
40	0	596.8	596.8	905.1	905.1	0.60	0.60	0.40	0.40
	4	368.4	516.2	474.7	632.1	0.76	0.66	0.69	0.58
	8	138.3	284.3	188.2	353.1	0.91	0.81	0.88	0.77
	12	-89.8	56.7	-67.7	99.9	1.00	0.96	1.00	0.93
	16	-316.5	-161.0	-306.2	-129.9	1.00	1.00	1.00	1.00
	20	-537.2	-380.1	-534.0	-350.6	1.00	1.00	1.00	1.00

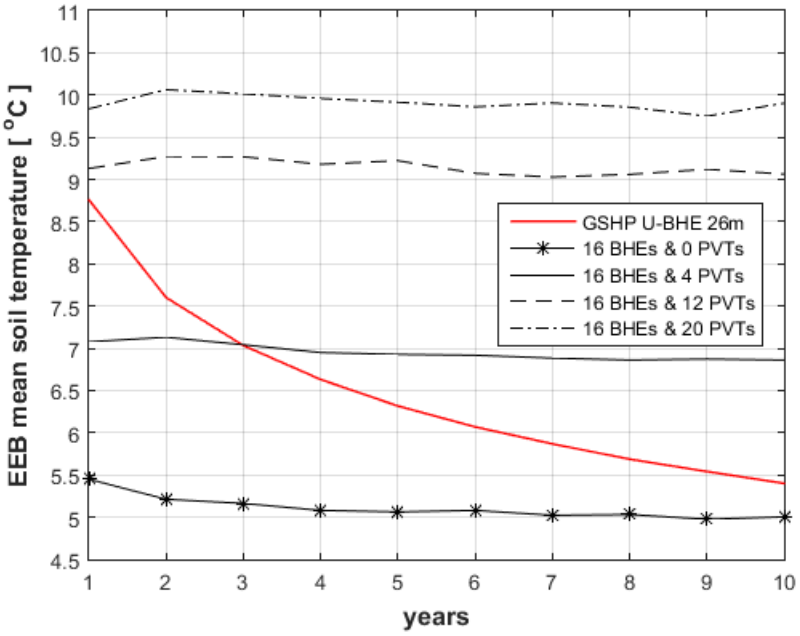

Figure 7.2. EEB mean soil temperature for the A_NE system of 16 BHEs and a variety of PVT arrays, along with the mean soil temperature resulting from the GSHP system use.

In Figure 7.3, the fraction of GHGs emission savings for the A_NB system are illustrated. A_NB system found less pollutant than the system based on the NGB for all system sizes. Likewise the A_NE system, the results for A_NB system can be analyzed by accepting two domains similar to those identified for A_NE system. The first part with the small PVT arrays illustrates a proportional increase of f_{sav_emis} to the system size, but relatively reduced to this found for the A_NE. The mean reason for this drop between the two systems is the increased power consumption by the A_NB system against the A_NE. Also, for the array of 12 PVTs, the system enters on a 100% reduction of GHGs emissions with the borefields of 32 and 40 BHEs. Similarly to the A_NE system, the size of the PVT array found to contribute more on the reduction of GHGs emissions than the borefield size. Finally, for the non-PVT system with the GHE as the only clean energy source, the carbon savings fraction is restricted to lower prices than these found for the A_NE system. This is caused by the reduced available heat of the EEB, which resulting to the increased auxiliary energy use. The reduced stored heat in the EEB is the product of the poor natural heat recovery process of the soil, as it is illustrated in subsection 5.1.1.

.

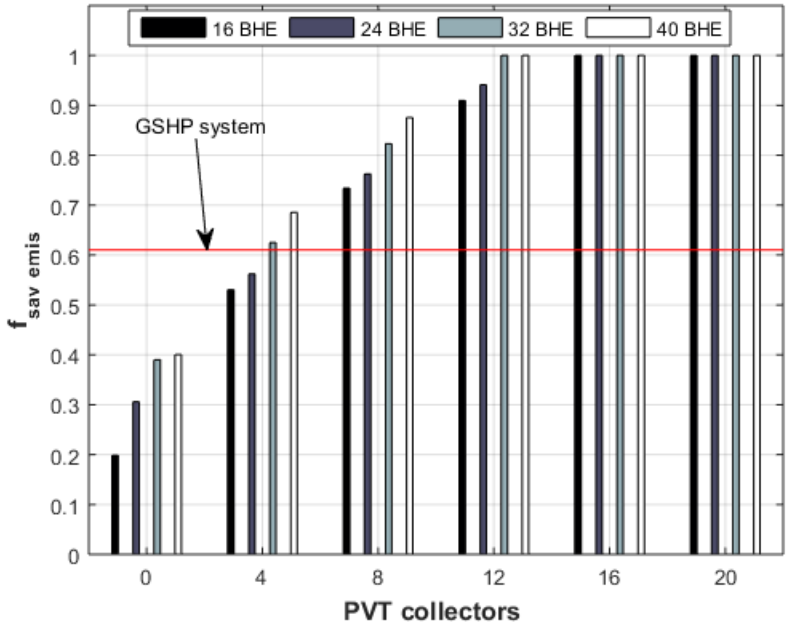

Figure 7.3. Fraction of GHGs emission savings fraction for A_NB system from the use of natural gas boiler-based system

With regards to systems with type B topology compared with A type, Figure 7.4 shows the f_{sav_emis} values obtained for borefields of 16 and 40 BHEs. In the same way as for the both systems with A topology, the systems with the direct use of solar heat follow similar pattern regarding the f_{sav_emis} dependence with the system size variation. Both systems with B topology found less capable of reducing the GHGs emissions than systems with A topology. The reasons for this lower performance to reduce the emissions are the dropped PVT electric SP (5.2.1) and the operation of the heat pump with higher electricity consumption. For the small GHE of 16 BHEs, the benchmark of 0.61 set by the GSHP system can be overcome by systems equipped with more than 4 PVTs, whereas the larger borefield can take this with any PVT array size. It is worth mentioning, that the hierarchy formed among the systems regarding the f_{sav_emis} values, follows the order shaped for systems' RPF (Figure 5.27). By bearing in mind the small fluctuation among all systems' PVT electric SP, it turns out that the system's electricity consumption is the factor which imposes the above-mentioned order.

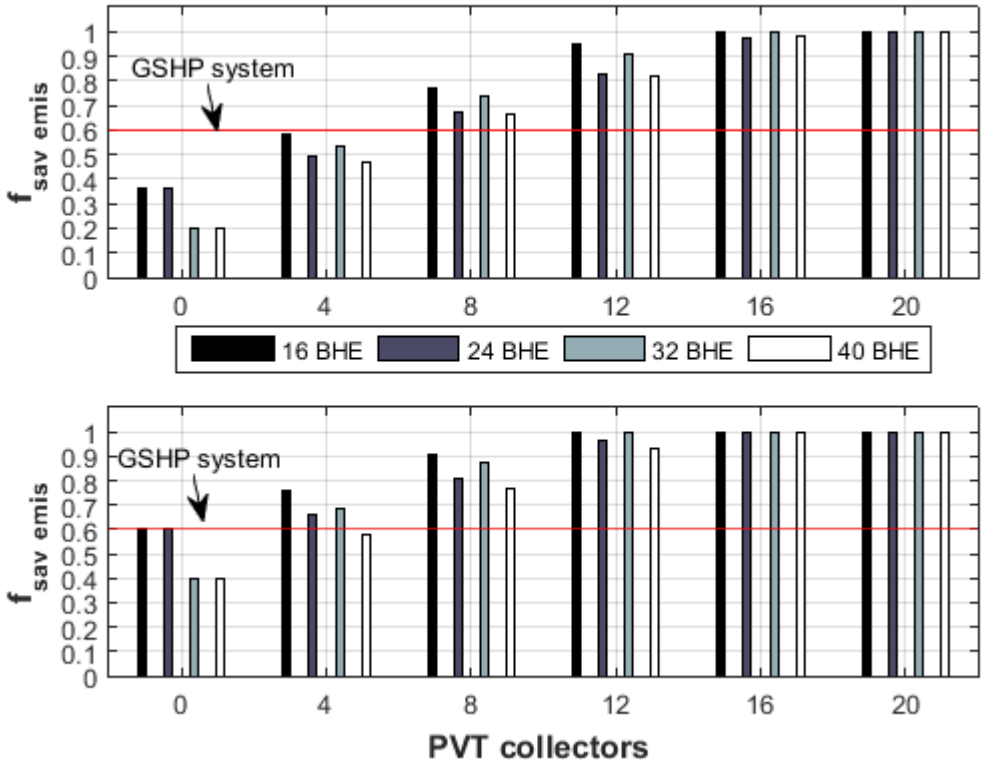

Figure 7.4. Fraction of GHGs emission savings for all systems installed with the new dwelling and for borefields of 16 and 40 BHEs.

7.2. Emissions comparison for the refurbished dwelling

Following the GHGs emission analysis conducted for the new dwelling, the NGB system installed in the renovated house is estimated to emit 3050.9 kg CO_2e per year. The GHGs emissions caused by the NGB system are comprised by 14874.2 kWh_{Th} (or 1070.1 kg of CH_4) and 44.8 kWh_e as parasitic energy. As regards the GSHP system installed for the refurbished house, the GHGs emissions are estimated to be 1512.4 kg CO_2e per year and are made by 5454.0 kWh_e. According to the results, the GSHP system can save half of the carbon emissions caused by the NGB system, thus the fractional savings are 0.5.

As it can been seen in Figure 7.5, the fractional emission savings for the A_RE system are lower than those estimated for all systems with the new dwelling. This significant reduction on f_{sav_emis} between the two-above scheme of systems is made by the extended power consumption, made by the systems paired with the refurbished dwelling. The fractional emission savings for A_RE system found to increase proportionally as the system size enlarges. Also, the f_{sav_emis} values

achieved for the A_RE system found to fluctuate from 0.18 to 0.80 (Table 7.2). As regards the comparison between the A_RE system and the GSHP system, in more than the half scenarios, the A_RE system found less emissive than the GSHP system. With more details, the A_RE system has obtained a f_{sav_emis} higher than 0.5 for all PVT arrays larger than 8 collectors, regardless the borefield size and for the array of 8 PVTs paired with 40 BHEs.

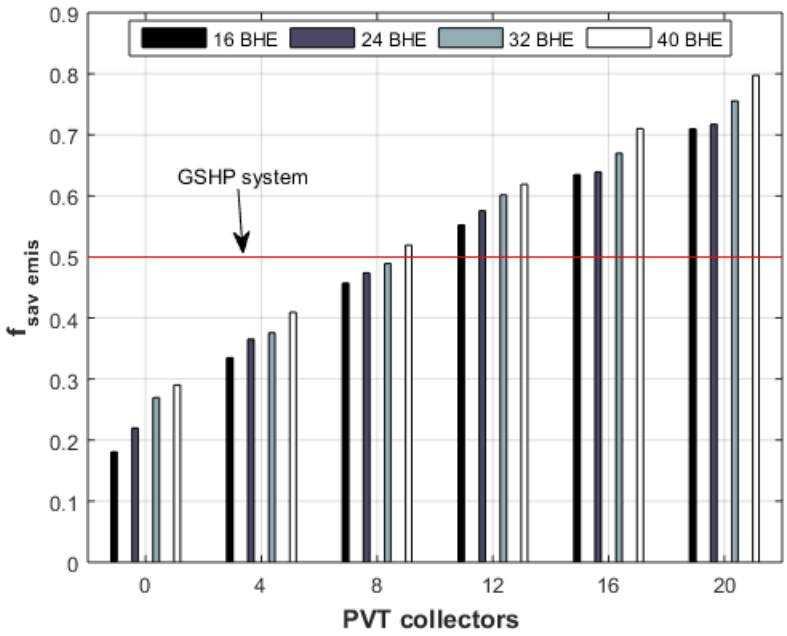

Figure 7.5. Fraction of GHGs emission savings for A_RE system from the use of natural gas boiler-based system.

According to the results illustrated in Table 7.2, the B_RE system found with lower capability to reduce the carbon emissions than the A_RE system. The achieved f_{sav_emis} values found to vary between 0.18 and 0.69, for the system of non-PVT with 16 BHEs and for the system with 20 PVTs with 40 BHEs respectively. Based on the results, twelve out of twenty-four systems illustrate fractional carbon savings better than the one found for the GSHP system (0.5). Also, the B_RE system is characterized as less carbon emissive than the NGB system for all investigated schemes.

Table 7.2. Annual GHGs emissions and fraction savings from SAGSHP systems against the NGB system, for both systems installed with the refurbished *dwelling.*

BHEs	PVTs	Annual GHGs emissions [kg CO_2e] A_RE	B_RE	f_{sav_emis} A_RE	B_RE
16	0	2499.1	2499.1	0.18	0.18
	4	2028.9	2109.0	0.33	0.31
	8	1656.0	1819.0	0.46	0.40
	12	1365.8	1589.2	0.55	0.48
	16	1114.5	1356.4	0.63	0.56
	20	885.4	1088.1	0.71	0.64
24	0	2380.8		0.21	
	4	1936.3		0.37	
	8	1605.1		0.47	
	12	1295.0		0.55	
	16	1100.6		0.64	
	20	862.6		0.72	
32	0	2228.8		0.27	
	4	1904.3		0.37	
	8	1558.6		0.49	
	12	1215.6		0.59	
	16	1007.4		0.67	
	20	745.9		0.76	
40	0	2165.7	2165.7	0.29	0.29
	4	1802.0	2209.1	0.41	0.28
	8	1466.9	1839.1	0.52	0.40
	12	1162.6	1531.9	0.62	0.50
	16	884.2	1296.1	0.71	0.58
	20	618.2	960.4	0.80	0.69

7.3. Comparison of the proposed systems with over PVT technologies

It is pertinent to compare the carbon emissions released by the SAGSHP system with this estimated from other studies for similar renewable energy systems. Thus, the benchmark of carbon emissions savings offered by two PVT based heating systems for UK climate is between 50 and 100 kg CO_2e per year and m^2 of PVT collector area (Herrando, Markides and Hellgardt, 2014; Herrando *et al.*, 2018). Similarly, a PVT based SAHP system investigated for Berlin (similar climatic conditions with London) was found to reduce the carbon emissions by 200 kg CO_2e per year and m^2 of PVT collector area (Ramos *et al.*, 2017). It is worth mentioning that, the presented studies have been conducted with different heating load and consumption profile than the

investigated SAGSHP system, thus the present comparison aims to offer only an indication regarding the emissions of the investigated system against other developed PVT technologies.

In Table 7.3, the carbon emissions savings are listed for all investigated schemes of the SAGSHP system and for the borefields of 16 and 40 BHEs. As it can be seen, the PVT based SAHP system is capable of reducing more carbon emissions per year and collector area than the investigated SAGSHP system for all configurations. As regard the PVT heating system, this is in the range of the values achieved by the SAGSHP for both dwellings. For the new dwelling, smaller arrays than 8 PVTs were found with less emission per collector area than the PVT system and for the refurbished dwelling, all arrays with less than 12 PVT were estimated with lower emissions per collector area than the PVT system.

Table 7.3. Carbon emission savings for all investigated SAGSHP schemes and for the borefields of 16 and 40 BHEs.

		A_NE	**B_NE**	**A_NB**	**B_NB**	**A_RE**	**B_RE**
	PVTs	kg CO_2e per year and m^2 of PVT collector area					
16 BHEs	4	139	118	127	113	162	149
	8	92	80	88	79	110	97
	12	76	66	72	65	89	77
	16	65	58	63	59	77	67
	20	60	54	58	54	69	62
40 BHEs	4	181	157	164	139	198	133
	8	108	97	105	92	125	96
	12	84	77	83	74	100	80
	16	72	66	72	65	86	69
	20	65	60	65	59	77	66

7.4. Carbon emission saving summary

As regards the new dwelling, the natural gas-based systems produced 1509.7 kg CO_2e annually for the space heating and DHW needs of the new dwelling, located in Birmingham. The GHSP systems obtained an emissions reduction of 61% (0.61 f_{sav_emis}) against the NGB systems, for equal heating load. The SAGSHP system was found capable of reducing significantly the carbon emissions against the NGB system at every configuration and system size. Also, most systems have achieved to decarbonize the emission by having more than 12 PVTs, regardless the

borefield size. The A_NE and A_NB got f_{sav_emis} equal to 1 by an even smaller PVT array of 8 PVTs and paired with borefield larger than 16 and 24 BHEs respectively. The SAGSHP system becomes less emissive than the GSHP systems from the array of 8 PVTs, with any configuration and borefield size. The A_NE and A_NB systems were established to be less emissive than the GHSP system from the array of 4 PVTs paired with the larger borefields. It is turned out that the generated power by the PVT collectors is the key parameter for the reduction on carbon emission illustrated by the SAGSHP system.

As regards the refurbished dwelling, the NGB system paired with the renovated dwelling was found to emit 3050.9 kg CO_2e per year. A reduction of 50% (0.5 f_{sav_emis}) on carbon emissions was estimated for the GSHP system. The SAGSHP system was less emissive than the NGB system at all configurations of the parametric analysis. Though for the refurbished dwelling scheme, the SAGSHP system did not managed to decarbonize totally the emissions at any system size. As regards the comparison with the GSHP system, the SAGSHP systems achieve better f_{sav_emi} than the conventional ground source system for all configurations with more than 8 PVT collectors. Finally, the fraction savings of the SAGSHP system found to rises proportionally as the number of BHEs and PVTs increases.

Chapter 8. Conclusions and further work

This chapter is divided in seven sections: the first section 8.1 offers a short summary of the conducted research, in section 8.2 the evaluation of the research objectives is illustrated, along with main finding from this process, the section 8.3 contains the conclusions about the metric used for the energy assessment of the systems, in section 8.4, the main results from the energy performance assessment of the systems are illustrated and discussed, by section 8.5 some design suggestions are illustrated, the proposals have been derived from the energy analysis of the systems, the section 8.6 illustrates the main findings from the carbon emissions assessment Chapter 7 and in section 8.7, a few research proposal for future works are offered along with proposed improvements for the studied system.

8.1. Introduction

With the current work, effort has been made to gain knowledge about the PVT based solar assisted ground source heat pump (SAGSHP) systems. By conducting the literature review, it emerged that the investigated type of systems cannot be treated by any existing designed method and are totally based on site specific approaches. Therefore, a model of the investigated SAGSHP system was formulated in TRNSYS and parametric analyses were conducted via simulation. The important variations of the analyses were the PVT array and borefield size, along with the dwelling's heating demand. Most of the components of the model are validated via experimental data from DMU's experiment (section 3.4), or with additional experimentation. Also, a new transient model for PVT collectors was developed along with a new modeling approach for the heat pump device. On top of the modelling procedure, a set of metrics was established with the aim to find out the best tool for the energy evaluation of the PVT-SAGSHP systems (section 3.5).

The illustrated methodology and approach have been deployed as an objective to provide answers on research questions and aim (section 1.3). The key points which were to be addressed are related to the size of the SAGSHP system and topology, and how these parameters influence the efficiency of the systems. Also, the energy independency from conventional energy sources was considered as an important index. The last task was to contrast the carbon emissions from SAGSHP systems with these released by the ground source heat pump (GSHP) and natural gas boiler (NGB) system.

8.2. Evaluation of the research objectives

One of the most fruitful tasks carried out during the research was the study of the existing scientific literature. The first effort was to clarify the investigated type of systems. Therefore, the SAGSHP systems were defined as these which are comprised by two main subsystems, the solar and the geothermal, with the solar system to be capable of providing heat. From the literature study, it came out that there are systems which are considered as solar assisted, but the provided energy source from the solar system is electricity. This definition proved useful, because narrowed down the large variety of solar and geothermal systems, to these with the particular characteristics.

Via the desk research important information about the SAGSHP systems was gained and evaluated. The bullet points list below illustrated the main findings:

- All the existing (built) systems are made from a particular set of components (solar collectors, geothermal heat exchangers). On top of the particularities of the systems, a variety of layouts and control prosses were identified. Based on the above facts, there is not a universal design method, and systems were built with site specific studies.
- By processing data from the investigated system, it was observed that PVT and uncover solar collectors tend to be paired more with horizontal or very shallow borehole heat exchanger. In contrast, the covered flat plate and vacuum solar collators is more likely to be installed with deep BHE. Additionally, from the data analysis the SAGSHP systems were split in two categories regarding their topology: the in series and the parallel. These two types of hydraulic connection were found capable to describe all the built systems.
- The majority of the theoretically studied have been carried out by utilizing TRNSYS simulation platform. The lion's share of the TRNSYS in this field is based on the fact of having numerus experimentally validated components.

The above findings create a prosperous ground for improvements and future works.

An important task made during the research was the investigation operation of the DMU's experimental system. The most well measured component of the systems was found to be the geothermal heat exchanger (GHE). Hence, data from the experiment were used to validate the utilised GHE's model. As regards the solar system, information about the PVTs' delivered heat and electricity were available. Thus, the lack of measurements of solar irradiance and the wind

speed become the reason to conducted additional experimentation. The aim of the data from the additional experiment was to validate the PVT's model. The transient nature of the new PVT model was found not to be useful during the final stage of parametrical analyses, and that because of adopting 1-hour simulation time step. Nevertheless, the model's ability to account the heat inertia of the PVT's absorber and its ability to describe the collector in detail, makes the extra effort worthwhile. Finally, the experiment conducted by the DMU and the additional experimentation about the PVT collector, were found to provide important information and self-confident on the carried research.

For the research needs, a new model for the heat pump was developed. As widely found in the literature, the heat pump devices are modeled by adopting performance data provided by the manufacturer. During the energy balancing procedure of the model, it was discovered, that what it is supposed to be absorbed by the heat pump does not mean that is available on the energy harvesting side. In other words, the solar and geothermal energy may be not capable to provide the heat pump's evaporator with the energy indicated in the performance data (Table 4.6). Therefore, the new model accepts the available energy as input and calculates the remaining parameters. The established model may be applied to a broader field of renewable energy systems which utilize heat pump.

The utilized modeling approach is made from substantial detail, by having the ability to vary many parameters and components. However, for a ten-year period simulation was found to require more than half hour for the execution. The main reason for extensive simulation time is the EEB's model which is based on numerical and analytical calculations. Therefore, it is proposed the creation of a lighter model in terms of calculations, with acceptable accuracy. The new model can be validated via the existing experimental data and can be embedded in a simplified modeling approach formulated in MATLAB. This new tool can be used to conduct further parametric studies and optimization without having the extensive simulation time. However, the ability of the TRNSYS's model to provide details about the parameters can be used at the final stage with the aim to emphasize on the interesting results. Another way to reduce the simulation span is to decrease the simulation period. Based on the results, all systems were entered in a soil temperature monotony after the 4^{th} year. Thus, someone can say to set a simulation period at 6 year instead of 10 year, which has been used. But, with the simulation time period to be reduced, important information regarding the magnitude of the soil's temperature variation is missed.

The parametric analyses of the systems were conducted via simulation, giving that the research must be carried out within a specific time frame and with limited budget (that concludes, now time and money for experimentation). Hence, most of the effort was made to create a model which can represent with acceptably accuracy the real system. One of the ways which can be achieved that is to utilize experimentally validated models, thus the two major sub systems (solar and geothermal) were simulated via verified models. At this point, it is difficult to compare the simulation results with these which are illustrated from similar studies in the existing literature, with the aim to quantify the model's correctness. The main reason for this limitation is that all systems have been found with different topology, components used, location and heat load. Additionally, in the literature, the SPF is the main metric which illustrates the energy performance of the systems, though the SPF was found not to fully describe the energy behaviour of the systems. However, the formulated model has experimentally validated the components required for the parametric analysis, also the heat pump's model was based on performance data provided by the manufacturer. It can be concluded that the built model is capable to predict the operation of the systems with acceptable accuracy. It is worth noticing, that up today, in the existing literature there is no system with the solar and geothermal systems to be experimentally verified.

For the research needs a set of metrics was established with the aim to find out which is the proper way to evaluate energetically the PVT-SAGSHP systems. During the results analysis and discussion process, it was revealed that this procedure of having many metrics for the same systems is a demanding task. However, the benefits derived from the evaluation process of the metrics are capable to compensate the extensive effort made. In other words, the system can be observed from a variety of perspectives, and via that to gain deeper understanding of its nature.

8.3. Metrics for the energy performance evaluation

Through the analysis and the discussion of the results, the renewable power fraction (RPF, subsection 3.5.4) is concluded to be the metric which can be used to determine the SAGSHP system with the higher energy performance. The RPF is the ratio between the generated and the consumed electricity of the system (equation 3.7). The numerator of equation 3.7 holds the generated electricity by PVT and the denominator contains all the electrical consumptions of the system, including the auxiliary heat (it is assumed to be offered via electricity). It turns out that, the higher is the RPF ratio, the more efficiently electricity is used by the system, with the higher

power yield by PVTs and/or lower electric consumption of the system. Bear in mind that, the denominator illustrates the total electricity required by the system to operate and to fulfill in total the heating demand. By obtaining a lower electricity consumption (denominator), a more electrical efficient operation is indicated. Also, a higher electric generation of PVTs' can be obtained via favorable conditions for power production, such as the lower inlet temperature of the PVT collectors. These conditions indicate interrelationships between the PVT and the system, and the RPF index is capable to consider these influences (subsection 5.2.3). It is important of mentioning that, the RPF can be used to compare system with equal number of PVTs and BHEs, otherwise the comparison is not valid.

The seasonal performance factor (SPF) indicated the ratio between the delivered heat and the consumed electricity by the system (subsection 3.5.1). In this study two versions of the SPF were considered: the consolidated SPF which includes the electricity delivered by PVTs and the SPF* which omits the electricity from PVT. Based on the results, the SPF was found capable to evaluate the SAGSHP system, but with a limitation related to the PVTs' capability to balance the electricity consumption of the system (it can get infinity values which are not useful for energy evaluation, equation 3.2). Unsuccessfully, the widely used seasonal performance factor which neglects the electricity from PVTs (SPF*), cannot track the overall energy performance of the systems, because the electricity generated by PVTs is neglected.

The specific productivity was used to illustrate the power or heat production per PVT collector (subsection 3.5.2). The system's heat specific productivity (SP_{sys_heat}) was established as a tool to estimate the heat with renewable energy origins used by the system. During the study, the SP_{sys_heat} was estimated for all schemes, but did not illustrate the ability to calculate the energy efficiency of the systems. That happened mainly due to the lack of considering the system's electricity. Although, additional studies have shown that, the SP_{sys_heat} can be an index capable of tracking the interaction of parameters with the energy harvested by the system. These parameters can be the flow rate of the solar system, the inclination of the collector and the plate heat exchanger's effectiveness. As regards the PVTs' specific productivity for heat and power, both found to be useful to determine the capabilities and improvements of the PVT collectors. These indexes can be used to optimize the harvest energy from the sun and to offer the maximum amount of energy resources to the system. Also, the heat and power of the collectors found to be linked to the collectors to boreholes ratio

(CBR), which must hold values lower than 0.2 (1 PVT per 5 borehole heat exchangers (BHE)), for improved energy absorption.

8.4. Energy performance and operation of the systems

For the new dwelling, by evaluating the systems as regards the renewable power fraction (RPF), the system with A topology and the EEB being exposed (A_NE) achieves the higher value. The second place belongs to the system with A topology and the EEB to be installed beneath (A_NB) the dwelling. As regards the third and the fourth place these belong to systems built with B topology and with the EEB being exposed (B_NE) and underneath the building (B_NB) respectively. System paired with the refurbished dwelling, follow the same order illustrated for the systems considered for the new dwelling. The above illustrated order of the system regarding the achieved RPF was remained stable throughout all the parametric analyses. Representatively, the RPF for the A_NE system was estimated to be 1.91 and for the A_NB slightly less to 1.9, for the larger PVT array and borefield (Table 5.21). About the RPF of the systems B_NE and B_NB, these were estimated at 1.54 and 1.47, accordingly.

The heat independency of the SAGSHP systems from conventional energy sources, this was estimated to be correlated with the size of borefield and the number of PVTs. As it was revealed, the main heat source of the systems was the EEB via the borefield. Then, by increasing the PVT array a further improvement on the renewable heat fraction (RHF, subsection 3.5.3) of the systems can be obtained. Systems paired with the new dwelling estimated to be capable of achieving up to 83% heat autonomy, while systems with the renovated solution get up to 74% heat independency. According to the analysis of the results, the systems with the higher RHF did not get also the best RPF, hence did not obtain the better energy efficiency (subsection 5.2.3). As it is already explained, the A topology got the higher energy performance (RPF), though, the B systems obtained the highest RHF. The better RHF of the B topology against the A, was caused by the increased synchronized part of heat. The part of the synchronized energy has been delivered mainly due to heat pump increased electricity consumption. It is important to reminded that, the heat autonomy of the SAGSHP systems cannot reach the 100%, due to the heat pump utilization, which does not allow the heat to be delivered without electricity consumption (COP).

According to the results, the direct use of solar heat for domestic hot water (DHW) has a negative effect on the energy efficiency of the systems. As this was illustrated, the systems with

B topology were estimated to obtain lower RPF than these with topology A (section 3.2), which does not utilize directly the solar heat. The elevated inlet temperature of the PVTs and the lack of solar heat to recharge the earth energy bank (EEB), are the main two reasons for the dropped efficiency of the B topology. It can be noted that, the PVTs connected in series to the borefield, elevate the soil and the evaporator's inlet temperature. The EEB location seems to not influence the efficiency of the systems, as much as the topology does. As regards the lack of the natural heat recovery of the EEB being beneath the dwelling, this can be compensated via solar heat. The array of 12 PVTs was found to offer substantial heat to the EEB of the A_NB system, in order this to achieve similar annual mean soil temperature with the A_NE system.

SAGSHP systems paired with the new dwelling, obtained a power self-sufficient state by being equipped with 12 or more PVT collectors for systems with A topology and with 16 or more PVTs for the B configuration respectively. The array of 20 PVTs for systems with A topology found to obtain almost two time more power than this consumed by the system. However, the B type of systems with the larger collector array managed to achieve only 1.5 times the consumed amount of electricity. The simulations have been conducted by a retrofitted PVT collector, which is experimentally validated of course. But a commercially available PVT may be more thermally and power efficient than the utilized one, which suffered from low absorber's bound heat conductance coefficient[21]. It can be deemed that, a more efficient PVT collector may reduce further the number of the devices required for the energy self-sufficiency of the systems (with higher power capacity and improved absorber's bound heat conductance coefficient). As regards the refurbished dwelling, this did not manage to enter in the 100% power self-sufficient mode, even with the bigger PVT array and borefield. Similarly, systems paired with the renovated house may benefited by a more energetical capable PVT collector.

As regards the variation of the soil temperature in the EEB, this was estimated to fluctuate until the 4th year for all systems and then to enter in a monotony (Figure 5.5). This behavior found to be related with the balancing procedure of the solar and the geothermal systems. Also, the EEB's mean annual soil temperature was found to be imposed by the PVT array size and the utilized control, both of these parameters are capable to regulate the soil's temperature (Figure 5.16). In the scenario where the EEB is placed beneath the house, the soil heat recovery mechanism

[21] The absorber's bound heat conductance coefficient indicates how easily is the heat transfer from the plate (PV) to the absorber (section 4.1).

was constrained by the building's footprint. This influence was estimated to eliminate as the borefield, and the PVT array enlarges.

The direct use of solar heat for the DHW need found to negatively influence the PVTs' thermal and electrical efficiency. The collectors' inlet temperature was elevated due to DHW tank higher temperature, which consequently rises the stream which returns to the PVT array. Also, the DHW demand covered via the solar heat was remained on low level due to heat pump's contribution (subsection 5.1.1). With the aim to improve the level of the direct utilized solar heat, two proposal have been developed and illustrated in subsection 5.1.1. In a nutshell the two proposal are: a) to determine the temperature up to where the PVTs may warm up the DHW tank efficiently, and the heat pump to provide the remaining heat and b) to set a second DHW tank which will be heated up totally from solar heat, and the remaining energy will be provided from the tank dedicated to the heat pump, via mixing.

Via the results analysis, the heating load found to be a crucial aspect regarding the energy performance of the systems. As it was revealed during the results analysis, by using the same size system but different dwelling type, the absorbed heat was increased significantly. Based on that, for the current location, the renewable energy absorbed as heat by the system is a function of three main parameters: the size of the PVT array, the size of the borefield and the heating demand. By neglecting the interaction of the heat pump sizing on the system's performance, these three aspects may be tabulated for the particular location (or for any location) and by that to shape a first sizing method.

The electricity generated by the PVTs was estimated to not be influenced by the CBR index but from the system's topology (section 3.2). As it already referred above, the B layout was found to reduce the electrical efficiency of the PVTs, due to high inlet temperature. Also, as it was discussed, the soil mean temperature is function of the size of the PVT array and the utilized control. Thus, for each PVT arrays an electric SP was achieved which is not a function of the borefield size (giving that the control procedure remains the same through the analysis).

8.5. Design aspects of the systems

By considering the above and the simulation results, it can be concluded that, new dwellings located in Midlands of the UK, can be energetic self-sufficient with 12 to 16 PVTs paired with borefields of 16 to 32 BHEs. Also, it is suggested to keep the CBR index as small it can be, because this found to improve the PVT heat SP. Thus, on the above range of PVT collectors and BHEs, it

is preferable to be installed with CBR less than 0.5 (1 PVT per 2 BHEs). As for the renovated dwelling, the heating system should be comprised by more than 24 BHEs, strictly built with A topology and with more efficient PVT collectors.

In addition to the above proposals for the design of SAGSHP systems, the following points can be made:

- By comparing systems built with the same topology (A or B), the difference on RPF eliminates as the PVT array enlarges regardless the location of the EEB, exposed or beneath the dwelling (Table 5.21). Practically, for the topology A and with large collector arrays (16 to 20 PVTs), someone can say that, the EEB can be installed with either option without resulting in any substantial RPF change (performance change).
- The topology B with the solar heat to be utilized directly should be avoided for any topology. Additional experimentation with simulations is required to provide the set up for direct use of solar heat.
- For climatic conditions as these of Birmingham, the electricity generated by PVT was found to not be influenced by the borefield size or the CBR ratio. But the heat production of the collectors was significantly influenced by the CBR ratio, and for the same PVT array and larger EEB the heat productivity was increased. It turns out that, the EEB should be the largest that can be achieved with the aim to maximize the heat offered by the PVT collector to the system. For a given borefield consisted of a certain number of boreholes, the volume of the EEB can enlarge by increasing the spacing among boreholes (equation 4.1).
- For new dwellings, the storage capacity (subsection 3.5.2) should be maintained below 10 m^3 m^{-2} (storage volume per PVT collectors' area), above this limit the PVT collectors are entering in a stagnation regime regarding the heat productivity (Figure 5.18). For the refurbished dwelling, throughout all the PVT arrays and borefields tried, no stagnation was traced.

8.6. Evaluation of the carbon emissions

The investigated PVT based SAGSHP system was found to be capable to reduce the carbon emissions at all system sizes and schemes. The comparison with the conventional GSHP system indicates that most systems with four or more PVTs turn out to be less emissive than the GSHP system. For the renovated dwelling, the required PVTs for the same objective are increased to

more than 8 PVT collectors. Also, all system found to decarbonize the emissions with collector array larger than 12 PVTs. It seems that for new dwellings, the two objectives of energy self-sufficient and zero carbon emissions can be achieved by a PVT array equal or larger than 12 collectors, while for renovated solutions more collectors are needed.

The gas boiler system was found to release 1510 kg CO_2e annually with the aim to cover the space heating and DHW needs of the new dwelling. Accordingly, the boiler's emissions for the refurbished dwelling were estimated to be 3051 kg CO_2e per year. Based on these annual emissions illustrated above for both dwellings, the GSHP system achieved a fractional emissions reduction of 0.61 for the new dwelling and 0.5 for the refurbished solution accordingly. As regards the SAGSHP systems, the fractional reduction was found to be from 0.2 up to total decarbonization for the new dwelling and from 0.18 up to 0.8 for the refurbished dwelling.

From the evaluation of the proposed systems against other PVT technologies, the SAHP system was found to be less emissive than the SAGSHP at all the investigated configurations. In details, an annual reduction on carbon emissions of 200 kg CO_2e m^{-2} was received for the SAHP system, while the best value achieved by the SAGHSP systems was estimated to be 198 kg CO_2e m^{-2} (Table 7.3). As regards the PVT system, this was found more emissive than the SAGSHP system for all PVT arrays with less than 8 collector and less than 12 collectors for the new and the refurbished dwelling, respectively. At the remaining PVT arrays, the PVT system was estimated to be with similar carbon emission with this of the SAGSHP system. By knowing that the current analysis offers a rough estimation of the comparison of the systems, a more rigorous investigation is proposed with the aim to obtain solid results. Thus, all systems can be modeled mathematically and simulated for the same climate by applying equal heating load for all competitors, hence a reference point for the analysis can be set.

8.7. Further work and improvements

Through the discussion of the research results, the limitation of the SAGSHP systems to utilize the available energy has emerged. That can be distinctively seen when from the same system size the refurbished dwelling got two times more heat that the new one (subsection 5.1.5). Based on the above observation, a smarter utilization of the available energy sources may improve the systems efficiency and their energy autonomy. Therefore, additional studies can be carried out with the aim to improve energetically the system. The new proposed topologies are listed below with bullet points:

- A phase change material (PCM) heat storage bank may be entered in parallel with the EEB, with the aim to store energy seasonally. The PVTs found capable of increasing their heat productivity with large storage capacities. Thus, the extra heat storage container can create the circumstances for risen heat production by PVTs. Then, the stored heat can be used independently or in parallel with the EEB, with the aim to cover the winter's peak loads. By this alteration, the required size of the system may be reduced along with its energy autonomy.
- A second scenario may be a buffer tank installed between the condenser of the heat pump and the heating load. This tank can be heated up when the level of the irradiance is substantial and capable to operate the heat pump by providing demanded electricity. Hence, by having the heat pump to run totally by the electricity from PVTs, the produced stored heat in the buffer tank is characterized as renewable energy. The size of the buffer tank can be determined via parametric analysis with the aim to define the preferable heat storage period and temperature.

From an engineering perspective, it is crucial to perform economic studies of the SAGSHP systems. Especially, the proposed technology should be compared with the conventional GSHP and NGB systems. Also, the optimum number of BHEs and PVTs can be offered via the higher net present value derived by the life cycle cost (LCC) analysis, by accounting the installation, the operation and the maintenance costs of the systems.

It is essential to estimate the parameters' values which cause the higher energy performance of the systems. Parameters like the flow rate of the PVTs and the spacing of the BHE directly influence the operation of the system. The optimization of the parameters' values can be carried out by aiming to maximize the exergy efficiency of the system. The exergetic study of the systems can be conducted along with their financial investigation because the operation and installation costs of the optimum values may differ from the utilized one.

Lastly, a holistic environmental assessment of the SAGSHP system should be carried out. Up to now, the system has been evaluated regarding the carbon emissions of its operation and the environmental impact in total has not been evaluated. The analysis can be conducted via the life cycle assessment (LCA) method and the system can be compared with the natural gas boiler system and the GSHP system.

References

Agemar, T., Weber, J. and Schulz, R. (2014) 'Deep geothermal energy production in Germany', *Energies*, 7(7), pp. 4397–4416. doi: 10.3390/en7074397.

Alkan, M. A., Keçebaş, A. and Yamankaradeniz, N. (2013) 'Exergoeconomic analysis of a district heating system for geothermal energy using specific exergy cost method', *Energy*, 60, pp. 426–434. doi: 10.1016/j.energy.2013.08.017.

Anderson, J. V., Mitchell, J. W. and Beckman, W. a. (1980) 'A design method for parallel solar-heat pump systems', *Solar Energy*, 25(2), pp. 155–163. doi: 10.1016/0038-092X(80)90471-5.

Argiriou, A. A. (1997) 'CSHPSS systems in Greece: Test of simulation software and analysis of typical systems', *Solar Energy*, 60(3–4), pp. 159–170. doi: 10.1016/S0038-092X(96)00154-5.

ASHRAE (2011) *ASHRAE Handbook - HVAC Applications*, *www.ansi.org American Society of Heating, Refrigerating and Air-Conditioning Engineers, Inc.*

Axaopoulos, P. J. and Fylladitakis, E. D. (2013) 'Performance and economic evaluation of a hybrid photovoltaic / thermal solar system for residential applications', 65, pp. 488–496.

Badache, M. *et al.* (2016) 'A new modeling approach for improved ground temperature profile determination', *Renewable Energy*. Elsevier Ltd, 85, pp. 436–444. doi: 10.1016/j.renene.2015.06.020.

Baetschmann, M. and Leibundgut, H. (2012) 'LowEx Solar Building System: Integration of PV/T Collectors into Low Exergy Building Systems', *Energy Procedia*, 30, pp. 1052–1059. doi: 10.1016/j.egypro.2012.11.118.

Bakirci, K. *et al.* (2011) 'Energy analysis of a solar-ground source heat pump system with vertical closed-loop for heating applications', *Energy*. Elsevier Ltd, 36(5), pp. 3224–3232. doi: 10.1016/j.energy.2011.03.011.

Bakker, M. *et al.* (2005) 'Performance and costs of a roof-sized PV/thermal array combined with a ground coupled heat pump', *Solar Energy*, 78(2), pp. 331–339. doi: 10.1016/j.solener.2004.09.019.

Bateson, A. (2014) 'CIBSE ASHRAE Technical Symposium, Dublin, Ireland, 3-4 April 2014', *CIBSE ASHRAE Technical Symposium*, (April), pp. 3–4.

Beier, R. A., Smith, M. D. and Spitler, J. D. (2011) 'Reference data sets for vertical borehole ground heat exchanger models and thermal response test analysis', *Geothermics*. CNR-Istituto di Geoscienze e Georisorse, 40(1), pp. 79–85. doi: 10.1016/j.geothermics.2010.12.007.

Bertram, E., Glembin, J. and Rockendorf, G. (2012) 'Unglazed PVT collectors as additional heat source in heat pump systems with borehole heat exchanger', *Energy Procedia*. The Authors, 30, pp. 414–423. doi: 10.1016/j.egypro.2012.11.049.

Bertsch, S. S. and Groll, E. A. (2008) 'Two-stage air-source heat pump for residential heating and cooling applications in northern U.S. climates', *International Journal of Refrigeration*, pp. 1282–1292. doi: 10.1016/j.ijrefrig.2008.01.006.

Bi, Y. *et al.* (2004) 'Solar and ground source heat-pump system', *Applied Energy*, 78(2), pp. 231–245. doi: 10.1016/j.apenergy.2003.08.004.

Bilbao, J. I. and Sproul, A. B. (2015) 'Detailed PVT-water model for transient analysis using RC networks', *Solar Energy*. Elsevier Ltd, 115, pp. 680–693. doi: 10.1016/j.solener.2015.03.003.

Blum, P. *et al.* (2010) 'CO2 savings of ground source heat pump systems - A regional analysis', *Renewable Energy*, pp. 122–127. doi: 10.1016/j.renene.2009.03.034.

Braun, J. E., Klein, S. A. and Mitchell, J. W. (1981) 'Seasonal storage of energy in solar heating', *Solar Energy*, 26(5), pp. 403–411. doi: 10.1016/0038-092X(81)90219-X.

Busato, F., Lazzarin, R. M. and Noro, M. (2013) 'Two years of recorded data for a multisource heat pump system: A performance analysis', *Applied Thermal Engineering*. Elsevier Ltd, 57(1–2), pp. 39–47. doi: 10.1016/j.applthermaleng.2013.03.053.

Busato, F., Lazzarin, R. and Noro, M. (2015) 'Ground or solar source heat pump systems for space heating: Which is better? Energetic assessment based on a case history', *Energy and Buildings*. Elsevier B.V., 102, pp. 347–356. doi: 10.1016/j.enbuild.2015.05.053.

Carbonell, D., Haller, M. Y. and Frank, E. (2014) 'Potential Benefit of Combining Heat Pumps with Solar Thermal for Heating and Domestic Hot Water Preparation', *Energy Procedia*, 57, pp. 2656–2665. doi: 10.1016/j.egypro.2014.10.277.

Cen, D. *et al.* (2006) 'Heating systems in buildings — Method for calculation of system energy requirements and system efficiencies — Part 4-7 Space heating generation systems , biomass combustion systems', *European Union*, pp. 1–22.

Chandrashekar, M. *et al.* (1982) 'A comparative study of solar assisted heat pump systems for canadian locations', *Solar Energy*, 28(3), pp. 217–226. doi: 10.1016/0038-092X(82)90160-8.

Chapuis, S. and Bernier, M. (2009) 'Seasonal storage of solar energy in borehole heat exchangers', *Eleventh International IBPSA Conference*, pp. 599–606. Available at: http://citeseerx.ist.psu.edu/viewdoc/summary?doi=10.1.1.172.4804.

Charalambous, P. G. *et al.* (2007) 'Photovoltaic thermal (PV/T) collectors: A review', *Applied Thermal Engineering*, 27(2–3), pp. 275–286. doi: 10.1016/j.applthermaleng.2006.06.007.

Commission, E. (2020) 'A policy framework for climate and energy in the period from 2020 to 2030', (2014), pp. 1–18.

D'Antoni, M., Fedrizzi, R. and Sparber, W. (2012) 'IEA – SHC Task 44 / Annex 38 Solar and Heat Pump Systems', *Iea-Shc*. Available at: http://task44.iea-shc.org/data/sites/1/publications/Task44-2012-06-Newsletter.pdf.

Dai, L. *et al.* (2015) 'Experimental performance analysis of a solar assisted ground source heat pump system under different heating operation modes', *Applied Thermal Engineering*. Elsevier Ltd, 75, pp. 325–333. doi: 10.1016/j.applthermaleng.2014.09.061.

Duffie, J. A. and Beckman, W. A. (2013) *Solar Engineering of Thermal Processes: Fourth Edition*, *Solar Engineering of Thermal Processes: Fourth Edition*. doi: 10.1002/9781118671603.

Emmi, G., Zarrella, A., De Carli, M., *et al.* (2015) 'An analysis of solar assisted ground source heat pumps in cold climates', *Energy Conversion and Management*. Elsevier Ltd, 106, pp. 660–675. doi: 10.1016/j.enconman.2015.10.016.

Emmi, G., Zarrella, A., Carli, M. De, *et al.* (2015) 'Solar Assisted Ground Source Heat Pump in Cold Climates'. Elsevier B.V., 82, pp. 623–629. doi: 10.1016/j.egypro.2015.12.010.

Energy Monitoring Company (2008) 'Measurement of Domestic Hot Water Consumption in Dwellings EXECUTIVE SUMMARY', p. 62.

Esen, H., Esen, M. and Ozsolak, O. (2017) 'Modelling and experimental performance analysis of solar-assisted ground source heat pump system', *Journal of Experimental & Theoretical Artificial Intelligence*, 29(1), pp. 1–17. doi: 10.1080/0952813X.2015.1056242.

Eslami-nejad, P. *et al.* (2009a) 'Solar heat injection into boreholes', *4Th Canadian Solar Building Conference*, (February), pp. 237–246.

Eslami-nejad, P. *et al.* (2009b) 'Solar heat injection into boreholes', *4Th Canadian Solar Building Conference*, (December), pp. 237–246.

Eslami-Nejad, P. and Bernier, M. (2011) 'Coupling of geothermal heat pumps with thermal solar collectors using double U-tube boreholes with two independent circuits', *Applied Thermal Engineering*. Elsevier Ltd, 31(14–15), pp. 3066–3077. doi: 10.1016/j.applthermaleng.2011.05.040.

European Parliament (2013) 'Guidelines for Member States on calculating renewable energy from heat pumps from different heat pump technologies pursuant to Article 5 of Directive 2009/28/EC', *Official Journal of the European Union*, (December), pp. 27–35.

European Parliament (2016) 'Decision (2013/114/EU) Establishing the Guidelines for Member States on Calculating Renewable Energy from Heat Pumps from Different Heat Pump Technologies pursuant to Article 5 of Directive 2009/28/EC of the European Parliament an dof the Council', *Official Journal of the European Union*, (December), pp. 27–35.

EUROSTAT (2015) *Consumption of energy: tables and figures excel*. Available at: https://ec.europa.eu/eurostat/statistics-explained/index.php?title=Archive:Consumption_of_energy#Further_Eurostat_information.

Fine, J. P. *et al.* (2018) 'A simplified ground thermal response model for analyzing solar-assisted ground source heat pump systems', *Energy Conversion and Management*. Elsevier, 165(March), pp. 276–290. doi: 10.1016/j.enconman.2018.03.060.

Florides, G. and Kalogirou, S. (2007) 'Ground heat exchangers-A review of systems, models and applications', *Renewable Energy*, 32(15), pp. 2461–2478. doi: 10.1016/j.renene.2006.12.014.

FLorschuetz, L. . (1979) 'Extension of the Hottel-Whillier Model To the Analysis of Combined Photovoltaic / Thermal Flat Plate Collectors', *Solar Energy*, 22, pp. 361–366.

Foulds, E., Abeysekera, M. and Wu, J. (2017) 'Modelling and analysis of a ground source heat

pump combined with a PV-T and earth energy storage system', *Energy Procedia*. Elsevier B.V., 142, pp. 886–891. doi: 10.1016/j.egypro.2017.12.142.

Franco, A. and Fantozzi, F. (2016) 'Experimental analysis of a self consumption strategy for residential building: The integration of PV system and geothermal heat pump', *Renewable Energy*. Elsevier Ltd, 86(September), pp. 1075–1085. doi: 10.1016/j.renene.2015.09.030.

Girard, A. *et al.* (2015) 'Higher ground source heat pump COP in a residential building through the use of solar thermal collectors', *Renewable Energy*. Elsevier Ltd, 80, pp. 26–39. doi: 10.1016/j.renene.2015.01.063.

Givoni, B. (1977) 'Underground longterm storage of solar energy-An overview', *Solar Energy*, 19(6), pp. 617–623. doi: 10.1016/0038-092X(77)90021-4.

de Gouw, J. A. *et al.* (2014) 'Reduced emissions of CO 2 , NOx , and SO 2 from U . S . power plants owing to switch from coal to natural gas Earth ' s Future', *Earth's Future*, 2, pp. 75–82. doi: 10.1002/2013EF000196.Abstract.

Guadalfajara, M., Lozano, M. A. and Serra, L. M. (2015) 'Simple calculation tool for central solar heating plants with seasonal storage', *Solar Energy*. Elsevier Ltd, 120, pp. 72–86. doi: 10.1016/j.solener.2015.06.011.

Guarracino, I. *et al.* (2016) 'Dynamic coupled thermal-and-electrical modelling of sheet-and-tube hybrid photovoltaic/thermal (PVT) collectors', *Applied Thermal Engineering*. Elsevier Ltd, 101, pp. 778–795. doi: 10.1016/j.applthermaleng.2016.02.056.

Guarracino, I. *et al.* (2019) 'Systematic testing of hybrid PV-thermal (PVT) solar collectors in steady-state and dynamic outdoor conditions', *Applied Energy*, pp. 1014–1030. doi: 10.1016/j.apenergy.2018.12.049.

Han, Z. *et al.* (2008) 'Numerical simulation of solar assisted ground-source heat pump heating system with latent heat energy storage in severely cold area', *Applied Thermal Engineering*, 28(11–12), pp. 1427–1436. doi: 10.1016/j.applthermaleng.2007.09.013.

Hellström, G. (1989) 'Duct Ground Heat Storage Model, Manual for Computer Code', *Energy*, (March). Available at: TESS type 557.

Hepbasli, A. *et al.* (2009) 'A review of gas engine driven heat pumps (GEHPs) for residential and industrial applications', *Renewable and Sustainable Energy Reviews*, 13(1), pp. 85–99. doi: 10.1016/j.rser.2007.06.014.

Hepbasli, A. and Kalinci, Y. (2009) 'A review of heat pump water heating systems', *Renewable and Sustainable Energy Reviews*, pp. 1211–1229. doi: 10.1016/j.rser.2008.08.002.

Herrando, M. *et al.* (2018) 'Technoeconomic modelling and optimisation of solar combined heat and power systems based on flat-box PVT collectors for domestic applications', *Energy Conversion and Management*, pp. 67–85. doi: 10.1016/j.enconman.2018.07.045.

Herrando, M., Ramos, A., *et al.* (2019) 'A comprehensive assessment of alternative absorber-exchanger designs for hybrid PVT-water collectors', *Applied Energy*. Elsevier, 235(July 2018), pp. 1583–1602. doi: 10.1016/j.apenergy.2018.11.024.

Herrando, M., Pantaleo, A. M., *et al.* (2019) 'Solar combined cooling, heating and power systems based on hybrid PVT, PV or solar-thermal collectors for building applications', *Renewable Energy*. Elsevier Ltd, 143, pp. 637–647. doi: 10.1016/j.renene.2019.05.004.

Herrando, M. and Markides, C. N. (2016) 'Hybrid PV and solar-thermal systems for domestic heat and power provision in the UK: Techno-economic considerations', *Applied Energy*. Elsevier Ltd, 161, pp. 512–532. doi: 10.1016/j.apenergy.2015.09.025.

Herrando, M., Markides, C. N. and Hellgardt, K. (2014) 'A UK-based assessment of hybrid PV and solar-thermal systems for domestic heating and power: System performance', *Applied Energy*, pp. 288–309. doi: 10.1016/j.apenergy.2014.01.061.

Herrando, M., Ramos, A. and Zabalza, I. (2018) 'Cost competitiveness of a novel PVT-based solar combined heating and power system: Influence of economic parameters and financial incentives', *Energy Conversion and Management*, 166(March), pp. 758–770. doi: 10.1016/j.enconman.2018.04.005.

HM Government. Ministry of Housing & Communities & Local Government (2010) *The Building Regulations 2010 Conservation, L1B*.

HM Government. Ministry of Housing & Communities & Local Government (2016) *The Building Regulations 2010 Conservation, L1A*.

HM UK Parliament (2008) 'Climate Change Act 2008', *HM Government*. doi: 10.1136/bmj.39469.569815.47.

Hossain, M. S. *et al.* (2011) 'Review on solar water heater collector and thermal energy performance of circulating pipe', *Renewable and Sustainable Energy Reviews*. Elsevier Ltd, 15(8), pp. 3801–3812. doi: 10.1016/j.rser.2011.06.008.

Hottel, H. C. and Whillier, A. (1955) 'Evaluation of flat-plate solar collector performance', in *Transcript of the Conference on the Use of Solar Energy, The Scientific Basis, Vol. II, Part 1, Section A*, pp. 74–104.

Incropera, F. P. *et al.* (2007a) *Fundamentals of Heat and Mass Transfer 6th Edition*, *Fundamentals of Heat and Mass Transfer 6th Edition*. doi: 10.1016/j.applthermaleng.2011.03.022.

Incropera, F. P. *et al.* (2007b) 'heat and mass transfer - Incropera 6e', *Fundamentals of Heat and Mass Transfer*, p. 997. doi: 10.1016/j.applthermaleng.2011.03.022.

J. Lund, B. Sanner, L. Rybach, R. Curtis, G. H. (2004) 'Geothermal (Ground-Source) Heat Pumps a World Overview.pdf', (January), pp. 1–10.

Ji, J. *et al.* (2009) 'Distributed dynamic modeling and experimental study of PV evaporator in a PV/T solar-assisted heat pump', *International Journal of Heat and Mass Transfer*. Elsevier Ltd, 52(5–6), pp. 1365–1373. doi: 10.1016/j.ijheatmasstransfer.2008.08.017.

Jradi, M., Veje, C. and Jrgensen, B. N. (2017) 'Performance analysis of a soil-based thermal energy storage system using solar-driven air-source heat pump for Danish buildings sector', *Applied Thermal Engineering*, 114, pp. 360–373. doi: 10.1016/j.applthermaleng.2016.12.005.

Kalogirou, S. A. (2004) *Solar thermal collectors and applications*, *Progress in Energy and Combustion Science*. doi: 10.1016/j.pecs.2004.02.001.

Kamel, R. S., Fung, A. S. and Dash, P. R. H. (2015) 'Solar systems and their integration with heat pumps: A review', *Energy and Buildings*. Elsevier B.V., 87, pp. 395–412. doi: 10.1016/j.enbuild.2014.11.030.

Kjellsson, E., Hellström, G. and Perers, B. (2010) 'Optimization of systems with the combination of ground-source heat pump and solar collectors in dwellings', *Energy*, 35(6), pp. 2667–2673. doi: 10.1016/j.energy.2009.04.011.

Klein, S. A. (2010) 'TRNSYS 17: A Transient System Simulation Program', *Solar Energy Laboratory, University of Wisconsin, Madison, USA*, 1, pp. 1–5.

Liu, L., Zhu, N. and Zhao, J. (2016) 'Thermal equilibrium research of solar seasonal storage system coupling with ground-source heat pump', *Energy*. Elsevier Ltd, 99, pp. 83–90. doi: 10.1016/j.energy.2016.01.053.

Loose, A. and Drück, H. (2014) 'Field test of an advanced solar thermal and heat pump system with solar roof tile collectors and geothermal heat source', *Energy Procedia*. Elsevier B.V., 48(0), pp. 904–913. doi: 10.1016/j.egypro.2014.02.104.

Lunde, P. J. (1979) 'Prediction of the performance of solar heating systems over a range of storage capacities', *Solar Energy*, 23(2), pp. 115–121. doi: 10.1016/0038-092X(79)90111-7.

Markides, C. N. (2013) 'The role of pumped and waste heat technologies in a high-efficiency sustainable energy future for the UK', *Applied Thermal Engineering*, pp. 197–209. doi: 10.1016/j.applthermaleng.2012.02.037.

Marx, R., Bauer, D. and Drueck, H. (2014) 'Energy efficient integration of heat pumps into solar district heating systems with seasonal thermal energy storage', *Energy Procedia*. Elsevier B.V., 57, pp. 2706–2715. doi: 10.1016/j.egypro.2014.10.302.

Mehrpooya, M., Hemmatabady, H. and Ahmadi, M. H. (2015) 'Optimization of performance of Combined Solar Collector-Geothermal Heat Pump Systems to supply thermal load needed for heating greenhouses', *Energy Conversion and Management*. Elsevier Ltd, 97, pp. 382–392. doi: 10.1016/j.enconman.2015.03.073.

Metz, P. D. (1980) 'DEVELOPMENT OF A VALIDATED MODEL OF GROUND COUPLING', *PRESENTED AT THE AMERICAN SECTION/INTERNATIONAL SOLAR ENERGY SOCIETY 1980 ANNUAL MEETING - PHOENIX, ARIZONA JUNE 2-6,*.

Molinaroli, L., Joppolo, C. M. and De Antonellis, S. (2014) 'Numerical Analysis of the Use of R-407C in Direct Expansion Solar Assisted Heat Pump', *Energy Procedia*. Elsevier B.V., 48, pp. 938–945. doi: 10.1016/j.egypro.2014.02.107.

Moran, M. J. and Shapiro, H. N. (2006) *Fundamentals of Engineering Thermodynamics, 5th Edition*, *Nature*. doi: 10.1038/1811028b0.

Morrone, B., Coppola, G. and Raucci, V. (2014) 'Energy and economic savings using geothermal heat pumps in different climates', *Energy Conversion and Management*, pp. 189–198. doi: 10.1016/j.enconman.2014.08.007.

Nagano, K., Katsura, T. and Takeda, S. (2006) 'Development of a design and performance prediction tool for the ground source heat pump system', *Applied Thermal Engineering*, pp. 1578–1592. doi: 10.1016/j.applthermaleng.2005.12.003.

Naranjo-Mendoza, C. *et al.* (2018) 'A comparison of analytical and numerical model predictions of shallow soil temperature variation with experimental measurements', *Geothermics*. Elsevier, 76(November 2017), pp. 38–49. doi: 10.1016/j.geothermics.2018.06.003.

Naranjo-Mendoza, C. *et al.* (2019) 'Experimental study of a domestic solar-assisted ground source heat pump with seasonal underground thermal energy storage through shallow boreholes', *Applied Thermal Engineering*, p. 114218. doi: 10.1016/j.applthermaleng.2019.114218.

Naranjo-Mendoza, C., Greenough, R. M. and Wright, A. J. (2018) 'Are shallow boreholes a suitable option for inter-seasonal ground heat storage for the small housing sector?', *conference IGSHPA*, pp. 1–10. doi: 10.22488/okstate.18.000040.

Nicholson-Cole, D. (2012a) '<Nicholson-Cole paper.pdf>', *CIBSE ASHRAE Technical Symposium, Imperial College, London UK – 18th and 19th April 2012*, (April), pp. 1–14.

Nicholson-Cole, D. (2012b) 'DOMESTIC SOLAR EARTH CHARGING ':, *11th International Conference on Sustainable Energy technologies (SET-2012)*, pp. 1–12.

Nouri, G., Noorollahi, Y. and Yousefi, H. (2019) 'Solar assisted ground source heat pump systems – A review', *Applied Thermal Engineering*. doi: 10.1016/j.applthermaleng.2019.114351.

Okafor, I. F. and Akubue, G. (2012) 'F-Chart Method for Designing Solar Thermal Water Heating Systems', 3(9).

Ozgener, O. and Hepbasli, A. (2005a) 'Experimental performance analysis of a solar assisted ground-source heat pump greenhouse heating system', *Energy and Buildings*, 37(1), pp. 101–110. doi: 10.1016/j.enbuild.2004.06.003.

Ozgener, O. and Hepbasli, A. (2005b) 'Performance analysis of a solar-assisted ground-source heat pump system for greenhouse heating: An experimental study', *Building and Environment*, 40(8), pp. 1040–1050. doi: 10.1016/j.buildenv.2004.08.030.

Ozgener, O. and Hepbasli, A. (2007) 'A review on the energy and exergy analysis of solar assisted heat pump systems', *Renewable and Sustainable Energy Reviews*, 11(3), pp. 482–496. doi: 10.1016/j.rser.2004.12.010.

Pärisch, P. *et al.* (2014) 'Investigations and model validation of a ground-coupled heat pump for the combination with solar collectors', *Applied Thermal Engineering*. Elsevier Ltd, 62(2), pp. 375–381. doi: 10.1016/j.applthermaleng.2013.09.016.

Philippe, M. *et al.* (2010) 'Vertical Geothermal Borefields', *Ashrae Journal*, (July), p. 10. Available at: http://www.freepatentsonline.com/article/ASHRAE-Journal/257352824.html.

Prins, G. and Rayner, S. (2008) 'The Kyoto Protocol', *Bulletin of the Atomic Scientists*. doi: 10.2968/064001011.

Putrayudha, S. A. *et al.* (2015) 'A study of photovoltaic/thermal (PVT)-ground source heat pump hybrid system by using fuzzy logic control', *Applied Thermal Engineering*. Elsevier Ltd, 89, pp. 578–586. doi: 10.1016/j.applthermaleng.2015.06.019.

Qi, Z. *et al.* (2014) 'Status and development of hybrid energy systems from hybrid ground source heat pump in China and other countries', *Renewable and Sustainable Energy Reviews*. Elsevier, 29, pp. 37–51. doi: 10.1016/j.rser.2013.08.059.

Raab, S., Mangold, D. and Müller-Steinhagen, H. (2005) 'Validation of a computer model for solar assisted district heating systems with seasonal hot water heat store', *Solar Energy*, 79(5), pp. 531–543. doi: 10.1016/j.solener.2004.10.014.

Rad, F. M. and Fung, A. S. (2016) 'Solar community heating and cooling system with borehole thermal energy storage - Review of systems', *Renewable and Sustainable Energy Reviews*, 60, pp. 1550–1561. doi: 10.1016/j.rser.2016.03.025.

Rad, F. M., Fung, A. S. and Leong, W. H. (2013) 'Feasibility of combined solar thermal and ground source heat pump systems in cold climate, Canada', *Energy and Buildings*. Elsevier B.V., 61, pp. 224–232. doi: 10.1016/j.enbuild.2013.02.036.

Ramos, A. *et al.* (2017) 'Hybrid photovoltaic-thermal solar systems for combined heating, cooling and power provision in the urban environment', *Energy Conversion and Management*, pp. 838–850. doi: 10.1016/j.enconman.2017.03.024.

Reda, F. *et al.* (2015) 'Energy assessment of solar technologies coupled with a ground source heat pump system for residential energy supply in Southern European climates', *Energy*, 91, pp. 294–305. doi: 10.1016/j.energy.2015.08.040.

Reda, F. (2015) 'Long term performance of different SAGSHP solutions for residential energy supply in Finland', *Applied Energy*, 144, pp. 31–50. doi: 10.1016/j.apenergy.2015.01.059.

Report, F., Engineering, T. and Station, E. (2001) 'Energy Systems', *Energy*, (September 2000), pp. 1–485.

Report, T. *et al.* (2010) *EHPA-DACH Testing Regulation Supplemental requirements for granting the international quality label for heat pumps Testing of Air / Water Heat Pumps Testing of Water / Water and Brine / Water Heat Pumps DIN EN 14511-1 , DIN EN 14511-2 , DIN EN 14511-3 , D*.

Sakellariou, E. and Axaopoulos, P. (2015) 'Experimental evaluation of a retrofitted PV / T collector', in *International Conference 'Science in Technology' SCinTE 2015 Experimental*, p. SCinTE-123-A03-068. Available at: http://www.scinte.gr/abstracts/3 Applied Mechanics, Civil and Energy Engineering/SCinTE-123-A03-068.pdf.

Sakellariou, E. and Axaopoulos, P. (2017) 'Simulation and experimental performance analysis of a modified PV panel to a PVT collector', *Solar Energy*. Elsevier Ltd, 155, pp. 715–726. doi: 10.1016/j.solener.2017.06.067.

Sakellariou, E. and Axaopoulos, P. (2018) 'An experimentally validated , transient model for sheet and tube PVT collector', *Solar Energy*, 174, pp. 709–718.

Sakellariou, E. I. *et al.* (2019) 'PVT based solar assisted ground source heat pump system : Modelling approach and sensitivity analyses', *Solar Energy*, pp. 37–50. doi: 10.1016/j.solener.2019.09.044.

Sarbu, I. and Sebarchievici, C. (2014) 'General review of ground-source heat pump systems for heating and cooling of buildings', *Energy and Buildings*. Elsevier B.V., 70, pp. 441–454. doi: 10.1016/j.enbuild.2013.11.068.

Schmidt, T. and Muller-Steinhagen, H. (2004) 'The Central Solar Heating Plant with Aquifer Thermal Energy Store in Rostock , Germany', *EuroSun 2004 – The 5th ISES Europe Solar Conference*, (June), pp. 1–6.

Schwarz, H. *et al.* (2018) 'Self-consumption through power-to-heat and storage for enhanced PV integration in decentralised energy systems', *Solar Energy*. Elsevier, 163(January), pp. 150–161. doi: 10.1016/j.solener.2018.01.076.

Si, Q., Okumiya, M. and Zhang, X. (2014) 'Performance evaluation and optimization of a novel solar-ground source heat pump system', *Energy and Buildings*. Elsevier B.V., 70, pp. 237–245. doi: 10.1016/j.enbuild.2013.11.065.

Sibbitt, B. *et al.* (2012) 'The performance of a high solar fraction seasonal storage district heating system - Five years of operation', *Energy Procedia*, 30, pp. 856–865. doi: 10.1016/j.egypro.2012.11.097.

Solar Angel (2016) 'Solar Angel DG-01 Module Specification'. Available at: www.solarangel.com.

Solar Energy Laboratory University of Wisconsin-Madison *et al.* (2009) 'TRNSYS 17 – a TRaNsientSYstem. Simulation program', *Simulation*.

Solaris, V. (2012) *Polysun Simulation Software*, *Velasolaris.Com*. doi: 10.1016/j.chroma.2004.11.083.

Sommerfeldt, N. and Madani, H. (2019) 'In-depth techno-economic analysis of PV / Thermal plus ground source heat pump systems for multi-family houses in a heating dominated climate', *Solar Energy*, 190(August), pp. 44–62.

Staffell, I. *et al.* (2012) 'A review of domestic heat pumps', *Energy and Environmental Science*. doi: 10.1039/c2ee22653g.

Stojanović, B. and Akander, J. (2010) 'Build-up and long-term performance test of a full-scale solar-assisted heat pump system for residential heating in Nordic climatic conditions', *Applied Thermal Engineering*, 30(2–3), pp. 188–195. doi: 10.1016/j.applthermaleng.2009.08.004.

Thorshaug Andresen, H. and Li, Y. (2015) 'Modelling the Heating of the Green Energy Lab in Shanghai by the Geothermal Heat Pump Combined with the Solar Thermal Energy and Ground Energy Storage', *Energy Procedia*. Elsevier B.V., 70, pp. 155–162. doi: 10.1016/j.egypro.2015.02.111.

Trillat-Berdal, V., Souyri, B. and Achard, G. (2007) 'Coupling of geothermal heat pumps with thermal solar collectors', *Applied Thermal Engineering*, 27(10), pp. 1750–1755. doi: 10.1016/j.applthermaleng.2006.07.022.

Trillat-Berdal, V., Souyri, B. and Fraisse, G. (2006) 'Experimental study of a ground-coupled heat pump combined with thermal solar collectors', *Energy and Buildings*, 38(12), pp. 1477–1484. doi: 10.1016/j.enbuild.2006.04.005.

UK-Gov (no date) 'Conversion-Factors-2019-Full-set-for-advanced-users'. Retrieved from https://www.gov.uk/government/publications/greenhouse-gas-reporting-conversion-factors-2019. Available at: https://www.gov.uk/government/publications/greenhouse-gas-reporting-conversion-factors-2019.

UN (2015) *Transforming our world: The 2030 agenda for sustainable development. A/RES/70/1*, *United Nations General Assembly*. doi: 10.1007/s13398-014-0173-7.2.

UNFCCC. Conference of the Parties (COP) (2015) 'ADOPTION OF THE PARIS AGREEMENT - Conference of the Parties COP 21', *Adoption of the Paris Agreement. Proposal by the President.*, 21932(December), p. 32. doi: FCCC/CP/2015/L.9/Rev.1.

Verma, V. and Murugesan, K. (2014) 'Optimization of solar assisted ground source heat pump system for space heating application by Taguchi method and utility concept', *Energy and Buildings*. Elsevier B.V., 82, pp. 296–309. doi: 10.1016/j.enbuild.2014.07.029.

Verma, V. and Murugesan, K. (2017) 'Experimental study of solar energy storage and space heating using solar assisted ground source heat pump system for Indian climatic conditions', *Energy and Buildings*. Elsevier B.V., 139, pp. 569–577. doi: 10.1016/j.enbuild.2017.01.041.

Wang, E. *et al.* (2012) 'Performance prediction of a hybrid solar ground-source heat pump system', *Energy and Buildings*. Elsevier B.V., 47, pp. 600–611. doi: 10.1016/j.enbuild.2011.12.035.

Wang, H. *et al.* (2009) 'A case study of underground thermal storage in a solar-ground coupled heat pump system for residential buildings', *Renewable Energy*, 34(1), pp. 307–314. doi: 10.1016/j.renene.2008.04.024.

Wang, X. *et al.* (2010) 'Experimental study of a solar-assisted ground-coupled heat pump system with solar seasonal thermal storage in severe cold areas', *Energy and Buildings*. Elsevier B.V., 42(11), pp. 2104–2110. doi: 10.1016/j.enbuild.2010.06.022.

Wang, Z. *et al.* (2017) 'Comprehensive review on the development of SAHP for domestic hot water', *Renewable and Sustainable Energy Reviews*, 72(January), pp. 871–881. doi: 10.1016/j.rser.2017.01.127.

Wright, A. J., Talbot, R. and Goddard, M. (2014) 'The solar house – a true low carbon solution for 2016?', in *CIBSE ASHRAE Technical Symposium*, pp. 3–4.

Wu, W. *et al.* (2013) 'A potential solution for thermal imbalance of ground source heat pump systems in cold regions: Ground source absorption heat pump', *Renewable Energy*. Elsevier Ltd, 59, pp. 39–48. doi: 10.1016/j.renene.2013.03.020.

Xi, C. *et al.* (2011) 'Experimental studies on a ground coupled heat pump with solar thermal collectors for space heating', *Energy*. Elsevier Ltd, 36(8), pp. 5292–5300. doi: 10.1016/j.energy.2011.06.037.

Xi, C., Lin, L. and Hongxing, Y. (2011) 'Long term operation of a solar assisted ground coupled heat pump system for space heating and domestic hot water', *Energy and Buildings*. Elsevier B.V., 43(8), pp. 1835–1844. doi: 10.1016/j.enbuild.2011.03.033.

Yang, L. *et al.* (2017) 'Smart Thermal Grid with Integration of Distributed and Centralized Solar Energy Systems', *Energy*. Elsevier Ltd, 122, pp. 471–481. doi: 10.1016/j.energy.2017.01.114.

Yang, W. B., Shi, M. H. and Dong, H. (2006) 'Numerical simulation of the performance of a solar-earth source heat pump system', *Applied Thermal Engineering*, 26(17–18), pp. 2367–2376. doi: 10.1016/j.applthermaleng.2006.02.017.

Yang, W., Sun, L. and Chen, Y. (2015) 'Experimental investigations of the performance of a solar-ground source heat pump system operated in heating modes', *Energy and Buildings*. Elsevier B.V., 89, pp. 97–111. doi: 10.1016/j.enbuild.2014.12.027.

Yang, W., Zhang, H. and Liang, X. (2018) 'Experimental performance evaluation and parametric study of a solar-ground source heat pump system operated in heating modes', *Energy*. Elsevier Ltd, 149, pp. 173–189. doi: 10.1016/j.energy.2018.02.043.

You, T. *et al.* (2016) 'An overview of the problems and solutions of soil thermal imbalance of ground-coupled heat pumps in cold regions', *Applied Energy*. Elsevier Ltd, 177, pp. 515–536. doi: 10.1016/j.apenergy.2016.05.115.

Zhu, N. *et al.* (2014) 'Recent research and applications of ground source heat pump integrated with thermal energy storage systems: A review', *Applied Thermal Engineering*. Elsevier Ltd, 71(1), pp. 142–151. doi: 10.1016/j.applthermaleng.2014.06.040.

Zhu, N., Wang, J. and Liu, L. (2015) 'Performance evaluation before and after solar seasonal storage coupled with ground source heat pump', *Energy Conversion and Management*, 103, pp. 924–933. doi: 10.1016/j.enconman.2015.07.037.

Zondag, H. (2008) 'Flat-plate PV-Thermal collectors and systems: A review', *Renewable and Sustainable Energy Reviews*, 12(4), pp. 891–959. doi: 10.1016/j.rser.2005.12.012.

ŻYLICZ, T. (2015) 'IPCC', *AURA*. doi: 10.15199/2.2015.4.7.